Alma Mater Studiorum – Università di Bologna

DOTTORATO DI RICERCA IN

TECNOLOGIE INNOVATIVE E USO SOSTENIBILE DELLE RISORSE DI PESCA E BIOLOGICHE DEL MEDITERRANEO (FISHMED-PHD)

Ciclo 34

Settore Concorsuale: 03/D1

Settore Scientifico Disciplinare: CHIM/11

IMPACT OF ANTHROPOGENIC STRESSORS ON THE MICROBIAL COMMUNITIES IN MARINE HOLOBIONTS AND ECOSYSTEMS

Presentata da: Giorgia Palladino

Coordinatore Dottorato

Prof. Stefano Goffredo

Supervisore

Prof. Marco Candela

Co-supervisore

Res. Sc. Gian Marco Luna

Esame finale anno 2022

This page is intentionally left blank

Table of contents

ABSTRACT

Marine microbiomes, either free-living or associated with multicellular hosts, play a determinant role in supporting the functioning and biodiversity of marine ecosystems, thus providing essential ecological services and promoting the health of the entire biosphere. In the Anthropocene, in which we now live, the fast and restless increase of World's human population strongly impacts life on Earth in the forms of ocean pollution, coastal zone destruction, overexploitation of marine resources, and climate change. Thanks to their phylogenetic, metabolic and functional diversity, marine microbiomes represent the Earth's biggest reservoir of solutions against the major threats that are now impacting marine ecosystems. In this scenario, it is of primary importance to study and exploit the mechanisms of microbial-derived adaptive response in marine holobionts, because they can provide valuable insights for deriving biotechnological applications to preserve the health of the ocean ecosystems. Moreover, microbial-based mitigation strategies heavily rely on the available knowledge on the specific role and composition of holobionts associated microbial communities, in order to assess whether variations can act as early bio-indicators of anthropogenic-induced stress, thus highlighting the importance of pioneer studies on microbial-mediated adaptive mechanisms in the marine habitats.

In this context, here we propose different study models representing ecologically important, widely distributed, and habitat-forming organisms, to further investigate the ability of marine holobionts to dynamically adapt to natural environmental variations, as well as to anthropogenic stress factors.

In this PhD thesis, we were able to supply a complete characterization of the microbial community associated with the model anthozoan cnidaria *Corynactis viridis* throughout a seasonal gradient, in order to provide critical insights into microbiome-host interactions in a biomonitoring perspective. We also dissected in details the microbial-derived mitigation strategies implemented by the benthonic anthozoan *Anemonia viridis* and the model gastropod *Patella caerulea* as models of adaptation to anthropogenic stressors, in the context of bioremediation of heavily human-impacted habitats and for the monitoring and preservation of coastal marine ecosystems, respectively. Finally, we provided a functional model of adaptation to future ocean acidification conditions by characterizing the microbial community associated with the temperate coral *Balanophyllia europaea* naturally living at low pH conditions, in order to implement microbial based actions to mitigate climate change.

CHAPTER 1 - INTRODUCTION

1.1 Microbiome research: historical overview and main concepts

From the discovery of microorganisms in the 1670 thanks to the Dutch businessman and scientist Antonie van Leeuwenhoek, commonly known as “the Father of Microbiology”, many major historical events defined the development of the microbiome research as it is nowadays, as summarized by Berg and co-workers (2020). Microbiology research has historically emerged as a branch of ecology, thus providing an interdisciplinary platform for many fields. The continuous innovation of investigation methods and technologies, combined with the most brilliant minds of the past two centuries, led to an impressively rapid development in the microbiology research field as a central topic for both the scientific community and the general public.

From the observation of microorganisms through the first developed microscope, it became evident that these invisible entities, originally called “animalcules", could be found in all kind of samples. Moreover, it became soon clear that these microorganisms were interacting with each other in complex communities, such as biofilms (Berg et al., 2020). Although the first focus of microorganisms research shifted towards pathogenic agents, advancements in microbial ecology during the ninetieth century highlighted that the majority of microbes — that can be found everywhere in natural environments and are often associated with pluricellular hosts — are essential for ecosystems functioning, where they establish beneficial interactions with other microbes as well as macroorganisms (Podolsky, 2012). In this scenario and given their complex interactions, microorganisms can hardly be considered as individual entities, but they establish interactions where crosstalk is essential for community structure and functional activity (Bassler, 2002). These communities have been defined as assemblages of microorganisms from different species living together and interacting with each other in a contiguous environment (Konopka, 2009). Starting from this definition, in 1988 the term microbiome was introduced for the first time as a “characteristic microbial community (micro)” living in a “reasonably well-defined habitat which has distinct physio-chemical properties (biome)” (Whipps, 1988). With the advancement of technologies that allowed to unravel all the potential of microbial communities, this first definition of microbiome has been modified many times in order to include the type of interactions that microorganisms could form between themself or within an environment (Lederberg and McCray, 2001; Marchesi and Ravel, 2015; del Carmen Orozco-Mosqueda et al., 2018), to describe their collective genome and genetic potential (Schlaeppi and Bulgarelli, 2015; Arevalo et al., 2019; Nature.com: Microbiome[1]; ScienceDirect: Microbiome[2]) and to define their possible associations and interactions with hosts (Merriam-Webster Dictionary: Definition of Microbiome[3]; Human Microbiome Project[4]).

The general consensus in the scientific community is that these “characteristic microbial communities” comprise all the living members of such communities (e.g., bacteria, archaea, fungi, etc.), whereas it is not as clear whether viruses and phages, but also relic DNA, should be included in this definition. In order to solve this controversy, it is possible to refer to all these components with the term microbiome, while

[1] https://www.nature.com/subjects/microbiome. Accessed 28 Oct 2021.
[2] https://www.sciencedirect.com/topics/immunology-and-microbiology/microbiome. Accessed 28 Oct 2021.
[3] https://www.merriam-webster.com/dictionary/microbiome. Accessed 28 Oct 2021.
[4] https://hmpdacc.org. Accessed 28 Oct 2021.

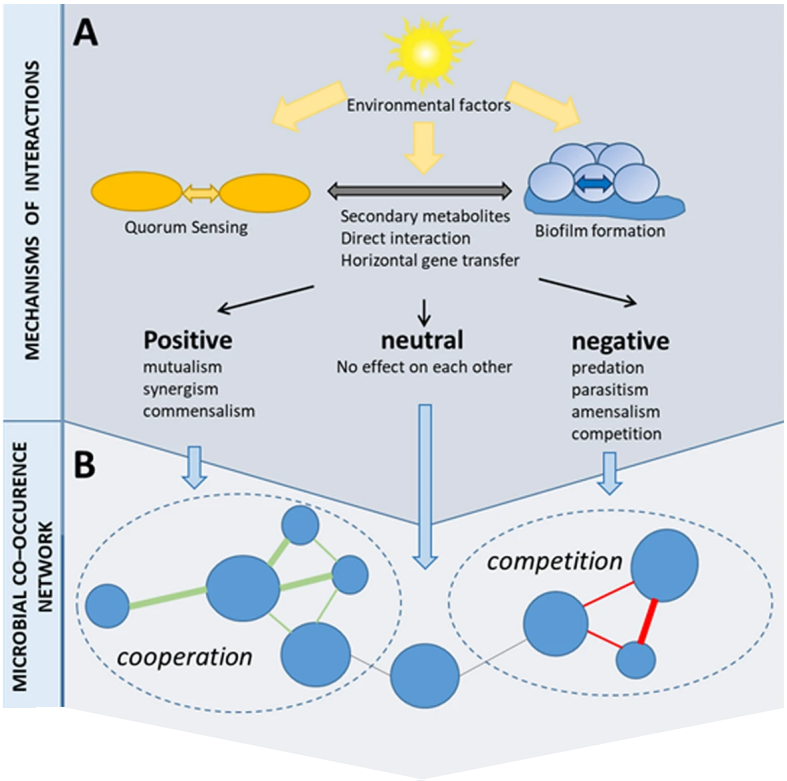

Figure 1 - Microbial interactions visualized through microbial co-occurence networks (adapted from Berg et al., 2020).

"microbiota" indicates only its living subsection (Marchesi and Ravel, 2015). Microbiome members not only share a well defined habitat with specific properties, but also interact with each other in different kind of relationships, with diverse effects on the microbial community phenotype (Banerjee et al., 2018). Microorganisms can indeed form positive networks, such as mutualistic and synergistic interactions or commensalism, negative networks , such as predation, parasitism or competitions, or even neutral interactions (Figure 1) (Berg et al., 2020). Microbiome composition, however, is not only influenced by the relationship between its different members. External factors drive the dynamics of environmental microbiomes according to the classic hypothesis that "everything is everywhere, but the environment selects" (De Wit and Bouvier, 2006), thus spatiotemporal dynamics also have a great effect in shaping microbiome structure and functions (Shade et al., 2013; Graham et al., 2016).

By observing subsequent compositional changes in a microbial community in response to environmental perturbation, it is possible to distinguish between stable and permanent members of a certain ecosystem and its intermittent part, that might be associated only with specific environmental conditions. The "core microbiome" has been typically defined "as the suite of members shared among microbial consortia from similar habitats" (Shade and Handelsman, 2012), although this definition has been subsequently widen to take into account the core genetic functions of a specific community (Lemanceau et al., 2017). Through the identification of the core species, the ecological role of microbial consortia can be assessed and community responses to perturbation can be predicted, assuming that commonly occurring organisms that appear in all assemblages associated with a particular habitat are stably present and essential for the functioning of that type of community (Shade and Handelsman, 2012).

All the concepts described here can be applied to microbe-microbe interactions, characterizing free-living communities in the environment, and microbiome-host interactions. The idea of studying complex systems in their entirety, focusing on the interconnection between different components rather than on individual parts, dates back to the 4th century BC with Aristotle and his philosophical notion defined holism. According to holism, complex systems have emerging properties resulting from the combination of their components, a notion described in the Metaphysics as "the totality is not, as it were, a mere heap, but the whole is something besides the parts" (Met. H.6). The holistic idea renewed his popularity at the beginning of the 1900s, when the endosymbiosis theory, according to which eukaryotic cells symbiotically assimilated

prokaryotes via phagocytosis to form mitochondria and later plastids, was proposed (Mereschkowski, 1905; Wallin, 1925). Although this theory was generally accepted, the term holobiont was introduced only later in the scientific scenario. This term was coined independently by Meyer-Abich (1943) and Lynn Margulis (1990), proposing that the main mechanism of evolution acted through symbiosis-driven leaps that merged organisms into new forms, referred to as holobionts, and only secondarily through gradual mutational changes (Dittami et al., 2021). The first time the word holobiont was used to identify a unit of selection was at the beginning of the XXI century by coral biologists, in order to describe the coral holobiont as the association of the cnidarian polyp, endocellular algae of the family *Symbiodiniaceae*, and ectosymbionts (i.e., prokaryotes, other unicellular eukaryotes, viruses) (Rohwer et al., 2002). Similarly to the study of microbe-microbe interactions, leading to the necessity to consider microbial communities as a whole, host-associated microorganisms also need to be considered in the nature of their association to gain insights into their ecological role in host physiology, health and behavior (Apprill, 2017).

1.2 Environmental marine microbiomes associated with seawater, sediments and air

Open oceans, soil, and oceanic and terrestrial subsurfaces are the biggest reservoirs of Earth's prokaryotes, where the number of cells has originally been estimated to be 1.2×10^{29}, 2.6×10^{29}, 3.5×10^{30}, and $0.25–2.5 \times 10^{30}$, respectively. They represent the largest pool of life's genetic diversity and they are an essential component of the Earth's biota (Whitman et al., 1998). Since 3.5 billions of years ago, when life on Earth originated as microorganisms in the oceans, these microorganisms established the necessary conditions of the Earth's biosphere for the evolution of complex biological communities. Being at the foundation of the biosphere and major determinants in the health and support of complex ecosystems, microbiomes play a primary, fundamental role in life on Earth, with their study being pivotal to the understanding of all living things (Schaechter et al., 2004). Microbial oceanography is a discipline born to integrate microbial ecology and oceanography to study the the role of microorganisms in biogeochemical dynamics of natural marine ecosystems (Karl, 2007). Oceans represent the largest contiguous habitat on Earth. Despite the absence of rigid physical barriers, the global ocean is composed by a set of different and semi-isolated habitats (Longhurst, 2010). Ocean circulation is responsible for the broad distribution of dissolved nutrients that, together with solar energy, represent the basis for life development in the sea. Closer to the costal environments, marine environments are influenced by the input of materials from the inland, such as sediments, freshwater, organic carbon and nutrients, affecting microbial productivity and increasing habitat variability. On the contrary, deeper environments (> 4 km) are characterized by relatively constant physical and chemical properties (Karl, 2007). Microorganisms inhabiting marine ecosystems in a planktonic state are estimated to be 10^4 to 10^6 cells per milliliter, thus accounting for the largest fraction on biomass and biodiversity in the ocean (Sunagawa et al., 2015). They collectively provide critical functions to the oceans and Earth by driving the global biogeochemical processes, such as carbon and nutrient cycling and organic matter degradation (Falkowski et al., 1998), and regulating the gaseous composition of the atmosphere through their roles in oxygen production (Apprill, 2017). Due to the high stratification of microbial assemblages on the vertical dimension (depth), it is important to characterize microbial genetic content within the epipelagic layer, both from the surface water and the deep chlorophyll maximum (DCM) layers, as well as the mesopelagic zone. The environmental parameters acting as the main drivers of microbial

community variability, both at taxonomic and functional level, have been shown to be depth and temperature, in the photic open ocean (Sunagawa et al., 2015). As for microbial functionality characterization, the functional core of the epipelagic zone is almost completely included in the mesopelagic functional core, that is instead enriched in aerobic respiration genes. This could be connected to the role of the mesopelagic zone as a key site for remineralization of organic matter and suggests microbial precipitation from the epipelagic layer into the mesopelagic zone, making it a fundamental area of carbon storage and burial in the biosphere (Arístegui et al., 2009).

The upper 10 cm of sediment in the open ocean is included in the oceanic habitat because it can be considered essentially contiguous with the overlying water column. On the other hand, oceanic subsurface is defined as marine sediments below the upper 10 cm (Whitman et al., 1998). The total microbial cell abundance in subseafloor sediment can vary between sites depending on mean sedimentation rate and distance from land. As for today, the global subseafloor sedimentary microbial abundance has been estimated to be 2.9×10^{29} cells, comprising only 0.18 to 3.6% of Earth's total living biomass (Kallmeyer et al., 2012). Depth is the main factor influencing microbial abundance in the oceanic subsurface, with a decrease in prokaryotic cells concentration associated with increasing depth (Hoshino et al., 2020). Different studies measured microbial concentration at decreasing depth. Parkes et al. (2000) showed that in more superficial sediments , microbial concentration can vary between 1.4 and 4×10^{9} cells/cm^3 in the top 1 m and decreases rapidly with depth. Schippers et al., (2005) measured the living component of microbial abundance in open ocean subsurfaces at different sites. The cell concentration varied from 10^{8} cells/cm^3 in the most superficial part to 10^{6} cells/m^3 at 40 m depth. Another factor that could limit bacterial distribution in deep sediments is the increasing temperature during burial. It is possible that only few bacteria are able to grow at elevated temperatures and/or that elevated temperatures may compound the limitation of organic matter during burial. However, some bacterial populations might be able to survive at very high temperature, being genetically equipped to bear thermophilic or hyper-thermophilic conditions (Parkes et al., 2000).

Open oceans not only act as one of the main reservoirs of prokaryotes concentration and genetic diversity, but marine aerosol constitute an important link between the oceans and the composition of the atmosphere, the hydrological cycles, and the Earth's temperature, with obvious impacts on human and ecosystems health. Primary sea spray aerosol (SSA) is generated at the ocean surface by bubble-bursting as the result of breaking waves. Secondary marine aerosol (SMA) is instead formed by the oxidation of volatile gasses from the ocean through nucleation processes, resulting in the formation of new particles. SMA can also condense onto already existing particles, influencing their chemical composition and properties (Mayer et al., 2020). Given the critical role of marine aerosols in impacting atmosphere composition and climate, it is important to understand how ocean biological activity can impact their formation. SSA is emitted over nearly three-quarters of our planet, as oceans cover more than 70% of the Earth's surface (Schiffer et al., 2018), thus the link between marine aerosol formation and air microbiome composition is extremely important. The complex system of particles in suspension in the atmosphere, either defines as aerosol or Airborne Particulate Matter (APM), can be constituted by a wide variety of sources, including marine aerosol. The "airborne microbiome" (AM) is the fraction of biological aerosol including microorganisms (Mescioglu et al., 2019). AM can be transported over large distances, across continents and oceans,

contributing to atmospheric events like ice nucleation and cloud processing (DeLeon-Rodriguez et al., 2013) and being responsible for the spreading of microorganisms over the planet surface, affecting the geographical biome and, ultimately, human health (Huang et al., 2014; Michaud et al., 2018).

1.3 Symbiotic associations between micro- and macroorganisms: the marine holobionts

From the beginning of the XXI century, when the term holobiont was firstly introduced, relationships and interactions between microorganisms and marine animals have been investigated over the past two decades, making holobionts a growing research area within the field of marine science. Technological advancements paved the way for a massively increased sequencing effort in the last decade, providing new important insights into the understanding of marine holobionts (Douglas, 2010; McFall-Ngai et al., 2013). In particular, key issues such as microbial community assembly and maintenance, as well as functional role of microbial components in different holobionts' ecosystems have been addressed.

Microbiome assembly is the mechanisms of selection used by the host to control the source and composition of its microbial partners. The microbial transmission pattern in marine hosts is a primary factor for the stability of their microbiome. Microbiomes can indeed follow different transmission modes, from vertical to horizontal and environmental acquisition (Simon et al., 2019). Funkhouser and Bordenstein (2013) described microbiome vertical transmission in the bivalves of the *Vesicomyidae* family and in marine sponges. Vesicomyid clams present a rudimentary gut and rely on sulfur-oxidizing bacteria found intracellularly within specialized host cells in the clam's gills. In this model, vertical transmission is the main mechanism for the maintenance of these symbionts. Another example of vertical transmission is represented by the sponge holobiont. Sponges are amongst the first multicellular animals that evolved over 600 million years ago, hosting a wide range of extracellular microbial symbionts. Many of these bacteria can be found in different sponge species from different areas, but they are not present in the surrounding seawater. Thus, it has been hypothesized that these sponge-specific microbes originated from ancient colonization events, before the diversification of marine sponges, and are maintained in sponge evolution via vertical transmission (Taylor et al., 2007; Schmitt et al., 2007 and 2008). However, in sponges vertical transmission is not the only path for microbial assembly: it has also been shown that rare taxa found at very low abundance in the surrounding seawater may serve as seed organisms for widely occurring symbionts in sponge hosts, thus defining a mixed mode of transmission, both vertical and horizontal (Webster et al., 2010). Corals can also present mixed forms of microbial transmission. For example, it has been shown that bacterial establishment is mainly environmentally driven in very early life stages but at least one bacterial strain is likely acquired within the parental environment. As for the coral associated microalgae, both vertical transmission and novel acquisition were observed (Epstein et al., 2019; Damjanovic et al., 2020).

Microbial community maintenance across the holobiont lifespan can be carried out as a selection by both the host and other components of the microbiome. A first method of host selection is represented by the secretion of specific antimicrobial peptides, that are able to shape species-specific bacterial associations (Franzenburg et al., 2013). Another chemical method of selection is the so-called microbial gardening, a concept firstly described in land plants, where root exudates manipulate microbiome composition (Lebeis et al., 2015). This finds some evidences in marine animals as well, although not much information is available yet. According to this theory, marine-specific chemical interactions can occur between the host and its

symbionts. For instance, seaweeds are able to chemically garden beneficial microbiomes and both seaweeds and corals shape their surface-associated microbiome by producing chemo-attractant and anti-bacterial compounds (Kessler et al., 2018; Ochsenkühn et al., 2018; Saha and Weinberger, 2019). Besides direct selection from the host, other events can shape holobionts microbial composition, such as ecological drift, dispersal (especially due to the high connectivity of aquatic environments), evolutionary diversification (coevolution or adaptation to host selection might also be driven by horizontal gene acquisition), or a combination of these processes and selection. However, the influence of these mechanisms on microbial composition is more difficult to estimate and studies are still in their infancy (Dittami et al., 2021).

Another main goal of marine ecology research is to understand which functions are delivered by the microbiota to the host and what are the resulting phenotypic and fitness effects (Simon et al., 2019). In order to do so, it is important to characterize the microbial phylogenetic and functional core (i.e., taxonomic composition and metabolic functionalities), common to different individuals of the same species and use this knowledge as a starting point to investigate how changes from standard conditions can affect host metabolism and physiology. Host species-specificity of microbiomes plays indeed a fundamental role for the characterization of microbial phylogenetic and functional core, with patterns of phylosymbiosis, where similarities in host-associated microbial communities summarize the phylogeny of their hosts, that can provide critical insights into microbiome-host interactions (Kohl, 2020; Mallott and Amato, 2021).

1.4 Marine holobionts model species

The characterization of microbial patterns of phylosymbiosis for the identification of species-specific associated microbiomes is particularly hard due to the big variety of marine species and their different physiological responses. To reduce this complexity, it is possible to consider some model species as representative marine animals carrying important ecological functions.

Sponges and corals are amongst the most studied model marine holobionts due to their important role as habitat-forming species, at the basis of the trophic chains, playing a major role in establishing and organizing the ecosystem structure and determining its productivity (Lemieux and Cusson, 2014). These organisms host exceptional diverse microbial communities and they are globally distributed in a wide range of benthic habitats (Pita et al., 2018).

Pita and co-workers (2018) reviewed the microbial ecological functions in sponges. The microbial core diversity across worldwide collected sponges, as a part of the Global Sponge Microbiome Project (Moitinho-Silva et al., 2017), defines species-specific microbial communities composed of both generalist microorganisms, detected in the majority of sponge species from diverse geographic regions, and specialists, enriched in certain species but rare or absent in most of them (Astudillo-García et al., 2017; Steinert et al., 2017). This highlights the importance of host-related factors in the selection and shaping of the core microbiome. Different environmental conditions, such as life stage or seasonality, depth, and habitat type, can also impact sponge microbial diversity in its variable fraction (Morrow et al., 2016; Steinert et al., 2016; Weigel and Erwin, 2017). Due to their major role as habitat-forming species, the study of sponge holobionts also expands to the interactions with the surrounding habitat, in the concept of nested ecosystems (Figure 2). Different metabolic features can be generally described for sponge associated microbiome, including auto- and heterotrophic pathways to exploit the nutrients available in the sponge

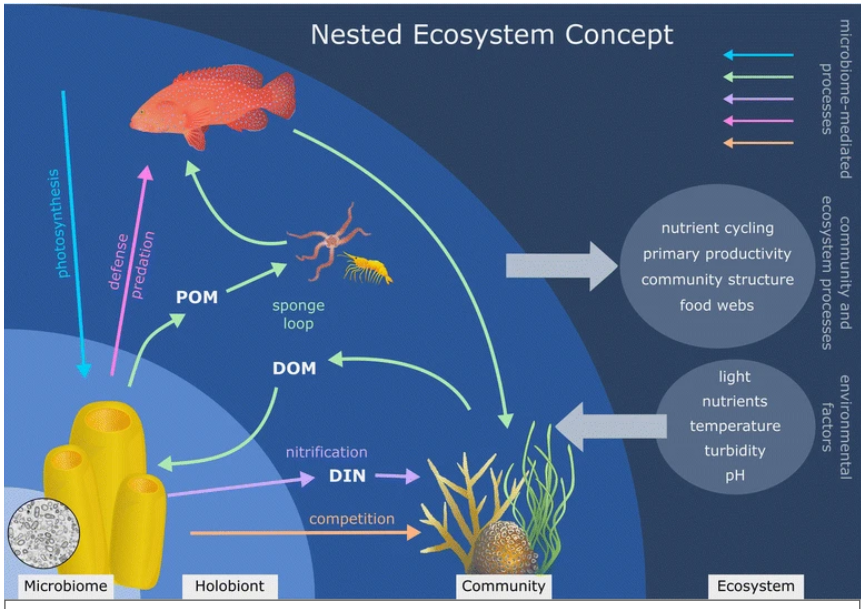

Figure 2 - The sponge holobiont as an example of nested ecosystem. Key functions carried out by the microbiome influence holobiont functioning and, consequently, community structure and ecosystem functioning. Thus, factors altering the microbiome functioning can lead to changes at the holobiont, community, or even ecosystem level. DOM, dissolved organic matter; POM, particulate organic matter; DIN, dissolved inorganic nitrogen (Pita et al., 2018).

environment, and pathways that contribute directly to the symbiotic relationship with the sponge host. For example, common photoautotrophic symbionts found in sponges provide their host with fixed carbon and nitrogen for its energy requirements, while contributing to the ecosystem primary productivity (Freeman and Thacker, 2011; Freeman et al., 2013). Nitrogen is a limiting nutrient in the marine environment and, since it is excreted by the the sponge host in the form of the waste product ammonia, it is coherent to find that sponge symbionts are enriched in nitrogen metabolism genes (Bayer et al., 2014; Li et al., 2016), meaning that sponge symbionts play a crucial role in the biogeochemical cycling of nitrogen (Hoffmann et al., 2009; Radax et al., 2012; Ribes et al., 2012; Li et al., 2014; Zhang et al., 2014; Ribes et al., 2015). Sponge associated microbiomes are also able to influence phosphorus availability, again affecting the ecosystem primary production (Colman, 2015; Zhang et al., 2015). Sponge associated microbial communities rely on nutrient sources from the sponge filtering activity or produced by the sponge itself, thus the degradation of complex carbohydrates is a common heterotrophic feature in sponge symbionts (Kamke et al., 2013; Webster and Thomas, 2016; Slaby et al., 2017). Sponge microbiome core functions can also benefit the host by producing and making available vitamins or secondary metabolites that contribute to the sponge chemical defense (Thomas et al., 2010; Wilson et al., 2014; Fiore et al., 2015), such as anti-predatory compounds (Della Sala et al., 2014; Rohde et al., 2015; Lackner et al., 2017), thereby influencing the benthonic community structure in terms of spatial competition.

Corals also occupy a key ecological position in the benthonic habitats, where they represent foundation species at the basis of the trophic chain. Although corals perform their nutrient intake via heterotrophic feeding, they largely rely on their symbiotic associations for a proficient nutrient acquisition. Indeed, the endosymbiotic dinoflagellates of the *Symbiodiniaceae* family provides nutrients and energy to the coral host through the transfer of photosynthates (Stat et al., 2006). The prokaryotic community associated with corals is also able to perform carbon fixation and to use simple and complex carbohydrates to recycle a portion of the carbon and energy invested in mucus production (Bourne et al., 2016; Robbins et al., 2019). Similarly to sponges, one of the core functions of the coral associated microbiome is represented by the metabolic

potential for complete nitrogen cycling. Potential nitrogen fixation bacteria have been indeed detected in all coral life stages across time and space (Rädecker et al., 2015; Benavides et al., 2017), together with many nitrifying, denitrifying and ammonifying microorganisms, potentially able remove ammonia waste products and control nitrogen availability, which is crucial to maintain a stable interaction between the coral and the *Symbiodiniaceae* algae (Siboni et al., 2008; Morris et al., 2019; Robbins et al., 2019). Corals microbial communities play a key role in the sulfur cycling as well. Reef-building corals are the largest producers of dimethylsulfoniopropionate (DMSP), a central molecule in the marine sulphur cycle, proposed to be involved in several protective physiological functions (Raina et al., 2013), such as osmo- and cryo-protection and antioxidant (Raina et al., 2010). Coral associated bacteria are able to use DMSP as a source for sulphur and carbon, indicating their involvement in coral reefs sulfur cycling (Vanwonterghem and Webster, 2020). Coral microbial symbionts are involved in the production of amino acids and secondary metabolites, i.e., vitamins, essential to the metabolic functioning of the host and algal symbionts. Finally, antimicrobial compound produced by coral microbial community can also be involved in pathogen control (Matthews et al., 2020) and regulation of the microbial colonization of the coral surface itself (Peixoto et al., 2017).

Other model organisms often taken into account by this field of research are bivalve mollusks and fish for their relevance in food production and, for mollusks, because their powerful filtering feeding activity makes them able to bioaccumulate and biomagnify of all kinds of environmental substances and molecules. Recent studies highlight the existence of tissue-specific microbiota in bivalve mollusks exerting key functions for the host physiology (Lokmer et al., 2016; Meisterhans et al., 2016; Pathirana et al, 2019). For example, Musella and co-workers (2020) described a specific pattern of microbial families characterizing the digestive gland, foot, gills, stomach, and hemolymph of the Mediterranean mussel *Mytilus galloprovincialis*, suggesting that the main determinant of the mussel microbiota variation is the niche-specificity rather than the individual differences. In particular, the digestive gland microbiota is found to be enriched in commensal microorganisms capable of fermenting complex polysaccharides from dietary fibers, such as such as cellulose and hemicellulose commonly found in bivalve food, to short-chain fatty acids (SCFAs). The stomach and foot microbiota are instead dominated by anaerobic microorganisms with animal tropism, whereas gills and hemolymph microbiota is characterized by aerobes of marine origin, being these tissues a primary biological barrier between the animal and the external environment, in direct contact with the surrounding seawater.

Fish-associated microbiomes have also gained increasing attention (Sehnal et al., 2021), especially considering the growing importance of fish farming for human consumption and the possible implications for human health (Grigorakis and Rigos, 2011; Rosa et al., 2012). For example, gills are the interface between fish and the surrounding environment for gas exchange, thus they are an important first line of defense against pathogenic infections that may come from the external habitat (Iijima et al., 2003). For this reason, gills associated microbiomes can reflect diseases and inflammatory states (Legrand et al., 2018), providing valuable knowledge of overall animal health. Fish skin surface also provides a barrier between the host and the surrounding environment, thus microbial communities associated with the epithelium exert an important role in fish immune system (Gomez et al., 2013), once again acting as a possible indicator for fish health status. Finally, fish carry complex intestinal microbiomes, strongly influenced by species-specificity, diet and living environment, that are involved in nutrient absorption, immune system, intestinal

development, homeostasis and xenobiotic metabolism (Sehnal et al., 2021), thus contributing to overall fish health.

Marine ecology research has also focused on the study of marine animals associated microbiome through non invasive sampling as a new key aspect to set health biomarkers. Many marine animals can be considered as "flagship species", defined as focal species, for ecological or social reasons, believed to be valuable for the understanding, management and conservation of natural environments (Zacharias and Roff, 2001). Also called sentinel animals, flagship species act as bioindicators to the ocean environment health, due to their rapid response to environmental conditions and disturbances (Apprill, 2017). An unfortunately famous example of flagship species is the loggerhead sea turtle (*Caretta caretta*), widespread across the whole Mediterranean Sea, as useful indicator of the general plastic pollution level of marine ecosystems (Biagi et al., 2021).

In conclusion, it is clear that microbiomes are tightly linked to the functioning and health of their host and, consequently, of the entire ecosystem. Modifications of these interactions caused by disturbances in the marine ecosystems can hence strongly impact holobionts and habitat homeostasis. The importance of the study of microbial core composition and functioning under healthy conditions is therefore essential to establish biomarkers, bioindicators, for host and environmental health (Sehnal et al., 2021) in a biomonitoring perspective, defined as the act of observing and assessing the state and ongoing changes in ecosystems, components of biodiversity, populations and species (Bondaruk et al., 2015).

1.5 Microbiome disturbances: long and short term responses to anthropogenic impacts

The fast and restless increase of World's human population is rising crescent concerns about the threads that human activity can pose to seas and oceans ecosystems (Fleming et al., 2019). Ocean pollution, costal zone destruction, overexploitation of marine resources, such as overfishing or seabeds exploitation, and the phenomena connected to climate change are all consequences of anthropogenically driven activities that are negatively impacting costal waters, the seas and global ocean (Fleming et al., 2019; Borja et al., 2020; Landrigan et al., 2020).

Ocean pollution is a complex and widespread mix of many different components (Figure 3) of both very old and new pollutants, in terms of release time and material (Landrigan et al., 2020). These include petroleum-based pollutants and plastic waste (PlasticsEurope, 2016), toxic metals, such as mercury pollution from coal combustion and gold-mining (Outridge et al., 2018), and chemical waste such as pharmaceuticals, pesticides and fertilizers from chemically intensive agriculture practice (Landrigan et al., 2020). About 80% of all the ocean pollution comes from land-based sources, e.g., via rivers or atmospheric deposition, whereas the remaining 20% is marine-based (Agardy et al., 2005; UNESCO. Facts and Figures on Marine Pollution[5]). The anthropogenic impact on the global ocean is also connected to climate change. Climate change has led to a constant increase of oceans temperature, causing glacials melting and sea level rising, with an almost doubled frequency of marine heat waves (Chen et al., 2021). Further consequences of climate change are the increased frequency and intensity of extreme weather events (Fasullo et al., 2018), such as storms and flooding, pathogenic algal and bacterial blooms and increased ocean acidification (Gruber et al., 2019).

[5] http://www.unesco.org/new/en/natural-sciences/ioc-oceans/focus-areas/rio-20-ocean/blueprint-for-the-future-we-want/marine-pollution/facts-and-figures-on-marine-pollution/. Accessed 22 Nov 2021.

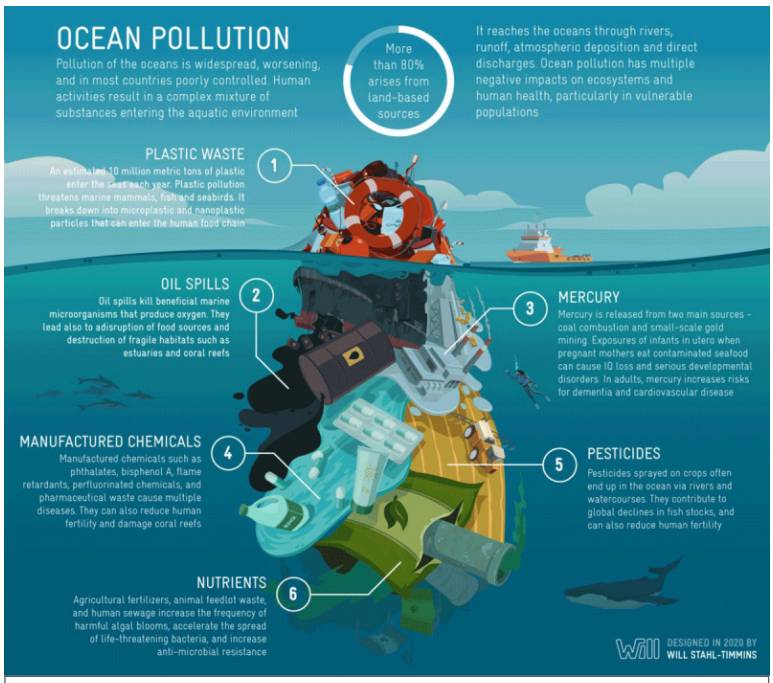

Figure 3 - The complex mixture representing ocean pollution (Landrigan et al., 2020).

Oceans have been always subjected to anthropogenic activities, with both direct (e.g., waste disposal) and indirect (e.g., climate change) impacts on marine environments, in the wrong belief that the global ocean would be able to absorb and mitigate all the contamination (Borja et al., 2020). The deterioration of marine environments can be brought back to two main dynamics. The impact of anthropogenic activities directly on marine organisms leads to low rate, slow acclimatization processes of the host physiology. Contrariwise, this deterioration can also indirectly act on marine holobionts through their associated microbiome. Due to the microbial fast population growth rate (Logue et al., 2015), this process leads to a faster acclimatization to rapid changes, with possible interesting biotechnological applications for marine restoration. Different types of disturbances can lead to different outcomes depending on the type or strength of the disturbance itself and on the holobiont properties (Pita et al., 2018). Homeostasis might be able to maintain a healthy state through the mechanisms of resistance and resilience that are, respectively, the ability to withstand perturbation unchanged and the capacity to recover upon disturbance. Alternatively, perturbations may disrupt this balance, leading to dysbiotic conditions. Finally, disturbances may act as a driver of selection for acclimatization, thus the holobiont reaches a new healthy state that allows it to better cope with environmental change (Figure 4). If these new features enhance holobiont fitness and can be transmitted to new generations, they may yield holobiont adaptation *sensu lato* (Webster and Reusch, 2017). In this contest, a major question in ocean global change biology is to determine whether short-term plastic responses might be linked to longer-term evolutionary responses or how they can co-occur to contribute to biological shifts (Collins et al., 2020).

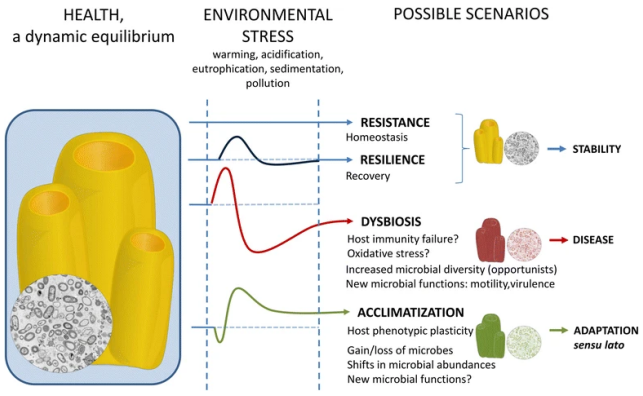

Figure 4 - Possible effect of disturbances and environmental changes on marine holobionts. Conceptual representation of holobiont health and potential outcomes upon environmental disturbances (Pita et al., 2018).

1.6 References

Agardy, T., Alder, J., Dayton, P., Curran, S., Kitchingman, A., Wilson, M., ... & Vorosmarty, C. (2005). Coastal systems.

Apprill, A. (2017). Marine animal microbiomes: toward understanding host–microbiome interactions in a changing ocean. *Frontiers in Marine Science*, *4*, 222.

Arevalo, P., VanInsberghe, D., Elsherbini, J., Gore, J., & Polz, M. F. (2019). A reverse ecology approach based on a biological definition of microbial populations. *Cell*, *178*(4), 820-834.

Arístegui, J., Gasol, J. M., Duarte, C. M., & Herndld, G. J. (2009). Microbial oceanography of the dark ocean's pelagic realm. *Limnology and Oceanography*, *54*(5), 1501-1529.

Astudillo-García, C., Bell, J. J., Webster, N. S., Glasl, B., Jompa, J., Montoya, J. M., & Taylor, M. W. (2017). Evaluating the core microbiota in complex communities: a systematic investigation. *Environmental Microbiology*, *19*(4), 1450-1462.

Banerjee, S., Schlaeppi, K., & van der Heijden, M. G. (2018). Keystone taxa as drivers of microbiome structure and functioning. *Nature Reviews Microbiology*, *16*(9), 567-576.

Bassler, B. L. (2002). Small talk: cell-to-cell communication in bacteria. *Cell*, *109*(4), 421-424.

Bayer, K., Moitinho-Silva, L., Brümmer, F., Cannistraci, C. V., Ravasi, T., & Hentschel, U. (2014). GeoChip-based insights into the microbial functional gene repertoire of marine sponges (high microbial abundance, low microbial abundance) and seawater. *FEMS microbiology ecology*, *90*(3), 832-843.

Benavides, M., Bednarz, V. N., & Ferrier-Pagès, C. (2017). Diazotrophs: overlooked key players within the coral symbiosis and tropical reef ecosystems?. *Frontiers in Marine Science*, *4*, 10.

Berg, G., Rybakova, D., Fischer, D., Cernava, T., Vergès, M. C. C., Charles, T., ... & Schloter, M. (2020). Microbiome definition re-visited: old concepts and new challenges. *Microbiome*, *8*(1), 1-22.

Biagi, E., Musella, M., Palladino, G., Angelini, V., Pari, S., Roncari, C., ... & Candela, M. (2021). Impact of Plastic Debris on the Gut Microbiota of Caretta caretta From Northwestern Adriatic Sea. *Frontiers in Marine Science*, *8*, 127.

Bondaruk, J., Janson, E., Wysocka, M., & Chałupnik, S. (2015). Identification of hazards for water environment in the Upper Silesian Coal Basin caused by the discharge of salt mine water containing particularly harmful substances and radionuclides. *Journal of Sustainable Mining*, *14*(4), 179-187.

Borja, A., White, M. P., Berdalet, E., Bock, N., Eatock, C., Kristensen, P., ... & Fleming, L. E. (2020). Moving toward an agenda on ocean health and human health in Europe. *Frontiers in Marine Science*, *7*, 37.

Bourne, D. G., Morrow, K. M., & Webster, N. S. (2016). Insights into the coral microbiome: underpinning the health and resilience of reef ecosystems. *Annual Review of Microbiology*, *70*, 317-340.

Chen, D., Rojas, M., Samset, B. H., Cobb, K., Diongue, A., Niang, A., ... & Tréguier, A. M. (2021). Framing, context, and methods. Climate Change 2021: The Physical Science Basis. Contribution of Working Group I to the Sixth Assessment Report of the Intergovernmental Panel on Climate Change.

Collins, S., Boyd, P. W., & Doblin, M. A. (2020). Evolution, microbes, and changing ocean conditions. *Annual review of marine science*, *12*, 181-208.

Colman, A. S. (2015). Sponge symbionts and the marine P cycle. *Proceedings of the National Academy of Sciences*, *112*(14), 4191-4192.

Damjanovic, K., Menéndez, P., Blackall, L. L., & van Oppen, M. J. (2020). Early life stages of a common broadcast spawning coral associate with specific bacterial communities despite lack of internalized bacteria. *Microbial ecology*, *79*(3), 706-719.

De Wit, R., & Bouvier, T. (2006). 'Everything is everywhere, but, the environment selects'; what did Baas Becking and Beijerinck really say?. *Environmental microbiology*, *8*(4), 755-758.

del Carmen Orozco-Mosqueda, M., del Carmen Rocha-Granados, M., Glick, B. R., & Santoyo, G. (2018). Microbiome engineering to improve biocontrol and plant growth-promoting mechanisms. *Microbiological research*, *208*, 25-31.

DeLeon-Rodriguez, N., Lathem, T. L., Rodriguez-R, L. M., Barazesh, J. M., Anderson, B. E., Beyersdorf, A. J., ... & Konstantinidis, K. T. (2013). Microbiome of the upper troposphere: species composition and prevalence, effects of tropical storms, and atmospheric implications. *Proceedings of the National Academy of Sciences*, *110*(7), 2575-2580.

Della Sala, G., Hochmuth, T., Teta, R., Costantino, V., & Mangoni, A. (2014). Polyketide synthases in the microbiome of the marine sponge Plakortis

halichondrioides: a metagenomic update. *Marine drugs*, *12*(11), 5425-5440.

Dittami, S. M., Arboleda, E., Auguet, J. C., Bigalke, A., Briand, E., Cárdenas, P., ... & Not, F. (2021). A community perspective on the concept of marine holobionts: current status, challenges, and future directions. *PeerJ*, *9*, e10911.

Douglas, A. E. (2010). *The Symbiotic Habit*. Princeton, NJ: University Press.

Epstein, H. E., Torda, G., Munday, P. L., & van Oppen, M. J. (2019). Parental and early life stage environments drive establishment of bacterial and dinoflagellate communities in a common coral. *The ISME journal*, *13*(6), 1635-1638.

Falkowski, P. G., Barber, R. T., & Smetacek, V. (1998). Biogeochemical controls and feedbacks on ocean primary production. S*cience*, *281*(5374), 200-206.

Fasullo, J. T., Otto-Bliesner, B. L., & Stevenson, S. (2018). ENSO's changing influence on temperature, precipitation, and wildfire in a warming climate. *Geophysical Research Letters*, *45*(17), 9216-9225.

Fiore, C. L., Labrie, M., Jarett, J. K., & Lesser, M. P. (2015). Transcriptional activity of the giant barrel sponge, Xestospongia muta Holobiont: molecular evidence for metabolic interchange. *Frontiers in microbiology*, *6*, 364.

Fleming, L. E., Maycock, B., White, M. P., & Depledge, M. H. (2019). Fostering human health through ocean sustainability in the 21st century. *People and Nature*, *1*(3), 276-283.

Franzenburg, S., Walter, J., Künzel, S., Wang, J., Baines, J. F., Bosch, T. C., & Fraune, S. (2013). Distinct antimicrobial peptide expression determines host species-specific bacterial associations. *Proceedings of the National Academy of Sciences*, *110*(39), E3730-E3738.

Freeman, C. J., & Thacker, R. W. (2011). Complex interactions between marine sponges and their symbiotic microbial communities. *Limnology and Oceanography*, *56*(5), 1577-1586.

Freeman, C. J., Thacker, R. W., Baker, D. M., & Fogel, M. L. (2013). Quality or quantity: is nutrient transfer driven more by symbiont identity and productivity than by symbiont abundance?. *The ISME journal*, *7*(6), 1116-1125.

Funkhouser, L. J., & Bordenstein, S. R. (2013). Mom knows best: the universality of maternal microbial transmission. *PLoS biology*, *11*(8), e1001631.

Gomez, D., Sunyer, J. O., & Salinas, I. (2013). The mucosal immune system of fish: the evolution of tolerating commensals while fighting pathogens. *Fish & shellfish immunology*, *35*(6), 1729-1739.

Graham, E. B., Crump, A. R., Resch, C. T., Fansler, S., Arntzen, E., Kennedy, D. W., ... & Stegen, J. C. (2016). Coupling spatiotemporal community assembly processes to changes in microbial metabolism. *Frontiers in Microbiology*, *7*, 1949.

Grigorakis, K., & Rigos, G. (2011). Aquaculture effects on environmental and public welfare–the case of Mediterranean mariculture. *Chemosphere*, *85*(6), 899-919.

Gruber, N., Clement, D., Carter, B. R., Feely, R. A., Van Heuven, S., Hoppema, M., ... & Wanninkhof, R. (2019). The oceanic sink for anthropogenic CO2 from 1994 to 2007. *Science*, *363*(6432), 1193-1199.

Hoffmann, F., Radax, R., Woebken, D., Holtappels, M., Lavik, G., Rapp, H. T., ... & Kuypers, M. M. (2009). Complex nitrogen cycling in the sponge Geodia barretti. *Environmental microbiology*, *11*(9), 2228-2243.

Hoshino, T., Doi, H., Uramoto, G. I., Wörmer, L., Adhikari, R. R., Xiao, N., ... & Inagaki, F. (2020). Global diversity of microbial communities in marine sediment. *Proceedings of the national academy of sciences*, *117*(44), 27587-27597.

Huang, R. J., Zhang, Y., Bozzetti, C., Ho, K. F., Cao, J. J., Han, Y., ... & Prévôt, A. S. (2014). High secondary aerosol contribution to particulate pollution during haze events in China. *Nature*, *514*(7521), 218-222.

Iijima, N., Tanimoto, N., Emoto, Y., Morita, Y., Uematsu, K., Murakami, T., & Nakai, T. (2003). Purification and characterization of three isoforms of chrysophsin, a novel antimicrobial peptide in the gills of the red sea bream, Chrysophrys major. *European Journal of Biochemistry*, *270*(4), 675-686.

Kallmeyer, J., Pockalny, R., Adhikari, R. R., Smith, D. C., & D'Hondt, S. (2012). Global distribution of microbial abundance and biomass in subseafloor sediment. *Proceedings of the National Academy of Sciences*, *109*(40), 16213-16216.

Kamke, J., Sczyrba, A., Ivanova, N., Schwientek, P., Rinke, C., Mavromatis, K., ... & Hentschel, U. (2013). Single-cell genomics reveals complex carbohydrate degradation patterns in poribacterial symbionts of marine sponges. *The ISME journal*, *7*(12), 2287-2300.

Karl, D. M. (2007). Microbial oceanography: paradigms, processes and promise. *Nature Reviews Microbiology*, *5*(10), 759-769.

Kessler, R. W., Weiss, A., Kuegler, S., Hermes, C., & Wichard, T. (2018). Macroalgal–bacterial interactions: role of dimethylsulfoniopropionate in microbial gardening by Ulva (Chlorophyta). *Molecular Ecology*, *27*(8), 1808-1819.

Kohl, K. D. (2020). Ecological and evolutionary mechanisms underlying patterns of phylosymbiosis in host-associated microbial communities. *Philosophical Transactions of the Royal Society B*, *375*(1798), 20190251.

Konopka, A. (2009). What is microbial community ecology?. *The ISME journal*, *3*(11), 1223-1230.

Lackner, G., Peters, E. E., Helfrich, E. J., & Piel, J. (2017). Insights into the lifestyle of uncultured bacterial natural product factories associated with marine sponges. *Proceedings of the National Academy of Sciences*, *114*(3), E347-E356.

Landrigan, P. J., Stegeman, J. J., Fleming, L. E., Allemand, D., Anderson, D. M., Backer, L. C., ... & Rampal, P. (2020). Human health and ocean pollution. *Annals of global health*, *86*(1).

Lebeis, S. L., Paredes, S. H., Lundberg, D. S., Breakfield, N., Gehring, J., McDonald, M., ... & Dangl, J. L. (2015). Salicylic acid modulates colonization of the root microbiome by specific bacterial taxa. *Science*, *349*(6250), 860-864.

Lederberg, J., & McCray, A. T. (2001). Ome SweetOmics--A genealogical treasury of words. *The scientist*, *15*(7), 8-8.

Legrand, T. P., Catalano, S. R., Wos-Oxley, M. L., Stephens, F., Landos, M., Bansemer, M. S., ... & Oxley, A. (2018). The inner workings of the outer surface: skin and gill microbiota as indicators of changing gut health in yellowtail kingfish. *Frontiers in microbiology*, *8*, 2664.

Lemanceau, P., Blouin, M., Muller, D., & Moënne-Loccoz, Y. (2017). Let the core microbiota be functional. *Trends in Plant Science*, *22*(7), 583-595.

Lemieux, J., & Cusson, M. (2014). Effects of habitat-forming species richness, evenness, identity, and abundance on benthic intertidal community establishment and productivity. *PloS one*, *9*(10), e109261.

Li, Z. Y., Wang, Y. Z., He, L. M., & Zheng, H. J. (2014). Metabolic profiles of prokaryotic and eukaryotic communities in deep-sea sponge Neamphius huxleyi indicated by metagenomics. *Scientific reports*, *4*(1), 1-12.

Li, Z., Wang, Y., Li, J., Liu, F., He, L., He, Y., & Wang, S. (2016). Metagenomic analysis of genes encoding nutrient cycling pathways in the microbiota of deep-sea and shallow-water sponges. *Marine Biotechnology*, *18*(6), 659-671.

Logue, J. B., Findlay, S. E., & Comte, J. (2015). Microbial responses to environmental changes. *Frontiers in Microbiology*, *6*, 1364.

Lokmer, A., Kuenzel, S., Baines, J. F., & Wegner, K. M. (2016). The role of tissue-specific microbiota in initial establishment success of Pacific oysters. *Environmental microbiology*, *18*(3), 970-987.

Longhurst, A. R. (2010). Ecological geography of the sea. Elsevier.

Mallott, E. K., & Amato, K. R. (2021). Host specificity of the gut microbiome. *Nature Reviews Microbiology*, 1-15.

Marchesi, J. R., & Ravel, J. (2015). The vocabulary of microbiome research: a proposal.

Margulis, L. (1990). Words as battle cries: symbiogenesis and the new field of endocytobiology. *Bioscience*, *40*(9), 673-677.

Matthews, J. L., Raina, J. B., Kahlke, T., Seymour, J. R., van Oppen, M. J., & Suggett, D. J. (2020). Symbiodiniaceae-bacteria interactions: rethinking metabolite exchange in reef-building corals as multi-partner metabolic networks. *Environmental microbiology*, *22*(5), 1675-1687.

Mayer, K. J., Sauer, J. S., Dinasquet, J., & Prather, K. A. (2020). CAICE Studies: Insights from a Decade of Ocean–Atmosphere Experiments in the Laboratory. *Accounts of Chemical Research*, *53*(11), 2510-2520.

McFall-Ngai, M., Hadfield, M. G., Bosch, T. C., Carey, H. V., Domazet-Lošo, T., Douglas, A. E., ... & Wernegreen, J. J. (2013). Animals in a bacterial world, a new imperative for the life sciences. *Proceedings of the National Academy of Sciences*, *110*(9), 3229-3236.

Meisterhans, G., Raymond, N., Girault, E., Lambert, C., Bourrasseau, L., De Montaudouin, X., ... & Jude-Lemeilleur, F. (2016). Structure of Manila clam (Ruditapes philippinarum) microbiota at the organ scale in contrasting sets of individuals. *Microbial ecology*, *71*(1), 194-206.

Meyer-Abich, A. (1943). Beiträge zur Theorie der Evolution der Organismen. I. Das typologische Grundgesetz und seine Folgerungen für Phylogenie und Entwicklungsphysiologie [Contributions to the evolutionary theory of organisms: I. The basic typological law and its implications for phylogeny and developmental physiology]. Acta Biotheoretica, 7, 1–80.

Mereschkowski, K. S. (1905). Über Natur und Ursprung der Chromatophoren im Pflanzenreiche, Biol.

Mescioglu, E., Rahav, E., Belkin, N., Xian, P., Eizenga, J. M., Vichik, A., ... & Paytan, A. (2019). Aerosol microbiome over the Mediterranean Sea diversity and abundance. *Atmosphere*, *10*(8), 440.

Michaud, J. M., Thompson, L. R., Kaul, D., Espinoza, J. L., Richter, R. A., Xu, Z. Z., ... & Prather, K. A. (2018). Taxon-specific aerosolization of bacteria and viruses in an

experimental ocean-atmosphere mesocosm. *Nature communications*, *9*(1), 1-10.

Moitinho-Silva, L., Nielsen, S., Amir, A., Gonzalez, A., Ackermann, G. L., Cerrano, C., ... & Thomas, T. (2017). The sponge microbiome project. *Gigascience*, *6*(10), gix077.

Morris, L. A., Voolstra, C. R., Quigley, K. M., Bourne, D. G., & Bay, L. K. (2019). Nutrient availability and metabolism affect the stability of coral–Symbiodiniaceae symbioses. *Trends in microbiology*, *27*(8), 678-689.

Morrow, K. M., Fiore, C. L., & Lesser, M. P. (2016). Environmental drivers of microbial community shifts in the giant barrel sponge, X estospongia muta, over a shallow to mesophotic depth gradient. *Environmental Microbiology*, *18*(6), 2025-2038.

Musella, M., Wathsala, R., Tavella, T., Rampelli, S., Barone, M., Palladino, G., ... & Candela, M. (2020). Tissue-scale microbiota of the Mediterranean mussel (Mytilus galloprovincialis) and its relationship with the environment. *Science of The Total Environment*, *717*, 137209.

Ochsenkühn, M. A., Schmitt-Kopplin, P., Harir, M., & Amin, S. A. (2018). Coral metabolite gradients affect microbial community structures and act as a disease cue. *Communications biology*, *1*(1), 1-10.

Outridge, P. M., Mason, R. P., Wang, F., Guerrero, S., & Heimburger-Boavida, L. E. (2018). Updated global and oceanic mercury budgets for the United Nations Global Mercury Assessment 2018. *Environmental science & technology*, *52*(20), 11466-11477.

Parkes, R. J., Cragg, B. A., & Wellsbury, P. (2000). Recent studies on bacterial populations and processes in subseafloor sediments: a review. *Hydrogeology Journal*, *8*(1), 11-28.

Pathirana, E., McPherson, A., Whittington, R., & Hick, P. (2019). The role of tissue type, sampling and nucleic acid purification methodology on the inferred composition of Pacific oyster (Crassostrea gigas) microbiome. *Journal of applied microbiology*, *127*(2), 429-444.

Peixoto, R. S., Rosado, P. M., Leite, D. C. D. A., Rosado, A. S., & Bourne, D. G. (2017). Beneficial microorganisms for corals (BMC): proposed mechanisms for coral health and resilience. *Frontiers in Microbiology*, *8*, 341.

Pita, L., Rix, L., Slaby, B. M., Franke, A., & Hentschel, U. (2018). The sponge holobiont in a changing ocean: from microbes to ecosystems. *Microbiome*, *6*(1), 1-18.

PlasticsEurope, E. P. R. O. (2016). Plastics—the facts 2016. An analysis of European plastics production, demand and waste data. *Plastics Europe*.

Podolsky, S. H. (2012). Metchnikoff and the microbiome. *The Lancet*, *380*(9856), 1810-1811.

Radax, R., Hoffmann, F., Rapp, H. T., Leininger, S., & Schleper, C. (2012). Ammonia-oxidizing archaea as main drivers of nitrification in cold-water sponges. *Environmental Microbiology*, *14*(4), 909-923.

Rädecker, N., Pogoreutz, C., Voolstra, C. R., Wiedenmann, J., & Wild, C. (2015). Nitrogen cycling in corals: the key to understanding holobiont functioning?. *Trends in microbiology*, *23*(8), 490-497.

Raina, J. B., Dinsdale, E. A., Willis, B. L., & Bourne, D. G. (2010). Do the organic sulfur compounds DMSP and DMS drive coral microbial associations?. *Trends in microbiology*, *18*(3), 101-108.

Raina, J. B., Tapiolas, D. M., Forêt, S., Lutz, A., Abrego, D., Ceh, J., ... & Motti, C. A. (2013). DMSP biosynthesis by an animal and its role in coral thermal stress response. *Nature*, *502*(7473), 677-680.

Ribes, M., Jiménez, E., Yahel, G., López-Sendino, P., Díez, B., Massana, R., ... & Coma, R. (2012). Functional convergence of microbes associated with temperate marine sponges. *Environmental Microbiology*, *14*(5), 1224-1239.

Ribes, M., Dziallas, C., Coma, R., & Riemann, L. (2015). Microbial diversity and putative diazotrophy in high-and low-microbial-abundance Mediterranean sponges. *Applied and Environmental Microbiology*, *81*(17), 5683-5693.

Robbins, S. J., Singleton, C. M., Chan, C. X., Messer, L. F., Geers, A. U., Ying, H., ... & Bourne, D. G. (2019). A genomic view of the reef-building coral Porites lutea and its microbial symbionts. *Nature microbiology*, *4*(12), 2090-2100.

Rohde, S., Nietzer, S., & Schupp, P. J. (2015). Prevalence and mechanisms of dynamic chemical defenses in tropical sponges. *PloS one*, *10*(7), e0132236.

Rohwer, F., Seguritan, V., Azam, F., & Knowlton, N. (2002). Diversity and distribution of coral-associated bacteria. *Marine Ecology Progress Series*, *243*, 1-10.

Rosa, R., Marques, A., & Nunes, M. L. (2012). Impact of climate change in Mediterranean aquaculture. *Reviews in Aquaculture*, *4*(3), 163-177.

Saha, M., & Weinberger, F. (2019). Microbial “gardening” by a seaweed holobiont: surface metabolites attract protective and deter pathogenic epibacterial settlement. *Journal of Ecology*, *107*(5), 2255-2265.

Schaechter, M., Kolter, R., & Buckley, M. (2004). Microbiology in the 21st century: where are we and where are we going?.

Schiffer, J. M., Mael, L. E., Prather, K. A., Amaro, R. E., & Grassian, V. H. (2018). Sea spray aerosol: where marine biology meets atmospheric chemistry. *ACS central science*, *4*(12), 1617-1623.

Schippers, A., Neretin, L. N., Kallmeyer, J., Ferdelman, T. G., Cragg, B. A., Parkes, R. J., & Jørgensen, B. B. (2005). Prokaryotic cells of the deep sub-seafloor biosphere identified as living bacteria. *Nature*, *433*(7028), 861-864.

Schlaeppi, K., & Bulgarelli, D. (2015). The plant microbiome at work. *Molecular Plant-microbe interactions*, *28*(3), 212-217.

Schmitt, S., Weisz, J. B., Lindquist, N., & Hentschel, U. (2007). Vertical transmission of a phylogenetically complex microbial consortium in the viviparous sponge Ircinia felix. *Applied and Environmental Microbiology*, *73*(7), 2067-2078.

Schmitt, S., Angermeier, H., Schiller, R., Lindquist, N., & Hentschel, U. (2008). Molecular microbial diversity survey of sponge reproductive stages and mechanistic insights into vertical transmission of microbial symbionts. *Applied and Environmental Microbiology*, *74*(24), 7694-7708.

Sehnal, L., Brammer-Robbins, E., Wormington, A. M., Blaha, L., Bisesi, J., Larkin, I., ... & Adamovsky, O. (2021). Microbiome composition and function in aquatic vertebrates: small organisms making big impacts on aquatic animal health. *Frontiers in microbiology*, *12*, 358.

Shade, A., & Handelsman, J. (2012). Beyond the Venn diagram: the hunt for a core microbiome. *Environmental microbiology*, *14*(1), 4-12.

Shade, A., Caporaso, J. G., Handelsman, J., Knight, R., & Fierer, N. (2013). A meta-analysis of changes in bacterial and archaeal communities with time. *The ISME journal*, *7*(8), 1493-1506.

Siboni, N., Ben-Dov, E., Sivan, A., & Kushmaro, A. (2008). Global distribution and diversity of coral-associated Archaea and their possible role in the coral holobiont nitrogen cycle. *Environmental Microbiology*, *10*(11), 2979-2990.

Simon, J. C., Marchesi, J. R., Mougel, C., & Selosse, M. A. (2019). Host-microbiota interactions: from holobiont theory to analysis. *Microbiome*, *7*(1), 1-5.

Slaby, B. M., Hackl, T., Horn, H., Bayer, K., & Hentschel, U. (2017). Metagenomic binning of a marine sponge microbiome reveals unity in defense but metabolic specialization. *The ISME journal*, *11*(11), 2465-2478.

Stat, M., Carter, D., & Hoegh-Guldberg, O. (2006). The evolutionary history of Symbiodinium and scleractinian hosts—symbiosis, diversity, and the effect of climate change. *Perspectives in Plant Ecology, Evolution and Systematics*, *8*(1), 23-43.

Steinert, G., Taylor, M. W., Deines, P., Simister, R. L., De Voogd, N. J., Hoggard, M., & Schupp, P. J. (2016). In four shallow and mesophotic tropical reef sponges from Guam the microbial community largely depends on host identity. *PeerJ*, *4*, e1936.

Steinert, G., Rohde, S., Janussen, D., Blaurock, C., & Schupp, P. J. (2017). Host-specific assembly of sponge-associated prokaryotes at high taxonomic ranks. *Scientific reports*, *7*(1), 1-9.

Sunagawa, S., Coelho, L. P., Chaffron, S., Kultima, J. R., Labadie, K., Salazar, G., ... & Velayoudon, D. (2015). Structure and function of the global ocean microbiome. *Science*, *348*(6237), 1261359.

Taylor, M. W., Radax, R., Steger, D., & Wagner, M. (2007). Sponge-associated microorganisms: evolution, ecology, and biotechnological potential. *Microbiology and molecular biology reviews*, *71*(2), 295-347.

Thomas, T., Rusch, D., DeMaere, M. Z., Yung, P. Y., Lewis, M., Halpern, A., ... & Kjelleberg, S. (2010). Functional genomic signatures of sponge bacteria reveal unique and shared features of symbiosis. *The ISME journal*, *4*(12), 1557-1567.

Vanwonterghem, I., & Webster, N. S. (2020). Coral reef microorganisms in a changing climate. *Iscience*, *23*(4), 100972.

Wallin, I. E. (1925). On the nature of mitochondria. IX. Demonstration of the bacterial nature of mitochondria. *American Journal of Anatomy*, *36*(1), 131-149.

Webster, N. S., Taylor, M. W., Behnam, F., Lücker, S., Rattei, T., Whalan, S., ... & Wagner, M. (2010). Deep sequencing reveals exceptional diversity and modes of transmission for bacterial sponge symbionts. *Environmental Microbiology*, *12*(8), 2070-2082.

Webster, N. S., & Thomas, T. (2016). The sponge hologenome. *MBio*, *7*(2), e00135-16.

Webster, N. S., & Reusch, T. B. (2017). Microbial contributions to the persistence of coral reefs. *The ISME journal*, *11*(10), 2167-2174.

Weigel, B. L., & Erwin, P. M. (2017). Effects of reciprocal transplantation on the microbiome and putative nitrogen

cycling functions of the intertidal sponge, Hymeniacidon heliophila. *Scientific Reports*, *7*(1), 1-12.

Whipps JM, In: *Fungi Biol Control Syst.* Burge N, editor. Manchester: Manchester University Press; 1988. Mycoparasitism and plant disease control. pp. 161–187.

Whitman, W. B., Coleman, D. C., & Wiebe, W. J. (1998). Prokaryotes: the unseen majority. *Proceedings of the National Academy of Sciences*, *95*(12), 6578-6583.

Wilson, M. C., Mori, T., Rückert, C., Uria, A. R., Helf, M. J., Takada, K., ... & Piel, J. (2014). An environmental bacterial taxon with a large and distinct metabolic repertoire. *Nature*, *506*(7486), 58-62.

Zacharias, M. A., & Roff, J. C. (2001). Use of focal species in marine conservation and management: a review and critique. *Aquatic conservation: marine and freshwater ecosystems*, *11*(1), 59-76.

Zhang, F., Vicente, J., & Hill, R. T. (2014). Temporal changes in the diazotrophic bacterial communities associated with Caribbean sponges Ircinia stroblina and Mycale laxissima. *Frontiers in microbiology*, *5*, 561.

Zhang, F., Blasiak, L. C., Karolin, J. O., Powell, R. J., Geddes, C. D., & Hill, R. T. (2015). Phosphorus sequestration in the form of polyphosphate by microbial symbionts in marine sponges. *Proceedings of the National Academy of Sciences*, *112*(14), 4381-4386.

CHAPTER 2 - THE STUDY OF MICROBIOMES ASSOCIATED WITH MARINE HOLOBIONTS IN THE PRESENTED THESIS

2.1 Holobionts models and study plan in the proposed research

There is a general lack of knowledge in the understanding of how host-associated microbes drive both the initial response as well as long-term, evolutionary adaptation to different anthropogenic stressors. First, microbial variability that might be able to confer adverse or beneficial outcomes for the host can be due to natural variability or selective pressure. Although this variability could be described by population genetics, basic ecological information is lacking for all but a few species (Taylor and Roterman, 2017). Also, temporal scales suitable for most research are usually not sufficient for understanding processes of acclimatization and adaptation that may occur over longer periods of time (Bénard et al., 2020). Furthermore, holobiont responses to stressors might be partly shaped by pre-existing environmental conditions or by previous generations, although that information is rarely considered or available (Leray et al., 2021). Finally, the understanding of how microbiomes genomic variations might contribute to host acclimatization and adaptation is limited due to a general lack of information coupling host and microbial genomes and variations at the individual level (Geier et al., 2020).

In order to deepen our knowledge on the influence of anthropogenic stressors on host-microbiome short-term responses and long-term evolutionary processes, here we propose different study models. All models take into account ecologically important, widely distributed, and habitat-forming organisms. Amongst them, the study of Cnidaria has gained increasing importance due to the growing awareness of their vulnerability to anthropogenic stressors, with cascade effects at the ecosystem level (Gerhardt, 2002; Rocha et al., 2014). This awareness highlighted the possible importance of Cnidaria microbiomes as a determinant of their adaptive response to climate-related and anthropogenic-induced stressors already impacting the ocean environment (Apprill, 2017), making the study of Cnidarians microbiomes, and its variations, a crucial point at the conjunction between animal and environmental health. In this context, we first aim at providing basic knowledge on the microbial community structure of the jewel anemone *Corynactis viridis*, a non-coral Cnidaria belonging to the order Corallimorpharia, and on its possible role in host physiology and health, as a model organism. In order to investigate possible short-term plastic responses in marine holobionts as a driver of selection for acclimatization, we exploit another model organism belonging to Cnidaria, namely the common sea anemone *Anemonia viridis*. This is a marine holobiont widely distributed across the world's oceans and has been recognized as a key member of marine ecosystems, playing several crucial roles in marine food webs and habitat structuring (Boero et al., 2005; Bosch, 2013; Coker et al., 2014). As second model to assess the impact of anthropogenic activities and, in particular, of fish farming cages on the microbiome of the surrounding wild holobionts, we select a common grazer gastropod from the genus Patella as a representative fouling holobiont. *Patella caerulea* is a common seaweed grazing marine limpet in all Mediterranean rocky shores (Della Santina and Chelazzi, 1991). As a result of their wide distribution, abundance, and sedentary lifestyle, limpets of this species have been proposed as biomonitors for the local water quality in terms of heavy metal accumulation and organic pollutants (Reguera et al., 2018; Viñas et al., 2018). In addition, limpets are considered keystone species for the coastal ecosystem because they can regulate the degree of algal coverage and, consequently, succession processes in rocky intertidal

communities (Coleman et al., 2006). Finally, we focus on possible long-term evolutionary responses to future oceanic scenarios by exploring coral microbiome variations in a coral population naturally living along a pH gradient generated by an underwater volcanic crater. We target the solitary, widespread, Mediterranean coral *Balanophyllia europaea* (Goffredo et al., 2007) as a study model because temperate species, compared to tropical and subtropical corals, might represent a winning model for more pronounced acclimatization capability, being exposed to a twice as high range of seasonal temperature fluctuations and intrinsically more capable to accommodate environmental variations (Maor-Landaw et al., 2017).

2.2 Technical aspects: sampling and molecular analysis

In order to avoid redundancy in the next paragraphs, common techniques which were repeatedly used throughout different studies are illustrated in this section. In the "Materials and methods" section of each study, only a brief recall of the appropriate protocol is mentioned, with the indication to look in this section for further details. Only techniques that are particular of a specific study are not illustrated here, but in the correspondent study.

Sample collection and DNA extraction

Specimen collection is very different depending on the sample origin and type. Sterility is preserved at the best of the sampling conditions by using sterile containers or previously sterilized tools. After specimen collection, all samples are transported to the laboratory as fast as possible where they are kept at -80 °C until further processing, unless some preliminary step is required before freezing.

Total microbial DNA extraction protocols are also dependent on the sample origin and type. Despite these differences, all the DNA extraction methods described in this thesis rely on Qiagen (Hilden, Germany) spin column-based nucleic acid purification kits. Extracted DNA samples are quantified with NanoDrop ND-1000 (NanoDrop Technologies, Wilmington, DE) and stored at -20 °C until further processing.

16S rRNA gene amplification and sequencing

Targeted gene sequencing is performed on the V3-V4 hypervariable region of the 16S rRNA gene. PCR amplification of this region is carried out in a 50-µL final volume containing 25 ng of microbial DNA, 2X KAPA HiFi HotStart ReadyMix (Roche, Basel, Switzerland), and 200 nmol/L of 341F and 785R primers carrying Illumina overhang adapter sequences. The thermal cycle consists of 3 min at 95°C, 30 cycles of 30 s at 95°C, 30 s at 55°C, and 30 s at 72°C, and a final 5-min step at 72°C (Biagi et al., 2020; Musella et al., 2020). PCR products are purified with Agencourt AMPure XP magnetic beads (Beckman Coulter, Brea, CA). Indexed libraries are prepared by limited-cycle PCR with Nextera technology and cleaned-up as above. Libraries are normalized to 4 nM and pooled. The sample pool is denatured with 0.2 N NaOH and diluted to a final concentration of 6 pM with a 20% PhiX control. Sequencing is performed on an Illumina MiSeq platform using a 2 × 250 bp paired-end protocol, according to the manufacturer's instructions (Illumina, San Diego, CA).

Bioinformatics and biostatistics

A pipeline combining PANDAseq (Masella et al., 2012) and QIIME 2 (Bolyen et al., 2019) is used to process raw sequences. The "fastq filter" function of the Usearch11 algorithm (Edgar, 2010) is applied to retain high-quality reads (min/max length = 350/550 bp), that are then binned into amplicon sequence variants (ASVs) using DADA2 (Callahan et al., 2016). Taxonomy assignment was performed using the VSEARCH algorithm (Rognes et al., 2016) and the SILVA database (December 2017 release) (Quast et al., 2012). All the sequences assigned to eukaryotes (i.e., chloroplasts and mitochondria) or unassigned are discarded. Different metrics, depending on the dataset, are used to evaluate alpha diversity, whereas beta diversity is estimated by computing the unweighted UniFrac distance.

All statistical analyses are performed using the R software[6] (R Core Team), version 3.6.1., with the packages "Made4" (Culhane et al., 2005) and "vegan"[7]. When unweighted UniFrac distances are plotted using the vegan package, the data separation in the Principal Coordinates Analysis (PCoA) is tested using a permutation test with pseudo-F ratios (function "adonis" in the vegan package). Significant data separation was assessed by Kruskal–Wallis test or Wilcoxon rank-sum test, based on the data. When necessary, *p*-values were corrected for multiple testing with Benjamini-Hochberg method, with a false discovery rate (FDR) ≤ 0.05 considered as statistically significant.

References

Apprill, A. (2017). Marine animal microbiomes: toward understanding host–microbiome interactions in a changing ocean. *Front. Mar. Sci.* 4:222. doi: 10.3389/fmars.2017.00222

Bénard, A., Vavre, F., & Kremer, N. (2020). Stress & Symbiosis: Heads or Tails?. *Frontiers in Ecology and Evolution*, *8*, 167.

Biagi, E., Caroselli, E., Barone, M., Pezzimenti, M., Teixido, N., Soverini, M., ... & Candela, M. (2020). Patterns in microbiome composition differ with ocean acidification in anatomic compartments of the Mediterranean coral Astroides calycularis living at CO2 vents. *Science of The Total Environment*, *724*, 138048.

Boero, F., Bouillon, J., & Piraino, S. (2005). The role of Cnidaria in evolution and ecology. *Italian Journal of Zoology*, *72*(1), 65-71.

Bolyen, E., Rideout, J. R., Dillon, M. R., Bokulich, N. A., Abnet, C. C., Al-Ghalith, G. A., ... & Caporaso, J. G. (2019). Reproducible, interactive, scalable and extensible microbiome data science using QIIME 2. *Nature biotechnology*, *37*(8), 852-857.

Bosch, T. C. (2013). Cnidarian-microbe interactions and the origin of innate immunity in metazoans. *Annual review of microbiology*, *67*, 499-518.

Callahan, B. J., McMurdie, P. J., Rosen, M. J., Han, A. W., & Johnson, A. (2016). JA, Holmes SP. 2016. *DADA2: high-resolution sample inference from Illumina amplicon data. Nature Methods*, *13*(7), 581-583.

Coleman, R. A., Underwood, A. J., Benedetti-Cecchi, L., Åberg, P., Arenas, F., Arrontes, J., ... & Hawkins, S. J. (2006). A continental scale evaluation of the role of limpet grazing on rocky shores. *Oecologia*, *147*(3), 556-564.

Coker, D. J., Wilson, S. K., & Pratchett, M. S. (2014). Importance of live coral habitat for reef fishes. *Reviews in Fish Biology and Fisheries*, *24*(1), 89-126.

Culhane, A. C., Thioulouse, J., Perrière, G., & Higgins, D. G. (2005). MADE4: an R package for multivariate analysis of gene expression data. *Bioinformatics*, *21*(11), 2789-2790.

Della Santina, P., & Chelazzi, G. (1991). Temporal organization of foraging in two Mediterranean limpets, Patella rustica L. and P. coerulea L. *Journal of experimental marine biology and ecology*, *153*(1), 75-85.

Edgar, R. C. (2010). Search and clustering orders of magnitude faster than BLAST. *Bioinformatics*, *26*(19), 2460-2461.

Geier, B., Sogin, E. M., Michellod, D., Janda, M., Kompauer, M., Spengler, B., ... & Liebeke, M. (2020). Spatial metabolomics of in situ host–microbe interactions at the micrometre scale. *Nature Microbiology*, *5*(3), 498-510.

[6] https://www.R-project.org; 2013

[7] https://cran.r-project.org/web/packages/vegan/index.html

Gerhardt, A. (2002). Bioindicator species and their use in biomonitoring. *Environ. Monit.* 1, 77–123.

Goffredo, S., Caroselli, E., Pignotti, E., Mattioli, G., & Zaccanti, F. (2007). Variation in biometry and population density of solitary corals with environmental factors in the Mediterranean Sea. *Marine biology, 152*, 351–361.

Masella, A. P., Bartram, A. K., Truszkowski, J. M., Brown, D. G., & Neufeld, J. D. (2012). PANDAseq: paired-end assembler for illumina sequences. *BMC bioinformatics*, *13*(1), 1-7.

Leray, M., Wilkins, L. G., Apprill, A., Bik, H. M., Clever, F., Connolly, S. R., ... & Eisen, J. A. (2021). Natural experiments and long-term monitoring are critical to understand and predict marine host–microbe ecology and evolution. *PLoS biology*, *19*(8), e3001322.

Maor-Landaw, K., Ben-Asher, H. W., Karako-Lampert, S., Salmon-Divon, M., Prada, F., Caroselli, E., ... & Levy, O. (2017). Mediterranean versus Red sea corals facing climate change, a transcriptome analysis. *Scientific reports*, *7*(1), 1-8.

Musella, M., Wathsala, R., Tavella, T., Rampelli, S., Barone, M., Palladino, G., ... & Candela, M. (2020). Tissue-scale microbiota of the Mediterranean mussel (Mytilus galloprovincialis) and its relationship with the environment. *Science of The Total Environment*, *717*, 137209.

Quast, C., Pruesse, E., Yilmaz, P., Gerken, J., Schweer, T., Yarza, P., Peplies, J., & Glöckner, F. O. (2012). The SILVA ribosomal RNA gene database project: improved data processing and web-based tools. *Nucleic acids research, 41*(D1), D590-D596.

Reguera, P., Couceiro, L., & Fernández, N. (2018). A review of the empirical literature on the use of limpets Patella spp. (Mollusca: Gastropoda) as bioindicators of environmental quality. *Ecotoxicology and environmental safety*, *148*, 593-600.

Rocha, J., Coelho, F. J., Peixe, L., Gomes, N. C., and Calado, R. (2014). Optimization of preservation and processing of sea anemones for microbial community analysis using molecular tools. *Sci. Rep.* 4:6986. doi: 10.1038/srep06986

Rognes, T., Flouri, T., Nichols, B., Quince, C., & Mahé, F. (2016). VSEARCH: a versatile open source tool for metagenomics. *PeerJ*, *4*, e2584.

Taylor, M. L., & Roterman, C. N. (2017). Invertebrate population genetics across Earth's largest habitat: The deep-sea floor. *Molecular Ecology*, *26*(19), 4872-4896.

Viñas, L., Pérez-Fernández, B., Soriano, J. A., López, M., Bargiela, J., & Alves, I. (2018). Limpet (Patella sp) as a biomonitor for organic pollutants. A proxy for mussel?. *Marine pollution bulletin*, *133*, 271-280.

2.3 Study I — Seasonal changes in microbial communities associated with the jewel anemone *Corynactis viridis*

Introduction

The Cnidaria are a large, diverse, and ecologically important group of organisms that are widely distributed in marine environments, where they represent important habitat-forming organisms (Marzinelli et al., 2018). The study of Cnidaria have gained increasing importance in recent years due to the growing awareness of their vulnerability to anthropogenic stressors, with obvious cascade impacts at the ecosystem level (Gerhardt, 2002; Rocha et al., 2014). As all marine animals, Cnidarians live as "holobionts," as a result of a close interaction with a complex microbial community (O'Brien et al., 2019), defined as microbiome (Berg et al., 2020). The "holobionts" microbiomes are inherent to the host physiology, being capable of providing the host with ecological functions crucial for its health (Pita et al., 2018). Particularly, several studies aimed at characterizing Cnidaria-associated microbes are now available, providing important information on their role in nutrition, defense, immunity and development (Littman et al., 2009; Liu et al., 2018; Pollock et al., 2018; Ziegler et al., 2019). This awareness also highlighted the possible importance of the Cnidaria microbiomes as a determinant of their adaptive or maladaptive response to stressors, including growing climate-related and anthropogenic-induced stressors already impacting the ocean environment (Apprill, 2017). Indeed, it has been proposed that variations in Cnidaria microbiome can be employed as early bio-indicator of both environmental and anthropogenic stressors (Stabili et al., 2018), making the study of Cnidarians microbiomes, and its variations, a crucial point at the conjunction between animal and environmental health. However, the vast majority of the studies on Cnidaria microbiomes are focused on corals, with a lack of information on all the other organisms belonging to this phylum. To the best of our knowledge, only a limited number of pioneering studies on non-coral Cnidaria have been performed (Di Camillo et al., 2012; Har et al., 2015; Murray et al., 2016; Brown et al., 2017) and no studies have been conducted to describe the microbes associated with Corallimorpharia, non-calcifying, close relatives of scleractinian corals (Lin et al., 2016). Although scleractinian corals are the most important reef builders, Corallimorpharia can also be extensively found on reefs either as solitary individuals or as colonies that may carpet vast reef areas, where they can exert important roles as habitat forming halobionts, being at the base of complex trophic chains (Kuguru et al., 2004). It is thus important to fill this knowledge gap, providing basic knowledge on the structure of the Corallimorpharia microbiome and on its possible role in host physiology and health. In this scenario, we aim to investigate the community structure, and its seasonal variations, of the microbes associated with the jewel anemone *Corynactis viridis*, an anthozoan Cnidaria belonging to the order Corallimorpharia. *C. viridis* is a brightly colored marine invertebrate similar in body form to a sea anemone. Its typical habitat encompasses the northeastern Atlantic Ocean, including Scotland, Ireland, and the southern and western coasts of Great Britain, the southwestern coasts of continental Europe and the Mediterranean Sea. It is found on rocks, caves or beneath overhangs sheltered from the light forming dense aggregations, and its depth range goes from the lower shore down to about 80 m (Hill and White, 2008). Specifically, in our work, we characterize the microbial communities associated with *C. viridis* from 30 individuals collected in three different seasons (winter 2018, spring and summer 2019) by next-generation sequencing (NGS) of the V3-V4 region of the 16S rRNA gene. According to our

data *C. viridis* possesses a characteristic associated microbiome whose inherent plasticity is possibly functional for the adaptation to seasonal changes.

Materials and methods

Sample collection and DNA extraction

Corynactis viridis individuals were collected at the "Il Paguro" site by the diving association "Dive Planet" (Rimini, Italy). "Il Paguro" is the wreck of a methane extraction platform located around 12 nautical miles offshore Ravenna, Italy. The wreck extends from a depth of 10 m in its most superficial part to 35 m, and it hosts a great variety of marine wildlife. In order to regulate the scuba activity on the site and preserve its coral reef-like ecosystem, an Italian association responsible for the site ("Associazione Paguro") has been established and, starting from July the 21st, 1995, the area was declared "Area of biological protection" by the Italian Ministry of Agricultural Resources. In February 2010, "Il Paguro" was declared "Site of community interest" by the Emilia-Romagna region (Rinaldi and Rambelli, 2004). "Associazione Paguro" kindly provided permission to sample *C. viridis* within the "Il Paguro" site for scientific purposes only and Italian Cost Guard was made aware of the sampling activity. We used satellite maps from NASA[8] to provide some data on the main environmental variables of the sampling site, including temperature and chlorophyll a to evidence eutrophication occurrence (Ignatiades, 2005). Ten anemone individuals were collected at three different time points in December 2018 (winter sampling), May 2019 (spring sampling) and July 2019 (summer sampling), for a total of 30 individuals (Supplementary Figure S1). For each site, 2 L of seawater were also sampled at the same depth as the anemones, by using previously sterilized polypropylene bottles. Anemones were collected using knives previously sterilized with alcohol, by placing 1–3 rocks hosting different individuals in sterile disposable plastic containers to avoid contamination. The picking of anemones from the respective rocks was performed once returned to the laboratory (within a few hours of sampling at sea), under a vertical laminar airflow cabinet using sterile tweezers and scalpels. Each individual was placed in a single 1.5-mL microtube and stored at −80°C until further processing. Seawater samples were filtered using vacuum filtration with MF-Millipore (Darmstadt, Germany) Membrane filters with 0.45-µm pore size, 47-mm diameter and mixed cellulose esters membrane. Each 2 L sample of seawater was filtered on a single filter, which was rolled on itself using sterilized forceps and placed in a 2-mL microtube, then stored at −80°C until further processing.

Total microbial DNA extraction was performed for each whole individual anemone (weighing approximately 0.15–0.20 g) using the DNeasy PowerBiofilm Kit (Qiagen, Hilden, Germany), whereas seawater microbial DNA extraction was carried out using the DNeasy PowerWater Kit (Qiagen). DNA samples were quantified using NanoDrop ND-1000 (NanoDrop Technologies, Wilmington, DE, United States) and stored at -20°C until further processing.

16S rRNA gene amplification and sequencing

Amplification of the V3-V4 hypervariable region of the 16S rRNA gene, PCR purification and sequencing library preparation were performed as described in paragraph 2.2. Sequencing was performed on Illumina

[8] https://giovanni.gsfc.nasa.gov/giovanni/. Accessed 10 Jan 2021.

MiSeq platform using a 2 × 250 bp paired end protocol, according to the manufacturer's instructions (Illumina, San Diego, CA, United States).

Bioinformatics and statistics

Raw sequences were processed as described in paragraph 2.2. The resulting ASV table was rarefied up to 1733 reads per sample, corresponding to the lowest read number observed among the samples. Alpha diversity was evaluated using Faith's Phylogenetic Diversity (PD_whole_tree) (Faith, 1992), Chao1 index for microbial richness and number of observed ASVs. The unweighted UniFrac distance was used to build Principal Coordinates Analysis (PCoA) plots.

Statistical analysis was performed using R software version 3.6.1[9]. PCoA, bacterial co-abundance groups (CAGs), box-and-whisker plots and Venn diagrams were generated using "Stats[10]", "Made4" (Culhane et al., 2005), "vegan[11]", "boxplot" (Murrell, 2018) and "VennDiagram[12]" packages. Unweighted UniFrac distance was used for PCoA, and the significance of separation was tested by permutation test with pseudo F-ratio (function "Adonis" in "vegan"). Bacterial groups with the largest contribution to the ordination space were found by using the function envfit of the R package vegan on the family relative abundances. Significant data separation was assessed by Kruskal–Wallis test or Wilcoxon rank-sum test, based on the data. When necessary, *p*-values were corrected for multiple testing with Benjamini-Hochberg method (see paragraph 2.2).

For graphical representation, anemone bacterial phyla whose relative abundance was less than 0.5% in at least 10% of the samples were filtered out under the name "other phyla." The same was done for microbial families and genera with a relative abundance lower than 2% in at least 10% of the samples ("other families" and "other genera," respectively). For the generation of CAGs, only bacterial genera present in at least 10% of the samples with relative abundance ≥ 0.5% were considered. Co-abundance was evaluated by the Kendall correlation test and displayed with hierarchical Ward-linkage clustering based on the Spearman correlation coefficient (Claesson et al., 2012). Wiggum plot networks were created using Cytoscape[13] software (Smoot et al., 2011), where the circle size represents the bacterial abundance and the connections between nodes represent significant Kendall correlations between genera (FDR ≤ 0.05). For Venn diagrams, the ASVs present in at least one sample of each season group were taken into account. We processed all the 4,623 ASVs obtained from DADA2 binning of high-quality reads through the R package VennDiagram, in order to produce a visual output of the ASVs sharing between seasons. The FASTA files of the ASV sequences shared between all seasons or couples of seasons were blasted against the 16S rRNA database through BLASTN algorithm (Altschul et al., 1990).

Results

C. viridis and seawater microbiota

A total of 30 individuals of *C. viridis* were sampled in three different seasons in December 2018 (winter), May 2019 (spring) and July 2019 (summer) at the "Il Paguro" site in the North Adriatic Sea. The monthly

[9] https://www.r-project.org/
[10] https://cran.r-project.org/web/packages/STAT/index.html
[11] https://cran.r-project.org/web/packages/vegan/index.html
[12] https://cran.r-project.org/web/packages/VennDiagram/index.html
[13] http://www.cytoscape.org/

satellite maps of temperature and surface chlorophyll a from NASA for each sampling period are provided in Supplementary Figure S2. Briefly, seawater temperature during the three sampling times variated between 10–12°C in winter, 15–17°C in spring, and 26–28°C in summer. Chlorophyll a concentration was always > 2 mg/m3 (ranging between 2.2 and 3.6), classifying the sampling region as eutrophic (Ignatiades, 2005; Ferreira et al., 2011). For each time point, 10 individuals and 2 L of seawater were collected at a depth of 20 m. From each sample, the microbiome compositional structure was obtained by NGS sequencing of the V3–V4 hypervariable region of the 16S rRNA gene, resulting in 252,160 high-quality reads and an average of 7,641.212 ± 5,177.348 (mean ± SD) reads per sample. High-quality reads were binned into 4,623 ASVs.

At first, we compared the alpha diversity between *C. viridis* and seawater communities. Although not significant, our data show a trend toward an overall higher microbial richness in seawater than in anemone, as measured by Chao1 metrics and number of observed ASV (Wilcoxon rank-sum test controlled for multiple testing using FDR, *p*-value > 0.05) (Supplementary Figure S3).

We next explored the community composition in *C. viridis* and seawater at different phylogenetic levels (Figure 5). At the phylum level, the *C. viridis* microbiota is characterized by five dominant phyla, Proteobacteria (mean relative abundance ± SD, 35.3 ± 14.4%), Firmicutes (15.3 ± 20.8%), Tenericutes (15.3 ± 21.3%), Planctomycetes (10.3 ± 8.4%) and Bacteroidetes (10.0 ± 9.1%). Less abundant phyla are represented by Actinobacteria (4.0 ± 4.3%), Cyanobacteria (2.7 ± 4.4%), Verrucomicrobia (1.9 ± 1.6%) and Chloroflexi (1.7 ± 2.2%). The most represented families are *Spiroplasmataceae* (15.2 ± 21.3%), *Planctomycetaceae* (9.8 ± 8.1%) and *Rhodobacteraceae* (7.1 ± 5.5%). Subdominant families are *Flavobacteriaceae* (4.5 ± 3.0%), Clostridiales family XII (2.9 ± 5.0%), *Vibrionaceae* (2.9 ± 3.8%) and *Clostridiaceae* (2.5 ± 4.0%). At the genus level, the dominant taxon is *Spiroplasma* (15.2 ± 21.3%), while less represented genera are *Fusibacter* (2.9 ± 5.0%), *Blastopirellula* (2.5 ± 2.6%) and Pir4 lineage (2.5 ± 3.5%). On the other hand, seawater shows a distinct microbial structure already at the phylum level, being dominated by Proteobacteria (57.1 ± 0.75), Bacteroidetes (19.6 ± 2.3%), Cyanobacteria (7.6 ± 2.7%) and Verrucomicrobia (6.2 ± 2.8%), with Planctomycetes (2.6 ± 2.2%), Actinobacteria (2.5 ± 2.5%) and Firmicutes (1.6 ± 2.8%) as subdominant taxa. The most represented families are *Flavobacteriaceae* (10.9 ± 3.3%), family I of Cyanobacteria subsection I (7.6 ± 2.8%) and *Rhodobacteraceae* (6.9 ± 2.9%), while *Halieaceae* (3.5 ± 3.8%), *Verrucomicrobiaceae* (3.0 ± 2.0%) and *Rhodospirillaceae* (3.0 ± 1.2%) are subdominant. *Synechococcus* (5.3 ± 5.3%) is the most abundant classified genus, while *Tenacibaculum* (2.5 ± 2.2%) the subdominant one.

In order to highlight the overall compositional differences between *C. viridis* and seawater microbial communities, a PCoA of the unweighted UniFrac distances was carried out. As expected, the *C. viridis* microbiome significantly segregates from that of seawater and such a segregation was found to be robust to seasonality (permutation test with pseudo-F ratio, *p*-value ≤ 0.01) (Supplementary Figure S4). To identify the bacterial families most contributing to the separation, their relative abundance was superimposed on the PCoA plots. According to our findings, the families *Planctomycetaceae*, *Spiroplasmataceae*, and Clostridiales family XII are the most characteristic of the *C. viridis* microbiome, but with a seasonality-specific pattern. Conversely, *Flavobacteriaceae* and family I of subsection I in the phylum Cyanobacteria are the most distinguishing of the seawater samples.

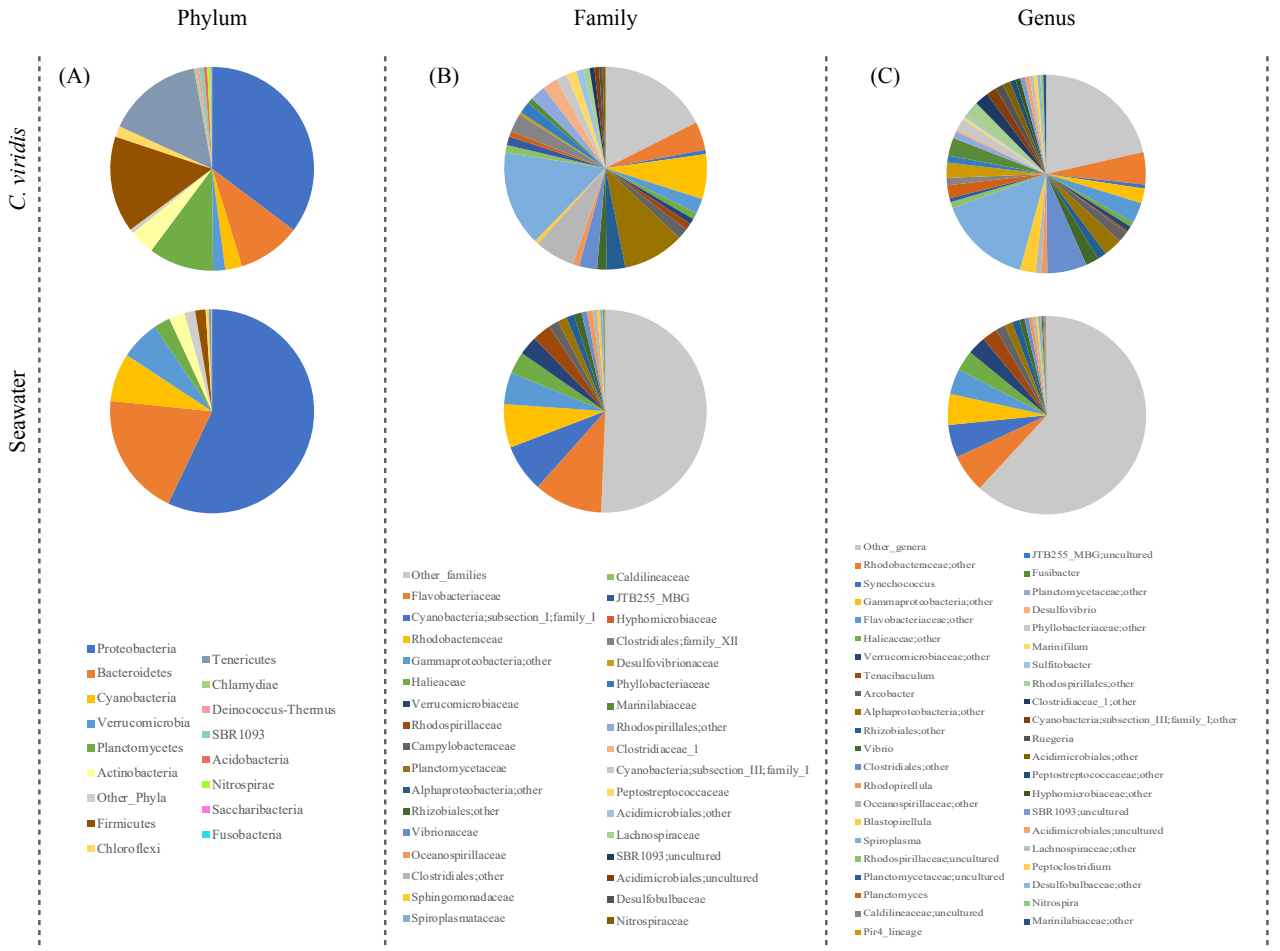

Figure 5 - Microbiota composition of *C. viridis* and seawater. Pie charts summarizing the phylum (A), family (B) and genus-level (C) microbiota composition of *C. viridis* and seawater. Only phyla with relative abundance > 0.5% in at least 10% of samples, and families and genera with relative abundance > 2% in at least 10% of samples are represented.

Seasonal trends in the *C. viridis* microbiome

We tested whether the *C. viridis*-associated microbial communities varied by season. To do this, we first assessed the existence of significant differences among seasons for alpha diversity. All metrics consistently indicated greater microbial diversity in winter and summer, compared to spring (Kruskal–Wallis test controlled for multiple testing using FDR, *p*-value ≤ 0.05) (Figure 6A). We next explored seasonal patterns in the community structure by analyzing beta diversity. Interestingly, the unweighted UniFrac-based PCoA revealed a sharp segregation of the microbiome structures through seasonality (permutation test with pseudo F-ratio, *p*-value ≤ 0.001) (Figure 6B). Conversely, seawater showed only a limited variation across the different seasons. When comparing the relative abundance of *C. viridis* microbial families among seasons (Figure 7), we found that during the winter, *Caldilineaceae*, *Nitrospiraceae*, and *Planctomycetaceae* were significantly more abundant, whereas the *Vibrionaceae* family was largely underrepresented. On the other hand, the spring samples were characterized by a higher proportion of the families *Rhodobacteraceae*, *Rhodospirillaceae*, *Campylobacteraceae*, *Oceanospirillaceae*, and *Spiroplasmataceae*. Finally, the relative abundance of *Marinilabiaceae*, family I of Cyanobacteria subsection III, *Clostridiaceae 1*, family XII of Clostridiales, *Lachnospiraceae*, *Peptostreptococcaceae*, *Desulfobulbaceae*, and *Desulfovibrionaceae* was significantly higher during the summer.

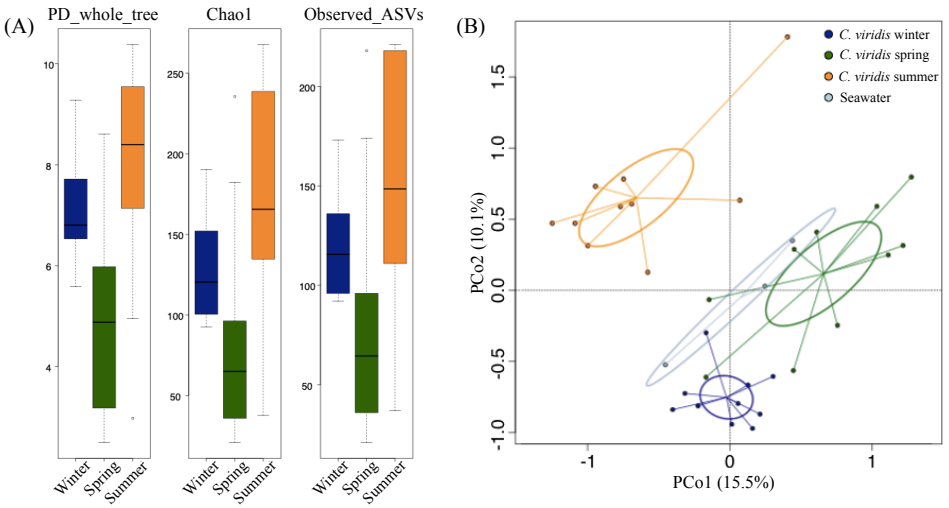

Figure 6 - Alpha and beta diversity of the *C. viridis* microbiota. (A) Box-and-whisker distribution of the Faith's Phylogenetic Diversity (PD_whole_tree), Chao1 index for microbial richness and number of observed ASVs, calculated for winter (dark blue), spring (dark green) and summer (orange) anemone samples. According to all metrics, greater microbial diversity was observed in winter and summer than in spring (Kruskal–Wallis test controlled for multiple testing using FDR, *p*-value ≤ 0.05). (B) Principal Coordinates Analysis (PCoA) based on unweighted UniFrac distances showing the variation of the anemone microbiota across seasons (same color code as in A) and seawater samples (light blue) (permutation test with pseudo F-ratio, *p*-value ≤ 0.001). The first and second principal components (PCo1 and PCo2) are plotted and the percentage of variance in the dataset explained by each axis is reported. Ellipses include 95% confidence area based on the standard error of the weighted average of sample coordinates.

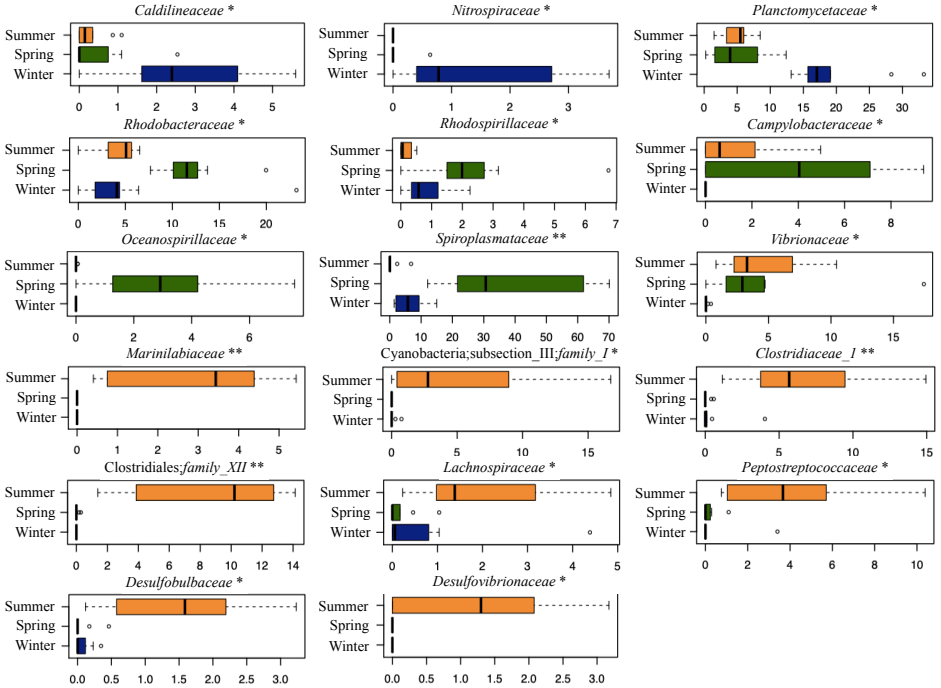

Figure 7 - *C. viridis*-associated bacterial families differently represented across seasons. Box-and-whisker plots showing the relative abundance distribution of bacterial families in the different seasons (winter, dark blue; spring, dark green; and summer, orange). The central box represents the distance between the 25th and 75th percentiles. The median is marked with a black line. Whiskers identify the 10th and 90th percentiles. ∗*p*-value ≤ 0.05; ∗∗*p*-value ≤ 0.01; Kruskal–Wallis test controlled for multiple testing using FDR.

To gain further insights into the *C. viridis*-associated microbiome, we explored its topological variation by clustering the bacterial genera into CAGs. Three CAGs were identified, and the prevalence and connections between the represented genera were obtained by a Wiggum plot network analysis (Supplementary Figure S5). Interestingly, we observed a peculiar declination of the *C. viridis* CAGs based on seasonality. CAGs were named according to the genus showing the higher overabundance in a seasonal-dependent pattern: "*Mycobacterium* CAG," "*Colwellia* CAG," and "*Desulfovibrio* CAG" (Figure 8). Winter communities were characterized by the "*Mycobacterium* CAG", which also included *Nitrospira*, *Planctomyces*, *Blastopirellula*, Pir4 lineage, OM60 (NOR5) clade and *Lysinibacillus*. Conversely, the "*Colwellia* CAG," including *Pseudoalteromonas*, *Aquibacter*, *Tenacibaculum*, *Spiroplasma*, *Vibrio*, *Sulfitobacter*, *Pseudofulvibacter*, and *Arcobacter*, dominated the spring microbiomes. Finally, the summer communities were characterized by the "*Desulfovibrio* CAG," including *Peptoclostridium*, *Marinifilum*, *Cetobacterium*, *Maribacter*, *Rhodopirellula*, *Fusibacter*, *Streptomyces*, and *Truepera*.

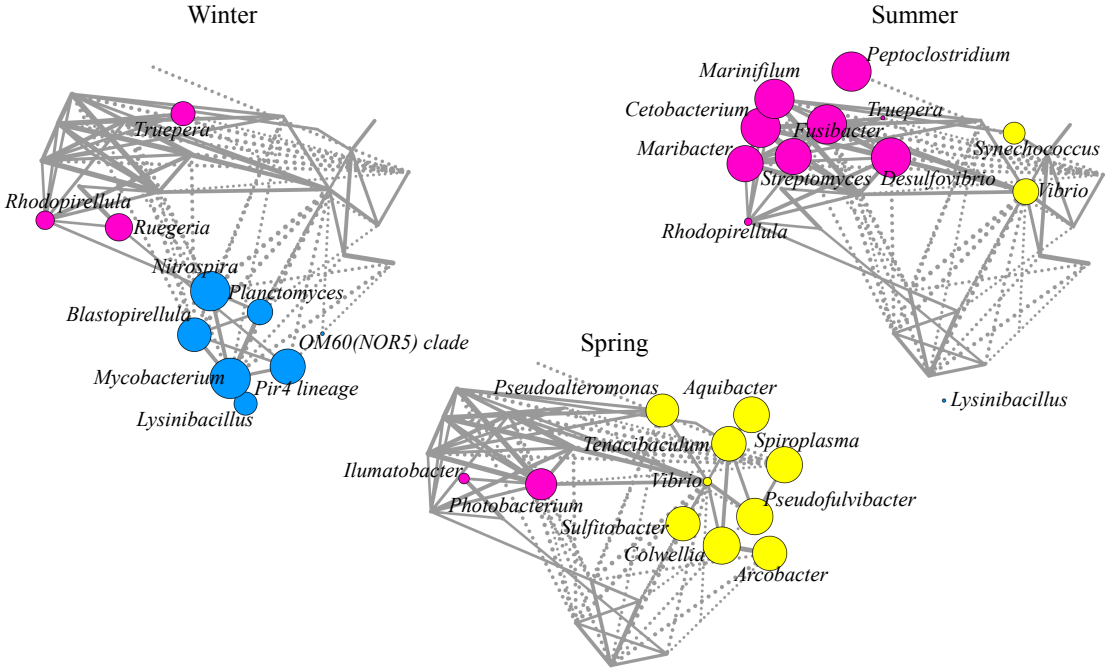

Figure 8 - Declination of *C. viridis* co-abundance groups according to seasonality. Co-abundance groups (CAGs) are named according to the dominant genus in each group: *Mycobacterium*, *Colwellia*, and *Desulfovibrio*. Each node represents a bacterial genus and its size is proportional to its overabundance on the average value within the population. The connections between nodes represent positive (solid lines) and negative (dashed lines) Kendall correlations between genera (FDR ≤ 0.05).

C. viridis core microbiome

Finally, we investigated whether *C. viridis* possesses a core microbiome, which is stably associated with the host and thus does not change with the seasons. As shown in Figure 9, only four ASVs were shared among all three seasons, whereas nine ASVs were shared between winter and spring samples, 18 ASVs between winter and summer samples, and seven ASVs between spring and summer samples, for a total of 38 shared ASVs in the three sampling seasons. According to a BLAST analysis, the four ASVs shared among the three seasons were all assigned to the bacterial family *Spiroplasmataceae* (Table 1). More detailed information on BLAST alignment for each ASV is provided in Supplementary Table S1.

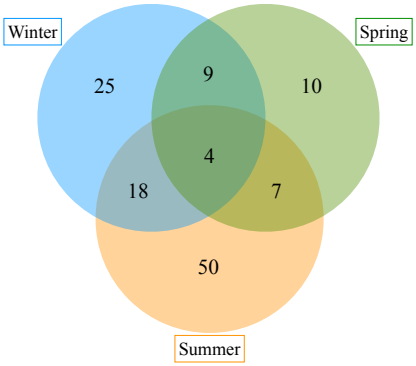

Figure 9 - ASVs sharing among *C. viridis* bacterial communities across seasons. Venn diagram showing the number of ASVs shared between the *C. viridis* bacterial communities in different seasons. Four ASVs are shared among all the three seasons, nine ASVs between winter and spring samples, 18 between winter and summer samples and seven between spring and summer samples.

Table 1 - ASVs sharing among *C. viridis*-associated microbial communities in winter, spring, and summer.

ASV no.	Family*	ASV no.	Family*
Winter-spring-summer shared ASVs		**Winter-summer shared ASVs**	
ASV_1	*Spiroplasmataceae*	ASV_14	*Xenococcaceae*
ASV_2	*Spiroplasmataceae*	ASV_15	*Planctomycetaceae*
ASV_3	*Spiroplasmataceae*	ASV_16	*Planctomycetaceae*
ASV_4	*Spiroplasmataceae*	ASV_17	*Rhodobacteraceae*
Winter-spring shared ASVs		ASV_18	*Mycoplasmataceae*
		ASV_19	*Flavobacteriaceae*
ASV_5	*Planctomycetaceae*	ASV_20	*Prochloraceae*
ASV_6	*Geminicoccaceae*	ASV_21	*Planctomycetaceae*
ASV_7	*Rhodobacteraceae*	ASV_22	*Ilumatobacteraceae*
ASV_8	*Phyllobacteriaceae*	ASV_23	*Thioprofundaceae*
ASV_9	*Nitrospiraceae*	ASV_24	*Flavobacteriaceae*
ASV_10	*Thiohalobacter*	ASV_25	*Flavobacteriaceae*
ASV_11	*Granulosicoccaceae*	ASV_26	*Sphingomonadaceae*
ASV_12	*Thiohalobacter*	ASV_27	*Nitrosomonadaceae*
ASV_13	*Veillonellaceae*	ASV_28	*Lachnospiraceae*
Spring-summer shared ASVs			*Defluviitaleaceae*
		ASV_29	*Flavobacteriaceae*
ASV_32	*Porphyromonadaceae*	ASV_30	*Planctomycetaceae*
ASV_33	*Vibrionaceae*	ASV_31	*Spirochaetaceae*
ASV_34	*Prochloraceae*		
ASV_35	*Planctomycetaceae*		
ASV_36	*Flavobacteriaceae*		
ASV_37	*Granulosicoccaceae*		
ASV_38	*Hyphomicrobiaceae*		
	Phyllobacteriaceae		

**The assignment is based on the BLASTN algorithm, taking into account the best hit for each corresponding ASV.*

Discussion

Given the fundamental role that microorganisms play in the functioning of eukaryotic hosts, investigating the diversity, community composition and seasonal changes of the host-associated microbial communities is crucial to understand the physiological significance of the association, also in light of anthropogenic threats. We show here that the microbial communities associated with *C. viridis* are unique and significantly different from those found in the surrounding seawater. In particular, *C. viridis* microbiome includes microorganisms belonging to nine main phyla, of which Proteobacteria, Firmicutes, Tenericutes, Planctomycetes, and Bacteroidetes are the dominant (relative abundance – r.a. – between 10 and 35%) and Actinobacteria, Cyanobacteria, Verrucomicrobia, and Chloroflexi are the subdominant (r.a. from 1.7 to 4%). Statistical analysis indicated that *Spiroplasmataceae*, *Planctomycetaceae*, and Clostridiales family XII are the families that most differentiate the *C. viridis* and seawater communities, allowing us to hypothesize, at least for these taxa, a non-neutral selection process from the surrounding environment. Supporting our findings, the communities associated with another sea anemone (i.e., *Nematostella vectensis*) show an overall phylum-level composition that well resembles what we observed for *C. viridis*, including Proteobacteria, Bacteroidetes, Firmicutes, Tenericutes, and Planctomycetes among the dominant phyla (Har et al., 2015). However, at lower taxonomic levels (i.e., family and genus levels), the microbial composition of different anthozoan cnidarians drastically changes (Murray et al., 2016; Brown et al., 2017), demonstrating a robust host-specific profile as already observed for other marine holobionts (Pita et al., 2018; Wilkins et al., 2019). Particularly, regarding Cnidaria, a robust specie-specific microbiome profile was demonstrated in three

highly abundant and widespread Indo-Pacific species (*Acropora aculeus*, *Mycedium elephantotus*, and *Pachyseris speciosa*), with very few bacterial phylotypes being shared between the three coral species (Hernandez-Agreda et al., 2018).

While the bacterioplankton communities in seawater only show slight variations across different seasons, the *C. viridis*-associated microbiota considerably changes, as previously shown for the coral-associated microbiome (Chen et al., 2011; Sharp et al., 2017; Cai et al., 2018). According to our data, *C. viridis* is capable of rearranging its associated microbial community along the transition from winter to spring and summer. In particular, the winter communities appear enriched in oligotrophic anaerobic microorganisms, such as *Planctomycetaceae*, *Caldilineaceae* and *Nitrospiraceae*, which are commonly found in other marine holobionts (Lee et al., 2018). Bacteria belonging to these taxa have been implicated in the cycling of important elements such as nitrogen, sulfur and iron, and provide key ecological functions to the marine ecosystem (Clum et al., 2009; Zhang et al., 2017 and 2018). Though being characterized by a different pattern in the dominant bacterial families, the spring communities show a structure similar to that observed in winter, being dominated by taxa such as *Rhodospirillaceae*, *Rhodobacteraceae*, and *Oceanospirillaceae*, microorganisms that are known to be anaerobic oligotrophic components of the microbiome of marine holobionts and play important roles in carbon and sulfur cycling (Pujalte et al., 2014; Cortés-Lara et al., 2015; Tinta et al., 2019). During the summer, *C. viridis* communities drastically increase their biodiversity and change their composition. Indeed, with the spring-summer transition, *C. viridis*-associated communities show dominance of heterotrophic anaerobic microorganisms, which generally populate the holobiont digestive tract. In particular, the *C. viridis* microbiome in summer is characterized by higher relative abundance of *Lachnospiraceae*, *Clostridiaceae* and *Desulfovibrionaceae*, well-known primary and secondary fermenters that populate the gastrointestinal tract of a wide range of terrestrial and marine holobionts, including mammalians (Rausch et al., 2019). During the summer, we also observed an increase in *Vibrionaceae* members that have been frequently detected as symbionts of marine holobionts and recently hypothesized to be involved in regulating host developmental processes (Tinta et al., 2019). Finally, although the *Spiroplasmataceae* family increases its relative abundance during spring, this taxon is the one that is most consistently present in all seasons. Being endosymbiotic commensals of several marine holobionts, such as the jellyfishes *Aurelia aurita*, *Cotylorhiza tuberculata*, and *Pelagia noctiluca* (Cortés-Lara et al., 2015; Weiland-Bräuer et al., 2015), members of this family might thus represent a stable component of the *C. viridis* communities and play an important physiological role for the host health and survival. Further experiments should demonstrate the role of these organisms in the holobiont functioning.

Conclusion

In conclusion, here we demonstrate that *C. viridis* possesses a characteristic host-associated microbiome. These anemone-associated microbial communities show significant variations with the seasons, moving from an anaerobic community cycling essential nutrients in winter to a community dominated by anaerobic heterotrophs, more specialized in fermenting proteins and complex polysaccharides, in summer. We hypothesize that seasonal change in community composition may reflect the corresponding seasonal changes in the host physiology. Indeed, in the phylum Cnidaria, the release of particulate and dissolved organic matter (including carbon and nitrogen) in the form of mucus is significantly higher in summer

(Kurihara et al., 2018). During the summer, Cnidaria typically produce and release more mucus, which can be used as a food source by holobiont microorganisms, thus supporting the transition to a more heterotrophic fermentative microbial community (Wright et al., 2019). Supporting our hypothesis, analogous shifts in the associated microbial community have been shown for *Astrangia Poculata* in the winter to summer transition, when the emergence from the host quiescence makes available to the associated microbiome host substrates supporting the heterotrophic growth (Sharp et al., 2017). A similar adaptive microbiome response to seasonal changes has been observed also for *Isopora palifera* (Chen et al., 2011). According to the authors, during the winter - when available nitrogen is limited - the corals enrich nitrogen fixing microorganisms in the associated communities. These microbes then decrease in the summer, when exogenous nitrogen sources become available. Although our findings led us to hypothesize an important role of the *C. viridis* microbiome for host biology, and *vice versa*, more evidences in this direction to prove it conclusively are still needed. For instance, the functional relevance of the observed seasonal changes for host physiology and health must be dissected. The study of the *C. viridis* microbes relationship will certainly benefit from further extension to other geographical sites and from matching the patterns of phylogenetic changes with the corresponding functional variations in the holobiont.

References

Altschul, S. F., Gish, W., Miller, W., Myers, E. W., & Lipman, D. J. (1990). Basic local alignment search tool. *Journal of molecular biology*, *215*(3), 403-410.

Apprill, A. (2017). Marine animal microbiomes: toward understanding host–microbiome interactions in a changing ocean. *Frontiers in Marine Science*, *4*, 222.

Berg, G., Rybakova, D., Fischer, D., Cernava, T., Vergès, M. C. C., Charles, T., ... & Schloter, M. (2020). Microbiome definition re-visited: old concepts and new challenges. *Microbiome*, *8*(1), 1-22.

Brown, T., Otero, C., Grajales, A., Rodriguez, E., & Rodriguez-Lanetty, M. (2017). Worldwide exploration of the microbiome harbored by the cnidarian model, Exaiptasia pallida (Agassiz in Verrill, 1864) indicates a lack of bacterial association specificity at a lower taxonomic rank. *PeerJ*, *5*, e3235.

Cai, L., Zhou, G., Tong, H., Tian, R. M., Zhang, W., Ding, W., ... & Qian, P. Y. (2018). Season structures prokaryotic partners but not algal symbionts in subtropical hard corals. *Applied microbiology and biotechnology*, *102*(11), 4963-4973.

Chen, C. P., Tseng, C. H., Chen, C. A., & Tang, S. L. (2011). The dynamics of microbial partnerships in the coral Isopora palifera. *The ISME Journal*, *5*(4), 728-740.

Claesson, M. J., Jeffery, I. B., Conde, S., Power, S. E., O'connor, E. M., Cusack, S., ... & O'Toole, P. W. (2012). Gut microbiota composition correlates with diet and health in the elderly. *Nature*, *488*(7410), 178-184.

Clum, A., Nolan, M., Lang, E., Del Rio, T. G., Tice, H., Copeland, A., ... & Lapidus, A. (2009). Complete genome sequence of Acidimicrobium ferrooxidans type strain (ICP T). *Standards in Genomic Sciences*, *1*(1), 38-45.

Cortés-Lara, S., Urdiain, M., Mora-Ruiz, M., Prieto, L., & Rosselló-Móra, R. (2015). Prokaryotic microbiota in the digestive cavity of the jellyfish Cotylorhiza tuberculata. *Systematic and applied microbiology*, *38*(7), 494-500.

Culhane, A. C., Thioulouse, J., Perrière, G., & Higgins, D. G. (2005). MADE4: an R package for multivariate analysis of gene expression data. *Bioinformatics*, *21*(11), 2789-2790.

Di Camillo, C. G., Luna, G. M., Bo, M., Giordano, G., Corinaldesi, C., & Bavestrello, G. (2012). Biodiversity of prokaryotic communities associated with the ectoderm of Ectopleura crocea (Cnidaria, Hydrozoa). *PLoS One*, *7*(6), e39926.

Faith, D. P. (1992). Conservation evaluation and phylogenetic diversity. *Biological conservation*, *61*(1), 1-10.

Ferreira, J. G., Andersen, J. H., Borja, A., Bricker, S. B., Camp, J., Da Silva, M. C., ... & Claussen, U. (2011). Overview of eutrophication indicators to assess environmental status within the European Marine Strategy Framework Directive. *Estuarine, Coastal and Shelf Science*, *93*(2), 117-131.

Gerhardt, A. (2002). Bioindicator species and their use in biomonitoring. *Environmental monitoring*, *1*, 77-123.

Har, J. Y., Helbig, T., Lim, J. H., Fernando, S. C., Penn, K., Reitzel, A. M., & Thompson, J. R. (2015). Microbial diversity and

activity in the Nematostella vectensis holobiont: insights from 16S rRNA gene sequencing, isolate genomes, and a pilot-scale survey of gene expression. *Frontiers in microbiology*, *6*, 818.

Hernandez-Agreda, A., Leggat, W., Bongaerts, P., Herrera, C., & Ainsworth, T. D. (2018). Rethinking the coral microbiome: simplicity exists within a diverse microbial biosphere. *MBio*, *9*(5), e00812-18.

Hill, J., and White, N. (2008). Biology and Sensitivity Key Information Sub-programme. The Marine Life Information Network (MarLIN). Available at: https://www.marlin.ac.uk (accessed November 9, 2020).

Ignatiades, L. (2005). Scaling the trophic status of the Aegean Sea, eastern Mediterranean. *Journal of Sea Research*, *54*(1), 51-57.

Kuguru, B. L., Mgaya, Y. D., Öhman, M. C., & Wagner, G. M. (2004). The reef environment and competitive success in the Corallimorpharia. *Marine Biology*, *145*(5), 875-884.

Kurihara, H., Ikeda, N., & Umezawa, Y. (2018). Diurnal and seasonal variation of particle and dissolved organic matter release by the coral Acropora tenuis. *PeerJ*, *6*, e5728.

Lee, M. D., Kling, J. D., Araya, R., & Ceh, J. (2018). Jellyfish life stages shape associated microbial communities, while a core microbiome is maintained across all. *Frontiers in microbiology*, *9*, 1534.

Lin, M. F., Chou, W. H., Kitahara, M. V., Chen, C. L. A., Miller, D. J., & Forêt, S. (2016). Corallimorpharians are not "naked corals": insights into relationships between Scleractinia and Corallimorpharia from phylogenomic analyses. *PeerJ*, *4*, e2463.

Littman, R. A., Willis, B. L., Pfeffer, C., & Bourne, D. G. (2009). Diversities of coral-associated bacteria differ with location, but not species, for three acroporid corals on the Great Barrier Reef. *FEMS microbiology ecology*, *68*(2), 152-163.

Liu, Y. C., Huang, R. M., Bao, J., Wu, K. Y., Wu, H. Y., Gao, X. Y., & Zhang, X. Y. (2018). The unexpected diversity of microbial communities associated with black corals revealed by high-throughput Illumina sequencing. *FEMS microbiology letters*, *365*(15), fny167.

Marzinelli, E. M., Qiu, Z., Dafforn, K. A., Johnston, E. L., Steinberg, P. D., & Mayer-Pinto, M. (2018). Coastal urbanisation affects microbial communities on a dominant marine holobiont. *npj Biofilms and Microbiomes*, *4*(1), 1-7.

Murray, A. E., Rack, F. R., Zook, R., Williams, M. J., Higham, M. L., Broe, M., ... & Daly, M. (2016). Microbiome composition and diversity of the ice-dwelling sea anemone, Edwardsiella andrillae. *Integrative and comparative biology*, *56*(4), 542-555.

Murrell, P. (2018). *R Graphics.* Boca Raton, FL: CRC Press.

O'Brien, P. A., Webster, N. S., Miller, D. J., & Bourne, D. G. (2019). Host-microbe coevolution: applying evidence from model systems to complex marine invertebrate holobionts. *MBio*, *10*(1), e02241-18.

Pita, L., Rix, L., Slaby, B. M., Franke, A., & Hentschel, U. (2018). The sponge holobiont in a changing ocean: from microbes to ecosystems. *Microbiome*, *6*(1), 1-18.

Pollock, F. J., McMinds, R., Smith, S., Bourne, D. G., Willis, B. L., Medina, M., ... & Zaneveld, J. R. (2018). Coral-associated bacteria demonstrate phylosymbiosis and cophylogeny. *Nature Communications*, *9*(1), 1-13.

Pujalte, M. J., Lucena, T., Ruvira, M. A., Arahal, D. R., & Macián, M. C. (2014). The Family Rhodobacteraceae. The Prokaryotes: Alphaproteobacteria and Betaproteobacteria. *Rosenberg E, Delong EF, Lory S, Stackebrandt E, and Thompson F.(eds.)*, 439-512.

Rausch, P., Rühlemann, M., Hermes, B. M., Doms, S., Dagan, T., Dierking, K., ... & Baines, J. F. (2019). Comparative analysis of amplicon and metagenomic sequencing methods reveals key features in the evolution of animal metaorganisms. *Microbiome*, *7*(1), 1-19.

Rinaldi, A., and Rambelli, F. (2004). *Sul Relitto Della Piattaforma Paguro.* Italy: La Mandragora.

Rocha, J., Coelho, F. J., Peixe, L., Gomes, N. C., & Calado, R. (2014). Optimization of preservation and processing of sea anemones for microbial community analysis using molecular tools. *Scientific reports*, *4*(1), 1-5.

Sharp, K. H., Pratte, Z. A., Kerwin, A. H., Rotjan, R. D., & Stewart, F. J. (2017). Season, but not symbiont state, drives microbiome structure in the temperate coral Astrangia poculata. *Microbiome*, *5*(1), 1-14.

Smoot, M. E., Ono, K., Ruscheinski, J., Wang, P. L., & Ideker, T. (2011). Cytoscape 2.8: new features for data integration and network visualization. *Bioinformatics*, *27*(3), 431-432.

Stabili, L., Parisi, M. G., Parrinello, D., & Cammarata, M. (2018). Cnidarian interaction with microbial communities: from aid to animal's health to rejection responses. *Marine drugs*, *16*(9), 296.

Tinta, T., Kogovšek, T., Klun, K., Malej, A., Herndl, G. J., & Turk, V. (2019). Jellyfish-associated microbiome in the marine environment: exploring its biotechnological potential. *Marine drugs*, *17*(2), 94.

Weiland-Bräuer, N., Neulinger, S. C., Pinnow, N., Künzel, S., Baines, J. F., & Schmitz, R. A. (2015). Composition of

bacterial communities associated with Aurelia aurita changes with compartment, life stage, and population. *Applied and environmental microbiology*, *81*(17), 6038-6052.

Wilkins, L. G., Leray, M., O'Dea, A., Yuen, B., Peixoto, R. S., Pereira, T. J., ... & Eisen, J. A. (2019). Host-associated microbiomes drive structure and function of marine ecosystems. *PLoS biology*, *17*(11), e3000533.

Wright, R. M., Strader, M. E., Genuise, H. M., & Matz, M. (2019). Effects of thermal stress on amount, composition, and antibacterial properties of coral mucus. *PeerJ*, *7*, e6849.

Zhang, B., Xu, X., & Zhu, L. (2017). Structure and function of the microbial consortia of activated sludge in typical municipal wastewater treatment plants in winter. *Scientific reports*, *7*(1), 1-11.

Zhang, B., Yu, Q., Yan, G., Zhu, H., yang Xu, X., & Zhu, L. (2018). Seasonal bacterial community succession in four typical wastewater treatment plants: correlations between core microbes and process performance. *Scientific reports*, *8*(1), 1-11.

Ziegler, M., Grupstra, C. G., Barreto, M. M., Eaton, M., BaOmar, J., Zubier, K., ... & Voolstra, C. R. (2019). Coral bacterial community structure responds to environmental change in a host-specific manner. *Nature communications*, *10*(1), 1-11.

2.4 Study II — Seasonal changes in microbial communities associated with the common anemone *Anemonia viridis*

Introduction

Cnidarians belong to an ancient phylum of metazoans widely distributed across the world's oceans. These organisms have been recognized as key members of marine ecosystems, playing several crucial roles in marine food webs and habitat structuring (Boero et al., 2005; Bosch, 2013; Coker et al., 2014). For these reasons, much attention is being paid to study the ecology and evolution of cnidarians, also considering their proved susceptibility to the ongoing climate change-related stressors (Weis, 2008; Hartman et al., 2020). Among such anthropogenic stressors, for instance, the persistent CO_2 emissions and the increasing environmental pollution, which may also lead to eutrophication of the sea, can damage living organisms, including cnidarians (Graham, 2001; Puce et al., 2009; ados Santos et al., 2015; Biagi et al., 2020). All living macroorganisms on the planet harbor complex microbial communities which comprise a wide range of viruses, bacteria, archaea, fungi and protists (Skillings, 2016; Pita et al., 2018; Palladino et al., 2021a) and cnidarians are no exception (Rohwer et al., 2002; van Oppen and Blackall, 2019; Maire et al., 2021). In cnidarians, several studies, performed mainly on corals, have confirmed that microbiome key functions are needed to support every aspect of the host life, like nutrition, growth and defense against pathogens (van Oppen and Blackall, 2019; Palladino et al., 2021b). Furthermore, it has been posited that microbiomes are capable of rapidly modifying their structure and functions (e.g., taxa relative abundance) to deal with suboptimal environmental conditions, providing the host with certain plasticity in a species-specific manner (Torda et al., 2017; Ziegler et al., 2017 and 2019; Biagi et al., 2020). For instance, previous studies hypothesized a connection between microbiome plasticity and the holobiont response to habitat pollution, global warming and ocean acidification (ados Santos et al., 2015; Grottoli et al., 2018). This could result in the swift acclimatization of the holobiont and may occur through the loss/gain of microbial species and also through horizontal gene transfer (Bang et al., 2018).

In this context, our study aims at elucidating how stable microbial communities of the species *Anemonia viridis* can be throughout different seasons and in different anatomic compartments, considering that cnidarians have been proved to shelter distinct microbiomes according to life stage and/or anatomic compartment (Sweet et al., 2011; Lee et al., 2018; van Oppen and Blackall, 2019; Biagi et al., 2020). *Anemonia viridis* (Cnidaria, Anthozoa) is a symbiotic sea anemone widely distributed in Europe, from the Mediterranean basin to the Azores and the North Sea, where it thrives on the shallow seafloor, being part of the benthic community (Porro et al. 2020). *A. viridis* (Figure 10) is a predator which can reproduce both sexually, by emitting sperm and eggs directly into the water column (external fertilization and

Figure 10 - *Anemonia viridis* as a member of benthic temperate habitats (https://commons.wikimedia.org/wiki/File:Anemone_de_mer_P1010222.JPG?uselang=it).

gonochorism), and asexually, by fission of the gastrovascular cavity, or coelenteron. Like all metazoans, this species hosts a complex microbial community made up of several microorganisms, thus it can be considered a holobiont. Specifically, sea anemones, just like a lot of corals and other marine invertebrates, live in close association with eukaryotic endosymbionts (mainly dinoflagellates of the family *Symbiodiniaceae*, which are absent in some species) and prokaryotic cells, which comprise bacteria and archaea. As previously mentioned, all of these symbionts play a crucial role in the host physiology, health, development and stress response (McDevitt-Irwin et al., 2017; Ziegler et al., 2019; Porro et al., 2020 and 2021). Although anthozoans in the order Scleractinia are regarded as the most important reef builders in several marine ecosystems (Ries et al., 2006; Palladino et al., 2021b), also sea anemones (order *Actiniaria)* play their part, by providing food and shelter to many aquatic animals, thus they should be considered remarkable habitat-forming species (Steinberg et al., 2020). For instance, tropical and subtropical fish of the genus *Amphiprion* (also known as clownfish or anemonefish), as well as several crustaceans, like crabs and shrimps, live amongst the toxic tentacles of different species of sea anemones, where they can find nutrients and protection (Valdivia and Stotz, 2006; Pratte et al., 2018; Huebner et al., 2019; Marcionetti et al., 2019; Roux et al., 2019). Similar symbiotic relationships, involving, for example, crabs, have been also observed in *A. viridis* (Vader and Tandberg, 2020).

In order to elucidate variations in the microbial community of *A. viridis* , it is important to shed light on the still overlooked biological features of this species, such as microbiome compositional structure and how it responds to seasonality, also given its potential to act as an early proxy of both environmental status and animal health (Stabili et al., 2018). Seasonality has indeed proved to be an important driver shaping the compositional structure of anthozoans microbiome from subtropical and temperate ecosystems (Sharp et al., 2017; Cai et al., 2018; Palladino et al., 2021b). This is in line with the strong seasonal variations that characterize the northwestern Adriatic Sea, which may alter several environmental parameters, including river inputs and oceanographic conditions (Alvisi and Cozzi, 2016). Specifically, the large runoff of this area is manly influenced by the persistent Po river freshwater and nutrient supplies (mainly N and P), which show a peak in late autumn and spring, thanks to high precipitation rates and snow melting from the mountains, respectively, with occasional peaks of discharge also during rainy winters (Cozzi and Giani, 2011). Besides, other than pluvio-nival conditions, also evaporation, exchanges with the aquifers and human activities linked to agriculture and industry, for instance, strongly affect the flow dynamics of northwestern Adriatic Sea rivers throughout the year (Cozzi and Giani, 2011).

In this work, the microbial communities of 20 individuals of *A. viridis* retrieved in three different seasons (winter, spring and summer 2019) were analyzed by means of NGS techniques (sequencing of the V3-V4 region of the 16S rRNA gene), taking into account also three different anatomic compartments (i.e., coelenteron sections, coelenteron content collected with a swab and tentacles). The samples belong to animals collected in the northwestern Adriatic Sea, a semi-enclosed basin characterized by warm shallow waters, low salinity, high productivity (mainly influenced by the Po river inputs) and a high level of anthropogenic pollution (Moodley et al., 1998; Franzellitti et al., 2004; Biagi et al., 2019 and 2021). Our data shows that, in this area, the microbiome of *A. viridis* is influenced by changing seasons, with a little degree of tissue-specificity as well.

Results

A total of 20 *A. viridis* specimens were collected along the northwestern Adriatic coast (Riccione, Italy) in three distinct seasons: winter (February and March 2019, 10 individuals), spring (May 2019, 6 individuals) and summer (July 2019, 4 individuals). For each season, seawater samples (2 L each) were taken close to the animals and at the same depth (2 samples for winter, 2 samples for spring and 1 sample for summer). All animal samples came from a 100-meter-long submerged barrier of reinforced concrete placed about 200 meters offshore. This framework, referred to as WMesh[14], was originally designed to prevent coastal erosion, but, thanks to its complex geometry, has provided a hard substrate that ended up hosting a wide variety of marine fauna, including fish, crustaceans, mollusks and sessile cnidarians. All samples were collected by scuba divers of the association "Blennius" (Riccione, Italy) in the first five meters of water depth. Both anemones and seawater samples were processed to unravel their microbiome compositional structure and how it may change across seasons (NGS Illumina sequencing of the V3–V4 hypervariable region of the 16S rRNA gene; refer to paragraph 2.2 for details). Furthermore, three different anatomic compartments of the anemones were analyzed individually, namely sections of the coelenteron, i.e., the primary organ of digestion and circulation, its content (collected with a swab) and the stinging tentacles.

As expected, the alpha diversity of the seawater is significantly higher than that of the anemones, suggesting the presence of a more biodiverse microbial community in the water column compared to the holobiont tissues (Figure 11A). As a matter of fact, three alpha diversity metrics confirmed this pattern: Faith's Phylogenetic Diversity (Wilcoxon rank-sum test controlled for multiple testing using FDR, p-value < 0.05), Chao1 (Wilcoxon rank-sum test controlled for multiple testing using FDR, p-value < 0.01) and number of observed ASVs (Wilcoxon rank-sum test controlled for multiple testing using FDR, p-value < 0.01). On the other hand, the assessment of *A. viridis* microbiome variations among seasons indicated that Faith's Phylogenetic Diversity is the only alpha diversity metric showing significant differences (Kruskal-Wallis test controlled for multiple testing using FDR, p-value < 0.01) and that microbial diversity is greater in winter and summer compared to spring (Figure 11B). As for the three different anatomic compartments, from now on referred to as coelenteron, swab and tentacle, no significant alpha diversity differences were found (Kruskal-Wallis test controlled for multiple testing using FDR, p-value > 0.05 for all the three metrics; not shown).

At the phylum level, *A. viridis* microbiome is dominated by Proteobacteria (mean relative abundance ± SD in winter: 47.22 ± 21.90%, in spring: 80.98 ± 15.96% and in summer: 58.82 ± 18.23%) (Figure 12A). Bacteroidetes is the second most abundant phylum only in winter (mean relative abundance ± SD: 13.40 ± 9.08%), while in spring and in summer this record goes to Firmicutes and Spirochaetae, respectively (mean relative abundance ± SD: 8.11 ± 8.33% and 9.43 ± 12.30%). As for subdominant phyla, members of Verrucomicrobia display the highest abundance values in summer (mean relative abundance ± SD: 7.19 ± 10.73%). Cyanobacteria are virtually absent in winter and spring (mean relative abundance < 1%) but show a significant increase in summer (mean relative abundance ± SD: 4.15 ± 6.30%). The opposite pattern can be observed for Actinobacteria, which are more common in winter (mean relative abundance ± SD: 3.49 ± 3.40%). Interestingly, unclassified phyla steeply decrease from winter to spring and summer (mean relative abundance ± SD in winter: 14.77 ± 21.31%, in spring: 1.23 ± 1.80% and in summer: 2.11 ± 2.56%). Bacteria

[14] https://www.wmesh.it/

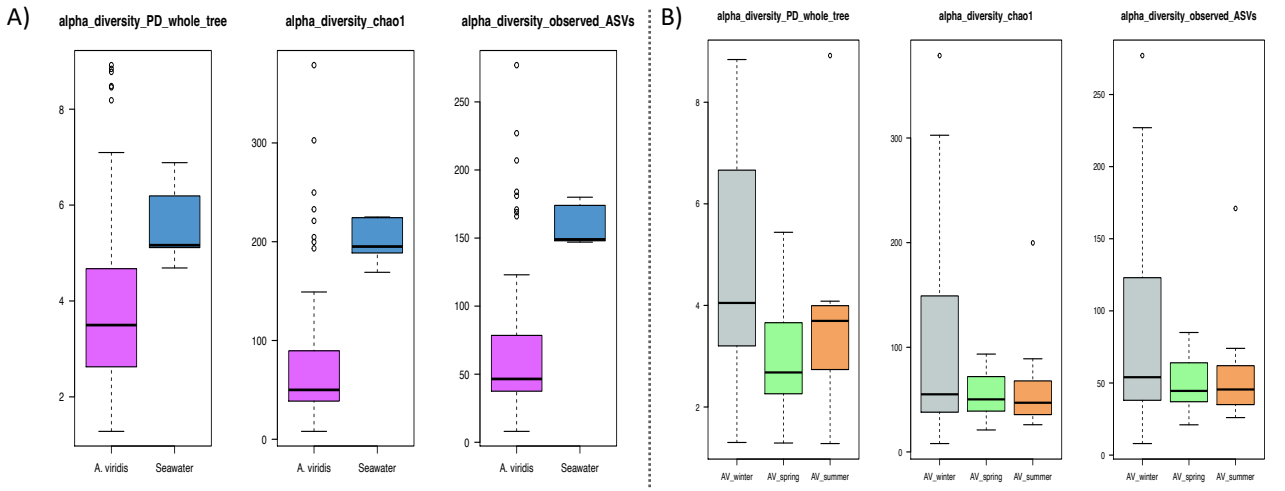

Figure 11 - Alpha diversity of *A. viridis* microbiome compared to the surrounding seawater (A) and in different sampling seasons (B). A) Box-and-whisker distribution of the Faith's Phylogenetic Diversity (PD_whole_tree), Chao1 index for microbial richness and number of observed ASVs of *A. viridis* (purple) and seawater (light blue). According to all metrics, seawater communities are more biodiverse than those of the anemones (Wilcoxon rank-sum test controlled for multiple testing using FDR, p-value < 0.05). B) Box-and-whisker distribution of the Faith's Phylogenetic Diversity (PD_whole_tree), Chao1 index for microbial richness and number of observed ASVs, calculated for winter (light gray), spring (light green) and summer (orange) anemone samples. Faith's Phylogenetic Diversity is the only metric consistently indicating a sample differentiation (Kruskal-Wallis test controlled for multiple testing using FDR, p-value < 0.01) and microbial diversity is greater in winter and summer rather that in spring.

phyla grouped as "Other" include phyla whose relative abundance was less than 1% in less that 20% of samples.

The seawater microbial ecosystem close to the anemones, on the other hand, shows a different structure and the vast majority of phyla-belonging sequences were classified (Figure 12B). Although Proteobacteria is still the dominant group (mean relative abundance ± SD in winter: 58.76 ± 1.83%, in spring: 56.92 ± 0.35% and in summer: 46.81%), the phylum Bacteroidetes shows a general abundance increase in every season (mean relative abundance ± SD in winter: 30.93 ± 4.86%, in spring: 22.56 ± 2.61% and in summer: 21.12%). Actinobacteria and Verrucomicrobia are subdominant taxa in every season. The former is more abundant in summer (relative abundance: 8.67%), whereas the latter prevails in spring (mean relative abundance ± SD: 9.21 ± 3.60%). Cyanobacteria relative abundance, again, is higher in summer (9.56%) than in the other two seasons (mean relative abundance ± SD in winter: 0.90 ± 1.13% and in spring: 4.38 ± 1.55%). It is noteworthy to highlight that Firmicutes and Spirochaetae, two important members of *A. viridis* microbiome, are almost absent in the surrounding seawater community (mean relative abundance < 1% in all seasons).

Seasonality of *A. viridis* microbiome taxonomy has been investigated also at the family level (data not shown). In winter, *Rhodobacteraceae* and *Flavobacteriaceae* are the dominant families (mean relative abundance ± SD: 10.99 ± 9.32% and 9.69 ± 6.95%, respectively), followed by an unclassified family of the class Alphaproteobacteria, *Spirochaetaceae* and *Vibrionaceae* as subdominant groups (mean relative abundance ± SD: 6.93 ± 16.79%, 6.50 ± 10.18% and 5.46 ± 9.62%, respectively). In spring, *Vibrionaceae* become more represented (mean relative abundance ± SD: 17.51 ± 14.83%), as well as

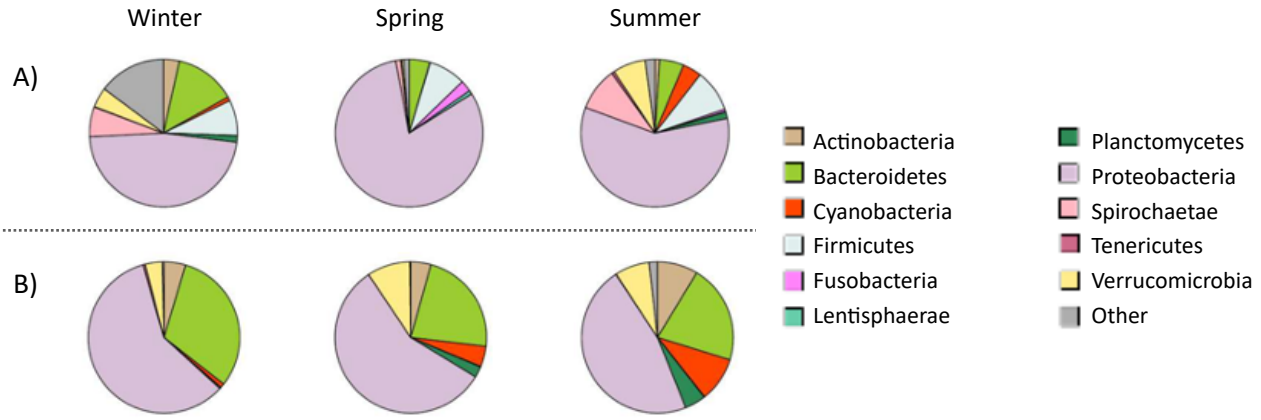

Figure 12 - Pie charts depicting the microbiome composition of *A. viridis* (A) and seawater (B) at the phylum level in the three different seasons (from left to right: winter, spring and summer). Only phyla with relative abundance > 1% in at least the 20% of samples are represented.

Pseudoalteromonadaceae and Clostridiales, *Family XII* (mean relative abundance ± SD: 5.95 ± 8.88% and 3.96 ± 5.29%, respectively). However, the most remarkable shift involves the family *Campylobacteraceae*, whose members are nearly absent in winter (mean relative abundance < 1%) and steeply peak in spring (mean relative abundance ± SD: 47.38 ± 24.78%). *Campylobacteraceae* remain abundant also in summer (mean relative abundance ± SD: 12.78 ± 10.65%), but the *Vibrionaceae* group is now the dominant family (mean relative abundance ± SD: 23.82 ± 17.51%). In summer, other well represented families are *Spirochaetaceae* (mean relative abundance ± SD: 9.43 ± 12.30%), an unclassified family of the order Verrucomicrobiales (mean relative abundance ± SD: 6.56 ± 9.99%) and *Family I* of the phylum Cyanobacteria (mean relative abundance ± SD: 4.15 ± 6.30%). Again, unclassified taxa, in this case families, prevail in winter and then decrease (mean relative abundance ± SD in winter: 33.26 ± 20.96%, in spring: 7.10 ± 7.23% and in summer: 16.00 ± 12.45%). The analysis focused on bacterial families whose relative abundance was > 2% in at least 20% of samples.

Seawater bacterial family composition shows a moderately different structure. In winter, *Flavobacteriaceae* and *Rhodobacteraceae* remain the dominant taxa (mean relative abundance ± SD: 24.00 ± 6.76% and 17.08 ± 4.30%, respectively) but amongst subdominant groups there are SAR86 clade, *Cryomorphaceae* and *Comamonadaceae* (mean relative abundance ± SD: 6.37 ± 4.79%, 4.88 ± 2.25% and 3.49 ± 0.28%, respectively). In spring, the major shifts encompass a notable abundance increase of *Halieaceae* and Cyanobacteria, *Family I* (mean relative abundance ± SD: 10.46 ± 1.55% and 4.38 ± 1.55%, respectively) and a decrease of *Cryomorphaceae* and *Comamonadaceae* (mean relative abundance ± SD: 1.99 ± 0.70% and 0.05 ± 0.07%, respectively). Moreover, *Flavobacteriaceae* and *Rhodobacteraceae* show a significant decrease (mean relative abundance ± SD: 16.48 ± 4.16% and 6.77 ± 0.42%, respectively). In summer, the seawater microbial ecosystem is dominated by Cyanobacteria, *Family I* (relative abundance: 9.46%) and *Rhodobacteraceae* (relative abundance: 8.67%), followed by *Flavobacteriaceae* and *Saprospiraceae* (relative abundance: 5.28% and 5.18%, respectively). Finally, every season is characterized by a high level of unclassified families (mean relative abundance ± SD in winter: 26.84 ± 1.48%, in spring: 32.12 ± 3.03% and in summer: 41.14%).

In order to provide additional information on *A. viridis* microbial differences across seasonality, we highlighted microbial variations in the host tridimensional structure through a graphic visualization by means of ternary plots representing *A. viridis* anatomic compartments in the three different seasons (Figure 13). The circle representing the phylum Verrucomicrobia, for example, is plotted closer to the coelenteron (C) vertex in winter, whereas it shifts towards the swab (S) and the tentacle (T) in summer. Cyanobacteria, which appear in summer, seem to be more associated with the coelenteron niche. Epsilonproteobacteria, which comprise, for instance, the family *Campylobacteraceae*, are plotted nearer to the coelenteron and tentacle vertexes in spring, while they tend to move a bit closer to the swab in summer. Another example is given by one family belonging to the phylum Planctomycetes, since its circle, from winter to summer, moves towards the tentacle vertex. Finally, the phylum Spirochaetae, well represented in winter and summer, is plotted closer to the coelenteron in winter and closer to the tentacle in summer.

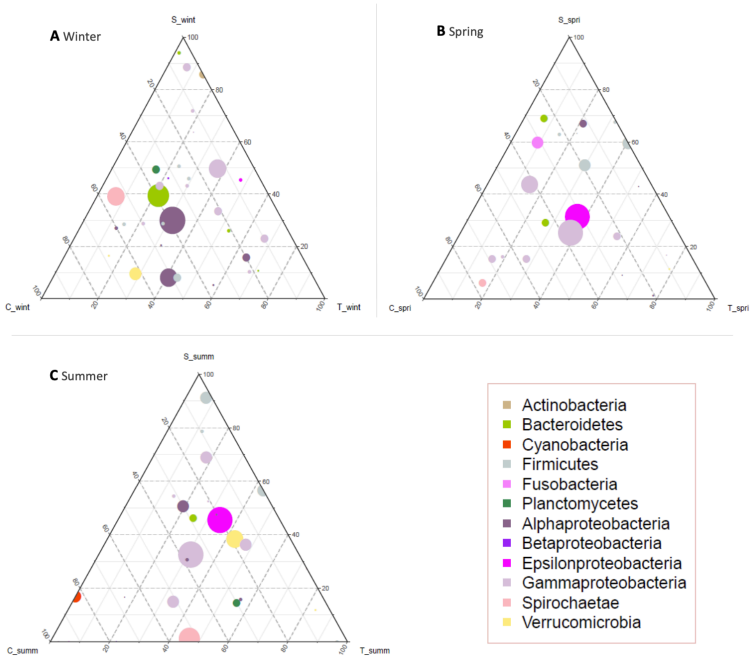

Figure 13 - Enrichment of bacterial families in the different anatomic compartments of the sea anemone *A. viridis* in the three different seasons. Ternary plots of bacterial families detected in the dataset with relative abundance > 2% in at least 4 samples. The samples were taken in winter (A), spring (B) and summer (C). The enrichment in the three anatomic compartments is plotted with the coelenteron (C), swab (S) and tentacle (T) ecosystems at the vertexes of the triangles. Each circle represents one bacterial family, and its size is proportional to the weighted relative abundance. Bacterial families are colored according to the phylum (or class, in the case of Proteobacteria) to which they belong (see the color legend on the right).

The overall compositional differences between *A. viridis* and seawater microbiomes were evaluated by performing a PCoA of the unweighted UniFrac distances. The results indicate a significant segregation between the two bacterial communities (permutation test with pseudo-F ratio, p-value = 0.001; not shown). The same beta diversity analysis was also carried out to highlight the seasonal and anatomic variations in the community structure of the sea anemones (Figure 14). As expected, the PCoA of the unweighted UniFrac distances shows a sharp separation of the microbiome structure across seasons, but only a slight

separation across different anatomic compartments (permutation test with pseudo-F ratio, p-value = 0.001 and < 0.05, respectively).

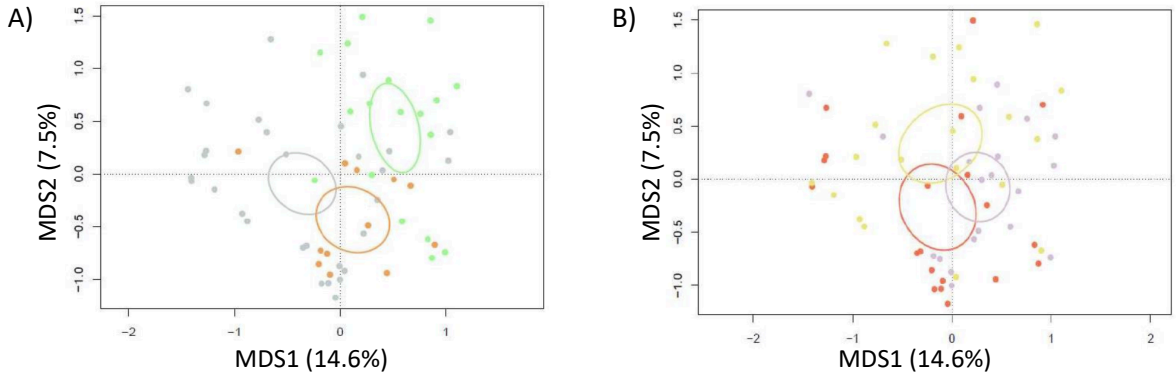

Figure 14 - Principal Coordinates Analyses (PCoA) based on unweighted UniFrac distances showing the variation of the *A. viridis* microbiome in winter (light gray), spring (light green) and summer (orange) (A) and in three different anatomic compartments (B), namely coelenteron (red), swab (dark yellow) and tentacle (light purple) (permutation test with pseudo-F ratio, p-value = 0.001 and < 0.05, respectively). The first and second principal components (MDS1 and MDS2) are reported in each plot and the percentage of variation in the dataset explained by each axis is indicated. Ellipses include the 95% confidence area based on the standard error of the weighted average of sample coordinates.

Discussion

The characteristic microbial community hosted by the sea anemone *A. viridis*, known to exert an influence on the many animal physiological processes, has been investigated in relation to seasonality in the northwestern Adriatic Sea, showing some interesting compositional changes from winter to summer.

Alpha and beta diversity measurements indicate that *A. viridis* microbiome is significantly different from that of the surrounding water column, besides being less biodiverse. Overall, these results hint at the presence of a non-neutral acquisition, mediated by the holobiont, of microorganisms from the nearby environment, as highlighted by previous studies showing a host-specific microbial profile for other anthozoans (Kvennefors et al., 2010; Pollock et al., 2018; Palladino et al., 2021b). According to our findings, seasonality is an important driver for shaping the compositional structure of *A. viridis* microbiome, both at the phylum and at the family level, with similar patterns that have already been observed for other subtropical and temperate anthozoans (Sharp et al., 2017; Cai et al., 2018; Palladino et al., 2021b). As already described, the northwestern Adriatic Sea is a shallow basin characterized by strong seasonality throughout the year, which may alter several environmental parameters, including river inputs and oceanographic conditions (Alvisi and Cozzi, 2016). It is interesting to notice the variation in the relative abundance of some bacterial families across seasonality. Individuals collected in winter are characterized by higher abundances of *Rhodobacteraceae* and *Flavobacteriaceae*, common components of microbial seawater ecosystems (Campbell et al., 2015). The *Vibrionaceae* family includes members with well-known opportunistic and pathogenic traits (Egan and Gardiner, 2016; Ziegler et al., 2016) and its relative abundance is higher in spring and summer. These observations are in line with a recent article on Corallimorpharia, a group of anthozoans closely related to sea anemones (Palladino et al., 2021b). This is

not surprising as *Vibrionaceae* are often associated with high seawater temperatures and coral bleaching (Littman et al., 2011; Pootakham et al., 2019). Besides, their high relative abundance in spring may be linked to a greater nutrient load, discharged from rivers, in which *Vibrionaceae* may thrive (Fan et al., 2013). However, this taxon also includes species frequently described as symbionts in marine macroorganisms (Palladino et al., 2021b), making it important for future studies to unravel the still controversial functions of *Vibrionaceae* in marine holobionts. In the spring season, a peak in *Campylobacteraceae* relative abundance is observed. *Campylobacteraceae* are a diverse group of pathogenic, commensal and environmental bacteria which comprises few genera with a vast array of functions (On and Zhang, 2014). Given their recorded presence in diseased corals (Daniels et al., 2015) and their clear dominance in *A. viridis* spring samples, further implications of the presence of this family in the complex holobiont will be worth investigating. These results indicate that *A. viridis* microbiome might be subjected to seasonal transitions, especially from winter to spring, leading to a marked compositional rearrangement of the holobiont-associated bacterial taxa. Such pattern, already highlighted in some anthozoan holobionts (Sharp et al., 2017; Palladino et al., 2021b), can be observed for other microbial families. Some of them, such as *Family XII* of the order Clostridiales, *Shewanellaceae* and *Pseudoalteromonadaceae*, are significantly more abundant in spring and include taxa with rich metabolic versatility and active in nutrient cycling pathways, as well as potential pathogens and opportunistic taxa capable of surviving in environments with high organic loads, like the northwestern Adriatic Sea (Leite et al., 2017; Conte et al., 2021). Moreover, the spring season is also enriched in families with nitrogen-fixing and denitrifying capabilities, such as *Marinilabiaceae*, which may be selected in periods of greater nutrient loads (Jessen et al., 2013). Last, the high relative abundance of Cyanobacteria *Family I* in summer, even though the differences across seasons are not statistically significant, is not surprising, as these phytoplanktonic microbes are known to flourish at mild temperatures and in good sunlight conditions (Kim et al., 2020). Moreover, Cyanobacteria higher abundance is an indicator for seawater eutrophication (Huisman et al., 2018) that can be linked to anthropogenic activities (Tsikoti and Genitsaris, 2021), such as tourism.

Taken together, these results show that seasonality combine with season-related anthropogenic stressors that can be a consistent driver capable of shaping microbiome taxonomy of the sea anemone *A. viridis* in the northwestern Adriatic Sea, a region characterized by strong annual fluctuations and severe anthropogenic stressors. Further studies should be focusing on the metabolic potential and on the actual microbial functions which may help the holobiont to cope with environmental shifts, given the greater magnitude that they are expected to have in the years to come.

References

ados Santos, H. F., Duarte, G. A. S., da Costa Rachid, C. T., Chaloub, R. M., Calderon, E. N., de Barros Marangoni, L. F., ... & Peixoto, R. S. (2015). Impact of oil spills on coral reefs can be reduced by bioremediation using probiotic microbiota. *Scientific reports*, *5*(1), 1-11.

Alvisi, F., & Cozzi, S. (2016). Seasonal dynamics and long-term trend of hypoxia in the coastal zone of Emilia Romagna (NW Adriatic Sea, Italy). *Science of the Total Environment*, *541*, 1448-1462.

Bang, C., Dagan, T., Deines, P., Dubilier, N., Duschl, W. J., Fraune, S., ... & Bosch, T. C. (2018). Metaorganisms in extreme environments: do microbes play a role in organismal adaptation?. *Zoology*, *127*, 1-19.

Biagi, E., D'Amico, F., Soverini, M., Angelini, V., Barone, M., Turroni, S., ... & Candela, M. (2019). Faecal bacterial communities from Mediterranean loggerhead sea turtles (Caretta caretta). *Environmental microbiology reports*, *11*(3), 361-371.

Biagi, E., Caroselli, E., Barone, M., Pezzimenti, M., Teixido, N., Soverini, M., ... & Candela, M. (2020). Patterns in microbiome composition differ with ocean acidification in anatomic compartments of the Mediterranean coral Astroides calycularis living at CO2 vents. *Science of The Total Environment*, *724*, 138048.

Biagi, E., Musella, M., Palladino, G., Angelini, V., Pari, S., Roncari, C., ... & Candela, M. (2021). Impact of Plastic Debris on the Gut Microbiota of Caretta caretta From Northwestern Adriatic Sea. *Frontiers in Marine Science*, *8*, 127.

Boero, F., Bouillon, J., & Piraino, S. (2005). The role of Cnidaria in evolution and ecology. *Italian Journal of Zoology*, *72*(1), 65-71.

Bosch, T. C. (2013). Cnidarian-microbe interactions and the origin of innate immunity in metazoans. *Annual review of microbiology*, *67*, 499-518.

Cai, L., Zhou, G., Tong, H., Tian, R. M., Zhang, W., Ding, W., ... & Qian, P. Y. (2018). Season structures prokaryotic partners but not algal symbionts in subtropical hard corals. *Applied microbiology and biotechnology*, *102*(11), 4963-4973.

Campbell, A. M., Fleisher, J., Sinigalliano, C., White, J. R., & Lopez, J. V. (2015). Dynamics of marine bacterial community diversity of the coastal waters of the reefs, inlets, and wastewater outfalls of southeast F lorida. *MicrobiologyOpen*, *4*(3), 390-408.

Coker, D. J., Wilson, S. K., & Pratchett, M. S. (2014). Importance of live coral habitat for reef fishes. *Reviews in Fish Biology and Fisheries*, *24*(1), 89-126.

Conte, C., Rotini, A., Winters, G., Vasquez, M. I., Piazza, G., Kletou, D., & Migliore, L. (2021). Elective affinities or random choice within the seagrass holobiont? The case of the native Posidonia oceanica (L.) Delile and the exotic Halophila stipulacea (Forssk.) Asch. from the same site (Limassol, Cyprus). *Aquatic Botany*, *174*, 103420.

Cozzi, S., & Giani, M. (2011). River water and nutrient discharges in the Northern Adriatic Sea: current importance and long term changes. *Continental Shelf Research*, *31*(18), 1881-1893.

Daniels, C., Baumgarten, S., Yum, L. K., Michell, C. T., Bayer, T., Arif, C., ... & Voolstra, C. R. (2015). Metatranscriptome analysis of the reef-building coral Orbicella faveolata indicates holobiont response to coral disease. *Frontiers in Marine Science*, *2*, 62.

Egan, S., & Gardiner, M. (2016). Microbial dysbiosis: rethinking disease in marine ecosystems. *Frontiers in Microbiology*, *7*, 991.

Fan, L., Liu, M., Simister, R., Webster, N. S., & Thomas, T. (2013). Marine microbial symbiosis heats up: the phylogenetic and functional response of a sponge holobiont to thermal stress. *The ISME journal*, *7*(5), 991-1002.

Franzellitti, S., Locatelli, C., Gerosa, G., Vallini, C., & Fabbri, E. (2004). Heavy metals in tissues of loggerhead turtles (Caretta caretta) from the northwestern Adriatic Sea. *Comparative Biochemistry and Physiology Part C: Toxicology & Pharmacology*, *138*(2), 187-194.

Graham, W. M. (2001). Numerical increases and distributional shifts of Chrysaora quinquecirrha (Desor) and Aurelia aurita (Linné)(Cnidaria: Scyphozoa) in the northern Gulf of Mexico. In *Jellyfish Blooms: Ecological and Societal Importance* (pp. 97-111). Springer, Dordrecht.

Grottoli, A. G., Dalcin Martins, P., Wilkins, M. J., Johnston, M. D., Warner, M. E., Cai, W. J., ... & Schoepf, V. (2018). Coral physiology and microbiome dynamics under combined warming and ocean acidification. *PloS one*, *13*(1), e0191156.

Hartman, L. M., van Oppen, M. J., & Blackall, L. L. (2020). The effect of thermal stress on the bacterial microbiome of Exaiptasia diaphana. *Microorganisms*, *8*(1), 20.

Huebner, L. K., Shea, C. P., Schueller, P. M., Terrell, A. D., Ratchford, S. G., & Chadwick, N. E. (2019). Crustacean symbiosis with Caribbean sea anemones Bartholomea annulata: occupancy modeling, habitat partitioning, and persistence. *Marine Ecology Progress Series*, *631*, 99-116.

Huisman, J., Codd, G. A., Paerl, H. W., Ibelings, B. W., Verspagen, J. M., & Visser, P. M. (2018). Cyanobacterial blooms. *Nature Reviews Microbiology*, *16*(8), 471-483.

Jessen, C., Villa Lizcano, J. F., Bayer, T., Roder, C., Aranda, M., Wild, C., & Voolstra, C. R. (2013). In-situ effects of eutrophication and overfishing on physiology and bacterial diversity of the Red Sea coral Acropora hemprichii. *PLoS One*, *8*(4), e62091.

Kim, M., Lee, J., Yang, D., Park, H. Y., & Park, W. (2020). Seasonal dynamics of the bacterial communities associated with cyanobacterial blooms in the Han River. *Environmental Pollution*, *266*, 115198.

Kvennefors, E. C. E., Sampayo, E., Ridgway, T., Barnes, A. C., & Hoegh-Guldberg, O. (2010). Bacterial communities of two ubiquitous Great Barrier Reef corals reveals both site-and species-specificity of common bacterial associates. *PloS one*, *5*(4), e10401.

Lee, M. D., Kling, J. D., Araya, R., & Ceh, J. (2018). Jellyfish life stages shape associated microbial communities, while a

core microbiome is maintained across all. *Frontiers in microbiology*, *9*, 1534.

Leite, L., Jude-Lemeilleur, F., Raymond, N., Henriques, I., Garabetian, F., & Alves, A. (2017). Phylogenetic diversity and functional characterization of the Manila clam microbiota: a culture-based approach. *Environmental Science and Pollution Research*, *24*(27), 21721-21732.

Littman, R., Willis, B. L., & Bourne, D. G. (2011). Metagenomic analysis of the coral holobiont during a natural bleaching event on the Great Barrier Reef. *Environmental microbiology reports*, *3*(6), 651-660.

Maire, J., Blackall, L. L., & van Oppen, M. J. (2021). Microbiome characterization of defensive tissues in the model anemone Exaiptasia diaphana. *BMC microbiology*, *21*(1), 1-12.

Marcionetti, A., Rossier, V., Roux, N., Salis, P., Laudet, V., & Salamin, N. (2019). Insights into the genomics of clownfish adaptive radiation: genetic basis of the mutualism with sea anemones. *Genome biology and evolution*, *11*(3), 869-882.

McDevitt-Irwin, J. M., Baum, J. K., Garren, M., & Vega Thurber, R. L. (2017). Responses of coral-associated bacterial communities to local and global stressors. *Frontiers in Marine Science*, *4*, 262.

Moodley, L., Heip, C. H., & Middelburg, J. J. (1998). Benthic activity in sediments of the northwestern Adriatic Sea: sediment oxygen consumption, macro-and meiofauna dynamics. *Journal of Sea Research*, *40*(3-4), 263-280.

On, A. J. L. S. L., & Zhang, L. (2014). 23 The Family Campylobacteraceae.

Palladino, G., Rampelli, S., Scicchitano, D., Musella, M., Quero, G. M., Prada, F., ... & Biagi, E. (2021a). Impact of Marine Aquaculture on the Microbiome Associated with Nearby Holobionts: The Case of Patella caerulea Living in Proximity of Sea Bream Aquaculture Cages. *Microorganisms*, *9*(2), 455.

Palladino, G., Biagi, E., Rampelli, S., Musella, M., D'Amico, F., Turroni, S., ... & Candela, M. (2021b). Seasonal changes in microbial communities associated with the jewel anemone Corynactis viridis. *Frontiers in Marine Science*, *8*, 57.

Pita, L., Rix, L., Slaby, B. M., Franke, A., & Hentschel, U. (2018). The sponge holobiont in a changing ocean: from microbes to ecosystems. *Microbiome*, *6*(1), 1-18.

Pollock, F. J., McMinds, R., Smith, S., Bourne, D. G., Willis, B. L., Medina, M., ... & Zaneveld, J. R. (2018). Coral-associated bacteria demonstrate phylosymbiosis and cophylogeny. *Nature Communications*, *9*(1), 1-13.

Pootakham, W., Mhuantong, W., Yoocha, T., Putchim, L., Jomchai, N., Sonthirod, C., ... & Tangphatsornruang, S. (2019). Heat-induced shift in coral microbiome reveals several members of the Rhodobacteraceae family as indicator species for thermal stress in Porites lutea. *MicrobiologyOpen*, *8*(12), e935.

Porro, B., Mallien, C., Hume, B. C., Pey, A., Aubin, E., Christen, R., ... & Forcioli, D. (2020). The many faced symbiotic snakelocks anemone (Anemonia viridis, Anthozoa): host and symbiont genetic differentiation among colour morphs. *Heredity*, *124*(2), 351-366.

Porro, B., Zamoum, T., Mallien, C., Hume, B. C., Voolstra, C. R., Röttinger, E., ... & Forcioli, D. (2021). Horizontal acquisition of Symbiodiniaceae in the Anemonia viridis (Cnidaria, Anthozoa) species complex. *Molecular ecology*, *30*(2), 391-405.

Pratte, Z. A., Patin, N. V., McWhirt, M. E., Caughman, A. M., Parris, D. J., & Stewart, F. J. (2018). Association with a sea anemone alters the skin microbiome of clownfish. *Coral reefs*, *37*(4), 1119-1125.

Puce, S., Bavestrello, G., Di Camillo, C. G., & Boero, F. (2009). Long-term changes in hydroid (Cnidaria, Hydrozoa) assemblages: effect of Mediterranean warming?. *Marine Ecology*, *30*(3), 313-326.

Ries, J. B., Stanley, S. M., & Hardie, L. A. (2006). Scleractinian corals produce calcite, and grow more slowly, in artificial Cretaceous seawater. *Geology*, *34*(7), 525-528.

Rohwer, F., Seguritan, V., Azam, F., & Knowlton, N. (2002). Diversity and distribution of coral-associated bacteria. *Marine Ecology Progress Series*, *243*, 1-10.

Roux, N., Lami, R., Salis, P., Magré, K., Romans, P., Masanet, P., ... & Laudet, V. (2019). Sea anemone and clownfish microbiota diversity and variation during the initial steps of symbiosis. *Scientific reports*, *9*(1), 1-13.

Sharp, K. H., Pratte, Z. A., Kerwin, A. H., Rotjan, R. D., & Stewart, F. J. (2017). Season, but not symbiont state, drives microbiome structure in the temperate coral Astrangia poculata. *Microbiome*, *5*(1), 1-14.

Skillings, D. (2016). Holobionts and the ecology of organisms: multi-species communities or integrated individuals?. *Biology & Philosophy*, *31*(6), 875-892.

Stabili, L., Parisi, M. G., Parrinello, D., & Cammarata, M. (2018). Cnidarian interaction with microbial communities: from aid to animal's health to rejection responses. *Marine drugs*, *16*(9), 296.

Steinberg, R. K., Dafforn, K. A., Ainsworth, T., & Johnston, E. L. (2020). Know thy anemone: A review of threats to

octocorals and anemones and opportunities for their restoration. *Frontiers in Marine Science*, *7*, 590.

Sweet, M. J., Croquer, A., & Bythell, J. C. (2011). Bacterial assemblages differ between compartments within the coral holobiont. *Coral Reefs*, *30*(1), 39-52.

Torda, G., Donelson, J. M., Aranda, M., Barshis, D. J., Bay, L., Berumen, M. L., ... & Munday, P. L. (2017). Rapid adaptive responses to climate change in corals. *Nature Climate Change*, *7*(9), 627-636.

Tsikoti, C., & Genitsaris, S. (2021). Review of Harmful Algal Blooms in the Coastal Mediterranean Sea, with a Focus on Greek Waters. *Diversity*, *13*(8), 396.

Vader, W., & Tandberg, A. H. S. (2020). Amphipods and sea anemones, an update. *The Journal of Crustacean Biology*, *40*(6), 872-878.

Valdivia, N., & Stotz, W. (2006). Feeding behavior of the porcellanid crab Allopetrolisthes spinifrons, symbiont of the sea anemone Phymactis papillosa. *Journal of Crustacean Biology*, *26*(3), 308-315.

van Oppen, M. J., & Blackall, L. L. (2019). Coral microbiome dynamics, functions and design in a changing world. *Nature Reviews Microbiology*, *17*(9), 557-567.

Weis, V. M. (2008). Cellular mechanisms of Cnidarian bleaching: stress causes the collapse of symbiosis. *Journal of Experimental Biology*, *211*(19), 3059-3066.

Ziegler, M., Roik, A., Porter, A., Zubier, K., Mudarris, M. S., Ormond, R., & Voolstra, C. R. (2016). Coral microbial community dynamics in response to anthropogenic impacts near a major city in the central Red Sea. *Marine pollution bulletin*, *105*(2), 629-640.

Ziegler, M., Seneca, F. O., Yum, L. K., Palumbi, S. R., & Voolstra, C. R. (2017). Bacterial community dynamics are linked to patterns of coral heat tolerance. *Nature communications*, *8*(1), 1-8.

Ziegler, M., Grupstra, C. G., Barreto, M. M., Eaton, M., BaOmar, J., Zubier, K., ... & Voolstra, C. R. (2019). Coral bacterial community structure responds to environmental change in a host-specific manner. *Nature communications*, *10*(1), 1-11.

2.5 Study III — Impact of marine aquaculture on the microbiome associated with nearby holobionts: the case of *Patella caerulea* living in proximity of sea bream aquaculture cages

Introduction

Fish farming is rapidly increasing in the Mediterranean Sea in order to respond to the rising demand for products for human consumption. Marine aquaculture (mariculture) is an integral part of growing coastal economy and is mainly carried out by caged open systems, with the farmed species in direct contact with the wild coastal ecosystem[15] (Grigorakis and Rigos, 2011; Rosa et al., 2012). Current finfish farming practices influence the marine biota at different trophic levels by changing environmental conditions in the surrounding water column, which undergoes severe eutrophication, as well as by impacting the chemical features of the sediments below the cages (San Diego-McGlone et al., 2008; Grigorakis and Rigos, 2011; Tičina et al., 2020). Indeed, sediments in proximity of the cages show an increase in organic matter, due to the sedimentation of uneaten feed and fish feces, as well as an accumulation of heavy metals (Moncada et al., 2019; Kalantzi et al., 2020). Consequences are shifts in nutrients and carbon fluxes, pH decline, and oxygen depletion in the sea floor, resulting in ammonia and hydrogen sulfide accumulation (Holmer et al., 2003; San Diego-McGlone et al., 2008). Such conditions modify the benthic assemblages of fauna and seagrass, affecting the whole food web (Karakassis et al., 2000). It has been demonstrated that the proximity of fish farming cages affects the survival of grazers and other macro-fauna trophic groups, even further than the mere sedimentation zone (Grigorakis and Rigos, 2011; Sanz-Lázaro et al., 2011).

All environments on our planet, including macro-organisms themselves (defined as holobionts), are colonized by microorganisms living in complex communities called microbiomes. All key biosphere processes, both terrestrial and aquatic, as well as many physiological aspects of animal and plant biology, deeply rely on microbiomes. Being aware of the microbiome importance as a life support system for the planet biosphere, there is now a huge concern about the impact of local and global anthropogenic factors on the planet microbiomes (Cavicchioli et al., 2019), making microbiome assessment a central point for a next-generation and more holistic evaluation of environmental health. In this scenario, the impact of aquaculture on seafloor microbiomes has recently been explored, reporting decreased bacterial biodiversity in the sediments below the cages, the overgrowth of microbial groups able to thrive in anaerobic, carbon-enriched conditions, as well as an accumulation of fecal bacteria and/or bacteria linked to the sulfur cycle (Luna et al., 2013; Hornick et al., 2018; Ape et al., 2019; Moncada et al., 2019; Rubio-Portillo et al., 2019; Shi et al., 2019; Zhang et al., 2020). The microbial community associated with the water column also appeared to be different within and outside the cage of farmed sea breams (Haro-Moreno et al., 2020). On the contrary, very little is known on the effect of the presence of farming cages on the microbiome of nearby wild organisms.

Animals and plants are not autonomous entities but need to be viewed as complex biomolecular networks composed by the host and its associated microbiome (Bordenstein and Theis, 2015). Microbiome structures result from a host-driven selection process. Nonetheless, in the case of marine holobionts that live in close, water-mediated interaction with microbiomes from the environment and the other holobionts living in their

[15] http://www.fao.org/documents/card/en/c/I9540EN/. *The State of World Fisheries and Aquaculture 2018 - Meeting the Sustainable Development Goals.* Rome: FAO. Accessed 07 Jan 2021.

proximity, host-associated microbial communities show a strong metacommunity behavior. In other words, the microbiome of a given host is presumably linked by dispersal to all other microbiomes in the same environment, and microbiome recruitment by one host can be affected by the exudate of another, nearby dwelling holobiont (Leibold et al., 2004; Adair and Douglas, 2017; Cleary et al., 2019; Trevathan-Tackett et al., 2019). Therefore, it is reasonable to expect that the microbiomes associated with wild marine holobionts living in proximity to the fish farms are somehow affected by the interaction with the microbiomes of farmed fish, both directly, by the transfer of fish microorganisms dispersed to the water column and/or sediments, and indirectly, by changing the surrounding environmental bacterial community. Eventually, the consequent colonization of the wild holobiont microbiomes with allochthonous microbial components would result in compositional changes with cascade impacts on the health and safety of the marine environment. In agreement with these hypotheses, it was recently reported that sponges living in proximity of fish farming sites in the Philippines harbor a microbial community enriched in genes involved in ammonia oxidation compared to sponges of the same species collected in pristine waters (Baquiran and Conaco, 2018).

In order to explore how the presence of fish farming cages influences the microbiome of the surrounding wild holobionts, we selected a common grazer gastropod from the genus Patella as a representative fouling holobiont. *Patella caerulea* is a common seaweed grazing marine limpet in all Mediterranean rocky shores (Della Santina and Chelazzi, 1991). As a result of their wide distribution, abundance, and sedentary lifestyle, limpets of this species have been proposed as biomonitors for the local water quality in terms of heavy metal accumulation and organic pollutants (Reguera et al., 2018; Viñas et al., 2018). In addition, limpets are keystone species for the coastal ecosystem because they regulate the degree of algal coverage and, consequently, succession processes in rocky intertidal communities (Coleman et al., 2006; Reguera et al., 2018; Viñas et al., 2018).

In this study, we compared (by next-generation sequencing 16S rDNA metabarcoding) the *P. caerulea* digestive gland microbiome structure in individuals collected close to sea bream (*Sparus aurata*) aquaculture cages located in a fish farm in Southern Sicily (Italy), Mediterranean Sea, with the one from individuals collected on a rocky coastal tract located at 1.2 km from the aquaculture facility, as a control site. The gut, skin, and gill microbiomes from the farmed fishes were also assessed, together with microbial assemblages from sediments and water at the aquaculture and control sites, allowing us to explore the variation of *P. caerulea* microbiomes at the aquaculture site in a holistic metacommunity context. Both sampling sites were located in the harbor of Licata, which is an ideal location to investigate the impact of aquaculture systems on the microbiome composition of nearby wild animals due to the limited hydrodynamic circulation inside the harbor and to its shallow depth (≈10 m), resulting in a large amount of organic matter accumulating on the sea floor under the cages (Ape et al., 2019). This comprehensive study design allowed us to dissect the interaction between the microbiomes from farmed fishes and surrounding wild holobionts at the metacommunity level, showing patterns of microbial dispersion from the former to the environment and, finally, to locally dwelling wild organisms.

Materials and Methods

Site description, samples collection, and environmental data

The sampling was performed on 25 September 2019, in a marine fish farm located in the harbor of Licata (Figure 15), in Southern Sicily (Mediterranean Sea, coordinates 37.087713°N, 13.943773°E). The facility is composed of 23 floating cages containing separately sea bream (*S. aurata*) and sea bass (*Dicentrarchus labrax*); further details on the sampling site are reported in Ape et al. (2019). Sea bream and sea bass have productive cycles of different length; thus, at the time of sampling, only sea bream cages contained a high number of adult fishes, representing a large biomass potentially influencing the local limpet microbiome. Indeed, in September, *S. aurata* individuals were almost at the end of their productive cycle, causing a progressive transformation of the benthic substrate into a muddy black sediment and making the sampling period ideal for the maximization of the aquaculture plant impact on the wild environment. We selected one of the sea bream cages as the sample site (37.086667°N, 13.943611°E), and we collected five *S. aurata* individuals and 12 *P. caerulea* individuals, the latter growing in adhesion to the cage plastic tubes. Surface sediment (0–1 cm) and seawater were collected under the cage as well as at two additional sites (37.089732°N, 13.937469°E and 37.091949°N, 13.933703°E, about 670 m and 1.2 km far from the aquaculture site, respectively) as controls, by coring and through a sterile plastic bottle, respectively. Limpet samples were detached using a previously sterilized knife and preserved into sterile plastic containers. We also collected 15 *P. caerulea* individuals from the shallow water rocks located along the pier (37.092222°N, 13.933056°E, 1.2 km far from the aquaculture site), as described above. From each fish, intestinal content (gut), gills, and skin were collected. In more detail, sea bream individuals (average 270 g) were euthanized by anesthesia (MS-222) following the national regulations and set on ice until processing. Within 2–5 h, gut tissues were obtained by aseptic dissection, and the intestinal content was squeezed out as described in Mente et al. (2018) and stored in sterile tubes. Finally, a 2 × 2 cm of skin (left side) and the second gill branch (left side) were aseptically collected with sterile scissors, rinsed with sterile phosphate buffer, and stored in sterile tubes. All samples were kept at −20 °C until shipping in the respective labs.

Seawater temperature and pH measurements were performed with an Onset HOBO Data Logger. Salinity was measured through an optical refractometer. Water samples for determination of total alkalinity (TA) were collected at both sites using sterile 120 mL syringes. The syringe samples were immediately transferred in labeled 100 mL amber glass bottles and fixed with saturated mercuric chloride ($HgCl_2$) to avoid biological alteration and stored in darkness at 4 °C prior to measurement. TA was determined by potentiometric titration (6 measurements per site) using a Metrohm 888 Titrando inter-faced with the data acquisition software TiAmo Light. The HCl (0.1 M) titrant solution was calibrated against certified reference materials distributed by A.G. Dickson (CRM, Batches #187). Seawater pH, TA, salinity, and temperature were used to calculate other carbonate chemistry parameters using the software CO2SYS with referenced dissociation constants (Mehrbach et al., 1973; Dickson and Millero, 1987; Dickson, 1990).

Figure 15 - **Sampling site description.** Map of the marine fish farm located in the harbor of Licata (37.087713°N, 13.943773°E). The sampling sites are indicated with red balloons and labelled accordingly. Aquaculture site is located at 37.086667°N, 13.943611°E, control sediment and water samples were collected far from the fish cages (37.089732°N, 13.937469°E and 37.091949°N, 13.933703°E) and *P. caerulea* individuals from the shallow water rocks located along the pier were collected at 37.092222°N, 13.933056°E (source: Google Earth, earth.google.com/web/; map data: SIO, NOAA, U.S. Navy, NGA, GEBCO, IBCAO).

Microbial DNA extraction, 16S rRNA gene amplification and sequencing

For limpet samples, we dissected the digestive gland from each individual under a vertical laminar airflow cabinet using sterile tweezers and scalpels, obtaining a weight range from 0.037 g to 0.460 g for all the glands, depending on each limpet size. Total microbial DNA extraction was performed on limpets digestive glands using the DNeasy PowerSoil Kit (Qiagen, Hilden, Germany) (Musella et al., 2020).

All feces collected from each sample were used for DNA extraction. Seawater samples (1 L) were filtered onto 0.22 µm cellulose nitrate membrane filters (Sartorius, ø 47 mm) and stored at −20 °C until processing; the entire membrane filters were used for DNA extraction. The top 1 cm of each sterile corer used for sediments collection was carefully extruded and stored at −20 °C and 1 g of this sediment was used for DNA extraction. DNA from sea bream feces and tissues, seawater and sediment samples was extracted using the DNeasy PowerSoil Kit (Qiagen) (Quero et al., 2017; Ape et al., 2019). Extracted DNA samples were quantified with NanoDrop ND-1000 (NanoDrop Technologies, Wilmington, DE) and stored at –20 °C until further processing.

PCR amplification of the V3-V4 hypervariable region of the 16S rRNA gene, library preparation and sequencing were carried out as described in paragraph 2.2.

Bioinformatics and statistics

Raw sequences were processed as described in paragraph 2.2. Two different metrics were used to evaluate alpha diversity - Faith's Phylogenetic Diversity (Faith_pd) (Faith, 1992) and number of observed ASVs. Beta diversity was estimated by computing the unweighted UniFrac distance. To further characterize the compositional specificities of the limpets digestive gland microbiome at aquaculture and control sites in the context of their respective marine metacommunities, PANDAseq assembled paired-end reads were also

processed with the QIIME1 (Caporaso et al., 2010) pipeline for OTUs (Operational Taxonomic Units) clustering based on 97% similarity threshold, with taxonomy assignment performed using the SILVA database. As above, all the sequences assigned to eukaryotes or unassigned were discarded.

All statistical analyses were performed using the R software[16] (R Core Team), version 3.6.1., with the packages "Made4" (Culhane et al., 2005) and "vegan[17]", except for environmental parameters that were compared between sites using Mann-Whitney, computed with IBM SPSS Statistics 26.0 (IBM Corporation). Ternary plots were prepared using the R packages "ggtern" (Hamilton and Ferry, 2018), "PMCMR" (Pohlert, 2014) and "vcd" (Meyer et al., 2020). Unweighted UniFrac distances were plotted using the vegan package and the data separation in the Principal Coordinates Analysis (PCoA) was tested using a permutation test with pseudo-F ratios (function "adonis" in the vegan package). Wilcoxon rank-sum test was used to assess differences in alpha diversity and ternary plots, and Kruskal-Wallis test for testing OTUs separation. P-values were corrected for multiple testing with the Benjamini-Hochberg method, with a false discovery rate (FDR) ≤ 0.05 considered statistically significant.

Results

Diversity and compositional structure of the marine microbial communities at aquaculture and control site in the Licata harbor

Sequencing of the V3-V4 hypervariable region of the 16S rRNA gene from the total microbial DNA resulted in 50 samples, from aquaculture and control sites, producing a high-quality output. These included three sediment and three seawater samples, 25 limpet digestive glands (DG) and 19 sea bream samples, consisting of 12 gut samples, three gill samples and four skin samples. The number of high-quality reads in the samples ranged between 1,690 and 20,252 per sample, with a subsequent normalization to the lowest number of reads (1,690), resulting into 6,450 ASVs and 8,701 OTUs.

According to our data, the overall structure of the limpet DG microbiome segregated from that of seawater and sediments microecosystems, as shown by the Principal Coordinates Analysis (PCoA) based on the unweighted UniFrac distances (Figure 16A) (permutation test with pseudo-F ratio, p-value ≤ 0.001). *P. caerulea* DG microbiome was also characterized by a lower diversity with respect to environmental communities (seawater and sediments) (Figure 16B), although the trend did not always reach the statistical significance (Wilcoxon rank-sum test controlled for multiple testing using FDR; limpets vs sediment p-value ≤ 0.05, limpets vs seawater p-value 0.09 and 0.2 for Faith PD index and number of observed ASVs, respectively).

Concerning their phylogenetic composition, the microbial assemblages associated with the three types of samples showed a characteristic layout in terms of dominant and subdominant components, with a specific declination according to the sampling site. Particularly, the microbiome of *P. caerulea* DG was characterized by two dominant phyla, Proteobacteria (mean relative abundance ± SD, 44.1 ± 12.6% and 43.7 ± 12.5% in limpets collected at the control and aquaculture sites, respectively) and Planctomycetes (29.7 ± 13.4% and 28.6 ± 22.4%). Alphaproteobacteria class represented the main fraction of Proteobacteria (72.0 ± 13.2% and 66.5 ± 23.0%). Relevant subdominant phyla (average relative abundance > 1%) were Firmicutes (6.4 ± 11.6%

[16] https://www.R-project.org; 2013

[17] https://cran.r-project.org/web/packages/vegan/index.html

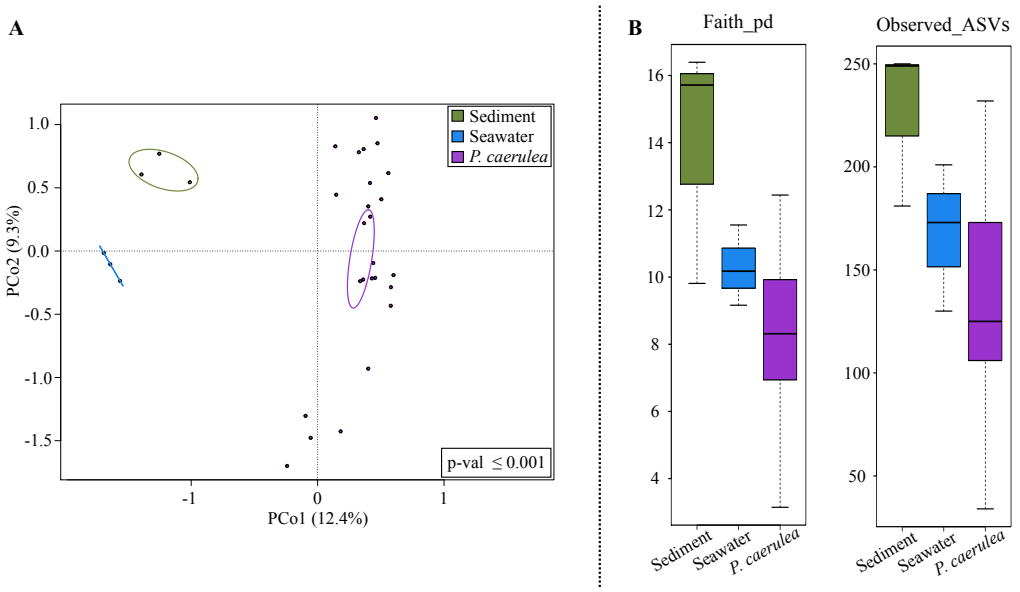

Figure 16 - **Alpha and beta diversity comparison between *P. caerulea* and the surrounding environment.** (A) Principal Coordinates Analysis (PCoA) based on the unweighted UniFrac distances between microbial profiles of sediments, seawater and limpets, showing a strong separation between the groups (permutation test with pseudo-F ratio, p-value ≤ 0.001). The percentage of variance in the dataset explained by each axis, first and second principal component (PCo1 and PCo2), is 12.4% and 9.3%, respectively. Ellipses include 95% confidence area based on the standard error of the weighted average of sample coordinates. (B) Box-and-whiskers distribution of Faith's Phylogenetic Diversity (Faith_pd) and number of observed ASVs as metrics of alpha diversity.

and 5.7 ± 4.6%), Actinobacteria (5.5 ± 7.3% and 3.7 ± 7.1%), Bacteroidetes (4.2 ± 8.5% and 2.8 ± 3.2%) and Cyanobacteria (2.1 ± 1.4% and 2.7 ± 3.2%). In the control site, we also found Verrucomicrobia (3.9 ± 3.4%), whereas Tenericutes (9.5 ± 16.5%) and Fusobacteria (1.2 ± 2.7%) were only present in the aquaculture site (Figure 17A). The detailed compositional structure of water and sediments microbiomes at the aquaculture and control sites is available in Supplementary Figures S6 and S7. Briefly, both sediments and seawater were mainly characterized by Proteobacteria and Bacteroidetes at all sampling sites. In the aquaculture site, the two matrices also included members of the Firmicutes phylum, whereas Verrucomicrobia were only characteristic of seawater. Finally, the microbiomes associated with different tissues of farmed sea breams were also characterized (Supplementary Figure S8). Our findings showed that all sea bream microbiomes were mainly characterized by Proteobacteria, with Firmicutes and Actinobacteria only represented in the gut samples.

Changes in the limpet microbiome and surrounding metacommunities at the aquaculture site in the Licata harbor

In order to highlight the impact of aquaculture cages on the limpet DG microbiome, a PCoA of the unweighted UniFrac distances of the microbiome structures in individuals collected at aquaculture and control sites was performed (Figure 17D). Data indicated a significant segregation between the two ecosystems (permutation test with pseudo-F ratio, p-value ≤ 0.001), demonstrating that the phylogenetic composition of *P. caerulea* DG microbiome changed at the aquaculture site. Further, DG samples collected in the aquaculture site showed a significantly lower alpha diversity, as shown by two different metrics (FDR-

corrected Wilcoxon rank-sum test, p-value 0.008 and 0.01 for Faith PD index and number of observed ASVs, respectively) (Figure 17C). For what concerns the main DG microbiome compositional specificities, limpets at the aquaculture site were characterized by a higher relative abundance in members belonging to the family *Mycoplasmataceae* (9.4 ± 16.5% in samples from the cages vs. 0.8 ± 3.3% in controls). Conversely, among the subdominant components, the DG microbiome of individuals at the aquaculture site was significantly depleted in members of the uncultured Verrucomicrobiales group DEV007, showing a relative abundance (r.a.) of 0.3 ± 0.5% compared to 2.1 ± 1.9% observed in controls (FDR-corrected Wilcoxon rank-sum test, p-value = 0.007) (Figure 17B).

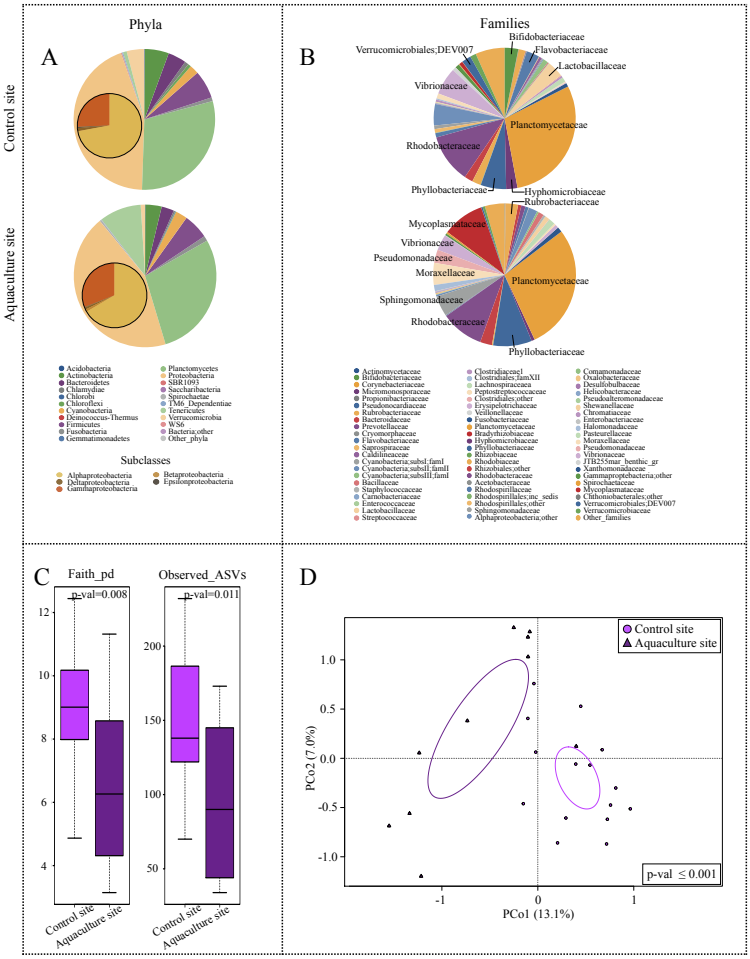

Figure 17 - Overall description of *P. caerulea* microbial communities and alpha and beta diversity comparison between *P. caerulea* from control and aquaculture sites. Pie charts summarizing the phylum (A) and family (B) level microbiota composition of *P. caerulea* in the two sampling sites. Phyla with relative abundance > 0.5% in at least one sample and families with relative abundance > 2% in at least 10% of samples are represented. Proteobacteria classes are expanded on the respective pie chart phylum slice. (C) Box-and-whiskers distribution of the alpha diversity metrics Faith's Phylogenetic Diversity (Faith_pd) and number of observed ASVs. (D) Principal Coordinates Analysis (PCoA) based on the unweighted UniFrac distances between microbial profiles of *P. caerulea* in the two sampling sites shows a strong separation between the groups (permutation test with pseudo-F ratio, p-value ≤ 0.001). The percentage of variance in the dataset explained by each axis, first and second principal component (PCo1 and PCo2), is 13.1% and 7.0%, respectively. Ellipses include 95% confidence area based on the standard error of the weighted average of sample coordinates.

A re-analysis of the sequences using a different strategy (UCLUST algorithm [38] with 97% similarity threshold) was subsequently carried out to characterize the compositional specificities of the limpet DG microbiome at the aquaculture and control site in the context of their respective marine metacommunities. The 97%-similarity threshold allowed us to obtain cluster of sequences (OTUs), possibly ascribable to small groups of species, that could play specific ecological roles within and across the analyzed ecosystems. Among the obtained 97%-similarity OTUs we filtered those detected with a relative abundance > 0.5% in at least one microbiome sample type (limpets, seawater, sediments and fish gut, gills and skin). The resulting subset of 192 OTUs was used for the production of ternary plots to highlight the OTUs ecological propensity toward the different local microbial communities (Figure 18A-C). While for the control site a single ternary plot was generated (Figure 18A), considering local water, sediments and the DG from limpets, for the aquaculture site two ternary plots were created, the first matching the one from the control site (Figure 18B) and the second in which seawater was substituted by S. aurata as the source ecosystem (Figure 18C). Furthermore, 50 OTUs showing a significantly different relative abundance in the DG microbiome from individuals collected at the aquaculture and control sites were identified (FDR-corrected Wilcoxon rank-sum test, p-value ≤ 0.05). Among these, 22 OTUs were more abundant in the control site (colored in purple in Figure 18A) whereas 28 OTUs showed a significant opposite trend (in purple in Figures 18B and C). The highest alignment scores against NCBI 16S rRNA database of these OTUs are reported in Supplementary Table S2.

Focusing on the 50 OTUs differentiating the limpet DG microbiome at aquaculture and control sites, the majority of those enriched in the latter were exclusive of limpets (plotted at the "*P. caerulea*" vertex in Figure 18A) (OTUs 4667, 11135, 4454, 12220, 1496, 4069, 4330, 14127, 5331, 14154, 3304, 11232, 11155, 14091, 11445, 3555 and 4234). These OTUs were assigned to species typically isolated from marine environment (e.g., species belonging to genera *Fodinicurvata*, *Rubinisphaera*, *Roseibacillus*) (Yoon et al., 2005; Infante-Dominguez et al., 2015; Ferreira et al., 2016; Kallscheuer et al., 2020) or from marine organisms, such as *Amorphus coralli*, firstly isolated from coral mucus (Yosef et al., 2008). Other OTUs characterizing the DG from the limpets collected at the control site, such as OTU5034 (genus *Robiginitalea*), OTU2911 (*Actibacter*) and OTU2120 (*Photobacterium*), were shared between limpets and sediments (plotted along the bottom plane of the ternary plot), whereas OTU2289 (*Psychrobacter*) was shared between limpets and water, with higher relative abundance in the latter (closer to the "Seawater" vertex in the ternary plot). Finally, OTU1355 (*Prochlorococcus*) was shared among all three ecosystems, with a higher proportion in seawater. Similar to what observed for the control site, the majority of OTUs characteristic of the limpets DG microbiome at the aquaculture site were exclusive of limpets (OTUs 4187, 11247, 11243, 11205, 6912, 5244, 4203, 2259, 4097, 2073, 12731, 11913, 4065, 4965, 2118, 2077, 2154, 11213, 1397, 11152, 4465, 4305, 6020, 3237 and 6006). Amongst these OTUs, four were assigned to the genus *Mycoplasma*, one to *Vibrio* and one to *Acinetobacter*, potential human pathogens found in marine organisms (Fraser et al., 1995; Wang et al., 2010; Abdel-Aziz et al., 2013; Sohn et al., 2019; Kuebutornye et al., 2020). Within the remaining OTUs characterizing the DG microbiome from limpets living in aquaculture proximity, we only found one OTU shared between limpets and sediments (OTU14234, belonging to the genus *Sulfurovum*), mainly present in sediments. Two OTUs were shared between limpets and seawater in the aquaculture site (OTU1919 and OTU2080, assigned to *Staphylococcus* and *Psychrobacter*, respectively),

with a higher relative abundance in limpet. Finally, limpets and farmed fishes shared four out of the 28 OTUs characteristic of the limpets DG microbiome at the aquaculture site, of which two more present in fish (OTU1919, *Staphylococcus*, and OTU6020, *Pseudomonas*) and two enriched in limpets (OTU12731, *Sphingomonas*, and OTU2080, *Psychrobacter*) (Figure 18B and C). Of these four OTUs, OTU1919 and OTU12731 were present at low relative abundance in all fish tissues, whereas OTU2080 specifically belonged to the ecosystem and OTU6020 was more abundant on the skin of fishes (Figure 18D).

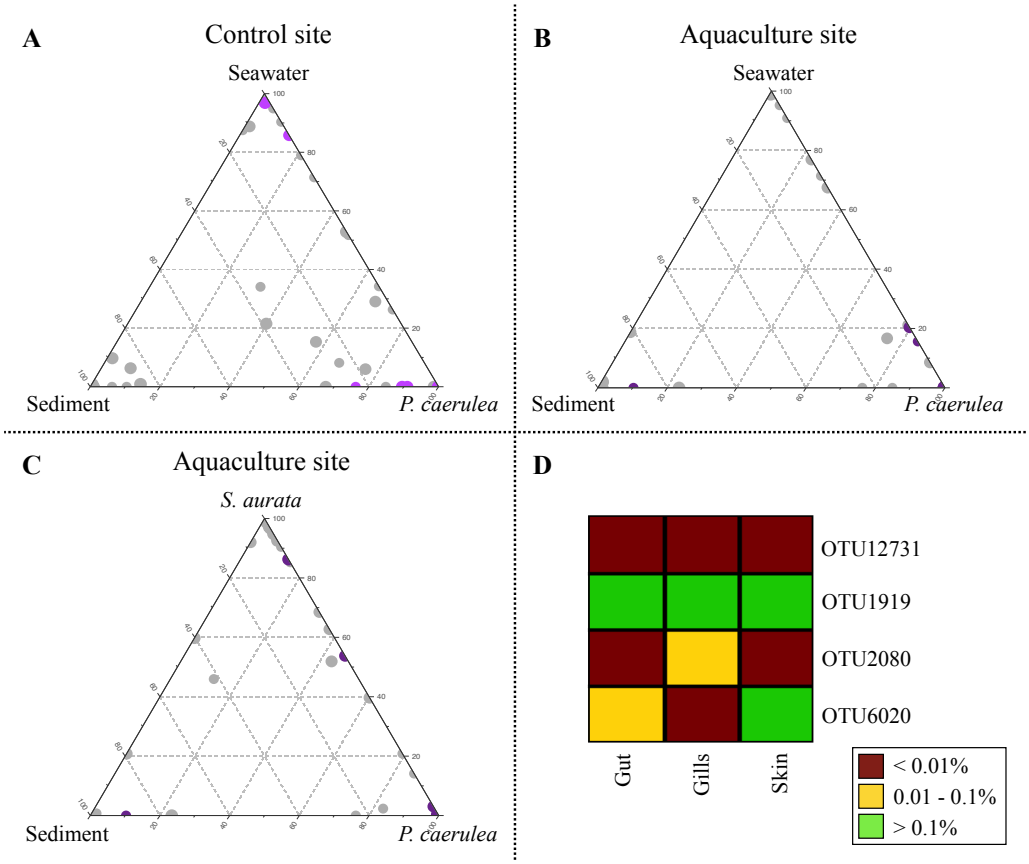

Figure 18 - **Impact of aquaculture cage proximity on *P. caerulea* microbiome at 97% similarity OTUs level.** (A, B, C) Ternary plots of all OTUs detected in the dataset with relative abundance > 0.5% in at least one sample. Each circle represents one OTU and the size is proportional to the weighted relative abundance. The position of each circle in the graphs represents its propensity toward the different ecosystems at the edges. (A) Purple circles represent the 22 OTUs whose mean relative abundance was significantly higher in the *P. caerulea* control site (FDR-corrected Wilcoxon rank-sum test, p-value ≤ 0.05). (B, C) Purple circles represent the 28 OTUs whose mean relative abundance was significantly higher in the *P. caerulea* aquaculture site (FDR-corrected Wilcoxon rank-sum test, p-value ≤ 0.05). (D) The heatmap represents the differential distribution of the OTUs shared between *P. caerulea* and farmed sea breams in the fish ecosystems (gut, gills and skin).

Discussion

Monitoring and preservation of coastal marine ecosystems are pivotal for the maintenance of the ecological and economical services that these environments provide, such as habitat provision, nutrient cycling, protection of the coast itself, and food provision through fishery and farming (Liquete et al., 2013; Trevathan-Tackett, et al., 2019). Aquaculture provides a relevant contribution to the food economy of

Mediterranean countries. However, similarly to most of the human food production activities, mariculture influences environmental conditions in the surrounding water column, as evidenced by the decline in seawater pH and subsequent shifts in carbonate-bicarbonate equilibria highlighted in the current study (Supplementary Table S3), with direct and indirect impacts on marine biota (Grigorakis and Rigos, 2011). Particularly, the health and functionality of the marine and coastal ecosystems are tightly linked to the resident environmental microbiomes, as well as to the ones associated with local holobionts. However, research focused on the impact of marine aquaculture on the coastal marine microbiomes is still in its infancy. While a considerable amount of work has been performed to assess the impact of aquaculture practices on the underlying seafloor microbial communities (Luna et al., 2013; Hornick and Buschmann, 2018; Ape et al., 2019; Moncada et al., 2019; Rubio-Portillo et al., 2019; Shi et al., 2019; Zhang et al., 2020), very few preliminary data have been provided linking the presence of fish farming cages to variations in the microbiome of benthic organisms living in close proximity (Baquiran and Conaco, 2018). In this scenario, we explored the impact of gilthead sea bream cage farming in the Licata harbor, Sicily, Italy, on the microbiome of locally dwelling wild species, by using a commonly found grazer gastropod (the limpet *Patella caerulea*) as a representative organism. In particular, we explained the variations of the limpet DG microbiomes at the aquaculture and control sites in the context of parallel changes in the local marine metacommunities, including water, sediments and farmed fish microbiomes.

In spite of being a crucial keystone species in coastal environments, very little information is available on the microbiome of limpets up to now, with the exception of a first exploration of the microbiome of *P. pellucida*, a prevalently Atlantic species that mostly parasitizes brown algae stems (Dudek et al., 2014). Consistently, the DG microbiome of *P. caerulea* analyzed in our work was dominated by Proteobacteria, but the most abundant class was Alphaproteobacteria instead of Betaproteobacteria, as reported for *P. pellucida*. Differences in proteobacterial classes could be related to several factors, including the different sustaining strategy of the two *Patella* species (with *P. caerulea* grazing on hard material algal coverage vs. *P. pellucida* parasitizing a single algal species), as well as the different environmental conditions characterizing the sampling areas (warm, shallow Mediterranean waters vs. Atlantic cold water). Also, while *P. pellucida* harbored a large amount of Firmicutes, the second most abundant phylum in *P. caerulea* was Planctomycetes. The DG microbiome of *P. caerulea* was significantly different from the microbiomes in the surrounding environment (water and nearby seafloor samples), confirming previous studies on aquatic holobionts and their ability to operate a non-neutral selection process of microbes from the surrounding environment (Pita et al., 2018; Cleary et al., 2019; Wilkins et al., 2019; Biagi et al., 2020).

In our work we were successful in demonstrating that limpets dwelling in proximity of aquaculture cages harbored a different DG microbiome compared to gastropods of the same species collected on distant rocky shores. Such difference was already evident when looking at the microbiome phylogenetic structure at phylum level, with Tenericutes largely abundant in samples collected on the cages, whereas samples from the rocky shores were enriched in Verrucomicrobia. Frequently in cooperation with Planctomycetes (Sizikov et al., 2020), members of Verrucomicrobia are capable of processing decaying organic materials and polysaccharides (Cabello-Yeves et al., 2017; Sichert et al., 2020). Several studies have highlighted their symbiotic lifestyle in marine invertebrates with recent findings showing metabolic adaptations enabling a more efficient utilization of specific carbon sources present in the host (King et al., 2012; Cleary et al., 2019;

Sizikov et al., 2020). However, we observed that the proximity to the aquaculture site was associated with the reduction of the Verrucomicrobia uncultured family DEV007 in the limpet microbiome of limpets. DEV007 is a marine group of bacteria recently pointed out as particularly sensitive to metal pollution in surface waters and marine sediments (Cornall et al., 2016; Baltar et al., 2018). Its decrease in limpets growing in adhesion to the aquaculture cage might be related to the increase in heavy metal accumulation that often accompanies aquaculture practices (Grigorakis and Rigos, 2011), and which can indirectly affect the most sensitive species in the microbiome of nearby wild organisms. Conversely, among the discriminant OTUs enriched in the microbiome of limpets collected on the aquaculture cage, we could find two OTUs putatively assigned to environmental bacteria that are instead reported as able to tolerate heavy metal pollution, namely *Acinetobacter guillouie* and *Mesorhizobium camelthorni* (Ontañon et al., 2018; Lamin et al., 2021).

Beside heavy metal contamination, the accumulation of organic matter on the seafloor beneath fish cages is considered one of the major impacts of aquaculture and may lead to a consequent depletion in oxygen availability in sediments, as well as to an increase in toxic products, such as sulphide and ammonium. Several studies have reported on the occurrence of sulfidobacteria in aquaculture, or nearby water, highlighting the potential importance of this taxa in the sulfur cycling within these systems (Duarte et al., 2019). Another bacterial species thriving in highly sulfidic fish-farm sediments is *Sulfurovum lithotrophicum*, a chemolithoautotroph ε-Proteobacteria able to use S^0 or $S_2O_3^{2-}$ as electron donors and O_2 or NO^{3-} as electron acceptors. *S. lithotrophicum* bacteria have been isolated in sediments from the oxic-anoxic interface where sulfides meet oxygenated seawater (Choi et al., 2018). The retrieval of higher relative abundances of OTU4065, assigned to *Sulfitobacter*, and OTU14234, belonging to the genus *Sulfurovum*, in *P. caerulea* individuals from the aquaculture site, as well as the observed sharing of the latter OTU with the aquaculture sediments, is in line with these previous findings, suggesting that the microbiome of locally dwelling holobionts might respond to environmental changes caused by the aquaculture practice (Cleary et al., 2019), i.e., heavy metal and sulphide accumulation, through the selection of environmental microorganisms allowing adaptive responses. Moreover, it was also shown that *Sulfitobacter* species might also have an inhibitory activity towards *Vibrio anguillarum*, an important fish pathogen (Sharifah and Eguchi, 2012). Thus, it is tempting to hypothesize that limpets might be pushed to select this particular bacterial group within their microbiome as a protective agent towards pathogens potentially enriched in the aquaculture site.

In relation to this, the possible pathogen flow from farmed to wild organisms in mariculture has been pointed out as an unavoidable problem of this particular aquaculture practice. Mollusks and other non-fish scavengers persist in the vicinity of sea cages for longer period than wild fishes, making them a target for pathogen transfer (Grigorakis and Rigos, 2011). We found that *Mycoplasmataceae*, the most abundant family within the phylum Tenericutes, tended to be more abundant in the DG microbiome from the limpets dwelling on the cages. Particularly, an OTU assigned to the genus *Mycoplasma* was the most relevant discriminating OTU between *P. cearulea* DG specimens taken at the two sites. Considering that many *Mycoplasma* species are parasitic or pathogenic to humans and other animals (Fraser et al., 1995; Feldman et al., 2006), these findings, together with the detection of OTUs assigned to potential fish pathogens from the genera *Vibrio* and *Acinetobacter* (Wang et al., 2010; Abdel-Aziz et al., 2013; Sohn et al., 2019;

Kuebutornye et al., 2020) as significantly most abundant in the DG microbiome from the limpets at the aquaculture cages, confirm that pathogen transfer between farmed fishes and wild limpets is possible. However, it must also be pointed out that Tenericutes, and particularly *Mycoplasma*, have been consistently observed as abundant, core members of several aquatic organisms' microbiome, mainly including bivalves, where they exhibit commensalism (Pierce, 2016; Aceves et al., 2018; Pierce and Ward, 2018 and 2019; Mathai et al., 2020; Marzocchi et al., 2021). A possible involvement in mutually beneficial interactions with the host - likely by assisting an efficient processing of complex organic compounds, abundant at aquaculture sites - is being progressively assumed (Fraune and Zimmer, 2008; Holm and Heidelberg, 2016; Marzocchi et al., 2021) and corroborates the idea of a possible role of fouling organisms in reducing the environmental impact of aquaculture (Montalto et al., 2020). Since the OTUs assigned to the genera *Mycoplasma*, *Vibrio* and *Acinetobacter* enriched in the DG microbiome from *P. caerulea* at the aquaculture site were not detectable in farmed fish samples and no disease was reported at the fish farming plant at the moment of sampling, we could hypothesize that relationships like commensalism, rather than parasitism or pathogenicity, occurred between *P. caerulea* and OTUs belonging to these genera. However, their detection in DG microbiomes from aquaculture still poses questions on their possible spread in the surrounding environment, in the nearby wild organisms as well as to humans, to which they are pathogens.

We also found two OTUs (12731 and 11913) assigned to the *Sphingomonas* genus, shared between limpets and fish, which were significantly more abundant in limpets at the aquaculture site. *Sphingomonas* is a bacterial genus commonly found in fish skin (Minich et al., 2020) and gut microbiome, and in farmed sea breams specifically, as reported by Floris *et al.* (2013) and Estruch *et al.* (2015). In particular, *Sphingomonas* has been reported as part of the fish beneficial microbiota (Legrand et al., 2020), and strains of this genus isolated from the gut microbiome of gilthead sea bream exhibited antibacterial activity against fish pathogens, such as *Vibrio alginolyticus* and *Photobacterium damselae* (Floris et al., 2018). It is thus tempting to speculate that the observed enrichment in these microorganisms in the DG microbiome of *P. caerulea* growing in the aquaculture site represents a protective feature, resulting from an adaptive selection of protective microbiome components from the farmed fish.

The study presented here has a preliminary nature and it cannot be excluded that our findings might specifically related to the considered model (i.e., the selected fish species, the selected wild grazing organism as well as the specific Licata harbor environment). However, it represents a successful application of an unprecedented approach, by considering a locally dwelling holobiont, i.e., the limpet, as a "proxy" for the pervasive effects that aquaculture cages can exert on wild life. Indeed, even if confirmation on different temporal and spatial scales are still needed, our results support the hypothesis that aquaculture impacts the surrounding microbial communities, not only the ones from underlying sediments, but also the microbiome of locally dwelling wild holobionts. According to our data, this seems to happen either directly, through the transfer of microorganisms from the farmed fish microbiomes to the microbiomes of local wild holobionts, and indirectly, with the aquaculture practice changing the chemical conditions of the environment, resulting in the selection of specific microbiome components in the local marine metacommunities. Changes in *P. caerulea* DG microbiome in individuals growing at the aquaculture site involve the loss of several microorganisms assigned to bacteria commonly found in wild marine organisms, as well as the concomitant acquisition of potential fish and human pathogens and parasites, resulting in an

overall significantly lower ecosystem biodiversity. Even if these features generally mirror dysbiotic changes, we were also able to observe possible adaptive microbiome variations, showing the inherent potential of holobiont microbiomes in enabling host adaptation to the changing environment, including changes resulting from marine aquaculture practices. Our study demonstrates the impact of using wider metacommunity approaches through the use of sedentary organisms as a proxy for metacommunity changes. Future studies may assess the viability and efficacy of other sedentary organisms that dwell on aquaculture cages (e.g., bivalves, tunicates polychaetes and fouling algae) to assess changes to different components of an ecosystem created by human activity, possibly using a longitudinal approach along the aquaculture productive cycles.

References

Abdel-Aziz, M., Eissa, A. E., Hanna, M., & Abou Okada, M. (2013). Identifying some pathogenic Vibrio/ Photobacterium species during mass mortalities of cultured Gilthead seabream (Sparus aurata) and European seabass (Dicentrarchus labrax) from some Egyptian coastal provinces. *International Journal of Veterinary Science and Medicine*, *1*(2), 87-95.

Aceves, A. K., Johnson, P., Bullard, S. A., Lafrentz, S., & Arias, C. R. (2018). Description and characterization of the digestive gland microbiome in the freshwater mussel Villosa nebulosa (Bivalvia: Unionidae). *Journal of Molluscan Studies*, *84*(3), 240-246.

Adair, K. L., & Douglas, A. E. (2017). Making a microbiome: the many determinants of host-associated microbial community composition. *Current Opinion in Microbiology*, *35*, 23-29.

Ape, F., Manini, E., Quero, G. M., Luna, G. M., Sarà, G., Vecchio, P., ... & Mirto, S. (2019). Biostimulation of in situ microbial degradation processes in organically-enriched sediments mitigates the impact of aquaculture. *Chemosphere*, *226*, 715-725.

Baltar, F., Gutiérrez-Rodríguez, A., Meyer, M., Skudelny, I., Sander, S., Thomson, B., ... & Morales, S. E. (2018). Specific effect of trace metals on marine heterotrophic microbial activity and diversity: Key role of iron and zinc and hydrocarbon-degrading bacteria. *Frontiers in microbiology*, *9*, 3190.

Baquiran, J. I. P., & Conaco, C. (2018). Sponge-microbe partnerships are stable under eutrophication pressure from mariculture. *Marine pollution bulletin*, *136*, 125-134.

Biagi, E., Caroselli, E., Barone, M., Pezzimenti, M., Teixido, N., Soverini, M., ... & Candela, M. (2020). Patterns in microbiome composition differ with ocean acidification in anatomic compartments of the Mediterranean coral Astroides calycularis living at CO2 vents. *Science of The Total Environment*, *724*, 138048.

Bordenstein, S. R., & Theis, K. R. (2015). Host biology in light of the microbiome: ten principles of holobionts and hologenomes. *PLoS biology*, *13*(8), e1002226.

Cabello-Yeves, P. J., Ghai, R., Mehrshad, M., Picazo, A., Camacho, A., & Rodriguez-Valera, F. (2017). Reconstruction of diverse verrucomicrobial genomes from metagenome datasets of freshwater reservoirs. *Frontiers in microbiology*, *8*, 2131.

Caporaso, J. G., Kuczynski, J., Stombaugh, J., Bittinger, K., Bushman, F. D., Costello, E. K., ... & Knight, R. (2010). QIIME allows analysis of high-throughput community sequencing data. *Nature methods*, *7*(5), 335-336.

Cavicchioli, R., Ripple, W. J., Timmis, K. N., Azam, F., Bakken, L. R., Baylis, M., ... & Webster, N. S. (2019). Scientists' warning to humanity: microorganisms and climate change. *Nature Reviews Microbiology*, *17*(9), 569-586.

Choi, A., Cho, H., Kim, B., Kim, H. C., Jung, R. H., Lee, W. C., & Hyun, J. H. (2018). Effects of finfish aquaculture on biogeochemistry and bacterial communities associated with sulfur cycles in highly sulfidic sediments. *Aquaculture Environment Interactions*, *10*, 413-427.

Cleary, D. F., Swierts, T., Coelho, F. J., Polónia, A. R., Huang, Y. M., Ferreira, M. R., ... & de Voogd, N. J. (2019). The sponge microbiome within the greater coral reef microbial metacommunity. *Nature communications*, *10*(1), 1-12.

Coleman, R. A., Underwood, A. J., Benedetti-Cecchi, L., Åberg, P., Arenas, F., Arrontes, J., ... & Hawkins, S. J. (2006). A continental scale evaluation of the role of limpet grazing on rocky shores. *Oecologia*, *147*(3), 556-564.

Cornall, A., Rose, A., Streten, C., McGuinness, K., Parry, D., & Gibb, K. (2016). Molecular screening of microbial communities for candidate indicators of multiple metal

impacts in marine sediments from northern Australia. *Environmental toxicology and chemistry*, *35*(2), 468-484.

Culhane, A. C., Thioulouse, J., Perrière, G., & Higgins, D. G. (2005). MADE4: an R package for multivariate analysis of gene expression data. *Bioinformatics*, *21*(11), 2789-2790.

Della Santina, P., & Chelazzi, G. (1991). Temporal organization of foraging in two Mediterranean limpets, Patella rustica L. and P. coerulea L. *Journal of experimental marine biology and ecology*, *153*(1), 75-85.

Dickson, A. G., & Millero, F. J. (1987). A comparison of the equilibrium constants for the dissociation of carbonic acid in seawater media. *Deep Sea Research Part A. Oceanographic Research Papers*, *34*(10), 1733-1743.

Dickson, A. G. (1990). Thermodynamics of the dissociation of boric acid in synthetic seawater from 273.15 to 318.15 K. *Deep Sea Research Part A. Oceanographic Research Papers*, *37*(5), 755-766.

Duarte, L. N., Coelho, F. J., Oliveira, V., Cleary, D. F., Martins, P., & Gomes, N. C. (2019). Characterization of bacterioplankton communities from a hatchery recirculating aquaculture system (RAS) for juvenile sole (Solea senegalensis) production. *PloS one*, *14*(1), e0211209.

Dudek, M., Adams, J., Swain, M., Hegarty, M., Huws, S., & Gallagher, J. (2014). Metaphylogenomic and potential functionality of the limpet Patella pellucida's gastrointestinal tract microbiome. *International journal of molecular sciences*, *15*(10), 18819-18839.

Estruch, G., Collado, M. C., Peñaranda, D. S., Tomás Vidal, A., Jover Cerdá, M., Pérez Martínez, G., & Martinez-Llorens, S. (2015). Impact of fishmeal replacement in diets for gilthead sea bream (Sparus aurata) on the gastrointestinal microbiota determined by pyrosequencing the 16S rRNA gene. *PloS one*, *10*(8), e0136389.

Faith, D. P. (1992). Conservation evaluation and phylogenetic diversity. *Biological conservation*, *61*(1), 1-10.

Feldman, S. H., Wimsatt, J., Marchang, R. E., Johnson, A. J., Brown, W., Mitchell, J. C., & Sleeman, J. M. (2006). A novel mycoplasma detected in association with upper respiratory disease syndrome in free-ranging eastern box turtles (Terrapene carolina carolina) in Virginia. *Journal of Wildlife Diseases*, *42*(2), 279-289.

Ferreira, C., Soares, A. R., Lamosa, P., Santos, M. A., & Da Costa, M. S. (2016). Comparison of the compatible solute pool of two slightly halophilic planctomycetes species, Gimesia maris and Rubinisphaera brasiliensis. *Extremophiles*, *20*(6), 811-820.

Floris, R., Manca, S., & Fois, N. (2013). Microbial ecology of intestinal tract of gilthead sea bream (Sparus aurata Linnaeus, 1758) from two coastal lagoons of Sardinia (Italy). *Transitional Waters Bulletin*, *7*(2), 4-12.

Floris, R., Scanu, G., Fois, N., Rizzo, C., Malavenda, R., Spanò, N., & Lo Giudice, A. (2018). Intestinal bacterial flora of Mediterranean gilthead sea bream (Sparus aurata Linnaeus) as a novel source of natural surface active compounds. *Aquaculture Research*, *49*(3), 1262-1273.

Fraser, C. M., Gocayne, J. D., White, O., Adams, M. D., Clayton, R. A., Fleischmann, R. D., ... & Venter, J. C. (1995). The minimal gene complement of Mycoplasma genitalium. *Science*, *270*(5235), 397-404.

Fraune, S., & Zimmer, M. (2008). Host-specificity of environmentally transmitted Mycoplasma-like isopod symbionts. *Environmental Microbiology*, *10*(10), 2497-2504.

Grigorakis, K., & Rigos, G. (2011). Aquaculture effects on environmental and public welfare–the case of Mediterranean mariculture. *Chemosphere*, *85*(6), 899-919.

Hamilton, N. E., & Ferry, M. (2018). ggtern: Ternary diagrams using ggplot2. *Journal of Statistical Software*, *87*(1), 1-17.

Haro-Moreno, J. M., Coutinho, F. H., Zaragoza-Solas, A., Picazo, A., Almagro-Moreno, S., & López-Pérez, M. (2020). Dysbiosis in marine aquaculture revealed through microbiome analysis: Reverse ecology for environmental sustainability. *FEMS Microbiology Ecology*, *96*(12), fiaa218.

Holm, J. B., & Heidelberg, K. B. (2016). Microbiomes of Muricea californica and M. fruticosa: comparative analyses of two co-occurring eastern Pacific octocorals. *Frontiers in Microbiology*, *7*, 917.

Holmer, M., Duarte, C. M., Heilskov, A., Olesen, B., & Terrados, J. (2003). Biogeochemical conditions in sediments enriched by organic matter from net-pen fish farms in the Bolinao area, Philippines. *Marine Pollution Bulletin*, *46*(11), 1470-1479.

Hornick, K. M., & Buschmann, A. H. (2018). Insights into the diversity and metabolic function of bacterial communities in sediments from Chilean salmon aquaculture sites. *Annals of microbiology*, *68*(2), 63-77.

Infante-Dominguez, C., Lawson, P. A., Johnson, C. N., Sanchez-Porro, C., & Ventosa, A. (2015). Fodinicurvata halophila sp. nov., a moderately halophilic bacterium from a marine saltern. *International journal of systematic and evolutionary microbiology*, *65*(Pt_3), 766-771.

Kalantzi, I., Rico, A., Mylona, K., Pergantis, S. A., & Tsapakis, M. (2021). Fish farming, metals and antibiotics in the eastern

Mediterranean Sea: Is there a threat to sediment wildlife?. *Science of The Total Environment*, *764*, 142843.

Kallscheuer, N., Jogler, M., Wiegand, S., Peeters, S. H., Heuer, A., Boedeker, C., ... & Jogler, C. (2020). Rubinisphaera italica sp. nov. isolated from a hydrothermal area in the Tyrrhenian Sea close to the volcanic island Panarea. *Antonie Van Leeuwenhoek*, *113*(12), 1727-1736.

Karakassis, I., Tsapakis, M., Hatziyanni, E., Papadopoulou, K. N., & Plaiti, W. (2000). Impact of cage farming of fish on the seabed in three Mediterranean coastal areas. *ICES Journal of Marine Science*, *57*(5), 1462-1471.

King, G. M., Judd, C., Kuske, C. R., & Smith, C. (2012). Analysis of stomach and gut microbiomes of the eastern oyster (Crassostrea virginica) from coastal Louisiana, USA. *PLoS one*, *7*(12), e51475.

Kuebutornye, F. K., Abarike, E. D., Lu, Y., Hlordzi, V., Sakyi, M. E., Afriyie, G., ... & Xie, C. X. (2020). Mechanisms and the role of probiotic Bacillus in mitigating fish pathogens in aquaculture. *Fish physiology and biochemistry*, 1-23.

Lamin, H., Alami, S., Bouhnik, O., Bennis, M., Benkritly, S., Abdelmoumen, H., ... & Missbah-El Idrissi, M. (2021). Identification of the endosymbionts from Sulla spinosissima growing in a lead mine tailings in Eastern Morocco as Mesorhizobium camelthorni sv. aridi. *Journal of Applied Microbiology*, *130*(3), 948-959.

Legrand, T. P., Wynne, J. W., Weyrich, L. S., & Oxley, A. P. (2020). A microbial sea of possibilities: current knowledge and prospects for an improved understanding of the fish microbiome. *Reviews in Aquaculture*, *12*(2), 1101-1134.

Leibold, M. A., Holyoak, M., Mouquet, N., Amarasekare, P., Chase, J. M., Hoopes, M. F., ... & Gonzalez, A. (2004). The metacommunity concept: a framework for multi-scale community ecology. *Ecology letters*, *7*(7), 601-613.

Liquete, C., Piroddi, C., Drakou, E. G., Gurney, L., Katsanevakis, S., Charef, A., & Egoh, B. (2013). Current status and future prospects for the assessment of marine and coastal ecosystem services: a systematic review. *PloS one*, *8*(7), e67737.

Luna, G. M., Corinaldesi, C., Dell'Anno, A., Pusceddu, A., & Danovaro, R. (2013). Impact of aquaculture on benthic virus–prokaryote interactions in the Mediterranean Sea. *Water research*, *47*(3), 1156-1168.

Marzocchi, U., Bonaglia, S., Zaiko, A., Quero, G. M., Vybernaite-Lubiene, I., Politi, T., ... & Cardini, U. (2021). Zebra mussel holobionts fix and recycle nitrogen in lagoon sediments. *Frontiers in microbiology*, 3620.

Mathai, P. P., Magnone, P., Dunn, H. M., & Sadowsky, M. J. (2020). Water and sediment act as reservoirs for microbial taxa associated with invasive dreissenid mussels. *Science of the Total Environment*, *703*, 134915.

Mehrbach, C., Culberson, C. H., Hawley, J. E., & Pytkowicx, R. M. (1973). Measurement of the apparent dissociation constants of carbonic acid in seawater at atmospheric pressure 1. *Limnology and oceanography*, *18*(6), 897-907.

Mente, E., Nikouli, E., Antonopoulou, E., Martin, S. A., & Kormas, K. A. (2018). Core versus diet-associated and postprandial bacterial communities of the rainbow trout (Oncorhynchus mykiss) midgut and faeces. *Biology Open*, *7*(6), bio034397.

Meyer, D.; Zeileis, A.; Hornik, K. vcd: Visualizing Categorical Data. *R package* version 1.4-8, 2020.

Minich, J. J., Poore, G. D., Jantawongsri, K., Johnston, C., Bowie, K., Bowman, J., ... & Allen, E. E. (2020). Microbial ecology of Atlantic salmon (Salmo salar) hatcheries: impacts of the built environment on fish mucosal microbiota. *Applied and environmental microbiology*, *86*(12), e00411-20.

Moncada, C., Hassenrück, C., Gärdes, A., & Conaco, C. (2019). Microbial community composition of sediments influenced by intensive mariculture activity. *FEMS microbiology ecology*, *95*(2), fiz006.

Montalto, V., Rinaldi, A., Ape, F., Mangano, M. C., Gristina, M., Sarà, G., & Mirto, S. (2020). Functional role of biofouling linked to aquaculture facilities in Mediterranean enclosed locations. *Aquaculture Environment Interactions*, *12*, 11-22.

Musella, M., Wathsala, R., Tavella, T., Rampelli, S., Barone, M., Palladino, G., ... & Candela, M. (2020). Tissue-scale microbiota of the Mediterranean mussel (Mytilus galloprovincialis) and its relationship with the environment. *Science of The Total Environment*, *717*, 137209.

Ontañon, O. M., Landi, C., Carleo, A., Gagliardi, A., Bianchi, L., González, P. S., ... & Bini, L. (2018). What makes A. guillouiae SFC 500-1A able to co-metabolize phenol and Cr (VI)? A proteomic approach. *Journal of hazardous materials*, *354*, 215-224.

Pierce, M. L. (2016). The Microbiome of the eastern oyster, Crassostrea virginica (Gmelin, 1791): Temporal and spatial variation, environmental influences, and its impact on host physiology.

Pierce, M. L., & Ward, J. E. (2018). Microbial ecology of the Bivalvia, with an emphasis on the family Ostreidae. *Journal of Shellfish Research*, *37*(4), 793-806.

Pierce, M. L., & Ward, J. E. (2019). Gut microbiomes of the eastern oyster (Crassostrea virginica) and the blue mussel (mytilus edulis): Temporal variation and the influence of marine aggregate-associated microbial communities. *Msphere*, *4*(6), e00730-19.

Pita, L., Rix, L., Slaby, B. M., Franke, A., & Hentschel, U. (2018). The sponge holobiont in a changing ocean: from microbes to ecosystems. *Microbiome*, *6*(1), 1-18.

Pohlert, T. (2014). The pairwise multiple comparison of mean ranks package (PMCMR). *R package*, *27*(2019), 9.

Quero, G. M., Perini, L., Pesole, G., Manzari, C., Lionetti, C., Bastianini, M., ... & Luna, G. M. (2017). Seasonal rather than spatial variability drives planktonic and benthic bacterial diversity in a microtidal lagoon and the adjacent open sea. *Molecular ecology*, *26*(21), 5961-5973.

Reguera, P., Couceiro, L., & Fernández, N. (2018). A review of the empirical literature on the use of limpets Patella spp. (Mollusca: Gastropoda) as bioindicators of environmental quality. *Ecotoxicology and environmental safety*, *148*, 593-600.

Rosa, R., Marques, A., & Nunes, M. L. (2012). Impact of climate change in Mediterranean aquaculture. *Reviews in Aquaculture*, *4*(3), 163-177.

Rubio-Portillo, E., Villamor, A., Fernandez-Gonzalez, V., Antón, J., & Sanchez-Jerez, P. (2019). Exploring changes in bacterial communities to assess the influence of fish farming on marine sediments. *Aquaculture*, *506*, 459-464.

San Diego-McGlone, M. L., Azanza, R. V., Villanoy, C. L., & Jacinto, G. S. (2008). Eutrophic waters, algal bloom and fish kill in fish farming areas in Bolinao, Pangasinan, Philippines. *Marine Pollution Bulletin*, *57*(6-12), 295-301.

Sanz-Lázaro, C., Belando, M. D., Marín-Guirao, L., Navarrete-Mier, F., & Marín, A. (2011). Relationship between sedimentation rates and benthic impact on Maërl beds derived from fish farming in the Mediterranean. *Marine Environmental Research*, *71*(1), 22-30.

Sharifah, E. N., & Eguchi, M. (2012). Mixed cultures of the phytoplankton Nannochloropsis oculata and the marine bacterium Sulfitobacter sp. RO3 inhibit the growth of virulent strains of the major fish pathogen Vibrio anguillarum. *Aquaculture Science*, *60*(1), 39-45.

Shi, R., Xu, S., Qi, Z., Zhu, Q., Huang, H., & Weber, F. (2019). Influence of suspended mariculture on vertical distribution profiles of bacteria in sediment from Daya Bay, Southern China. *Marine pollution bulletin*, *146*, 816-826.

Sichert, A., Corzett, C. H., Schechter, M. S., Unfried, F., Markert, S., Becher, D., ... & Hehemann, J. H. (2020). Verrucomicrobia use hundreds of enzymes to digest the algal polysaccharide fucoidan. *Nature microbiology*, *5*(8), 1026-1039.

Sizikov, S., Burgsdorf, I., Handley, K. M., Lahyani, M., Haber, M., & Steindler, L. (2020). Characterization of sponge-associated Verrucomicrobia: microcompartment-based sugar utilization and enhanced toxin–antitoxin modules as features of host-associated Opitutales. *Environmental microbiology*, *22*(11), 4669-4688.

Sohn, H., Kim, J., Jin, C., & Lee, J. (2019). Identification of Vibrio species isolated from cultured olive flounder (Paralichthys olivaceus) in Jeju Island, South Korea. *Fisheries and Aquatic Sciences*, *22*(1), 1-8.

Tičina, V., Katavić, I., & Grubišić, L. (2020). Marine Aquaculture Impacts on Marine Biota in Oligotrophic Environments of the Mediterranean Sea–A Review. *Frontiers in Marine Science*, *7*, 217.

Trevathan-Tackett, S. M., Sherman, C. D., Huggett, M. J., Campbell, A. H., Laverock, B., Hurtado-McCormick, V., ... & Macreadie, P. I. (2019). A horizon scan of priorities for coastal marine microbiome research. *Nature ecology & evolution*, *3*(11), 1509-1520.

Viñas, L., Pérez-Fernández, B., Soriano, J. A., López, M., Bargiela, J., & Alves, I. (2018). Limpet (Patella sp) as a biomonitor for organic pollutants. A proxy for mussel?. *Marine pollution bulletin*, *133*, 271-280.

Wang, Y., Zhang, X. H., Yu, M., Wang, H., & Austin, B. (2010). Vibrio atypicus sp. nov., isolated from the digestive tract of the Chinese prawn (Penaeus chinensis O'sbeck). *International journal of systematic and evolutionary microbiology*, *60*(11), 2517-2523.

Wilkins, L. G., Leray, M., O'Dea, A., Yuen, B., Peixoto, R. S., Pereira, T. J., ... & Eisen, J. A. (2019). Host-associated microbiomes drive structure and function of marine ecosystems. *PLoS biology*, *17*(11), e3000533.

Yoon, J. H., Lee, C. H., Kang, S. J., & Oh, T. K. (2005). Psychrobacter celer sp. nov., isolated from sea water of the South Sea in Korea. *International Journal of Systematic and Evolutionary Microbiology*, *55*(5), 1885-1890.

Yosef, D. Z. B., Ben-Dov, E., & Kushmaro, A. (2008). Amorphus coralli gen. nov., sp. nov., a marine bacterium isolated from coral mucus, belonging to the order Rhizobiales.

International journal of systematic and evolutionary microbiology, *58*(12), 2704-2709.

Zhang, K., Zheng, X., He, Z., Yang, T., Shu, L., Xiao, F., ... & Yan, Q. (2020). Fish growth enhances microbial sulfur cycling in aquaculture pond sediments. *Microbial biotechnology*, *13*(5), 1597-1610.

2.6 Study IV — Functional and taxonomic shifts of bacterial communities associated with mucus, tissue and skeleton of the coral *Balanophyllia europea* living along a natural CO_2 gradient

Introduction

Scleractinian corals live in close association with a diverse array of phylogenetically disparate microorganisms, including endocellular photoautotrophic dinoflagellate symbionts (belonging to the Symbiodiniaceae family) and complex communities of bacteria, archaea, viruses, and unicellular eukaryotes (i.e., microbiomes). Indeed, each coral anatomic compartment (i.e., surface mucus, soft tissue, and skeleton) constitutes a microhabitat characterized by specific conditions supporting different micro-ecosystems (Vanwonterghem and Webster, 2020). The consortium of coexisting pluri- and unicellular organisms is termed "coral holobiont" and acts as a single entity to maintain organismal function under varying environmental conditions (Goulet et al., 2020; Voolstra and Ziegler, 2020). Indeed, complex bacteria communities inhabiting coral mucus, tissue, and skeleton exert a crucial role in ensuring the health and survival of the coral as they provide their host with a variety of functions, such as assistance in recovering and recycling of nutrients (carbon, nitrogen and sulfur, but also vitamins and essential amino acids), protection against pathogens invasion, and production of chemicals that drive larval settlement (McDevitt-Irwin et al., 2017; McFall-Ngai et al., 2013; Morrow et al., 2012; O'Brien et al., 2018; Rohwer et al., 2001 and 2002; Rosenberg et al., 2007).

Besides being tightly related to the host phylogeny, the composition and metabolism of coral microbiomes change temporally (across seasons and along coral lifespan), spatially (across the compartments defined by the coral anatomy), and in response to environmental variations (Dunphy et al., 2019; van Oppen and Blackall, 2019; Vanwonterghem and Webster, 2020). Shifts in coral microbiome composition in response to environmental changes may affect the co-metabolic networks, possibly contributing to the acclimatization of coral holobiont. Indeed, microbial communities as a whole have the possibility to acclimatize faster than their metazoan host to environmental changes, thanks to their greater genetic diversity, shorter generational time, and remarkable metabolic potential (Bourne et al., 2016; Torda et al., 2017). Such propensity for a fast response to environmental changes has been investigated as possibly involved in the acclimatization and adaptation of coral holobiont to climate change-related phenomena, such as ocean warming and ocean acidification (OA) (Stocker et al., 2013; Rosenberg et al., 2007; Torda et al., 2017; Voolstra and Ziegler, 2020; Putnam, 2021).

Ocean acidity has increased worldwide by 25–30% (0.1 pH units) since the beginning of the nineteenth century, and it is expected to drop by a further 0.29 pH units by 2080-2100 (Stocker et al., 2013; Bindoff *et al.*, 2019). OA is expected to alter the survival, growth, and reproduction of key components of marine ecosystems, especially calcifying species (Hoegh-Guldberg et al., 2017), both at microbial and multicellular levels (Kroeker et al., 2010; Gattuso et al., 2015; Yu and Chen, 2019). Thus, it is of outmost importance, for projecting ecological processes in the forthcoming oceans, to understand how OA will affect the microbiome of important ecosystem forming organisms such as corals (Ingrosso et al., 2018). In this context, natural underwater CO_2 seeps represent a precious study system to understand how corals will respond to OA (Hassenrück et al., 2016; Tangherlini et al., 2021). The Mediterranean Sea, which will likely be one of the most affected seas by climate change (Lejeusne et al., 2010), hosts naturally acidified shallow sites with

relatively stable underwater CO_2 emission at ambient temperature with no detection of toxic compounds, that have been recognized as fundamental study models for OA (Teixido et al., 2020; Goffredo et al., 2014; Fantazzini et al., 2015).

To date, few studies have explored coral microbiome variations in natural coral populations at CO_2 seeps (Morrow et al., 2015; O'Brien et al., 2018; Kenkel et al., 2018; Biagi et al., 2020; Shore et al., 2021), showing different microbiome responses depending on the host species. For instance, at natural CO_2 seeps in Papua New Guinea, the endolithic community associated with massive *Porites* spp. does not change with pH (Marcelino et al., 2017; O'Brien et al., 2018), while large shifts in tissue-associated bacterial communities were found in *Acropora millepora* and *Porites cylindrica* (Morrow et al., 2015). Indeed, as recently highlighted by Shore and colleagues (2021), the response to decreasing pH of the microbiome associated with *Porites* corals seems to be species-specific and does not reflect a breakdown in bacteria-host symbiosis. In the Mediterranean coral *Astroides calycularis* growing at the Ischia CO_2 vents, the mucus-associated microbiome was more affected by acidification than soft tissue and skeleton, with a general increase in subdominant bacterial groups with OA, some of which may be involved in the nitrogen cycle (Biagi et al., 2020).

The target species of the present study is the solitary Mediterranean coral *Balanophyllia europaea* that naturally lives along a pH gradient generated by an underwater volcanic crater located close to Panarea Island (Italy). *B. europaea* is a temperate, zooxanthellate, scleractinian coral, widespread in the Mediterranean Sea, where it thrives on rocky substrates at a depth of 0-50 m (Goffredo et al., 2007). Populations of this simultaneous hermaphrodite and brooding coral (Goffredo et al., 2002) naturally growing along the CO_2 gradient are less abundant, less stable and decrease their net calcification rate with OA, while preserving their linear extension rate at the expense of skeletal bulk density, which strongly decreases (Goffredo et al., 2014; Fantazzini et al., 2015; Caroselli et al., 2019). Coral skeletons of *B. europaea* become more porous and less resistant to breakage as pH decreases, while nanoscale properties of calcium carbonate crystals are preserved (Fantazzini et al., 2015).

To date, the majority of the studies aiming at understanding the involvement of coral microbiomes in acclimatization to future acidified water conditions were focused on tropical and subtropical corals (Webster et al., 2016; Okazaki et al., 2017; O'Brien et al., 2018; Klein et al., 2021). However, temperate species, such as *B. europaea*, might represent a model for more pronounced acclimatization capability, being exposed to a twice as high range of seasonal temperature fluctuations and intrinsically more capable to accommodate environmental variations (Maor-Landaw et al., 2017). Here, we focus on the bacterial component of the *B. europaea* holobiont and on the variations in the metabolic potential of the microbial communities residing in surface mucus, soft tissue, and skeleton to the decreasing pH. The CO_2 seep near Panarea Island (Italy) from which samples were taken is an underwater crater at 10 m depth releases persistent gaseous emissions (98–99% CO_2 without instrumentally detectable toxic compounds), resulting in a stable pH gradient at ambient temperature that has been characterized in detail (Goffredo et al., 2014; Fantazzini et al., 2015; Prada et al., 2017). Sampling sites along this gradient match mean pH values projected for 2100 under different IPCC scenarios (Chen et al., 2021). Our approach, combining both 16S rRNA sequencing and shotgun metagenomics, allowed to highlight genetic functions included in the

microbial metagenome, their changes in coral holobionts acclimatized to different OA levels under natural conditions, and possible bacteria-related acclimatization processes.

Materials and methods

Samples collection

Nine coral specimens were haphazardly collected in July 2019 along a pH gradient at a CO_2 seep near Panarea Island (Italy) by SCUBA divers using a hammer and chisel and placed in plastic containers. Mucus was collected using cotton swabs on individual polyps immediately upon coral sampling (Biagi et al., 2020). At each site, close to corals collection point, three sediments (one for each site) were sampled in 50mL falcon tubes using a small shovel, and seawater was collected with sterile plastic bottles (2L per site). All samples were transported in ice to the laboratory and frozen at -80 °C until further processing.

Coral specimens processing and DNA extraction

Coral samples were processed to separate the different coral compartments (mucus, tissue, and skeleton) using standard protocols (Apprill et al., 2016; Rubio-Portillo et al., 2016; Biagi et al., 2020). Briefly, for mucus samples, the cotton tip of each swab was transferred into a 2 mL Eppendorf tube to which 500 µL of sterile artificial seawater (NaCl 450 mM, KCl 10 mM, $CaCl_2$ 9 mM, $MgCl_2{\cdot}6H_2O$ 30 mM, $MgSO_4{\cdot}7H_2O$ 16 mM, pH 7.8) were added. Samples were vortexed for 1 min and sonicated for 2 min, repeating these steps twice and finally vortexing for 1 min. Cotton swabs were then transferred in a new 2 mL Eppendorf tube and the process was repeated. Finally, cotton swabs were discarded and the suspensions of the same samples were joined and centrifuged at 9000 g for 5 min at 4 °C. Pellets were then stored at −80 °C until further processing. We processed each coral specimen by mechanical fragmentation using an agate mortar to separate coral soft tissue and carbonate skeletal matrix. Coral specimens were transferred into the mortar using sterile forceps and fragmented with the pestle with 10 mL of sterile artificial seawater (Biagi et al., 2020). Fragmented samples were transferred into a 250 mL beaker and an additional 20 mL of artificial seawater was used to wash the mortar and pestle from residues. The homogenates were incubated at RT for 15 minutes to allow skeletal fragments to settle. Afterwards, the suspension containing coral tissue was collected and transferred into two 15 mL tubes. Both tubes were centrifuged for 15 min at 9300 g at 4 °C to pellet the coral tissue fraction. The pellets were stored at -80 °C until further processing. For the skeletal fraction, skeleton samples were washed three times with 10 mL of artificial seawater with an incubation of 7 min at RT after each washing to allow the fragments to settle. After discarding the supernatant, skeletal fragments were collected and transferred into a 2 mL Eppendorf tube and kept frozen at -80 °C until further processing.

Total bacterial DNA was extracted from each sample using the DNeasy PowerBiofilm Kit (Qiagen, Hilden, Germany) (Palladino et al., 2021). About 0.1-0.2 g of skeleton samples were weighted and transferred into a PowerBiofilm Bead Tube before being resuspended in 350 mL of MBL solution. Mucus and tissue pellets were instead resuspended in 350 mL of MBL solution first and then transferred into a PowerBiofilm Bead Tube. Extracted DNA samples were quantified with NanoDrop ND-1000 (NanoDrop Technologies, Wilmington, DE, USA) and stored at -20 °C until further processing.

Environmental samples processing and DNA extraction

Each 2L of seawater sample was processed via vacuum filtration under sterile conditions using MF-Millipore (Darmstadt, Germany) membrane filters with 0.45-µm pore size, 47-mm diameter and mixed cellulose esters membrane. Each membrane filter was folded using sterilized forceps and placed into a PowerWater DNA Bead Tube and then stored at -80 °C until further processing. Seawater microbial DNA extraction was carried out using the DNeasy PowerWater Kit (Qiagen, Hilden, Germany) following the manufacturer's instructions.

Finally, 0.25-0.35 g of sediment samples was weighted into PowerBead Tubes and total bacterial DNA was extracted using the DNeasy PowerSoil Kit (Qiagen, Hilden, Germany) following the manufacturer's instructions.

Environmental DNA samples were quantified using NanoDrop ND-1000 (NanoDrop Technologies, Wilmington, DE, United States) and stored at -20°C until further processing.

16S rRNA gene amplification and sequencing

PCR amplification of the V3-V4 hypervariable region of the 16S rRNA gene, library preparation and sequencing were performed as described in paragraph 2.2.

Bacterial DNA enrichment, library preparation and shotgun sequencing

Coral DNA samples were subjected to a further processing for shotgun sequencing. Microbial DNA extracted from skeleton and tissue was enriched with the NEBNext Microbiome DNA Enrichment Kit to maximize the protocol efficiency (Feehery et al., 2013) following manufacturer's instructions. Both enriched DNA and total microbial DNA from mucus samples was quantified using Qubit fluorometer (Invitrogen, Waltham, MA, USA) and DNA libraries were prepared using the QIAseq FX DNA library kit (Qiagen, Hilden, Germany) in accordance with the manufacturer's instructions. Briefly, 100 ng of each DNA sample were fragmented to a 450-bp size, end-repaired, and A-tailed using FX enzyme mix with the following thermal cycle: 4°C for 1 min, 32°C for 8 min, and 65°C for 30 min. Adapter ligation was performed by incubating DNA samples at 20 °C for 15 min in the presence of DNA ligase and Illumina adapter barcodes. Following, a first purification step with Agencourt AMPure XP magnetic beads (Beckman Coulter, Brea, CA, USA), library amplification with a 10-cycle PCR amplification and a further step of purification were performed. Samples were pooled at equimolar concentrations of 4 nM to obtain the final library. Sequencing was performed on an Illumina NextSeq platform using a 2 x 150-bp paired-end protocol, following the manufacturer's instructions (Illumina, San Diego, CA, USA).

Bioinformatics and biostatistics

For the 16S rRNA gene analysis, aw sequences for a total of 33 samples were processed as described in paragraph 2.2.

For the shotgun sequencing analysis, raw reads for a total of 27 samples were filtered for PCR duplicates with Picard tool (EstimatedlibraryComplexity) (Toolkit, 2019). Next, Trimmomatic (v. 0.39) (Bolger et al., 2014) was adopted to remove adapters and low-quality bases, setting a minimum quality of 20, with reads length ranging from 35 to 151 bp. Fastqc was then applied to examine the quality of the reads prior and after the reads pre-processing steps (Andrews, 2010). Megahit was used to generate a co-assembly of all the 27 samples, setting a kmer list of 21, 41, 61, 81 and 99 (Liu et al., 2015). EukRep (v. 0.6.6) (West et al., 2018) was adopted to classify the contigs in prokaryotic and eukaryotic bins. The reads mapping to the

eukaryotic bin (Bowtie2, v. 2.3.5) (Langmead and Salzberg, 2012) were identified with Samtools (v 1.9) (Li et al., 2009) and eliminated from each sample (BBMap v. 38.22[18]). The taxonomic classification, at family, genus and species level was obtained with Kaiju (v. 1.7.0) (Menzel et al., 2016), with greedy mode, match length and match score of 11 and 65 respectively and considering both the paired and unpaired reads for each sample. Next, we performed reads functional annotation via MetaCV (v. 2059) (Liu et al., 2013), obtaining KO numbers and their associated KEGG pathway at different functional levels. For each KO, the associated reads were retrieved, and their corresponding taxonomic annotation was collected as obtained from Kaiju. Functional analysis at KO level was also performed by identifying increasing or decreasing trends for genes in samples at different conditions, considering the prevalence of genes among the three replicates from the same site.

Processed reads for 16S rRNA sequencing and for metagenomic sequencing are openly available in European Nucleotide Archive (ENA), reference number PRJEB48073.

All statistical analyses were performed using the R software[19], version 3.6.1, with the packages "Made4" (Culhane et al., 2005) and "vegan[20]". Beta diversity was estimated by computing the Bray-Curtis distance and the data separation in the Principal Coordinates Analysis (PCoA) was tested using a permutation test with pseudo-F ratios (function "adonis" in the vegan package). Wilcoxon rank-sum test was used to assess differences between replicates taken at different sites. P-values were corrected for multiple testing using the Benjamini–Hochberg method, with a false discovery rate (FDR) ≤ 0.05 considered statistically significant. A procrustean randomized test (function "protest" in the vegan package) was performed to highlight a significant association between the taxonomic and functional profiles on the microbiome across the entire dataset.

Results

Nine specimens of the coral *Balanophyllia europaea*, 3 sediment samples and 3 seawater samples were collected in July 2019 from three sites (3 coral individuals per site and 2 environmental samples per site, respectively) along a pH gradient at a CO_2 seep near Panarea Island (Italy). Site 1 (control) mean total scale pH (pH_{TS}) is 8.07, corresponding to surface pH of modern oceans; Site 2 (moderate acidification) mean pH_{TS} is 7.87, aligning with a conservative IPCC CO_2 emission scenario (SSP2-4.5); Site 3 (high acidification) mean pH_{TS} is 7.74 and it is aligned with a worst-case IPCC scenario (SSP3-7.0). Coral samples were processed to separate the 3 different compartments (mucus, soft tissue, and skeleton), obtaining 27 coral samples (Table 2).

Table 2 - Summary of *B. europaea* and environmental samples and features of the sampling sites.

	Environmental parameters		***B. europaea* samples**				**Environmental samples**		
	Sampling site	mean pH	Individuals	Mucus	Soft tissue	Skeleton	Seawater	Sediments	
	Site 1 (control)	8.07	3	3	3	3	1	1	
	Site 2 (mild acidification)	7.87	3	3	3	3	1	1	
	Site 3 (high acidification)	7.74	3	3	3	3	1	1	
Total				**9**	**9**	**9**	**3**	**3**	**33**

[18] http://sourceforge.net/projects/bbmap/

[19] R Core Team; www.r-project.org

[20] https://cran.r-project.org/web/packages/vegan/index.html

The microbiome compositional structure of the total 33 samples was obtained by NGS sequencing of the V3-V4 hyper variable region of the 16S rRNA gene, resulting in 298,545 high-quality reads with an average of 9,046 ± 3,764 reads per sample. High-quality reads were binned into 8,007 Amplicon Sequence Variants (ASVs). Shotgun sequencing analysis was then applied on the 27 coral samples. A total of 179,644,167 paired-end raw reads were generated, with an average of 6,653,487 ± 1,959,146 paired-reads per sample. After quality filtering, reads taxonomic classification resulted in a total of 4,174,277 taxonomically assigned reads (average 154,602 ± 241,549 per sample). The reads functional annotation per each sample yielded a total number of functionally classified reads of 72,222,759 (average 2,674,917 ± 3,028,259 per sample).

Balanophyllia europaea overall microbial compositional structure across compartments and acidification conditions

B. europaea mucus, tissue and skeleton microbiomes constituted separate communities from those of the surrounding environment, in terms of phylogenetic composition at genus level, as shown by the Principal Coordinate Analysis (PCoA) based on the Bray-Curtis distance based of 16S rRNA data (Figure 19A). Segregation of coral microbiomes was significant with respect to both seawater and sediment microbial communities (permutation test with pseudo-F ratio, p-value = 0.001), regardless of the coral compartment, although sediment and skeleton samples slightly overlapped on the PCoA plot.

The microbiomes of the 3 coral compartments significantly differed among each other, in terms of phylogenetic composition at the genus level, as observed by computing Bray-Curtis distances among samples using both 16S rRNA (Figure 19B) and shotgun metagenomic data (Figure 19C) (permutation test with pseudo-F ratio, p-value = 0.001 for both). Indeed, concordance between metagenomic and 16S rRNA data was highlighted by using a procrustean randomized test ("protest") (p-value = 0.001).

The compositional structure of the three compartments, as assigned using Kaiju on metagenomic data at phylum level (Supplementary Figure S9), was coherent with the available literature on the same coral species (Meron et al., 2012). In particular, Proteobacteria was the most abundant phylum in all coral compartments, with a prevalence of Alphaproteobacteria followed by Beta and Gammaproteobacteria, and with Bacteroidetes also listed among the dominant phyla.

Microbiome composition of corals living at different pH conditions along the Panarea gradient (i.e., at different distances from the crater) was assessed separately on the 3 anatomic compartments (Figures 19D to F). Microbial communities associated with mucus from corals taken at the control site (Site 1) and at both the acidified locations (Site 2 and 3) significantly differed in terms of composition, as shown by the separation in the PCoA based on Bray-Curtis distances among samples calculated using phylogenetic data obtained from shotgun metagenomic (Figure 19D; permutation test with pseudo-F ratio, p-value = 0.03). Such significant differences were not observed among microbial communities from soft tissue and skeleton (Figures 19E and F, respectively). Confirming these data, the community composition at the family level in mucus samples showed some noticeable trends of increasing relative abundance in members of the family Burkholderiaceae and decreasing relative abundance in reads assigned to the family Rhodobacteraceae from Site 1 to Site 3 (Supplementary Figure S10) (Wilcoxon rank sum test of Site 1 compared to Site 2 and 3, p-value = 0.05 and 0.02 respectively).

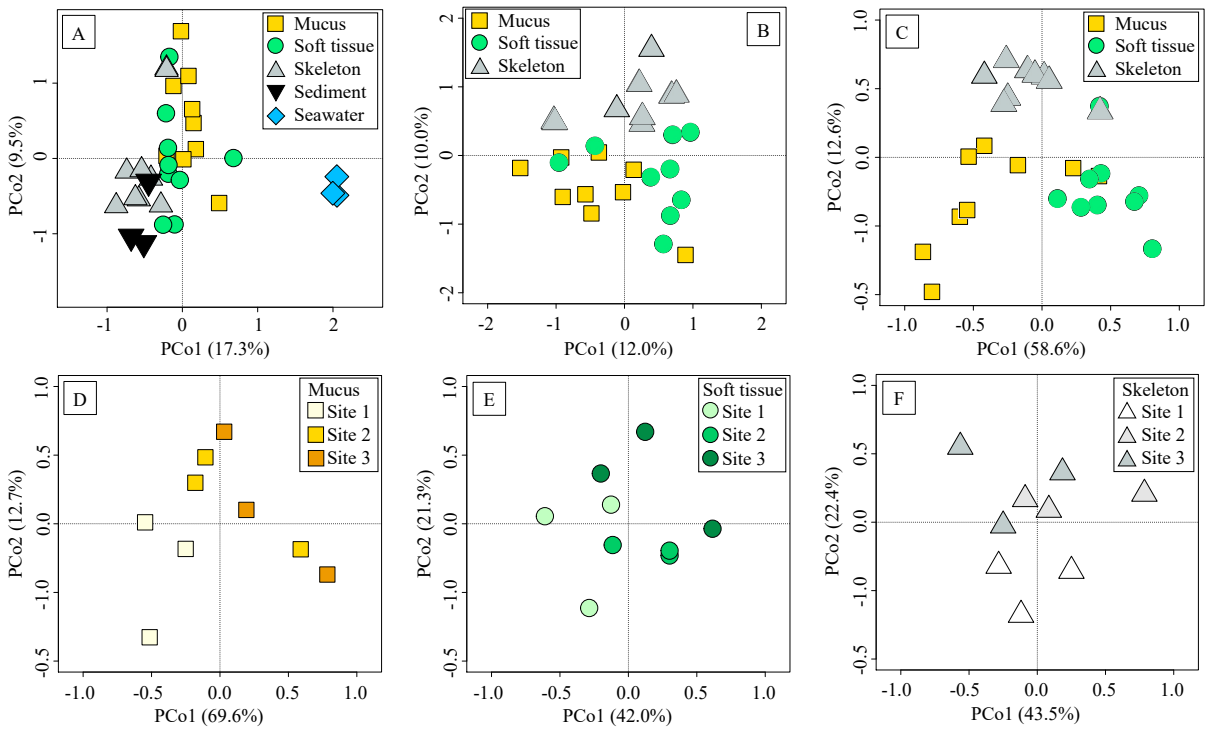

Figure 19 - **Overall microbiome compositional structure of *B. europaea* and the surrounding environment.** Principal Coordinate Analyses (PCoAs) of the Bray-Curtis distances calculated on microbiome profiles at genus taxonomic level, obtained from 16S rRNA sequencing (A and B) and phylogenetic assignation of metagenomic reads (C-F), describing different features of the available coral and environmental samples. The first and second principal components (PCo1 and PCo2) are plotted in all graphs and the percentage of variance in the dataset explained by each axis is reported. (A) PCoA based on 16S rRNA data showing the structure of *B. europaea* associated microbiomes (mucus samples, yellow squares; soft tissue samples, green circles; skeleton samples, grey triangles) compared to the surrounding environment (water samples, light blue diamonds; sediment samples, black reversed triangles) (permutation test with pseudo-F ratio, p-value = 0.001). (B) PCoA based on 16S rRNA data showing *B. europaea* microbiomes associated with the 3 different coral compartments (mucus in yellow, soft tissue in green, skeleton in gray) (permutation test with pseudo-F ratio, p-value = 0.001). (C) PCoA based on metagenomics data showing *B. europaea* microbiomes associated with the 3 different coral compartments (mucus in yellow, soft tissue in green, skeleton in gray) (permutation test with pseudo-F ratio, p-value = 0.001). (D) PCoA based on metagenomics data comparing *B. europaea* mucus microbiome in samples collected at different acidified conditions. Samples are depicted as squares filled in shades of color from lighter (Site 1, control site, non-acidified) to darker yellow (Site 2, moderate acidification, and Site 3, strong acidification). Permutation test with pseudo-F ratio, Site 1 *vs.* Site 2 and 3 together, p-value = 0.03. (E) PCoA based on metagenomics data comparing *B. europaea* microbiome associated with soft tissue compartment in samples collected at different acidified conditions. Samples are depicted as circles filled filled in shades of colors from lighter (Site 1) to darker green (Site 2 and Site 3). Permutation test with pseudo-F ratio, Site 1 *vs.* Site 2 and 3 together, p-value ≥ 0.05. (F) PCoA based on metagenomics data comparing *B. europaea* microbiome associated with skeleton compartment in samples collected at different acidified conditions. Samples are depicted as triangles filled in shades of color from white (Site 1) to light grey (Site 2) to dark grey (Site 3).

Gain and loss of metagenomic functions in *Balanophyllia europaea* living in acidification conditions

To highlight changes associated with water acidification on metabolic potential of the coral microbiome, in terms of gain and loss of genetic functions, we focused at the level of KEGG orthologs (KO entries), i.e., groups of genes performing the same function. Starting from a dataset of over 3,000 assigned KO, we selected in each tissue the KO entries showing a prevalence of 100% (i.e., detected in 3 out of 3 replicates) in the control site (Site 1) and 0% (i.e., none of the 3 replicates) in the highly acidified site (Site 3) or *vice versa*. The result of the analysis was a prevalence-based model for deriving functions that were under selection pressure by the different pH/pCO_2 levels at the 3 sites. Indeed, through this reductive approach, we were able to focus on microbial functions that were gained or lost in host grown under low pH/high pCO_2 levels (Figure 20).

In mucus and skeleton, a wide set of microbial genes underwent a rearrangement in the presence/absence profile of coral specimens collected at highly acidified conditions, whereas in coral soft tissue a smaller number of KO entries showed a clear trend. Indeed, mucus and skeleton metagenomes showed a rearrangement in KOs assigned to proteins involved in transport systems and functions associated with the stress response. Coherently with recent studies showing rearrangements of the ion transport system in both tropical and temperate corals subjected to pH variations (Glazier et al., 2020; Strader et al., 2020), metals transporters (i.e., K11709 in mucus, K11707 and K04758 in skeleton) were lost in samples from the acidified sites, whereas other genes with similar functions appeared (i.e., K09820 in mucus). Other transporters acquired by the microbiome of corals growing in acidified conditions were the transporter ppdA (both in mucus and skeleton) (Tjalsma et al., 2000), two transporters connected to histidine kinase sensor protein (K07706 and K07777, in mucus) (Kabbara et al., 2019), a short chain fatty acid transporter (K02106, in skeleton), and the bacterial outer membrane lipoprotein Blc (K03098, in skeleton), involved in transport of lipids for membrane maintenance (Campanacci et al., 2004).

In the mucus metagenome, a group of functions that can be associated with stress response was consistently gained by corals growing in highly acidified conditions: the mazE gene (K07172) is a toxin-antitoxin system activated during adverse environmental conditions (Nikolic, 2019), the tyrosinase function (K00505) can be involved in production of protective pigments during environmental stress (Pavan et al., 2020; Contreras-Llano et al., 2019), the gluconate 2-dehydrogenase (K06151) is an enzyme showing pH dependence in the regulation of catabolism (Maurer et al., 2015), the pyrroloquinoline quinone (pqq) biosynthesis protein (K06136) synthesizes a redox cofactor for bacterial dehydrogenases under environmental stress conditions (Naveed et al., 2016), the gene mmuM (K00547) is a homocysteine S-methyltransferase previously found upregulated under osmotic stress in corals (Aguilar et al., 2019), the gene rhaB (K00848) is a rhamnulokinase involved in the response to cell wall and membrane stress in bacteria (Bury-Moné et al., 2009). Moreover, the penicillin-binding protein B2 (K08724), which increased its prevalence in tissue samples beside being acquired by mucus samples from the acidified site, is known for its involvement in polymerization of peptidoglycan (Zawadzka-Skomiał et al., 2006). Finally, the competence protein ComFA (K02240, gained by samples from acidified sites in both mucus and skeleton) has a role in DNA uptake during horizontal gene transfer (Chilton et al., 2017), which represents an adaptive stress-response mechanism in different bacteria (Johnsen and Kroer, 2007).

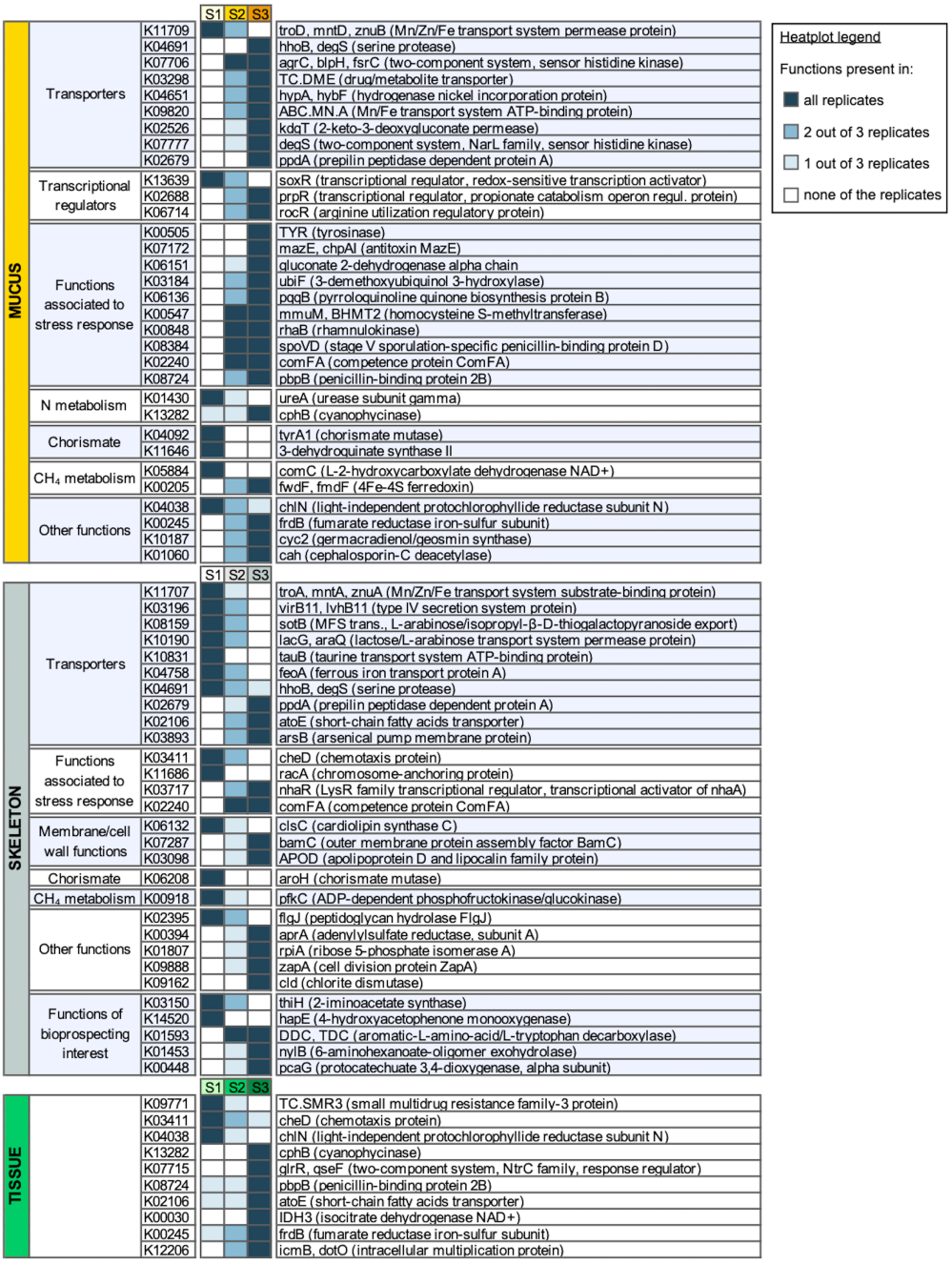

Figure 20 - **Prevalence-based model for deriving acidification-related gain/loss of metagenomic functions. KEGG orthologs (KO genes)** List of KO entries (KEGG orthologs) in the metagenome obtained from the 3 *B. europaea* anatomic compartments (mucus, soft tissue, and skeleton) in different acidification conditions (S1, control site; S2, moderate acidification; S3, high acidification). KO genes showing a prevalence of 100% (i.e., detected in 3 out of 3 replicates) in S1 and 0% (i.e., none of the 3 replicates) in S3 or *vice versa*, are reported, identifying functions lost or gained with acidification, respectively. A heatplot with a color gradient corresponding to the number of replicates in which each KO is detected is provided (see legend top-right for color key). For each KO, listed with KO identification number (left), the KEGG description is given on the right of the heatplot. KO entries are grouped by coherence of involvement in different physiological functions (i.e., genes classified as involved in transcriptional regulation, membrane transport, membrane or cell wall functionality maintenance, stress response, nitrogen (N) metabolism, chorismate pathway, methane (CH_4) metabolism), as well as by their increasing or decreasing trends among acidification conditions in the same coral compartment, whenever possible.

Highly acidified conditions were also associated with the gain of the transcriptional regulator nhaR (K03717), responsible for the osmotic induction of a promoter of the stress-inducible gene osmC (Toesca et al., 2001), in skeleton. Conversely, in the same compartment, we observed the loss of the arabinose transport system permease protein (K10190) and of the taurine transport system (K10831). Both arabinose and taurine represent important coral osmolytes used by the metaorganisms to cope with environmental fluctuations (Luo et al., 2021).

Most of the above-mentioned functions were detected in 1 or 2 out of 3 replicates in samples taken at Site 2 (Figure 20), showing how corals growing in moderately acidified waters could represent a transition state towards acclimatization.

For what concern nitrogen (N) metabolism, the urease ureA (K01430) was progressively lost in mucus metagenomes with the increase of acidification, whereas the cyanophycinase cphB (K13282) was gained both in mucus and tissue samples from acidified sites. Cyanophycin is a storage biopolymer [multi-L-arginyl-poly (L-aspartic acid)] acting as N reservoir (Burnat et al., 2014). The enzyme cyanophycinase is responsible for the hydrolytic cleavage of this polymer into aspartate-arginine dipeptides (Law et al., 2009). In order to thoroughly explore N organication and storage pathways, we observed the prevalence of the cyanophycin synthetase (CphA) gene (K03802) and of the Nif gene cluster (i.e., genes responsible for N fixation) in the different acidification sites. These genes were consistently detected in all acidification conditions (Supplementary Tables S4 and S5). Hence, the gain of the cphB function points at an acidification-induced gain of potential for N mobilization. Supporting this data, a regulatory protein of arginine utilization (K06714) also appeared in mucus samples from the acidified site, with arginine being a building block of cyanophycin (Zhang and Yang, 2019; Flores et al., 2019).

Other peculiar functions that were lost in acidified conditions (both Site 2 and Site3) were two chorismate mutases (tyrA1, K04092, and aroH, K06208, in mucus and skeleton respectively) and the 3-dehydroquinate synthase (K11646, mucus) (Figure 20), which are part of the chorismate pathway, involved in the production of aromatic precursors of a wide range of secondary metabolites (Pérez et al., 2015).

We also noticed the rearrangement of a few genes involved in functions that could be considered of bioprospecting interest, meaning that the coral growing close to underwater CO_2 seeps might represent a future useful source of genetic functions exploitable for bioremediation applications or pharmaceutical, agro- and food industrial processes (Ahila et al., 2017). In particular, the genes nylB (K01453) and pcaG (K00448), respectively involved in the nylon degradation pathway (Ohki et al., 2006) and in PAH degradation (Velupillaimani and Muthaiyan, 2019), were acquired in skeleton samples from the acidified site.

Functional metagenomic shifts in *Balanophyllia europaea* living in acidification conditions

Given the above described gain/loss of metagenomic functions, in particular in the mucus and skeleton metagenomes, we explored shifts in relative abundance of the different pathways within selected KEGG networks possibly connected with the functional rearrangements observed at orthologs level in corals growing at different acidified conditions (Figure 21). In the mucus metagenome, the network “Carbohydrate metabolism” (KEGG classification 1.1) showed changes in the carbon utilization, with the percentage of reads assigned to the pathways “amino sugar and nucleotide sugar metabolism” and “starch and sucrose metabolism” significantly increasing between the control site and the two acidified sites (Wilcoxon rank

sum test of Site 1 *vs*. Site 2 and 3 together, p-value = 0.02 and 0.05, respectively). Specifically, the former increased from an average (avg.) of 7.9% in the control to 9.5% and 10.8% in the two acidified sites (Site 2 and Site 3, respectively), whereas the latter increased from avg. 5.9% to 9.8% and 9.0%, respectively. At the same time, we observed a significant decrease in the relative abundance of "glycolysis/gluconeogenesis" pathway, from avg. 11.6% to 8.0% and 9.8% (Wilcoxon test Site 1 *vs*. Site 2 and 3, p-value = 0.05). Among the pathways included in the network "Amino acid metabolism" (KEGG classification 1.5), we observed in the mucus metagenome a significant increase in the reads assigned to "cysteine and methionine metabolism" (from avg. 7.4% in the control site to 10.2% and 9.1% in the acidified sites, Wilcoxon test Site 1 *vs*. Site 2 and 3, p-value = 0.05) and also in the "alanine, aspartate and glutamate metabolism" (from avg. 9.0% in the control site to 14.3% and 11.6% in the acidified sites, Wilcoxon test Site 1 *vs*. Site 2 and 3, p-value = 0.05). Finally, we observed a rearrangement in the relative abundance of pathways connected to the production or degradation of a wide variety of secondary metabolites (i.e., within the networks "Metabolism of terpenoids and polyketides" – KEGG classification 1.9 – and "Biosynthesis of other secondary metabolites" – KEGG classification 1.10). In mucus metagenome, we found the "geraniol degradation" and the "limonene and pinene degradation" pathways to significantly decrease in terms of relative abundance with acidification (from avg. 16.1% to 5.6% and 6.4% and from 28.3% to 6.8% and 9.9%

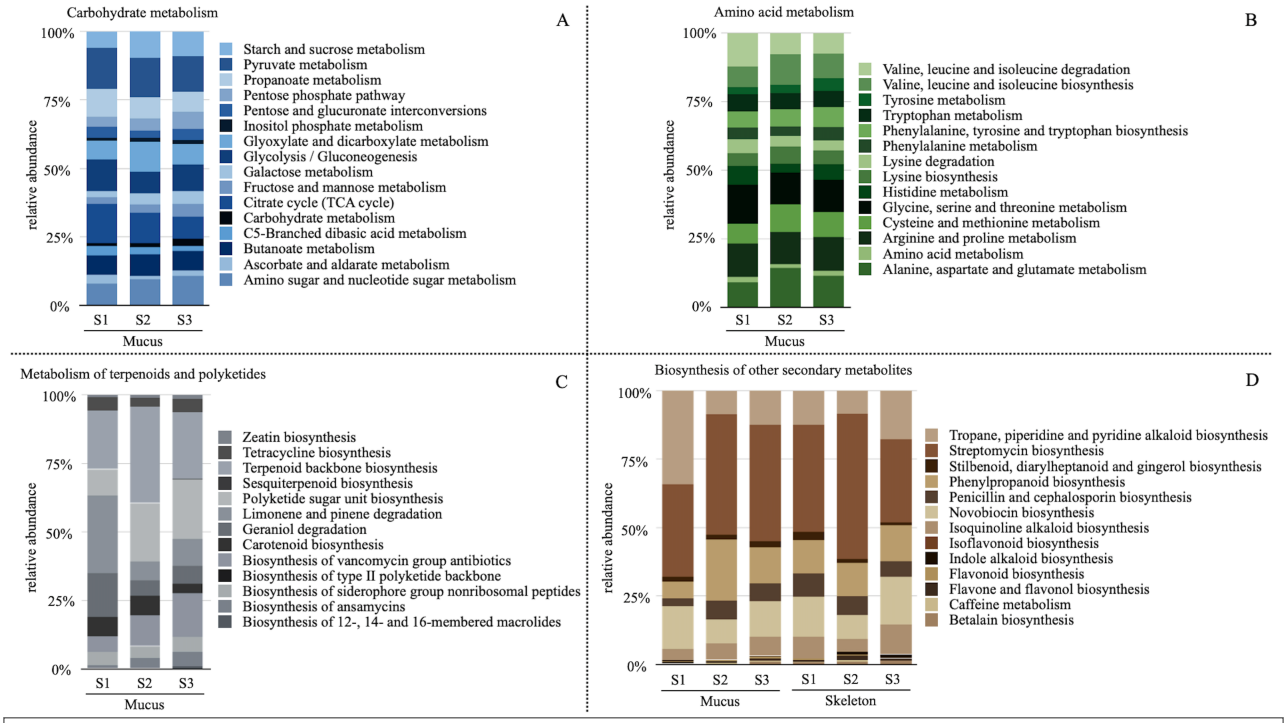

Figure 21 - **Distribution of functional pathways in selected KEGG networks in *B. europaea* metagenomes.** Bar plots representing average relative abundance of KEGG pathways expressed as percentages of reads assigned to specific pathways with respect to the total number of reads assigned to the networks "Carbohydrate metabolism" (KEGG classification 1.1) (A), "Amino acids metabolism" (KEGG classification 1.5) (B), "Metabolism of terpenoids and polyketides" (KEGG classification 1.9) (C), and "Biosynthesis of other secondary metabolites" (KEGG classification 1.10) (D). All bar plots refer to the metagenome obtained by mucus samples of *B. europaea* collected at Site 1 (S1), Site 2 (S2) and Site 3 (S3), with the exception of the network "Biosynthesis of other secondary metabolites" (D) for which data referring to skeleton samples are also plotted. Color legend is provided for each plot.

respectively, Wilcoxon test Site 1 *vs*. Site 2 and 3, p-value = 0.02 for both), whereas the "polyketide sugar unit biosynthesis" increased with acidification (from avg. 9.6% to 21.3% and 21.6%, Wilcoxon test Site 1 *vs*. Site 2 and 3 p-value = 0.02). Furthermore, the percentage of reads mapped in "tropane, piperidine and pyridine alkaloid biosynthesis" pathway decreased with acidification (from avg. 34.1% to 8.7% and 12.4%, Wilcoxon test Site 1 *vs*. Site 2 and 3 p-value = 0.05). Moreover, in the skeleton we observed a shift in pathways connected with the synthesis of secondary metabolites, with "stilbenoid, diarylheptanoid and gingerol biosynthesis" pathway decreasing with acidification (from avg. 2.9% to 1.3% and 1.1%, Wilcoxon test Site 1 *vs*. Site 2 and 3 p-value = 0.03) and with indole alkaloid biosynthesis increasing with acidification (from avg. 0.04% to 1.0% and 1.4%, Wilcoxon test Site 1 *vs*. Site 2 and 3 p-value = 0.02).

Discussion

Ocean acidification (OA) poses a massive threat to the marine ecosystems due to its possible impact on calcifying organisms (Wannicke et al., 2018). In spite of the intensive research efforts lately devoted to the exploration of the effects of global changes on corals, our understanding on how their biological and physiological processes may change under OA is still limited (Kaniewska et al., 2012). To this concern, temperate species such as *B. eurapaea* targeted in our study, may represent a valuable model given its more pronounced acclimatization capability with respect to tropical species, being naturally able to accommodate wider seasonal environmental variations (Maor-Landaw et al., 2017). Our aim was to highlight genetic functions, included in the microbial metagenome of the anatomic compartments of *B. europaea*, changing along with OA, and ultimately identify possible bacteria-related acclimatization processes.

In terms of phylogenetic composition, we observed a rearrangement at the family-level in the microbial community associated with the surface mucus of corals with increasing acidification, whereas significant shifts were not observed in soft tissue and skeleton samples, which are confirmed as ecologically distinct habitats (Luo et al., 2021). This is in line with previous findings on microbiome variations induced by acidification in another temperate but non-zooxanthellate coral species (i.e., *Astroides calycularis*; Biagi et al., 2020) and coherent with the fact that mucus niche is a "first line" defense layer, located at the interface between the coral itself and the surrounding environment (Shnit-Orland and Kushmaro, 2009; O'Brien et al., 2018). The phylogenetic rearrangement associated with increasing acidification in the mucus microbial community is in line with the observed variation in microbiome metabolic potential. The mucus microbiome was the one in which a wider and more consistent gain of functions associated with stress response was observed. Indeed, some of the functions acquired with acidification are known to be involved in resistance to acidic stress in model bacteria; these functions include gluconate 2-dehydrogenase alpha chain (Maurer et al., 2005) and 2-octaprenyl-3-methyl-6-methoxy-1,4-benzoquinol hydroxylase (Ma et al., 2010). This observation points at a possible mechanism of selection of stress-adaptable microbiome components, which could contribute to the coral acclimatization process.

Secondly, the microbiome of corals living in acidified conditions showed quantitative shifts in the pathways of carbohydrate metabolism and rearrangements in processes involving metabolites necessary for maintaining protective cell structures, such as lipid membranes and cell walls. Our findings indicate that carbohydrate metabolism in coral microbiome under OA, in particular in the mucus compartment, was

subjected to a shift from energy production to maintenance of cell membrane and wall integrity, with a decrease in direct sugar consumption and an increase in structural sugar biosynthesis pathways (Figure 22). According to our data, the utilization of carbon sources in the mucus ecosystems underwent a shift in favor of amino and nucleotide sugars metabolism, which are important precursors of the lipidic membranes and cell wall (Benner and Kaiser, 2003; Mills et al., 2020), to the detriment of energetic pathways, such as glycolysis/gluconeogenesis. Environmental changes, including lowering pH, might lead to cell membrane damages (Labare et al., 2010) or alteration in cell structural lipids (Sogin et al., 2016), meaning that membrane bioenergetics and lipid physiology are closely related to the stress response (Yang et al., 2014). Since a wide range of nucleotide sugars are required for lipopolysaccharide (LPS) biosynthesis (Mills et al., 2020), we can assume that changes in environmental conditions might influence the metabolism of nucleotide sugar production by provoking alterations in bacterial cells membranes. Moreover, nucleotide sugars are also essential for sucrose synthesis, with sucrose synthase enzyme having a dual role in producing both UDP-glucose, necessary for cell wall and glycoprotein biosynthesis, and ADP-glucose, necessary for starch biosynthesis (Diricks et al., 2017). Hence, the increasing trend of both nucleotide sugar pathway and sucrose metabolism that we observed under high acidification is coherent with the strong interconnection between these two pathways and the damages possibly induced by OA. These findings are also supported by the gain of a short chain fatty acid transporter and of an outer membrane protein involved in membrane repair (Blc) in the metagenome of skeleton samples collected under highly acidified conditions. Among their multiple roles, fatty acids are indeed important structural constituents of phospholipids, which are the building blocks of cell membranes (De Carvalho and Caramujo, 2018). In addition, the ability of Blc to bind several fatty acids and lysophospholipids (LPLs), key inner membrane intermediates of phospholipid metabolism, makes this membrane protein likely involved in cell envelope LPL transport in case of membrane damage (Campanacci et al., 2004 and 2006).

Amino sugars also have an important structural role as components of the prokaryotic cell walls, where they occur in peptidoglycan, LPS, and pseudopeptidoglycan (Benner and Kaiser, 2003). For example, it has been shown in a model cyanobacterium that peptidoglycan incorporates L-alanine, D-alanine, D-glutamate and meso-diaminopimelate into peptide bridges, which are linked to polymers consisting of alternating amino sugar (acetyl-glucosamine and acetyl-muramate) monomers (Mills et al., 2020). This is in line with the increasing relative abundance in the pathway of alanine, aspartate and glutamate metabolism within the amino acids metabolism that we observed with augmented OA, although we could not find a direct link between ocean acidification and cell wall rearrangement in the available literature. Supporting this possible rearrangement of peptidoglycan structure due to highly acidified conditions, we also observed the penicillin-binding protein B2 function, involved in the polymerization of peptidoglycan (Zawadzka-Skomiał et al., 2006), appearing in mucus and increasing in prevalence in tissue metagenomes under high acidification conditions (Figure 22).

Finally, in our model of coral acclimatized to low pH, we observed an acidification-induced selection of functions related to Nitrogen (N) mobilization in the mucus metagenome. As OA alters microorganism biogeochemical environment, it is of particular relevance to understand whether and how it is able to affect N cycling in ecologically relevant benthic holobionts (Wannicke et al., 2018). Our results suggest that organic N mobilization is promoted by acidification, especially in the mucus, through the gain of the cyanophycinase

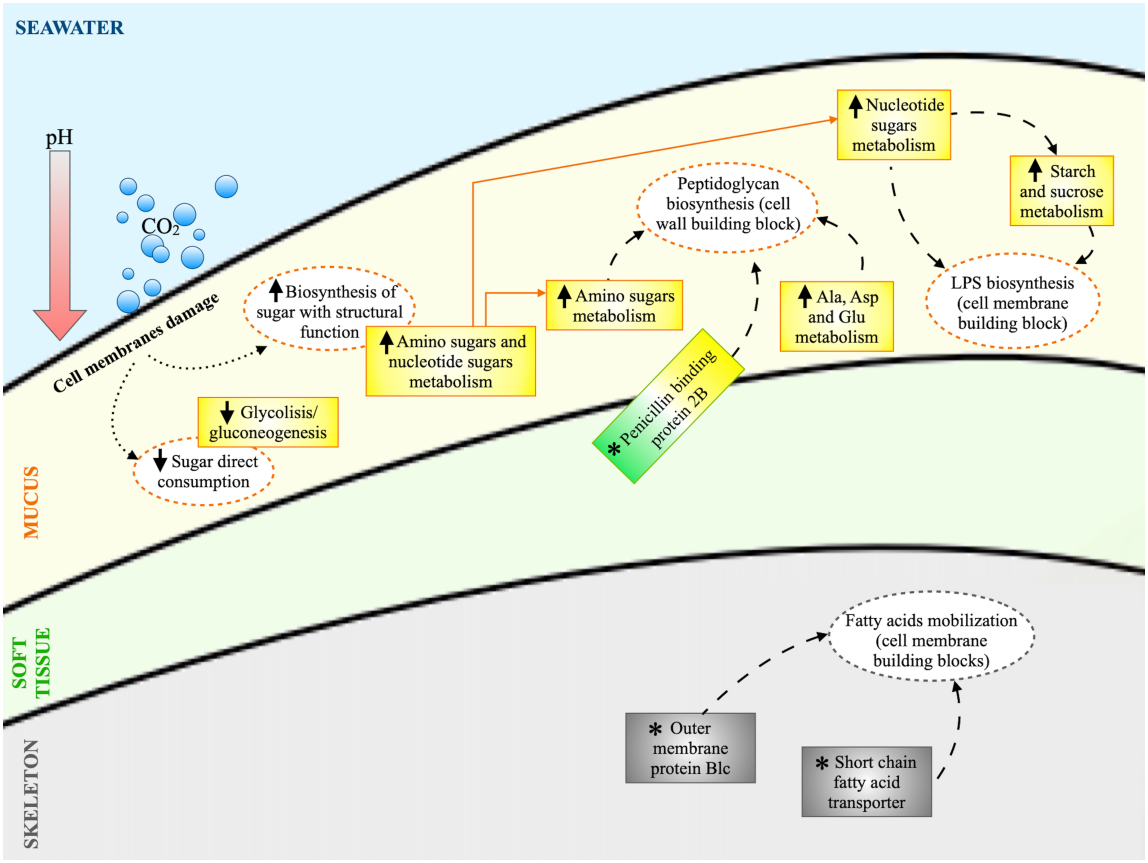

Figure 22 - **Proposed model of carbohydrate metabolism shift in coral microbiomes under acidification conditions, from direct energy production to structural maintenance pathways.** KEGG pathways and KO entries showing acidification related modifications in relative abundance or prevalence, respectively, are reported in rectangles using the same color code of the coral compartment in which variations were observed (mucus, yellow; soft tissue, green; skeleton, grey). Upward and downward arrows indicate that the KEGG pathway increased or decreased in terms of relative abundance with the increasing acidification, respectively. Reported KO entries (*) were detected in all replicates from the highly acidified site while absent in samples from control sites. Cell functions hypothesized to be connected with the variations of KEGG pathways abundance and KO entries detection are reported in dashed circles. Dotted arrows represent the influence of acidification on carbohydrates utilization. Dashed arrows represent connections between observed increasing/decreasing pathways and cell functions. Abbreviations: LPS, lipopolysaccharides; Ala, Alanine; Asp, Aspartate; Glu, Glutamate.

function. Cyanophycin is a water-insoluble storage biopolymer acting as N reservoir and synthesized by the enzyme cyanophycin synthetase (Burnat et al., 2014). Cyanophycinase, responsible for the release of the dipeptide β-aspartyl-arginine from cyanophycin and subsequent hydrolyzation to aspartate and arginine by an isoaspartyl dipeptidase (Burnat et al., 2014; Zhang and Yang, 2019), only appears in the microbiome associated with corals growing under highly acidified conditions. Accordingly, the appearance of a regulatory protein of arginine utilization in coral mucus growing in acidified sites supports our hypothesis. On the contrary, N fixation did not show acidification-related rearrangements in the involved genetic functions, in our Mediterranean coral model, confirming the importance of this pathway for coral survival pointed out by previous studies using $^{15}N_2$ tracer technique (Bednarz et al., 2021). Growth and density of Symbiodiniaceae algal symbiont within the coral host is highly dependent on N availability, and N fixation

performed by bacteria could contribute to the stability of the coral–algae symbiosis, in particular under sub-optimal scenarios (Rädecker et al., 2015). It is tempting to hypothesize that, with the increased acidification, the N demand in either all or one among the components of the *B. eurapaea* holobiont (i.e., the prokaryotic community, the coral host, the symbiotic algae) might increase, and that the gain in terms of functions for N mobilization from storage polymers in the microbial community might be a coping strategy for the sub-optimal environmental conditions.

Studies linking coral N metabolism and environmental variations, in particular heat and eutrophic stresses, have provided a wide array of different, sometimes contrasting, results, depending on the species. For instance, increased ammonia availability allows the maintenance of photosynthesis and calcification rates in the coral *Turbinaria reniformis* under thermal stress (Béraud et al., 2013), whereas an excess of N of anthropogenic origin exacerbates the bleaching reaction to thermal stress in *Acropora* and *Pocillopora* (Tong et al., 2020). Pogoreutz et al. (2017) proposed a coral bleaching model in which an increased N fixation is synergic with ocean warming in determining the loss of control over the symbiosis with Symbiodiniaceae in *Pocillopora* model. However, the balance in nutrients exchange among bacteria, the coral host, and the zooxanthellae is deemed extremely complex, and it involves mechanisms of N limitation and phosphorous starvation to allow the host to exert control on the photosynthesis in the algal symbiont and maintain the symbiotic homeostasis under changing environmental conditions (Pogoreuzt et al., 2017). To the best of our knowledge, mechanistic studies linking N cycle and tolerance to OA in temperate corals are still unavailable, and our results highlight that any attempt at deepening our knowledge in this field needs to consider the N storage and mobilization pathways and, most importantly, take into account the crosstalk among all the components of the holobiont (coral, algae, and bacteria).

Another peculiar rearrangement involved in N metabolism observed in the mucus metagenome was loss of the urease gene (ureA). Urea has been proposed to represent an important metabolite for coral calcification through degradation by urease (Zhou et al., 2020), which catalyzes the hydrolysis of urea to inorganic carbon and ammonia that are involved in the calcification process (Biscéré et al., 2018). The net calcification rate of *B. europaea* are actually reduced with increasing acidification (Fantazzini et al., 2015), thus it is possible that a loss in the urease activity might be involved in the process.

Conclusions

Changes in microbiome metabolic networks are essential to trigger the fast response of the coral holobiont to modifications in external conditions and promote corals tolerance to climate change-related phenomena that might alter their survival, growth, and reproduction (Rosenberg et al., 2007; Stocker et al., 2013; Torda et al., 2017; Voolstra and Ziegler, 2020; Putnam, 2021). In this context, we explored variations in the composition and metabolic potential of the microbiomes residing in surface mucus, soft tissue and skeleton of *Balanophyllia europaea* naturally living along an acidification gradient as an approximation of forthcoming ocean conditions. The metagenomic changes observed in corals acclimatized to low pH suggest a functional rearrangement able to mitigate the sub-optimal environmental conditions at three different levels. First, at mucus level, the low pH of surrounding water could exert a selective pressure on microbiome composition promoting the acquisition of bacteria genetically equipped for dealing with environmental stress, as demonstrated by the gain of functions related to stress resistance. Secondly, the carbohydrate

metabolism of the coral microbiome, especially in the mucus compartment, is affected by acidification in ways that hint at a more efficient maintenance of cell protective structures. Our findings highlighted a quantitative shift in the carbohydrate metabolism from energy production to the maintenance of the integrity of cell membranes and walls. In line with previous findings, indicating that acidification might lead to cell membrane damages (Labare et al., 2010) or alteration in cell structural lipids (Sogin et al., 2016), we confirmed the importance of membrane bioenergetics in connection to the response to acidification (Yang et al., 2014). Thirdly, acidification promote the selection of genetic functions that can respond to variations in nitrogen needs at the holobiont level. In fact, our findings sustain the hypothesis that genes devoted to organic N mobilization are gained in coral growing under acidified conditions, in particular in the mucus niche, thus possibly increasing the availability of this major limiting element (Glaze et al., 2021) for the holobiont and for its control over the algal symbiont. Growth and density of Symbiodiniaceae within the coral host are indeed highly dependent on N availability and nutrients of bacterial origin have been proposed to impact the stability of the symbiosis between coral host and the zooxanthellae under sub-optimal environmental conditions (Rädecker et al., 2015; Bourne et al., 2016; Pogoreutz et al., 2017). Our results point at the importance to consider the crosstalk among all the three components (coral host, symbiotic algae, and bacterial communities) of the holobiont to further unveil nitrogen-involving processes that allow photosynthetic corals to maintain their functionality under adverse environmental conditions.

Our study expands the current knowledge on processes of coral acclimatization to OA and confirms that temperate corals represent a promising model of microbiome adaptation. When confirmed by future mechanistic studies, the processes hypothesized in the present work represent an important step towards a holistic comprehension of the tripartite crosstalk between coral host, symbiotic algae and bacterial communities, as well as a deepened understanding on how this relationship changes under environmental variations allowing for the survival and health of these ecosystem forming holobionts in the forthcoming oceans.

References

Aguilar, C., Raina, J. B., Fôret, S., Hayward, D. C., Lapeyre, B., Bourne, D. G., & Miller, D. J. (2019). Transcriptomic analysis reveals protein homeostasis breakdown in the coral *Acropora millepora* during hypo-saline stress. *BMC genomics, 20*(1), 1-13.

Ahila, N. K., Prakash, S., Manikandan, B., Ravindran, J., Prabhu, N. M., & Kannapiran, E. (2017). Bio-prospecting of coral (*Porites lutea*) mucus associated bacteria, Palk Bay reefs, Southeast coast of India. *Microbial pathogenesis*, *113*, 113-123.

Andrews, S. (2010). Fastqc: a quality control tool for high throughput sequence data. Available online at: http://www.bioinformatics.babraham.ac.uk/projects/fastqc/.

Apprill, A., Weber, L. G., & Santoro, A. E. (2016). Distinguishing between microbial habitats unravels ecological complexity in coral microbiomes. *mSystems, 1*(5), e00143-16.

Bednarz, V. N., Van De Water, J. A., Grover, R., Maguer, J. F., Fine, M., & Ferrier-Pagès, C. (2021). Unravelling the importance of diazotrophy in corals–combined assessment of nitrogen assimilation, diazotrophic community and natural stable isotope signatures. *Frontiers in microbiology*, *12*, 1638.

Benner, R., & Kaiser, K. (2003). Abundance of amino sugars and peptidoglycan in marine particulate and dissolved organic matter. *Limnology and oceanography, 48*(1), 118-128.

Béraud, E., Gevaert, F., Rottier, C., & Ferrier-Pagès, C. (2013). The response of the scleractinian coral *Turbinaria reniformis* to thermal stress depends on the nitrogen status of the coral holobiont. *Journal of experimental biology*, *216*(14), 2665-2674.

Biagi, E., Caroselli, E., Barone, M., Pezzimenti, M., Teixido, N., Soverini, M., ... & Candela, M. (2020). Patterns in

microbiome composition differ with ocean acidification in anatomic compartments of the Mediterranean coral Astroides calycularis living at CO2 vents. *Science of The Total Environment*, *724*, 138048.

Bindoff, N. L., Cheung, W. W., Kairo, J. G., Arístegui, J., Guinder, V. A., Hallberg, R., ... & Williamson, P. (2019). Changing ocean, marine ecosystems, and dependent communities. *IPCC special report on the ocean and cryosphere in a changing climate*, 477-587.

Biscéré, T., Ferrier-Pagès, C., Grover, R., Gilbert, A., Rottier, C., Wright, A., ... & Houlbrèque, F. (2018). Enhancement of coral calcification via the interplay of nickel and urease. *Aquatic Toxicology*, *200*, 247-256.

Bolger, A.M., Lohse, M., & Usadel, B. (2014). Trimmomatic: A flexible trimmer for Illumina sequence data. *Bioinformatics, 30*(15), 2114–2120.

Bourne, D. G., Morrow, K. M., & Webster, N. S. (2016). Insights into the coral microbiome: underpinning the health and resilience of reef ecosystems. *Annual review of microbiology, 70*, 317-340.

Burnat, M., Herrero, A., & Flores, E. (2014). Compartmentalized cyanophycin metabolism in the diazotrophic filaments of a heterocyst-forming cyanobacterium. *Proceedings of the national academy of sciences of the united states of america, 111*(10), 3823-3828.

Bury-Moné, S., Nomane, Y., Reymond, N., Barbet, R., Jacquet, E., Imbeaud, S., ... & Bouloc, P. (2009). Global analysis of extracytoplasmic stress signaling in Escherichia coli. *PLoS genetics*, *5*(9), e1000651.

Campanacci, V., Nurizzo, D., Spinelli, S., Valencia, C., Tegoni, M., & Cambillau, C. (2004). The crystal structure of the *Escherichia coli* lipocalin Blc suggests a possible role in phospholipid binding. *FEBS letters, 562*(1-3), 183-188.

Campanacci, V., Bishop, R. E., Blangy, S., Tegoni, M., & Cambillau, C. (2006). The membrane bound bacterial lipocalin Blc is a functional dimer with binding preference for lysophospholipids. *FEBS letters, 580*(20), 4877-4883.

Caroselli, E., Gizzi, F., Prada, F., Marchini, C., Airi, V., Kaandorp, J., ... & Goffredo, S. (2019). Low and variable pH decreases recruitment efficiency in populations of a temperate coral naturally present at a CO2 vent. *Limnology and Oceanography*, *64*(3), 1059-1069.

Chen, D., Rojas, M., Samset, B. H., Cobb, K., Niang, A. D., Edwards, P., ... & Zhou, B. (2021). Framing, Context, and Methods. In: *Climate change 2021: the physical science basis. Contribution of working group I to the sixth assessment report of the intergovernmental panel on climate change*.

Chilton, S. S., Falbel, T. G., Hromada, S., & Burton, B. M. (2017). A conserved metal binding motif in the Bacillus subtilis competence protein ComFA enhances transformation. *Journal of bacteriology*, *199*(15), e00272-17.

Contreras-Llano, L. E., Guerrero-Rubio, M. A., Lozada-Ramírez, J. D., García-Carmona, F., & Gandía-Herrero, F. (2019). First betalain-producing bacteria break the exclusive presence of the pigments in the plant kingdom. *MBio, 10*(2), e00345-19.

Culhane, A. C., Thioulouse, J., Perrière, G., & Higgins, D. G. (2005). MADE4: an R package for multivariate analysis of gene expression data. *Bioinformatics, 21*(11), 2789-2790.

De Carvalho, C. C., & Caramujo, M. J. (2018). The various roles of fatty acids. *Molecules, 23*(10), 2583.

Diricks, M., Gutmann, A., Debacker, S., Dewitte, G., Nidetzky, B., & Desmet, T. (2017). Sequence determinants of nucleotide binding in Sucrose Synthase: improving the affinity of a bacterial Sucrose Synthase for UDP by introducing plant residues. *Protein engineering, design and selection, 30*(3), 143-150.

Dunphy, C. M., Gouhier, T. C., Chu, N. D., & Vollmer, S. V. (2019). Structure and stability of the coral microbiome in space and time. *Scientific reports, 9*(1), 1-13.

Fantazzini, P., Mengoli, S., Pasquini, L., Bortolotti, V., Brizi, L., Mariani, M., ... & Goffredo, S. (2015). Gains and losses of coral skeletal porosity changes with ocean acidification acclimation. *Nature Communications*, *6*(1), 1-7.

Feehery, G. R., Yigit, E., Oyola, S. O., Langhorst, B. W., Schmidt, V. T., Stewart, F. J., ... & Pradhan, S. (2013). A method for selectively enriching microbial DNA from contaminating vertebrate host DNA. *PloS one*, *8*(10), e76096.

Flores, E., Arévalo, S., & Burnat, M. (2019). Cyanophycin and arginine metabolism in cyanobacteria. *Algal research, 42,* 101577.

Gattuso, J. P., Magnan, A., Billé, R., Cheung, W. W., Howes, E. L., Joos, F., ... & Turley, C. (2015). Contrasting futures for ocean and society from different anthropogenic CO2 emissions scenarios. *Science*, *349*(6243).

Glaze, T. D., Erler, D. V., & Siljanen, H. M. (2021). Microbially facilitated nitrogen cycling in tropical corals. *The ISME journal*, 10.1038/s41396-021-01038-1. Advance online publication.

Glazier, A., Herrera, S., Weinnig, A., Kurman, M., Gómez, C. E., & Cordes, E. (2020). Regulation of ion transport and

energy metabolism enables certain coral genotypes to maintain calcification under experimental ocean acidification. *Molecular ecology, 29*(9), 1657-1673.

Goffredo, S., Arnone, S., & Zaccanti, F. (2002). Sexual reproduction in the Mediterranean solitary coral *Balanophyllia europaea* (Scleractinia, Dendrophylliidae). *Marine ecology progress series, 229*, 83–94.

Goffredo, S., Caroselli, E., Pignotti, E., Mattioli, G., & Zaccanti, F. (2007). Variation in biometry and population density of solitary corals with environmental factors in the Mediterranean Sea. *Marine biology, 152*, 351–361.

Goffredo, S., Prada, F., Caroselli, E., Capaccioni, B., Zaccanti, F., Pasquini, L., ... & Falini, G. (2014). Biomineralization control related to population density under ocean acidification. *Nature climate change*, *4*(7), 593-597.

Goulet, T.L., Erill, I., Ascunce, M.S., Finley, S.J., & Javan, G.T. (2020). Conceptualization of the holobiont paradigm as it pertains to corals. *Frontiers in physiology, 11*, 566968.

Hassenrück, C., Fink, A., Lichtschlag, A., Tegetmeyer, H.E., de Beer, D., & Ramette, A. (2016). Quantification of the effects of ocean acidification on sediment microbial communities in the environment: the importance of ecosystem approaches. *FEMS microbiology ecology, 92*(5), fiw027.

Hoegh-Guldberg, O., Poloczanska, E.S., Skirving, W., & Dove, S. (2017). Coral reef ecosystems under climate change and ocean acidification. *Frontiers in marine science, 4,* 158.

Ingrosso, G., Abbiati, M., Badalamenti, F., Bavestrello, G., Belmonte, G., Cannas, R., ... & Boero, F. (2018). Mediterranean bioconstructions along the Italian coast. *Advances in marine biology*, *79*, 61-136.

Johnsen, A. R., & Kroer, N. (2007). Effects of stress and other environmental factors on horizontal plasmid transfer assessed by direct quantification of discrete transfer events. *FEMS microbiology ecology, 59*(3), 718-728.

Kabbara, S., Hérivaux, A., Dugé de Bernonville, T., Courdavault, V., Clastre, M., Gastebois, A., ... & Papon, N. (2019). Diversity and evolution of sensor histidine kinases in eukaryotes. *Genome biology and evolution*, *11*(1), 86-108.

Kaniewska, P., Campbell, P. R., Kline, D. I., Rodriguez-Lanetty, M., Miller, D. J., Dove, S., & Hoegh-Guldberg, O. (2012). Major cellular and physiological impacts of ocean acidification on a reef building coral. *PloS one, 7*(4), e34659.

Kenkel, C. D., Moya, A., Strahl, J., Humphrey, C., & Bay, L. K. (2018). Functional genomic analysis of corals from natural CO_2-seeps reveals core molecular responses involved in acclimatization to ocean acidification. *Global change biology*, *24*(1), 158-171.

Klein, S. G., Geraldi, N. R., Anton, A., Schmidt-Roach, S., Ziegler, M., Cziesielski, M. J., ... & Duarte, C. M. (2021). Projecting coral responses to intensifying marine heatwaves under ocean acidification. *Global Change Biology*.

Kroeker, K. J., Kordas, R. L., Crim, R. N., & Singh, G. G. (2010). Meta-analysis reveals negative yet variable effects of ocean acidification on marine organisms. *Ecology letters*, *13*(11), 1419-1434.

Labare, M. P., Bays, J. T., Butkus, M. A., Snyder-Leiby, T., Smith, A., Goldstein, A., ... & LaBranche, R. (2010). The effects of elevated carbon dioxide levels on a Vibrio sp. isolated from the deep-sea. *Environmental Science and Pollution Research*, *17*(4), 1009-1015.

Langmead, B., & Salzberg, S. L. (2012). Fast gapped-read alignment with Bowtie 2. *Nature methods, 9*(4), 357–359.

Law, A. M., Lai, S. W., Tavares, J., & Kimber, M. S. (2009). The structural basis of beta-peptide-specific cleavage by the serine protease cyanophycinase. *Journal of molecular biology, 392*(2), 393–404.

Lejeusne, C., Chevaldonné, P., Pergent-Martini, C., Boudouresque, C. F., & Pérez, T. (2010). Climate change effects on a miniature ocean: the highly diverse, highly impacted Mediterranean Sea. *Trends in ecology and evolution, 25*(4), 250–260.

Li, H., Handsaker, B., Wysoker, A., Fennell, T., Ruan, J., Homer, N., ... & Durbin, R. (2009). The sequence alignment/map format and SAMtools. *Bioinformatics*, *25*(16), 2078-2079.

Liu, J., Wang, H., Yang, H., Zhang, Y., Wang, J., Zhao, F., & Qi, J. (2013). Composition-based classification of short metagenomic sequences elucidates the landscapes of taxonomic and functional enrichment of microorganisms. *Nucleic acids research, 41*(1), e3-e3.

Li, D., Liu, C. M., Luo, R., Sadakane, K., & Lam, T. W. (2015). MEGAHIT: an ultra-fast single-node solution for large and complex metagenomics assembly via succinct de Bruijn graph. *Bioinformatics*, *31*(10), 1674-1676.

Luo, D., Wang, X., Feng, X., Tian, M., Wang, S., Tang, S. L., ... & Luo, H. (2021). Population differentiation of Rhodobacteraceae along with coral compartments. *The ISME Journal*, 1-17.

Ma, C., Sim, S., Shi, W., Du, L., Xing, D., & Zhang, Y. (2010). Energy production genes sucB and ubiF are involved in persister survival and tolerance to multiple antibiotics and

stresses in *Escherichia coli*. *FEMS microbiology letters*, *303*(1), 33-40.

Maor-Landaw, K., Ben-Asher, H. W., Karako-Lampert, S., Salmon-Divon, M., Prada, F., Caroselli, E., ... & Levy, O. (2017). Mediterranean versus Red sea corals facing climate change, a transcriptome analysis. *Scientific reports*, *7*(1), 1-8.

Marcelino, V.R., Morrow, K.M., van Oppen, M.J.H., Bourne, D.G., & Verbruggen, H. (2017). Diversity and stability of coral endolithic microbial communities at a naturally high pCO_2 reef. *Molecular ecology, 26*(19), 5344–5357.

Maurer, L. M., Yohannes, E., Bondurant, S. S., Radmacher, M., & Slonczewski, J. L. (2005). pH regulates genes for flagellar motility, catabolism, and oxidative stress in *Escherichia coli* K-12. *Journal of bacteriology*, *187*(1), 304-319.

McDevitt-Irwin, J. M., Baum, J. K., Garren, M., & Vega Thurber, R. L. (2017). Response of coral-associated bacterial communities to local and global stressor. *Frontiers in marine science, 4*, 262.

McFall-Ngai, M., Hadfield, M. G., Bosch, T. C., Carey, H. V., Domazet-Lošo, T., Douglas, A. E., ... & Wernegreen, J. J. (2013). Animals in a bacterial world, a new imperative for the life sciences. *Proceedings of the National Academy of Sciences*, *110*(9), 3229-3236.

Menzel, P., Ng, K. L., & Krogh, A. (2016). Fast and sensitive taxonomic classification for metagenomics with Kaiju. *Nature communications, 7*(1), 1-9.

Meron, D., Rodolfo-Metalpa, R., Cunning, R., Baker, A. C., Fine, M., & Banin, E. (2012). Changes in coral microbial communities in response to a natural pH gradient. *The ISME journal*, *6*(9), 1775-1785.

Mills, L. A., McCormick, A. J., & Lea-Smith, D. J. (2020). Current knowledge and recent advances in understanding metabolism of the model cyanobacterium *Synechocystis* sp. PCC 6803. *Bioscience reports, 40*(4), BSR20193325.

Morrow, K. M., Moss, A. G., Chadwick, N. E., & Liles, M. R. (2012). Bacterial associates of two Caribbean coral species reveal species-specific distribution and geographic variability. *Applied and environmental microbiology, 78*(18), 6438-6449.

Morrow, K. M., Bourne, D. G., Humphrey, C., Botté, E. S., Laffy, P., Zaneveld, J., ... & Webster, N. S. (2015). Natural volcanic CO 2 seeps reveal future trajectories for host–microbial associations in corals and sponges. *The ISME journal*, *9*(4), 894-908.

Naveed, M., Tariq, K., Sadia, H., Ahmad, H., & Mumtaz, A. S. (2016). The life history of pyrroloquinoline quinone (PQQ): a versatile molecule with novel impacts on living systems. *International journal of molecular biology Open Access, 1*, 29-46.

Nikolic, N. (2019). Autoregulation of bacterial gene expression: lessons from the MazEF toxin–antitoxin system. *Current genetics, 65*(1), 133-138.

O'Brien, P. A., Smith, H. A., Fallon, S., Fabricius, K., Willis, B. L., Morrow, K. M., & Bourne, D. G. (2018). Elevated CO_2 has little influence on the bacterial communities associated with the pH-tolerant coral, massive *Porites* spp. *Frontiers in microbiology, 9*, 2621.

Ohki, T., Wakitani, Y., Takeo, M., Yasuhira, K., Shibata, N., Higuchi, Y., & Negoro, S. (2006). Mutational analysis of 6-aminohexanoate-dimer hydrolase: relationship between nylon oligomer hydrolytic and esterolytic activities. *FEBS letters, 580*(21), 5054-5058.

Okazaki, R. R., Towle, E. K., van Hooidonk, R., Mor, C., Winter, R. N., Piggot, A. M., ... & Langdon, C. (2017). Species-specific responses to climate change and community composition determine future calcification rates of Florida Keys reefs. *Global change biology*, *23*(3), 1023-1035.

Palladino, G., Biagi, E., Rampelli, S., Musella, M., D'Amico, F., Turroni, S., ... & Candela, M. (2021). Seasonal changes in microbial communities associated with the jewel anemone Corynactis viridis. *Frontiers in Marine Science*, *8*, 57.

Pavan, M. E., López, N. I., & Pettinari, M. J. (2020). Melanin biosynthesis in bacteria, regulation and production perspectives. *Applied microbiology and biotechnology, 104*(4), 1357-1370.

Pérez, E., Rubio, M. B., Cardoza, R. E., Gutiérrez, S., Bettiol, W., Monte, E., & Hermosa, R. (2015). The importance of chorismate mutase in the biocontrol potential of *Trichoderma parareesei. Frontiers in microbiology, 6*, 1181.

Pogoreutz, C., Rädecker, N., Cardenas, A., Gärdes, A., Voolstra, C. R., & Wild, C. (2017). Sugar enrichment provides evidence for a role of nitrogen fixation in coral bleaching. *Global change biology*, *23*(9), 3838-3848.

Prada, F., Caroselli, E., Mengoli, S., Brizi, L., Fantazzini, P., Capaccioni, B., ... & Goffredo, S. (2017). Ocean warming and acidification synergistically increase coral mortality. *Scientific reports*, *7*(1), 1-10.

Putnam, H. M. (2021). Avenues of reef-building coral acclimatization in response to rapid environmental change. *The Journal of experimental biology, 224*(Pt Suppl 1), jeb239319.

Rädecker, N., Pogoreutz, C., Voolstra, C. R., Wiedenmann, J., & Wild, C. (2015). Nitrogen cycling in corals: the key to

understanding holobiont functioning? *Trends in microbiology*, *23*(8), 490-497.

Rohwer, F., Breitbart, M., Jara, J., Azam, F., & Knowlton, N. (2001). Diversity of bacteria associated with the Caribbean coral *Montastraea franksi. Coral reefs, 20*(1), 85-91.

Rohwer, F., Seguritan, V., Azam, F., & Knowlton, N. (2002). Diversity and distribution of coral-associated bacteria. *Marine ecology progress series, 243*, 1-10.

Rosenberg, E., Koren, O., Reshef, L., Efrony, R., & Zilber-Rosenberg, I. (2007). The role of microorganisms in coral health, disease and evolution. *Nature reviews. Microbiology, 5*(5), 355–362.

Rubio-Portillo, E., Santos, F., Martínez-García, M., de Los Ríos, A., Ascaso, C., Souza-Egipsy, V., ... & Anton, J. (2016). Structure and temporal dynamics of the bacterial communities associated to microhabitats of the coral O culina patagonica. *Environmental microbiology*, *18*(12), 4564-4578.

Shnit-Orland, M., & Kushmaro, A. (2009). Coral mucus-associated bacteria: a possible first line of defense. *FEMS microbiology ecology, 67*(3), 371-380.

Shore, A., Day, R. D., Stewart, J. A., & Burge, C. A. (2021). Dichotomy between regulation of coral bacterial communities and calcification physiology under ocean acidification conditions. *Applied and environmental microbiology, 87*(6), e02189-20.

Sogin, E. M., Putnam, H. M., Anderson, P. E., & Gates, R. D. (2016). Metabolomic signatures of increases in temperature and ocean acidification from the reef-building coral, *Pocillopora damicornis. Metabolomics, 12*(4), 71.

Stocker, T. F., Qin, D., Plattner, G. K., Alexander, L. V., Allen, S. K., Bindoff, N. L., ... & Xie, S. P. (2013). Technical summary. In Climate change 2013: the physical science basis. Contribution of Working Group I to the Fifth Assessment Report of the Intergovernmental Panel on Climate Change (pp. 33-115). Cambridge University Press.

Strader, M. E., Wong, J. M., & Hofmann, G. E. (2020). Ocean acidification promotes broad transcriptomic responses in marine metazoans: a literature survey. *Frontiers in zoology, 17*(1), 1-23.

Tangherlini, M., Corinaldesi, C., Ape, F., Greco, S., Romeo, T., Andaloro, F., & Danovaro, R. (2021). Ocean acidification induces changes in virus-host relationships in Mediterranean benthic ecosystems. *Microorganisms, 9*(4), 769.

Teixidó, N., Caroselli, E., Alliouane, S., Ceccarelli, C., Comeau, S., Gattuso, J. P., ... & Gambi, M. C. (2020). Ocean acidification causes variable trait-shifts in a coral species. *Global Change Biology*, *26*(12), 6813-6830.

Toesca, I., Perard, C., Bouvier, J., Gutierrez, C., & Conter, A. (2001). The transcriptional activator NhaR is responsible for the osmotic induction of osmCp1, a promoter of the stress-inducible gene osmC in *Escherichia coli*. *Microbiology, 147*(10), 2795-2803.

Tong, H., Cai, L., Zhou, G., Zhang, W., Huang, H., & Qian, P. Y. (2020). Correlations between prokaryotic microbes and stress-resistant algae in different corals subjected to environmental stress in Hong Kong. *Frontiers in microbiology*, *11*, 686.

Toolkit, P. (2019). Broad Institute, GitHub Repository. http://broadinstitute.github.io/picard/; Broad Institute.

Torda, G., Donelson, J. M., Aranda, M., Barshis, D. J., Bay, L., Berumen, M. L., ... & Munday, P. L. (2017). Rapid adaptive responses to climate change in corals. *Nature Climate Change*, *7*(9), 627-636.

Tjalsma, H., Bolhuis, A., Jongbloed, J. D., Bron, S., & van Dijl, J. M. (2000). Signal peptide-dependent protein transport in *Bacillus subtilis*: a genome-based survey of the secretome. *Microbiology and molecular biology reviews, 64*(3), 515-547.

van Oppen, M. J., & Blackall, L. L. (2019). Coral microbiome dynamics, functions and design in a changing world. *Nature reviews. Microbiology, 17*(9), 557-567.

Vanwonterghem, I., & Webster, N. S. (2020). Coral reef microorganisms in a changing climate. *Iscience*, *23*(4), 100972.

Velupillaimani, D., & Muthaiyan, A. (2019). Potential of *Bacillus subtilis* from marine environment to degrade aromatic hydrocarbons. *Environmental sustainability, 2*(4), 381-389.

Voolstra, C. R., & Ziegler, M. (2020). Adapting with microbial help: microbiome flexibility facilitates rapid responses to environmental change. *BioEssays: news and reviews in molecular, cellular and developmental biology, 42*(7), e2000004.

Wannicke, N., Frey, C., Law, C. S., & Voss, M. (2018). The response of the marine nitrogen cycle to ocean acidification. *Global change biology, 24*(11), 5031-5043.

Webster, N. S., Negri, A. P., Botté, E. S., Laffy, P. W., Flores, F., Noonan, S., ... & Uthicke, S. (2016). Host-associated coral reef microbes respond to the cumulative pressures of

ocean warming and ocean acidification. *Scientific reports*, *6*(1), 1-9.

West, P.T., Probst, A.J., Grigoriev, I.V., Thomas, B.C., & Banfield, J.F. (2018). Genome-reconstruction for eukaryotes from complex natural microbial communities. *Genome research, 28*(4), 569-580.

Yang, Y., Kadim, M. I., Khoo, W. J., Zheng, Q., Setyawati, M. I., Shin, Y. J., ... & Yuk, H. G. (2014). Membrane lipid composition and stress/virulence related gene expression of Salmonella Enteritidis cells adapted to lactic acid and trisodium phosphate and their resistance to lethal heat and acid stress. *International journal of food microbiology*, *191*, 24-31.

Yu, T., & Chen, Y. (2019). Effects of elevated carbon dioxide on environmental microbes and its mechanisms: A review. *The Science of the total environment, 655*, 865–879.

Zawadzka-Skomiał, J., Markiewicz, Z., Nguyen-Disteche, M., Devreese, B., Frere, J. M., & Terrak, M. (2006). Characterization of the bifunctional glycosyltransferase/ acyltransferase penicillin-binding protein 4 of *Listeria monocytogenes*. *Journal of bacteriology, 188*(5), 1875-1881.

Zhang, H., & Yang, C. (2019). Arginine and nitrogen mobilization in cyanobacteria. *Molecular microbiology, 111*(4), 863-867.

Zhou, Y., Tang, K., Wang, P., Wang, W., Wang, Y., & Wang, X. (2020). Identification of bacteria-derived urease in the coral gastric cavity. *Science China Earth sciences, 63*(10), 1553-1563.

CHAPTER 3 - THE STUDY OF ENVIRONMENTAL MICROBIOMES IN THE PRESENTED THESIS

3.1 Study V — Particulate matter emission sources and meteorological parameters combine to shape the airborne microbiome communities in the Ligurian coast, Italy

Introduction

Airborne Particulate Matter (APM) is a complex system of particles in suspension in the atmosphere, usually defined as aerosol. Atmospheric aerosol is contributed by a multiplicity of sources of both natural and anthropogenic origin, including both biogenic and abiotic chemical components, and producing extremely complex and variable matrices that can be processed and solved for their origin using appropriate analytical processing and computational tools (Tositti, 2018a and b). In particular, the aerosol composition consists of a series of macrocomponents, which make up the mass of APM, as well as an even larger series of different trace components, the latter being of primary relevance as including the most toxic species and providing the highest chemical fingerprinting potential (Hopke, 2016). These aerosol bulk components can be emitted directly into the atmosphere (Primary Aerosol) or, otherwise, they can be abundantly produced within the atmosphere, following chemical reactions on gaseous precursors previously emitted (Secondary Aerosol). Primary Biological Aerosol (PBA), in short bioaerosol, represents the APM fraction including atmospheric particles released from the biosphere to the atmosphere (Fröhlich-Nowoisky et al., 2016). PBA comprise living and dead organisms, their dispersal units (e.g., pollen and spores) as well as tissue fragments from decay processes (Womack et al., 2010; Castillo et al., 2012). The overall mass contribution of PBA to conventional APM metrics is to date a very challenging task though some authors have recently estimated that it may account for about 16% of PM_{10} in different cities examined (Hyde and Mahalov, 2020). The PBA fraction including microorganisms is defined as “airborne microbiome” (AM) and represents a highly dynamic and diversified assemblage of active and inactive microorganisms (Mescioglu et al., 2019). Indeed, AM can originate from multiple terrestrial and marine sources - including resident microbiomes in soil, waterbodies, plants and animal faeces (Després et al., 2012; Fröhlich-Nowoisky et al., 2016; Mhuireach and Betancourt-Román, 2019) - whose relative importance depends season, location, altitude and meteorological and atmospheric factors. Further, in agricultural and suburban locations, other sources relevant to AM emissions are represented by man-made systems, such as agricultural waste, composting, and wastewater treatment plants. AM emission mechanisms include erosion or abrasive dislodgement from terrestrial sources and, from open waters, bubble-bursting at the air-water interface (Veron, 2015; Wilson et al., 2015). PBA size spans from a few nanometres up to about a tenth of a millimeter (Castillo et al., 2012), with bacteria-containing particles ranging around 2-4 µm in diameter (Dommergue et al., 2019) and accounting for “5–50% of the total number of atmospheric particles >0.2 µm in diameter” (Delort and Amato, 2017). Due to the small size, AM can be transported over large distances, across continents and oceans, and reach the upper troposphere, where it actively contributes to ice nucleation and cloud processing (DeLeon-Rodriguez et al., 2013). In the troposphere, the AM concentration ranges from 10^2 to 10^5 cells/m^3 (Dommergue et al., 2019), being the densest in the planetary boundary layer, whose thickness depends on micrometeorological factors and geographic location, with marked daily and seasonal fluctuations (Sesartic et al., 2012; Toprak and Schnaiter, 2013). In particular, the near-ground AM is the one most influenced by local sources, including local meteorology and atmospheric composition. AM is then

removed from the troposphere by wet and dry deposition processes. The former is the major sink for atmospheric aerosol particles, in the form of precipitation (Renard et al., 2019), while the latter, being less important on the global scale, is particularly relevant with respect to local air quality (Fröhlich-Nowoisky et al., 2016; Mescioglu et al., 2019).

Recently, an increasing perception of the strategic importance of PBA - AM in particular - for the Earth system and, ultimately, for the planet and human health, has arisen (Cao et al., 2014; Huang et al., 2014; Michaud et al., 2018). For instance, besides its relevance to atmospheric processes, AM has been found to control the spread of microorganisms over the planet surface, affecting the geographical biome, with key implications on agriculture and, ultimately, human health. This awareness raised concern about the potential impact of anthropogenic activities on PBA and, in particular, on the AM fraction. For example, changes in aerosol composition due to extensive human influence on the planetary scale give rise to air pollution, the inherent modification of atmospheric reactivity and, ultimately, climate change (von Schneidemesser et al., 2015). These factors may likely interfere with AM, shaping its structure and dispersion throughout the troposphere, with direct consequences on the terrestrial biome (Qin et al., 2020). However, as far as we know, the current state of knowledge on the connections between AM, atmospheric processes and atmospheric pollution is still fragmentary, with relatively few pioneer studies that take into account multidimensional datasets to analyze the connection between air chemical composition and its microbiome structure and variations, e.g., comparing different land-use types (Bowers et al., 2013; Liu et al., 2019), different sites within cities (Woo et al., 2013; Gandolfi et al., 2015; Innocente et al., 2017; Li et al., 2019), or worldwide locations (Graham et al., 2018; Mescioglu et al., 2019; Tignat-Perrier et al., 2019).

Our work fits in this scenario by exploring the ability of an interdisciplinary approach combining chemical speciation and metagenomics in shedding light on the complex relationships among abiotic and microbiome components of local ambient aerosol. The study is based on a series of about one hundred PM_{10} samples from a coastal district in north-western Italy, collected daily over six months, from February to July 2012, to cover the cold-to-warm seasonal transition. The chemical composition of each sample was obtained, and a receptor modelling approach was used to identify and quantitatively apportion the chemical species determined in the samples to their sources. Owing to the cutoff adopted in APM sampling, the samples were deemed suitable for total DNA extraction and microbiome characterization by Next-Generation Sequencing using the 16S rRNA gene as target. In our work, we were able to finely reconstruct the overall aerosol behavior in an area affected by both natural and anthropogenic emission sources, determining the local bacterial microbiome from PBA contained in PM_{10} and its main features as a function of local meteorological and environmental characteristics.

Materials and methods

Site description

The PM_{10} samples treated in this work were collected in Savona, one of the main towns in the Ligurian region (Figure 23). The whole region overlooks the Tyrrhenian sea but is entirely occupied by the Apennine range down to the coast, where only a narrow strip of plain is present. Therefore, the coastal area is densely inhabited and crossed by an extremely busy traffic road mainly connecting Italy to France. Besides being

occupied by a medium-size heavily inhabited urban settlement, the Savona district also hosts a wide industrial area, including a coal-fired power plant active at the time of our experimental field activity and a large and very busy harbour. The climate of this site is classified as warm-temperate (Csa, according to Köppen and Geiger classification) (Köppen, 1900; Geiger, 1954) with an average annual temperature of 14.6°C and average precipitation of 910 mm[21]. Intense northern winds characterize the circulation in winter (Burlando et al., 2013), while sea-land breeze regimes prevail in the warm season, usually starting from March (Bentamy et al., 2007; Tositti et al., 2018). The air sampling site was located at an altitude of 12 m on the sea level in a rural area as classified according to the EU Directive 2008/50/EC on Air quality, with a distance of 2 km from the sea.

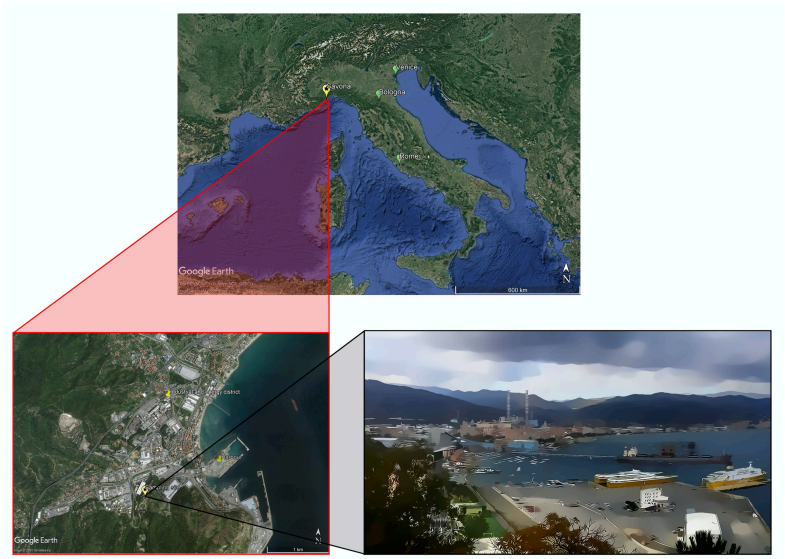

Figure 23 - **Location of the sampling site.** Map providing the location of Savona in Italy (indicated with a yellow balloon with a star; other Italian cities are indicated with a green balloon) (top panel), and snapshot of the PM_{10} sampling site with a 3D view of the surroundings (bottom panel) (source: Google Earth; map data: SIO, NOAA, U.S. Navy, NGA, GEBCO, TerraMetrics). Adapted from the original file of P. Christener (https://commons.wikimedia.org/wiki/File:Vado-Ligure.jpg), CC BY-SA 3.0 (https://creativecommons.org/licenses/by-sa/3.0), via Wikimedia Commons.

Sample collection and atmospheric parameters

A total of 184 daily PM_{10} samples were collected from February 1, 2012, until July 20, 2012 with low-volume samplers (SWAM Dual Channel, 55.6 m^3/day, FAI, Italy) to allow simultaneous collection of both quartz (Whatman ®QM-A quartz) and PTFE membranes (Whatman $PM_{2.5}$ PTFE). Samples were stored frozen in the dark at -10°C until processing. In this work, PTFE membranes were used for gravimetry, ion chromatography and elemental analysis with particle induced X-ray emission and inductively coupled plasma mass spectrometry, while quartz membranes were used for the analysis of carbonaceous macrocomponents and microbiology. A subset of 98 samples, uniformly distributed across the sampling period, was used for the analyses reported in the present paper. During the sampling campaign, meteorological parameters were measured simultaneously on site using a Davis Vantage Pro2 Weather Station (Davis Instruments, Hayward, CA), placed in proximity of the PM_{10} sampler, for the measurement of temperature, pressure, relative

[21] https://en.climate-data.org, accessed 28/07/2020

humidity, rainfall, and wind direction and speed with a time resolution of 30 min. Subsequently, the data obtained were averaged on a daily scale (Supplementary Table S6), i.e., at the same time resolution as the PM_{10} samples, using the "openair" package (Carslaw and Ropkins, 2012) of the R software[22] (version 3.6.1).

Chemical characterization of the samples

Chemical characterization of PM_{10} filters was carried out using several analytical techniques. First, PM_{10} mass load (µg/m^3) was determined by gravimetric analysis. Elemental and organic carbon were determined on quartz membranes by thermal-optical transmittance analysis (TOT), as previously described (Piazzalunga et al., 2011). For inorganic speciation, several analytical techniques were performed on PTFE filter portions: Ion Chromatography (IC) for the determination of the main water-soluble ion composition (NH_4^+, K^+, Mg^{2+}, NO_3^-, $SO4^{2-}$, Na^+, Cl^-, Ca^{2+}, and a few low-level organic compounds, i.e., oxalates and methanesulfonate), and Particle Induced X-ray Emission (PIXE) and Inductively Coupled Plasma Mass Spectrometry (ICP-MS) for the simultaneous analysis of a series of metals and metalloids (Na, Al, Si, Cl, Ca, Ti, V, Cr, Mn, Fe, Ni, Cu, Zn, Br, Pb, Li, Co, Rb, Sr, Cd, La, Ce, Sb, Cs, Ba, Ti, Bi, As, Se, Sn). Elemental analysis by PIXE was carried out at the Tandetron 3 MeV of LABEC-INFN, Florence (Italy), according to the method previously reported (Lucarelli et al., 2011). Elemental analysis by ICP-MS was carried out according to the UNI EN 14902, 2005 for PM_{10} as an extension of the DL 155, 2010 in agreement with the EU Directive 2008/50/EC on ambient air quality and cleaner air for Europe. In order to prevent data redundancy, insoluble magnesium (Mg ins) and insoluble potassium (K ins) were calculated as the difference between PIXE and IC concentrations and replaced the corresponding elementary concentration data.

Positive Matrix Factorization analysis

Positive Matrix Factorization (PMF) is an advanced multivariate factor analysis technique widely used in receptor modelling for the chemometric evaluation and modelling of environmental datasets (Paatero and Tapper, 1994; Hopke, 2000; Comero et al., 2009; Hopke, 2016; Tositti et al., 2014; Belis et al., 2019; Masiol et al., 2020). PMF allows the identification and quantification of the emissive profile of a receptor site, i.e., the monitoring site where an air quality station is operated. We applied EPA PMF 5.0 software (Norris et al., 2014). The dataset was checked and re-arranged prior to PMF modelling according to the model criteria previously described (Norris et al., 2014) and, after data pre-processing, a concentration matrix of 98 samples × 25 variables was obtained. After careful evaluation of the input data and uncertainty matrices, an optimum number of factors was found by analysing the values of Q, a parameter estimating the goodness of the fit performed (Brown et al., 2015), and the distribution of residuals. In order to assess the reliability of the model reconstruction, measured (input data) and reconstructed (modeled) values together with the distribution of residuals were compared. Our results indicated a good general performance of the model in reconstructing PM_{10} (coefficient of determination equal to 0.79) for most variables. In order to confirm the results of receptor modelling, the origin of the air masses associated with the factors obtained was investigated through the creation of wind polar plots using the source contribution of the factors produced by PMF. In particular, polar plots were produced for each single PMF factor using the "openair" package of R (Carslaw and Ropkins, 2012), utilizing the conditional probability function (CPF) (Ashbaugh et al., 1985) with an arbitrary threshold set to the 75th percentile.

[22] R Core Team; www.r-project.org

Microbial DNA extraction, 16S rRNA gene amplification and sequencing

Microbial DNA extraction was performed on quartz membrane filter using the DNeasy PowerSoil Kit (Qiagen, Hilden, Germany) (Jiang et al., 2015; Shin et al., 2015). Extracted DNA samples were quantified with NanoDrop ND-1000 (NanoDrop Technologies, Wilmington, DE) and stored at -20°C until further processing. The PCR amplification of the V3-V4 hypervariable region of the 16S rRNA gene and the library preparation were performed as described in paragraph 2.2. Sequencing was performed on an Illumina MiSeq platform using a 2 × 250 bp paired-end protocol, according to the manufacturer's instructions (Illumina, San Diego, CA).

Bioinformatics and statistics

Raw sequences were processed as described in paragraph 2.2. Three different metrics were used to evaluate alpha diversity - Faith's Phylogenetic Diversity (PD whole tree) (Faith, 1992), Chao1 index for microbial richness, and number of observed ASVs - and unweighted UniFrac distance was used for Principal Coordinates Analysis (PCoA). Permutation test with pseudo-F ratio (function "adonis" in the "vegan" package of R), Kruskal-Wallis test or Wilcoxon rank-sum test were used to assess data separation. Kendall correlation test was used to determine associations between the PCoA coordinates of each sample and the factors identified by the PMF analysis. P-values were corrected for multiple testing with the Benjamini-Hochberg method, with a false discovery rate (FDR) ≤ 0.05 considered statistically significant. All statistical analyses and respective figures were produced with the R software using "Made4" (Culhane et al., 2005) and "vegan[23]" packages. Clustering analysis of family-level AM profiles, filtered for family subject prevalence of at least 20%, based on the SILVA taxonomy assignment, was carried out using hierarchical Ward-linkage clustering based on the Spearman correlation coefficients. We verified that each cluster showed significant correlations between samples within the group (multiple testing using the Benjamini–Hochberg method) and that the clusters were statistically significantly different from each other (permutational MANOVA using the Spearman distance matrix as input, function adonis of the vegan package in R).

Additionally, PANDAseq assembled paired-end reads were also processed with the QIIME1 (Caporaso et al., 2010) pipeline for OTUs (Operational Taxonomic Units) clustering based on 97% similarity threshold. Taxonomy was then assigned using the SILVA database. OTUs were processed through the R package "MaAsLin2" (Mallick et al., 2021) to determine their association with microbial clusters. Kruskal-Wallis test was used to find OTUs whose relative abundance was significantly different among microbial clusters. The resulting OTUs were taxonomically assigned against the NCBI 16S rRNA database using the BLAST[24] algorithm.

Results

Particulate Matter emission sources and atmospheric parameters

The PMF model application on PM_{10} samples resulted in a solution with an optimum number of seven source factors at the receptor site, i.e., the station where the PM_{10} samples were collected. Like other multivariate methods, these factors correspond to linear combinations of the original compositional

[23] https://cran.r-project.org/web/packages/vegan/index.html
[24] https://blast.ncbi.nlm.nih.gov/

parameters, each potentially identifiable as an emission source profile. The fractional contribution per sample for each of the seven factors is reported in Supplementary Table S7.

In order to associate the factors with specific emission sources, prior knowledge about the receptor site (Savona, Italy) was used together with a critical analysis of the factor fingerprints (Figure 24A). Moreover, the percentage contribution of the seven identified sources to the total variable was reported (PM_{10}, Figure 24B). As a result, the seven factors extracted by PMF analysis can be described as follows. Factor 1 is characterized by the prevalence of elements attributable to the geochemical composition because of the high percentages of Si, Al, and Ti. Therefore, this factor was identified as "crustal material and road dust resuspension", deriving from the soil and/or road surface (Tositti et al., 2014; Chow et al., 2015). Factor 2 is linked to organic carbon (OC), Cu, Zn, Cr, and K^+. OC and K^+ are strictly related to combustion processes, including biomass burning, as previously described (Pachon et al., 2013). Cu, Zn, and Cr are associated with traffic: Cu and Cr are well-known tracers of the brakes of motor vehicles, while Zn is known as a tracer of tire wear (Alastuey et al., 2007; Thorpe and Harrison, 2008; Gietl et al., 2010). Therefore, this factor was identified as a combination of "traffic and biomass burning" sources. Factor 3 is mainly associated with NO_3^- from gas-to-particle conversion of NO_x (g) in the atmosphere to which traffic and other high-temperature combustion processes may contribute (Schaap et al., 2004; Pathak et al., 2009); as such it can hardly be attributed to a single well-defined source, especially in such a complex emissive scenario. Therefore, this

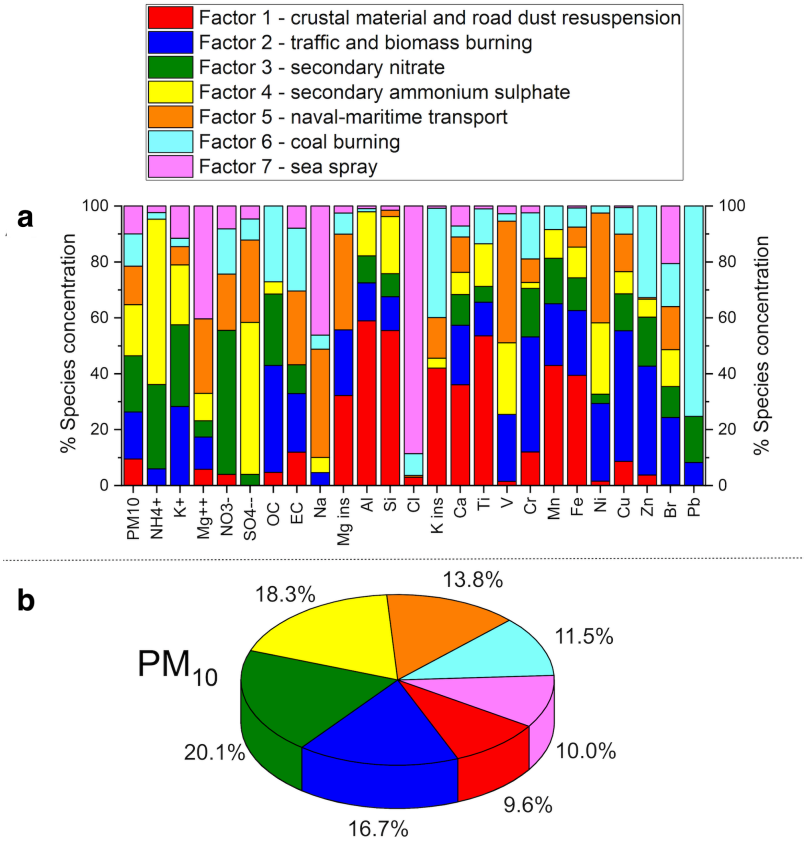

Figure 24- Emission sources identified by PMF analysis. (**a**) Stacked bar chart of the percentage concentration of each chemical species contributing to each of the seven factors that represent the chemical profile of each source identified in the PMF model. (**b**) Pie chart representing the contribution of the seven sources to PM_{10} mass. The seven factors were identified as reported at the top.

factor was identified collectively as “secondary nitrate”. Factor 4 relates to SO_4^{2-} and NH_4^+ from gas-to particle reactions, leading to secondary ammonium sulphate (Rodríguez et al., 2004; Vecchi et al., 2004; Hueglin et al., 2005). Similarly to secondary nitrate, this component can be contributed by various sources (both natural and anthropogenic) due to the multiplicity of fossil fuel sources of the precursor gaseous SO_2 and the ubiquity of NH_3 (g) (Behera et al., 2013; Fioletov et al., 2017). Therefore, this factor was collectively identified as “secondary ammonium sulphate”. Factor 5 is associated with Na, Mg ins, V, and Ni. The distinctive association of V and Ni reveals emissions attributable to the combustion of heavy oil (Jang et al., 2007; Becagli et al., 2012; Viana et al., 2014). The association of these species with Na and Mg suggests a "naval-maritime transport" source. Factor 6 is mainly characterized by high scores of Pb, K ins, Zn, OC, and elemental carbon (EC). The fine particles produced by coal combustion are characterized by significant fractions of OC and K together with typical elements such as Zn, while other semi-volatile elements condense on the surface of fine particles of K ins (Yu et al., 2018). Therefore, this factor was identified as “coal burning”. Factor 7 is connected to a large score of Cl^-, Na, and Mg^{++}, and clearly identified as “sea spray” aerosol (Grythe et al., 2014).

In order to confirm the PMF analysis results, the origin of the polluted air masses was investigated by analyzing the PMF factors as a function of wind direction, calculating the respective cumulative distribution functions and generating the corresponding wind polar plots. This method associates the emissive profile obtained by PMF with wind direction and intensity to which the receptor site is downwind. The plots obtained are shown in Supplementary Figure S11. In particular, factors 1, 3, 4, and 6 (respectively crustal material and road dust resuspension, secondary nitrate, secondary ammonium sulphate, and coal burning) are associated with winds blowing from the inland towards the coast covering traffic and industrial sources. Factor 5 (naval-maritime transport) is oriented downwind from the sea, confirming that it is associated with the fuel oil used for sea shipping. Finally, while factor 2 shows a local origin indicating sources in the proximity of the receptor site, factor 7 is meridionally oriented, indicating once more a marine origin. It should be noted, however, that, unlike factor 5 characterized by elements typical of the submicron fraction likely flushed back and forth by sea-land breezes from the harbor, factor 7 is associated with coarse particles requiring different meteorological conditions (possibly more intense winds from the open sea in order to sustain heavier particles).

AM overall composition

Next generation sequencing of the V3-V4 hypervariable region of the 16S rRNA gene from the total microbial DNA extracted from PM_{10} air filters resulted in 98 samples containing more than 1 000 reads per samples which were retained for the rest of the study, for a total of 797,781 high-quality sequences with an average of 8,058 ± 3,410 (mean ± SD) paired-end reads per sample, binned into 4 189 ASVs. According to our data, AM is dominated by the phyla Proteobacteria (mean relative abundance ± SD = 42.8 ± 19.4%) and Firmicutes (27.4 ± 18.9%), with Actinobacteria (14.8 ± 10.9%) and Bacteroidetes (9.2 ± 8.6%) being subdominant. At the family level, the most represented taxa are *Comamonadaceae* (6.1 ± 13.4%) and *Sphingomonadaceae* (4.3 ± 5.0%), both belonging to Proteobacteria. Other represented families are *Ruminococcaceae* (3.9 ± 7.6%), *Enterobacteriaceae* (3.7 ± 5.9%), *Clostridiaceae* (3.6 ± 6.8%), *Bacillaceae* (3.5

± 5.0%) and *Flavobacteriaceae* (3.4 ± 5.7%). Please see Supplementary Figure S12 for a graphical representation of the overall compositional structure of AM throughout the entire sampling period.

In order to explore connections between the AM structure and seasonality, we compared the levels of AM diversity over the different months (Figure 25). Diversity measurements indicated a general trend of microbial richness to decrease from winter to summer, although the differences did not reach statistical significance (Kruskal-Wallis test, FDR corrected p-value > 0.05) (Figure 25A). Conversely, the PCoA of unweighted UniFrac distances between the AM compositional profiles showed sample segregation according to the month of sampling (Figure 25B) (FDR-corrected permutation test with pseudo-F ratio, p-value = 0.012), meaning that seasonality significantly affects the overall compositional AM structure.

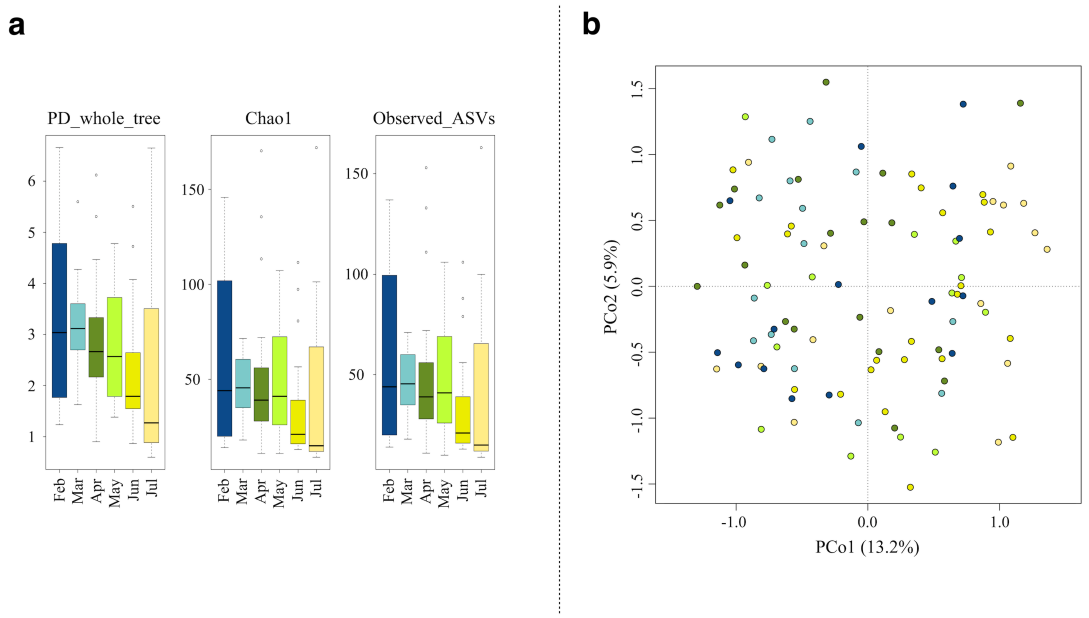

Figure 25 - **AM alpha and beta diversity throughout the sampling period.** (**a**) Box-and-whiskers distribution of Faith's Phylogenetic Diversity (PD_whole_tree), Chao1 index for microbial richness and number of observed ASVs, for each month of sampling. The data show a trend towards reduced microbial richness from winter to summer, although the differences did not reach statistical significance (Kruskal-Wallis test, FDR-corrected p-value > 0.05). (**b**) Principal Coordinates Analysis (PCoA) based on unweighted UniFrac distances between AM profiles, showing separation by sampling month (permutation test with pseudo-F ratio, p-value = 0.012) (same colour code as in panel A). The first and second principal components (PCo1 and PCo2) are plotted and the percentage of variance in the dataset explained by each axis is reported.

Variation of the AM topological structure and association with PM emission sources and meteorological parameters

To further explore the overall AM variation across the sampling period, a clustering analysis of the AM compositional profiles was carried out. Hierarchical Ward-linkage clustering based on the Spearman correlation coefficients of family-level AM profiles resulted in the significant separation of 4 clusters, named C1, C2, C3 and C4, respectively (FDR-corrected permutation test with pseudo-F ratio, p-value ≤ 0.001) (Figure 26). Confirming the robustness of the identified clusters, the PCoA of the unweighted UniFrac distances between samples revealed a sharp segregation based on the assigned cluster (Figure 27). Interestingly, when we searched for correlations between PCoA coordinates and measured meteorological

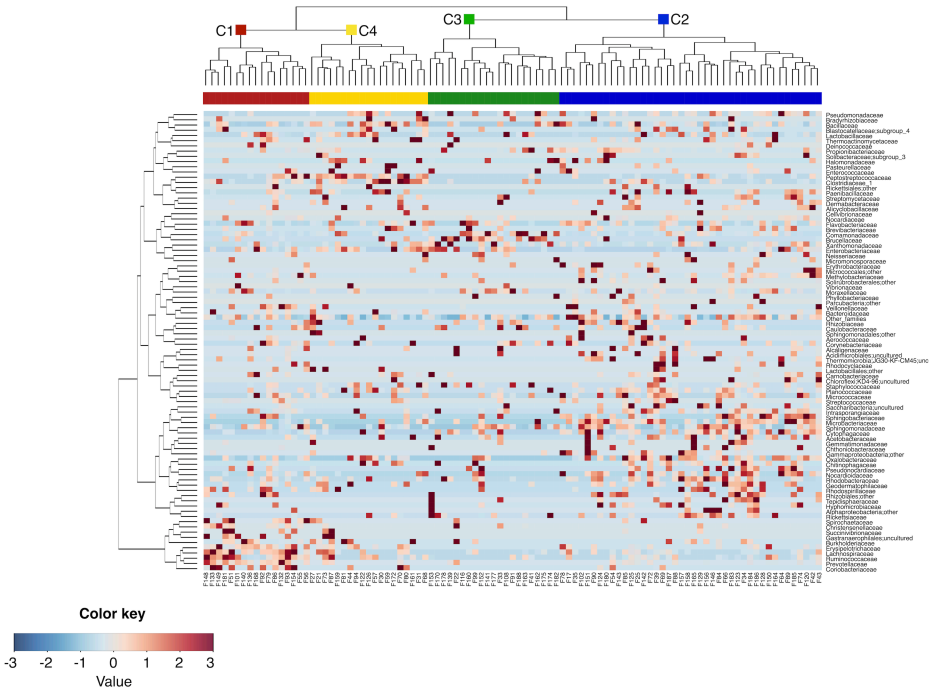

Figure 26 - **Family-level clusters of the airborne microbiome.** Hierarchical Ward-linkage clustering based on the Spearman correlation coefficients of the proportion of families in the AM samples. Only families with relative abundance >2% in at least 3 samples were retained. The four identified clusters (FDR-corrected permutation test with pseudo-F ratio, p-value ≤ 0.001) are labelled in the top tree and highlighted by different coloured squares (red, blue, green and yellow for the clusters C1, C2, C3 and C4, respectively).

parameters or PMF factors (Supplementary Tables S6 and S7, respectively), we found that factor 5 (naval-maritime transport) and relative humidity (RH) were both positively correlated with the PCo1 axis (Kendall's test, FDR-corrected p-value ≤ 0.001), while factor 6 (coal burning) was negatively correlated with the PCo1 coordinates (p-value ≤ 0.001) (Figure 27). This indirect gradient analysis allowed to highlight positive associations between clusters C1 and C3 and factors 6 and 5, respectively. Further, cluster C3 was found to be positively related to RH. As for seasonality, the clusters C3 and C4 are the most prevalent in summer and winter, respectively, while for C1 and C2 we did not observe any prevalence for a particular sampling period. We also compared the microbial diversity values of samples included in the different clusters, using three different diversity metsrics. Our data indicated higher biodiversity in clusters C1 and C2 (PD whole tree, chao1, and observed ASVs, mean ± SD: 3.6±1.3, 67.2±43.9, and 65.0±40.5 for C1, 3.2±1.4, 59.1±38.2 and 57.6±36.0 for C2, respectively) compared to C3 and C4 (1.4±0.7, 18.7±9.4, and 18.5±9.3 for C3, 2.4±1.2, 31.2±18.4 and 31.2±18.3 for C4), with C3 having the lowest biodiversity (Kruskal-Wallis test, FDR corrected p-value ≤ 0.001).

Compositional specificity and prevalent microbiological source of the four AM clusters

We subsequently compared the relative abundance of AM families among the four clusters in order to find out the most distinctive families of each of them (Supplementary Figure S13). According to our findings, the discriminating families (i.e., families with significantly different relative abundance, based on Kruskal-Wallis test) for the microbial cluster C1 are *Prevotellaceae*, *Erysipelotrichaceae*, *Coriobacteriaceae*, *Christensenellaceae*, *Lachnospiraceae*, *Ruminococcaceae,* and *Spirochaetaceae*. The microbial cluster C2 is

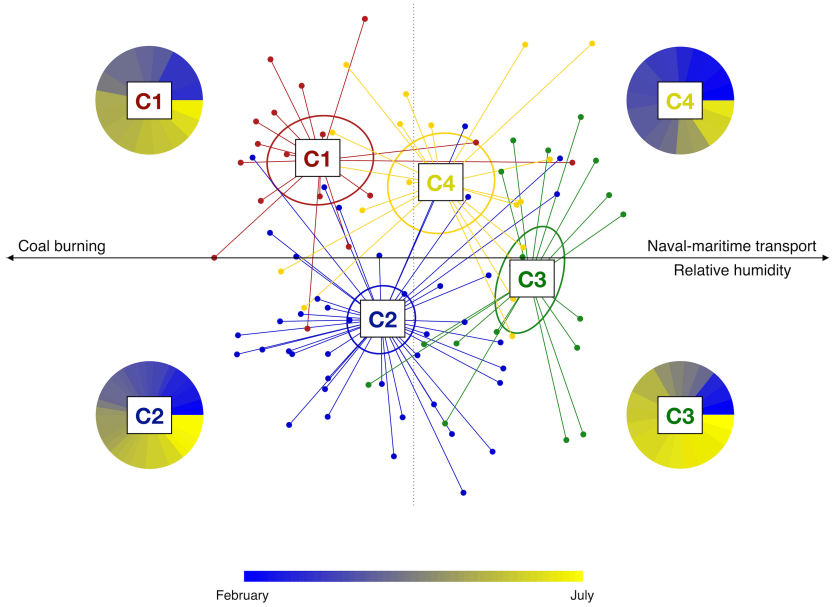

Figure 27 - Variation of the AM topological structure and association with PM emission sources and meteorological parameters. Principal coordinates analysis (PCoA) based on the unweighted UniFrac distance shows separation between the microbial clusters (C1 to C4; permutation test with pseudo F-ratio, p-value ≤ 0.001; see also Figure 3). The percentage of variance in the dataset explained by each axis, first and second principal component (PCo1 and PCo2), is 13.2% and 5.9%, respectively. Ellipses include 95% confidence area based on the standard error of the weighted average of sample coordinates. Significant Kendall correlations between PCoA axes and PMF factors and measured meteorological parameters are reported with a black arrow. Specifically, the emission source factor 5 (naval-maritime transport) and relative humidity are both positively correlated with the PCo1 axis (Kendall correlation test, FDR-corrected p-value ≤ 0.001), while the emission source factor 6 (coal burning) is negatively correlated with the PCo1 coordinates (p-value ≤ 0.001). For each AM cluster, the proportion of samples based on the sampling time (from February (dark blue) to July (yellow)) is shown as a pie chart.

instead characterized by higher abundance in the families *Microbacteriaceae*, *Cytophagaceae*, *Oxalobacteraceae*, *Sphingobacteriaceae*, *Nocardioidaceae*, *Methylobacteriaceae*, *Intrasporangiaceae*, *Rhodobacteraceae* and *Acetobacteraceae*. Only two proteobacterial families, namely *Brucellaceae* and *Comamonadaceae,* have a significantly higher abundance in cluster C3. Four families show higher abundance in cluster C4, i.e., *Peptostreptococcaceae*, *Clostridiaceae*, *Bacillaceae* and *Enterobacteriaceae*. It is also worth noting that the families *Planococcaceae* and *Paenibacillaceae* are highly represented in both C2 and C4 clusters, whereas *Sphingomonadaceae* members are equally represented in all clusters except for C4.

In an attempt to identify the most likely prevalent microbial origin of the four AM clusters, we first derived the respective compositional peculiarities at the OTU level. To this aim, 16S rRNA gene reads were clustered at 97% homology, resulting in 3 821 OTUs. By linear regression, we subsequently obtained 80 OTUs specifically discriminating the four clusters. In particular, for 52 of these OTUs a significantly different distribution in the four clusters was confirmed by a Kruskal-Wallis test, as shown in Supplementary Figure S14. For each of them, the isolation source of the closest BLAST match within the NCBI 16S rRNA sequence database was recovered (Supplementary Table S8). Interestingly, according to our findings, the cluster C1 is

mainly characterized by OTUs of faecal origin. These OTUs include sequences assigned to typical components of the human gut microbiome, such as *Faecalibacterium prausnitzii*, *Ruminococcus faecis*, *Prevotella copri*, *Eubacterium eligens*, *Ruminococcus bromii*, *Roseburia inulinivorans* and *Blautia faecis* (Zhang et al., 2015; Lloyd-Price et al., 2016; Rinninella et al., 2019), the cattle rumen components *Succinivibrio dextrinosolvens* (Wang et al., 2017) and *Oscillibacter ruminantium* (Lee et al., 2012), and the porcine gut microbiome member *Treponema porcinum* (Nordhoff et al., 2005). Differently, the cluster C2 is characterized by OTUs assigned to microorganisms isolated from plant roots and leaves, including *Curtobacterium flaccumfaciens* (Chen et al., 2021), *Glutamicibacter halophytocola* (Feng et al., 2017) and *Frigoribacterium endophyticum* (Wang et al., 2015), as well as by a specific pattern of environmental bacteria, from soil, air, and fresh and marine water ecosystems. Similarly, both clusters C3 and C4 are characterized by a peculiar combination of environmental microorganisms from different sources, including soil, fresh and marine waters, and airborne microbial ecosystems.

Discussion

In order to explore connections between the local air microbiome, atmospheric pollution and meteorological factors, here we provide a longitudinal survey of the near-ground AM, atmospheric particulate and atmospheric parameters in Savona, Italy. According to our findings, the local AM appears dominated by the phyla Proteobacteria, Firmicutes, Actinobacteria and Bacteroidetes, well matching the general layout of an AM community (Fröhlich-Nowoisky et al., 2016; Liu et al., 2019). The application of the PMF receptor modelling on the chemical compositional pattern of the PM_{10} samples collected during the field campaign allowed the identification of seven emission sources: “crustal material and road dust resuspension”, “traffic and biomass burning”, “secondary nitrate”, “secondary ammonium sulphate”, “naval-maritime transport”, “coal burning” and “sea spray”. Each source factor was subsequently subjected to anemological analysis based on polar plots, allowing each emission source to be associated with the corresponding wind direction to which the receptor site is downwind, similarly to the approach used by Innocente et al. (2017). Specifically, emission sources as “crustal material and road dust resuspension”, “secondary nitrate”, “secondary ammonium sulphate” and “coal burning” were associated with winds blowing from the inland toward the sampling site, intercepting substantially traffic and industrial particulate sources. Conversely, emission sources such as “naval-maritime transport” and “sea spray” were associated with a sea breeze, supporting a marine origin for both. Finally, the “traffic and biomass burning” emission source mostly showed a local origin.

It is known that bacterial communities structure and composition can be influenced by environmental conditions, such as seasons, air masses origin and landscape characteristics (Innocente et al., 2017; Tignat-Perrier et al., 2019; Bowers et al., 2011), as well as PM_{10} chemical compositional pattern (Gandolfi et al., 2015). When we explored the AM structure variation during the observation period, we were able to identify four distinct clusters of samples, named C1 to C4. Interestingly, the four clusters were associated with a peculiar combination of seasonality, meteorological variables and emission sources, as integrated into factors by PMF analysis.

In particular, the AM cluster C1 was associated with the “coal burning” emission source, suggesting not actually the industrial facility as a microbiome source, but rather the influence of an air mass whose

transport over a given district harvests chemical and microbiological components along the same tropospheric path. Instead, the cluster C3, most represented in the warm period, probably has a marine origin due to its association with the “naval-marine transport” emission source and high relative humidity. Finally, the clusters C2 and C4 did not show any specific association with the aerosol sources assessed by PMF, even if they showed a different seasonal behaviour, with C4 being more represented in the cold period. The results obtained by the application of such double-step multivariate analysis – associating multidimensional microbiome and chemical datasets – represent the true novelty of our study. Indeed, we were able to associate the AM composition to well discriminated emission sources, each with a characteristic chemical composition and origin.

The four AM clusters revealed a distinct, well-defined compositional structure, each being enriched with a specific set of microbial families and OTUs. The specificity of each bacterial profile de facto serves as a microbiological fingerprint, allowing to single out the probable microbiome sources characterizing each cluster that, similar to what occurs to abiotic particles, allow to trace back the origin of the air mass. In particular, the clusters C3 and C4 substantially reflect interconnected environmental microbiomes, encompassing a specific combination of microorganisms from soil resuspension, as well as from marine and fresh waters (possibly from rivers and streams flowing into the Ligurian Sea) and from the air. C2 cluster reveals the plant microbiome as an additional source, showing a further combination of plant-associated and environmental microorganisms, due to the contact of air masses over a vegetation landscape. Interestingly, the feasibility of air mass tracing also using bacterial species clearly emerges when we observe in detail the compositional structure of C1. This is in fact the only AM cluster carrying a recognizable pool of bacterial moieties of faecal origin, which are consistently part of the animal gut microbiome, suggesting not only a well-defined origin but also the potential use of this information in the assessment of microbiological impacts. Faecal material as a potential source of bacteria was already reported by Bowers et al. (2013). It should be noted that in the area upwind C1 no sewage treatment plant as a possible source of faecal microbiome was present at the time of sampling. However, the area is very densely populated and forested areas populated by local fauna are closely found within a few kilometres.

Taken together, our data on the temporal dynamics of the near-ground AM in Savona, highlight the relevant degree of plasticity of AM over time. As such, we demonstrated how meteorological factors (i.e., wind direction and humidity) and atmospheric pollution (particles emission sources) can combine in shaping the AM configuration. In particular, coal burning and winds blowing from the inlands mix to establish a characteristic AM with a prevalence of aerosolized faecal microorganisms, regardless of seasonality. Conversely, in the summer season, humidity, sea breeze and naval-marine transport pollutants result in an AM mainly originating from environmental microbiomes, including microorganisms that are typically found in seawater and soil. Even if we were not able to establish connections between the other identified emission sources and specific AM clusters, we would stress the importance of seasonality in shaping the AM structure. Indeed, the variation between the clusters C2 and C4, for which no connection with any emission source was observed, was shown to be dependent on the sampling period, with the cluster C2 most prevalent during the warm season and including plant microbiomes as possible characteristic sources, as previously observed by Franzetti et al. (2011) and Bertolini et al. (2013).

In conclusion, our results suggest that, in an urban settlement, the influence of air masses harvesting chemical components from industrial sources may increase the proportion of aerosolized faecal microorganisms in the atmosphere, ultimately increasing citizens' exposure to faecal microbes. Similar results have recently been obtained by exploring AM in Beijing over 6 months (Qin et al., 2020). Our findings strengthen the importance of including the monitoring of the AM compositional structure as a determinant factor in the currently used air quality indexes. Indeed, in urban areas, the possible increased exposure to faecal-associated microbiomes as a result of increasing pollution can pose a possible threat to human health, particularly in regions with high-intensity animal farming, due to the inherent propensity of opportunistic pathogens to aerosolize.

References

Alastuey, A., Moreno, N., Querol, X., Viana, M., Artíñano, B., Luaces, J. A., ... & Guerra, A. (2007). Contribution of harbour activities to levels of particulate matter in a harbour area: Hada Project-Tarragona Spain. *Atmospheric Environment*, *41*(30), 6366-6378.

Ashbaugh, L. L., Malm, W. C., & Sadeh, W. Z. (1985). A residence time probability analysis of sulfur concentrations at Grand Canyon National Park. *Atmospheric Environment (1967)*, *19*(8), 1263-1270.

Becagli, S., Sferlazzo, D. M., Pace, G., Sarra, A. D., Bommarito, C., Calzolai, G., ... & Udisti, R. (2012). Evidence for heavy fuel oil combustion aerosols from chemical analyses at the island of Lampedusa: a possible large role of ships emissions in the Mediterranean. *Atmospheric Chemistry and Physics*, *12*(7), 3479-3492.

Behera, S. N., Sharma, M., Aneja, V. P., & Balasubramanian, R. (2013). Ammonia in the atmosphere: a review on emission sources, atmospheric chemistry and deposition on terrestrial bodies. *Environmental Science and Pollution Research*, *20*(11), 8092-8131.

Belis, C. A., Harrison, R. M., & Hopke, P. K. (2019). European guide on air pollution source apportionment with receptor models.

Bentamy, A., Ayina, H. L., Queffeulou, P., Croize-Fillon, D., & Kerbaol, V. (2007). Improved near real time surface wind resolution over the Mediterranean Sea. *Ocean Science*, *3*(2), 259-271.

Bertolini, V., Gandolfi, I., Ambrosini, R., Bestetti, G., Innocente, E., Rampazzo, G., & Franzetti, A. (2013). Temporal variability and effect of environmental variables on airborne bacterial communities in an urban area of Northern Italy. *Applied microbiology and biotechnology*, *97*(14), 6561-6570.

Bowers, R. M., McLetchie, S., Knight, R., & Fierer, N. (2011). Spatial variability in airborne bacterial communities across land-use types and their relationship to the bacterial communities of potential source environments. *The ISME journal*, *5*(4), 601-612.

Bowers, R. M., Clements, N., Emerson, J. B., Wiedinmyer, C., Hannigan, M. P., & Fierer, N. (2013). Seasonal variability in bacterial and fungal diversity of the near-surface atmosphere. *Environmental science & technology*, *47*(21), 12097-12106.

Brown, S. G., Eberly, S., Paatero, P., & Norris, G. A. (2015). Methods for estimating uncertainty in PMF solutions: examples with ambient air and water quality data and guidance on reporting PMF results. *Science of the Total Environment*, *518*, 626-635.

Burlando, M., De Gaetano, P., Pizzo, M., Repetto, M. P., Solari, G., & Tizzi, M. (2013). Wind climate analysis in complex terrains. *Journal of Wind Engineering and Industrial Aerodynamics*, *123*, 349-362.

Cao, C., Jiang, W., Wang, B., Fang, J., Lang, J., Tian, G., ... & Zhu, T. F. (2014). Inhalable microorganisms in Beijing's PM2. 5 and PM10 pollutants during a severe smog event. *Environmental science & technology*, *48*(3), 1499-1507.

Caporaso, J. G., Kuczynski, J., Stombaugh, J., Bittinger, K., Bushman, F. D., Costello, E. K., ... & Knight, R. (2010). QIIME allows analysis of high-throughput community sequencing data. *Nature methods*, *7*(5), 335-336.

Carslaw, D. C., & Ropkins, K. (2012). Openair—an R package for air quality data analysis. *Environmental Modelling & Software*, *27*, 52-61.

Castillo, J. A., Staton, S. J., Taylor, T. J., Herckes, P., & Hayes, M. A. (2012). Exploring the feasibility of bioaerosol analysis as a novel fingerprinting technique. *Analytical and bioanalytical chemistry*, *403*(1), 15-26.

Chen, G., Khojasteh, M., Taheri-Dehkordi, A., Taghavi, S. M., Rahimi, T., & Osdaghi, E. (2021). Complete genome sequencing provides novel insight into the virulence

repertories and phylogenetic position of dry beans pathogen Curtobacterium flaccumfaciens pv. flaccumfaciens. *Phytopathology®*, *111*(2), 268-280.

Chow, J. C., Lowenthal, D. H., Chen, L. W. A., Wang, X., & Watson, J. G. (2015). Mass reconstruction methods for PM 2.5: a review. *Air Quality, Atmosphere & Health*, *8*(3), 243-263.

Comero, S., Capitani, L., & Gawlik, B. M. (2009). Positive Matrix Factorisation (PMF)–An introduction to the chemometric evaluation of environmental monitoring data using PMF. *Office for Official Publications of the European Communities, Luxembourg*, *59*.

Culhane, A. C., Thioulouse, J., Perrière, G., & Higgins, D. G. (2005). MADE4: an R package for multivariate analysis of gene expression data. *Bioinformatics*, *21*(11), 2789-2790.

DeLeon-Rodriguez, N., Lathem, T. L., Rodriguez-R, L. M., Barazesh, J. M., Anderson, B. E., Beyersdorf, A. J., ... & Konstantinidis, K. T. (2013). Microbiome of the upper troposphere: species composition and prevalence, effects of tropical storms, and atmospheric implications. *Proceedings of the National Academy of Sciences*, *110*(7), 2575-2580.

Delort, A. M., & Amato, P. (Eds.). (2017). *Microbiology of aerosols*. John Wiley & Sons.

Després, V., Huffman, J. A., Burrows, S. M., Hoose, C., Safatov, A., Buryak, G., ... & Jaenicke, R. (2012). Primary biological aerosol particles in the atmosphere: a review. *Tellus B: Chemical and Physical Meteorology*, *64*(1), 15598.

Dommergue, A., Amato, P., Tignat-Perrier, R., Magand, O., Thollot, A., Joly, M., ... & Larose, C. (2019). Methods to investigate the global atmospheric microbiome. *Frontiers in microbiology*, *10*, 243.

Faith, D. P. (1992). Conservation evaluation and phylogenetic diversity. *Biological conservation*, *61*(1), 1-10.

Feng, W. W., Wang, T. T., Bai, J. L., Ding, P., Xing, K., Jiang, J. H., ... & Qin, S. (2017). Glutamicibacter halophytocola sp. nov., an endophytic actinomycete isolated from the roots of a coastal halophyte, Limonium sinense. *International journal of systematic and evolutionary microbiology*, *67*(5), 1120-1125.

Fioletov, V., McLinden, C. A., Kharol, S. K., Krotkov, N. A., Li, C., Joiner, J., ... & Denier van der Gon, H. A. (2017). Multi-source SO 2 emission retrievals and consistency of satellite and surface measurements with reported emissions. *Atmospheric Chemistry and Physics*, *17*(20), 12597-12616.

Franzetti, A., Gandolfi, I., Gaspari, E., Ambrosini, R., & Bestetti, G. (2011). Seasonal variability of bacteria in fine and coarse urban air particulate matter. *Applied microbiology and biotechnology*, *90*(2), 745-753.

Fröhlich-Nowoisky, J., Kampf, C. J., Weber, B., Huffman, J. A., Pöhlker, C., Andreae, M. O., ... & Pöschl, U. (2016). Bioaerosols in the Earth system: Climate, health, and ecosystem interactions. *Atmospheric Research*, *182*, 346-376.

Gandolfi, I., Bertolini, V., Bestetti, G., Ambrosini, R., Innocente, E., Rampazzo, G., ... & Franzetti, A. (2015). Spatio-temporal variability of airborne bacterial communities and their correlation with particulate matter chemical composition across two urban areas. *Applied microbiology and biotechnology*, *99*(11), 4867-4877.

Geiger, R. (1954) Landolt-Börnstein – Zahlenwerte und Funktionen aus Physik, Chemie, Astronomie, Geophysik und Technik, alte Serie Vol. 3, Ch. Klassifikation der Klimate nach W. Köppen. 603–607 (Springer, Germany)

Gietl, J. K., Lawrence, R., Thorpe, A. J., & Harrison, R. M. (2010). Identification of brake wear particles and derivation of a quantitative tracer for brake dust at a major road. *Atmospheric Environment*, *44*(2), 141-146.

Graham, K. E., Prussin, A. J., Marr, L. C., Sassoubre, L. M., & Boehm, A. B. (2018). Microbial community structure of sea spray aerosols at three California beaches. *FEMS microbiology ecology*, *94*(3), fiy005.

Grythe, H., Ström, J., Krejci, R., Quinn, P., & Stohl, A. (2014). A review of sea-spray aerosol source functions using a large global set of sea salt aerosol concentration measurements. *Atmospheric Chemistry and Physics*, *14*(3), 1277-1297.

Hopke, P. K. (2000, February). A guide to positive matrix factorization. In *Workshop on UNMIX and PMF as Applied to PM2* (Vol. 5, No. 5, p. 600).

Hopke, P. K. (2016). Review of receptor modeling methods for source apportionment. *Journal of the Air & Waste Management Association*, *66*(3), 237-259.

Huang, R. J., Zhang, Y., Bozzetti, C., Ho, K. F., Cao, J. J., Han, Y., ... & Prévôt, A. S. (2014). High secondary aerosol contribution to particulate pollution during haze events in China. *Nature*, *514*(7521), 218-222.

Hueglin, C., Gehrig, R., Baltensperger, U., Gysel, M., Monn, C., & Vonmont, H. (2005). Chemical characterisation of PM2. 5, PM10 and coarse particles at urban, near-city and rural sites in Switzerland. *Atmospheric Environment*, *39*(4), 637-651.

Hyde, P., & Mahalov, A. (2020). Contribution of bioaerosols to airborne particulate matter. *Journal of the Air & Waste Management Association*, *70*(1), 71-77.

Innocente, E., Squizzato, S., Visin, F., Facca, C., Rampazzo, G., Bertolini, V., ... & Bestetti, G. (2017). Influence of seasonality, air mass origin and particulate matter chemical composition on airborne bacterial community structure in the Po Valley, Italy. *Science of the Total Environment*, *593*, 677-687.

Jang, H. N., Seo, Y. C., Lee, J. H., Hwang, K. W., Yoo, J. I., Sok, C. H., & Kim, S. H. (2007). Formation of fine particles enriched by V and Ni from heavy oil combustion: Anthropogenic sources and drop-tube furnace experiments. *Atmospheric Environment*, *41*(5), 1053-1063.

Jiang, W., Liang, P., Wang, B., Fang, J., Lang, J., Tian, G., ... & Zhu, T. F. (2015). Optimized DNA extraction and metagenomic sequencing of airborne microbial communities. *Nature protocols*, *10*(5), 768-779.

Köppen, W. (1900). Versuch einer Klassifikation der Klimate, vorzugsweise nach ihren Beziehungen zur Pflanzenwelt. *Geographische Zeitschrift*, *6*(11. H), 593-611.

Lee, G. H., Kumar, S., Lee, J. H., Chang, D. H., Kim, D. S., Choi, S. H., ... & Kim, B. C. (2012). Genome sequence of Oscillibacter ruminantium strain GH1, isolated from rumen of Korean native cattle.

Li, H., Zhou, X. Y., Yang, X. R., Zhu, Y. G., Hong, Y. W., & Su, J. Q. (2019). Spatial and seasonal variation of the airborne microbiome in a rapidly developing city of China. *Science of the Total Environment*, *665*, 61-68.

Liu, H., Hu, Z., Zhou, M., Hu, J., Yao, X., Zhang, H., ... & Hu, B. (2019). The distribution variance of airborne microorganisms in urban and rural environments. *Environmental Pollution*, *247*, 898-906.

Lloyd-Price, J., Abu-Ali, G., & Huttenhower, C. (2016). The healthy human microbiome. Genome Med 8: 51.

Lucarelli, F., Nava, S., Calzolai, G., Chiari, M., Udisti, R., & Marino, F. (2011). Is PIXE still a useful technique for the analysis of atmospheric aerosols? The LABEC experience. *X-Ray Spectrometry*, *40*(3), 162-167.

Mallick H., Rahnavard A., McIver L. J., Ma S., Zhang Y., Nguyen L. H., Tickle T. L., Weingart G., Ren B., Schwager E. H., Chatterjee S., Thompson K. N., Wilkinson J. E., Subramanian A., Lu Y., Waldron L., Paulson J. N., Franzosa E. A., Bravo H. C., & Huttenhower C. (2021). Multivariable Association Discovery in Population-scale Meta-omics Studies. *PLoS Computational Biology*, 17(11):e1009442

Masiol, M., Squizzato, S., Formenton, G., Khan, M. B., Hopke, P. K., Nenes, A., ... & Pavoni, B. (2020). Hybrid multiple-site mass closure and source apportionment of PM2. 5 and aerosol acidity at major cities in the Po Valley. *Science of the Total Environment*, *704*, 135287.

Mescioglu, E., Rahav, E., Belkin, N., Xian, P., Eizenga, J. M., Vichik, A., ... & Paytan, A. (2019). Aerosol microbiome over the Mediterranean Sea diversity and abundance. *Atmosphere*, *10*(8), 440.

Mhuireach, G. Á., Betancourt-Román, C. M., Green, J. L., & Johnson, B. R. (2019). Spatiotemporal controls on the urban aerobiome. *Frontiers in Ecology and Evolution*, *7*, 43.

Michaud, J. M., Thompson, L. R., Kaul, D., Espinoza, J. L., Richter, R. A., Xu, Z. Z., ... & Prather, K. A. (2018). Taxon-specific aerosolization of bacteria and viruses in an experimental ocean-atmosphere mesocosm. *Nature communications*, *9*(1), 1-10.

Nordhoff, M., Taras, D., Macha, M., Tedin, K., Busse, H. J., & Wieler, L. H. (2005). Treponema berlinense sp. nov. and Treponema porcinum sp. nov., novel spirochaetes isolated from porcine faeces. *International journal of systematic and evolutionary microbiology*, *55*(4), 1675-1680.

Norris, G., Duvall, R., Brown, S. & Bai, S. (2014). Epa positive matrix factorization (PMF) 5.0 fundamentals and user guide prepared for the us environmental protection agency office of research and development. United States Environmental Protection Agency report. https://www.epa.gov/sites/production/files/2015-02/documents/pmf_5.0_user_guide.pdf.

Paatero, P., & Tapper, U. (1994). Positive matrix factorization: A non-negative factor model with optimal utilization of error estimates of data values. *Environmetrics*, *5*(2), 111-126.

Pachon, J. E., Weber, R. J., Zhang, X., Mulholland, J. A., & Russell, A. G. (2013). Revising the use of potassium (K) in the source apportionment of PM2. 5. *Atmospheric Pollution Research*, *4*(1), 14-21.

Pathak, R. K., Wu, W. S., & Wang, T. (2009). Summertime PM 2.5 ionic species in four major cities of China: nitrate formation in an ammonia-deficient atmosphere. *Atmospheric Chemistry and Physics*, *9*(5), 1711-1722.

Piazzalunga, A., Bernardoni, V., Fermo, P., Valli, G., & Vecchi, R. (2011). on the effect of water-soluble compounds removal on EC quantification by TOT analysis in urban aerosol samples. *Atmospheric chemistry and physics*, *11*(19), 10193-10203.

Qin, N., Liang, P., Wu, C., Wang, G., Xu, Q., Xiong, X., ... & Zhu, T. F. (2020). Longitudinal survey of microbiome associated with particulate matter in a megacity. *Genome biology*, *21*(1), 1-11.

Renard, P., Canet, I., Sancelme, M., Matulova, M., Uhliarikova, I., Eyheraguibel, B., ... & Delort, A. M. (2019). Cloud microorganisms, an interesting source of biosurfactants. *Surfactants and Detergents*.

Rinninella, E., Raoul, P., Cintoni, M., Franceschi, F., Miggiano, G. A. D., Gasbarrini, A., & Mele, M. C. (2019). What is the healthy gut microbiota composition? A changing ecosystem across age, environment, diet, and diseases. *Microorganisms*, *7*(1), 14.

Rodrıguez, S., Querol, X., Alastuey, A., Viana, M. M., Alarcon, M., Mantilla, E., & Ruiz, C. R. (2004). Comparative PM10–PM2. 5 source contribution study at rural, urban and industrial sites during PM episodes in Eastern Spain. *Science of the Total Environment*, *328*(1-3), 95-113.

Schaap, M., Loon, M. V., Ten Brink, H. M., Dentener, F. J., & Builtjes, P. J. H. (2004). Secondary inorganic aerosol simulations for Europe with special attention to nitrate. *Atmospheric Chemistry and Physics*, *4*(3), 857-874.

Sesartic, A., Lohmann, U., & Storelvmo, T. (2012). Bacteria in the ECHAM5-HAM global climate model. *Atmospheric Chemistry and Physics*, *12*(18), 8645-8661.

Shin, S. K., Kim, J., Ha, S. M., Oh, H. S., Chun, J., Sohn, J., & Yi, H. (2015). Metagenomic insights into the bioaerosols in the indoor and outdoor environments of childcare facilities. *PLoS One*, *10*(5), e0126960.

Thorpe, A., & Harrison, R. M. (2008). Sources and properties of non-exhaust particulate matter from road traffic: a review. *Science of the total environment*, *400*(1-3), 270-282.

Tignat-Perrier, R., Dommergue, A., Thollot, A., Keuschnig, C., Magand, O., Vogel, T. M., & Larose, C. (2019). Global airborne microbial communities controlled by surrounding landscapes and wind conditions. *Scientific reports*, *9*(1), 1-11.

Toprak, E., & Schnaiter, M. (2013). Fluorescent biological aerosol particles measured with the Waveband Integrated Bioaerosol Sensor WIBS-4: laboratory tests combined with a one year field study. *Atmospheric Chemistry and Physics*, *13*(1), 225-243.

Tositti, L., Brattich, E., Masiol, M., Baldacci, D., Ceccato, D., Parmeggiani, S., ... & Zappoli, S. (2014). Source apportionment of particulate matter in a large city of southeastern Po Valley (Bologna, Italy). *Environmental Science and Pollution Research*, *21*(2), 872-890.

Tositti, L. (2018a). Physical and chemical properties of airborne particulate matter. In *Clinical Handbook of Air Pollution-Related Diseases* (pp. 7-32). Springer, Cham.

Tositti, L. (2018b). The relationship between health effects and airborne particulate constituents. *Clinical Handbook of Air Pollution-Related Diseases*, 33-54.

Tositti, L., Brattich, E., Parmeggiani, S., Bolelli, L., Ferri, E., & Girotti, S. (2018). Airborne particulate matter biotoxicity estimated by chemometric analysis on bacterial luminescence data. *Science of the Total Environment*, *640*, 1512-1520.

Vecchi, R., Marcazzan, G., Valli, G., Ceriani, M., & Antoniazzi, C. (2004). The role of atmospheric dispersion in the seasonal variation of PM1 and PM2. 5 concentration and composition in the urban area of Milan (Italy). *Atmospheric Environment*, *38*(27), 4437-4446.

Veron, F. (2015). Ocean spray. Annual Review of Fluid Mechanics, 47, 507-538.

Viana, M., Hammingh, P., Colette, A., Querol, X., Degraeuwe, B., de Vlieger, I., & van Aardenne, J. (2014). Impact of maritime transport emissions on coastal air quality in Europe. *Atmospheric Environment*, *90*, 96-105.

Von Schneidemesser, E., Monks, P. S., Allan, J. D., Bruhwiler, L., Forster, P., Fowler, D., ... & Sutton, M. A. (2015). Chemistry and the linkages between air quality and climate change. *Chemical Reviews*, *115*(10), 3856-3897.

Wang, H. F., Zhang, Y. G., Chen, J. Y., Guo, J. W., Li, L., Hozzein, W. N., ... & Li, W. J. (2015). Frigoribacterium endophyticum sp. nov., an endophytic actinobacterium isolated from the root of Anabasis elatior (CA Mey.) Schischk. *International journal of systematic and evolutionary microbiology*, *65*(Pt_4), 1207-1212.

Wang, Y., Cao, P., Wang, L., Zhao, Z., Chen, Y., & Yang, Y. (2017). Bacterial community diversity associated with different levels of dietary nutrition in the rumen of sheep. *Applied microbiology and biotechnology*, *101*(9), 3717-3728.

Wilson, T. W., Ladino, L. A., Alpert, P. A., Breckels, M. N., Brooks, I. M., Browse, J., ... & Murray, B. J. (2015). A marine biogenic source of atmospheric ice-nucleating particles. *Nature*, *525*(7568), 234-238.

Womack, A. M., Bohannan, B. J., & Green, J. L. (2010). Biodiversity and biogeography of the atmosphere. *Philosophical Transactions of the Royal Society B: Biological Sciences*, *365*(1558), 3645-3653.

Woo, A. C., Brar, M. S., Chan, Y., Lau, M. C., Leung, F. C., Scott, J. A., ... & Pointing, S. B. (2013). Temporal variation in airborne microbial populations and microbially-derived allergens in a tropical urban landscape. *Atmospheric Environment*, *74*, 291-300.

Yu, J., Yan, C., Liu, Y., Li, X., Zhou, T., & Zheng, M. (2018). Potassium: a tracer for biomass burning in Beijing?. *Aerosol and Air Quality Research*, *18*(9), 2447-2459.

Zhang, J., Guo, Z., Xue, Z., Sun, Z., Zhang, M., Wang, L., ... & Zhang, H. (2015). A phylo-functional core of gut microbiota in healthy young Chinese cohorts across lifestyles, geography and ethnicities. *The ISME journal*, *9*(9), 1979-1990.

CHAPTER 4 - CONCLUDING REMARKS

The presented thesis work aims at filling the general lack of knowledge in the understanding of how host-associated microbes drive marine holobionts response to anthropogenic stressors and the host acclimatization to abiotic stressors, as a natural model of future climate change scenarios, by proposing different study models representing ecologically important, widely distributed, and habitat-forming organisms. By means of these study models, here we demonstrated how marine holobionts are able to dynamically adapt to natural environmental variations as well as related anthropogenic stress factors.

In particular, we showed that model benthonic organisms such as anthozoans and gastropods develop a microbial-derived adaptive response to anthropogenic stressors that allows their acclimatization under environmental disturbances. We described how natural seasonal variations combine with seasonal-related anthropogenic stressors acting as a consistent driver capable of shaping the microbial composition of the model organisms *Anemonia viridis* in the northwestern Adriatic Sea, a region characterized by strong annual fluctuations and severe anthropogenic stressors. In this context, *Anemonia viridis* acts as a natural filtration system able to select health-promoting microorganisms from the microbial communities populating the surrounding environment, possibly removing pathogens in a heavily human-impacted habitat, where waters can carry traces of fecal contamination from domestic wastage, agricultural runoff, river discharges and massive tourism. This highlights the importance of the role of this model organism for ecosystem restoration. Regarding the monitoring and preservation of coastal marine ecosystems, we dissected the interactions between the microbiomes from farmed fishes and the surrounding wild holobionts at the metacommunity level, in consideration of the strong impact of mariculture on environmental conditions in the surrounding water column. Particularly, we showed patterns of microbial dispersion from the farmed fishes to the environment and, finally, to locally dwelling wild organisms, through the use of the sedentary organism *Patella caerulea* as a proxy for metacommunity changes.

Moreover, we proposed the temperate, solitary, and widespread scleractinian coral *Balanophyllia europaea* as a natural model of acclimatization to low seawater pH, aiming at expanding our current knowledge on processes of acclimatization for marine holobionts to future ocean acidification conditions. Due to the massive threat posed by ocean acidification to the marine ecosystems, we investigated variations in the composition and metabolic potential of the microbiomes associated with *Balanophyllia europaea*. In this thesis work, we showed that corals naturally living at low pH conditions develop microbial dependent mechanisms of adaptation, providing a valuable model to implement microbial based actions to mitigate climate change.

ACKNOWLEDGMENTS

During this long journey that has been my PhD period, I met many people that contributed greatly to all my scientific and personal achievements.

Among all the scientific collaborations that allowed me to develop my research studies, I would like to thank Associazione Paguro (Ravenna, Italy) and Dive Planet (Rimini, Italy) for their primary contribution to the *Corynactis viridis* samples collection and for the pictures of "Il Paguro." I would also like to thank Cooperativa Bagnini Riccione (Riccione, Italy), Associazione BLENNIUS (Riccione, Italy) and Fondazione Cetacea Onlus (Riccione, Italy) for their involvement in all the scientific and citizen science activities, for their spirit of cooperation, their passion, and for their availability in samples collection. Finally, I would like to thank the Italian National Research Council group (CNR), in particular in the figure of my co-supervisor Gian Marco Luna, and the Environmental Chemistry and Radioactivity Laboratory of the University of Bologna, in particular prof. Laura Tositti, because of their precious collaboration in the production of high quality scientific data.

From both a personal and professional perspective, I would like to thank my research group, the Microbiome Science and Biotechnology Unit, and our affiliate group, the Microbiomics Unit.
Marco, thank you because your role is not limited to our group leader, but you are also a great mentor and motivator. Thank you for your trust.
Silvia, thank you because you are always present for any question and advice in the most easy going way, making everyone feel comfortable. And thank you for your desk!
Simone, thank you because any time I have a doubt, it doesn't matter whether lab related or not, you always have a valuable opinion to share.
Daniel, I would like to define you as my lab buddy, but we all know that partner is definitively a more accurate definition! Thank you, because it would not have been the same without you.
Margherita, we started this journey together. Thank you for making it easier.
Enrico, our collaboration definitively started in a rush, but we managed to deal with everything so far. I'm confident it can only improve for the best.
Patrizia, thank you because you started all this and nobody would be here if it wasn't for you.
Federica, we had a rough start, being us both stubborn in our own way. I'm glad of how much our relationship improved, you really are a great person to rely on.
Monica, thank you for always being kind and available. I would not have survived all the didactic activities without your help!
Marco, you are one of the most effective and efficient people I know. Thank you because of your great problem solving ability whenever I needed it.
Gabriele, Mariachiara and Giulia, we just started our collaboration. I'm looking forward to seeing its progresses.
Elena, I need to put you at the end of this list, but not for importance. This thesis would definitely not have been completed without your great help. I am very happy for your last professional achievements, even tough this means we are not working together anymore. I wish you all the best, because you deserve it. And I would never thank you enough for how much you thought me.

Finally, I would like to make my most personal acknowledgments.
I would like to thank my family for always being supportive throughout all these years, allowing me to reach this last milestone in my education. None of my achievements would have been possible without you.
I would like to thank my CrossFit Box as my second home. Or maybe as my first one, I literally spend more time there than in my own house! Thank you to CFZP and its amazing coaches for all your help in my personal improvement. You gave me the motivation to always push my boundaries and overcome my limits, making me growing not only as an athlete, but as a person. And thank you to my CrossFit mates I Bagagli del Signor Tiro, you have no idea how much you helped me with stress relieve and how much you supported me. With this, our group name is officially on paper!
My final thanks goes to Andrea. This is the third thesis where I need to thank you for supporting me in this journey. I started thanking you as my boyfriend and I finish thanking you as my husband. I don't think I have any more word to express my gratitude towards you. So I will just say thank you one more time.

LIST OF PUBLICATIONS FROM THE AUTHOR

1. **Palladino, G.**, Rampelli, S., Scicchitano, D., Musella, M., Quero, G.M., Prada, F., Mancuso, A., Seyfarth, A.M., Turroni. S., Candela, M., Biagi, E. (2021). Impact of marine aquaculture on the microbiome associated with nearby holobionts: the case of *Patella caerulea* living in proximity of sea bream aquaculture cages. *Microorganisms*. https://doi.org/10.3390/microorganisms9020455

2. Biagi, E., Musella, M., **Palladino, G.**, Angelini, V., Pari, S., Roncari, C., Scicchitano, D., Rampelli, S., Franzellitti, S., Candela, M. (2021). Impact of Plastic Debris on the Gut Microbiota of *Caretta caretta* From Northwestern Adriatic Sea. *Frontiers in Marine Science*. https://doi.org/10.3389/fmars.2021.637030.

3. **Palladino, G.**, Biagi, E., Rampelli, S., Musella, M., D'Amico, F., Turroni, S., Brigidi, P., Luna, G.M., Candela, M. (2021). Seasonal Changes in Microbial Communities Associated With the Jewel Anemone *Corynactis viridis*. *Frontiers in Marine Science*. https://doi.org/10.3389/fmars.2021.627585.

4. **Palladino, G.**, Morozzi, P., Biagi, E., Brattich, E., Turroni, S., Rampelli, S., Tositti, L., Candela, M. (2021). Particulate Matter emission sources and meteorological parameters combine to shape the airborne microbiome communities in the Ligurian coast, Italy. *Scientific reports*, 11, 175. https://doi.org/10.1038/s41598-020-80642-1.

5. Taylor, J.A., **Palladino, G.**, Wemheuer, B., Steinert, G., Sipkema, D., Williams, T.J., and Thomas, T. (2020). Phylogeny resolved, metabolism revealed: functional radiation within a widespread and divergent clade of sponge symbionts. *The ISME journal.* https://doi.org/10.1038/s41396-020-00791-z.

6. Musella, M., Wathsala, R., Tavella, T., Rampelli, S., Barone, M., **Palladino, G.**, Biagi, E., Brigidi, P., Turroni, S., Franzellitti, S., and Candela, M. (2020). Tissue-scale microbiota of the Mediterranean mussel (*Mytilus galloprovincialis*) and its relationship with the environment. *The Science of the total environment, 717*, 137209. https://doi.org/10.1016/j.scitotenv.2020.137209.

7. Chaib De Mares, M., Jiménez, D.J., **Palladino, G.**, Gutleben, J., Lebrun, L.A., Muller, E., Wilmes, P., Sipkema, D., and van Elsas, J.D. (2018). Expressed protein profile of a Tectomicrobium and other microbial symbionts in the marine sponge *Aplysina aerophoba* as evidenced by metaproteomics. *Scientific reports*, *8*(1), 11795. https://doi.org/10.1038/s41598-018-30134-0.

SUPPLEMENTARY MATERIAL

Supplementary figures

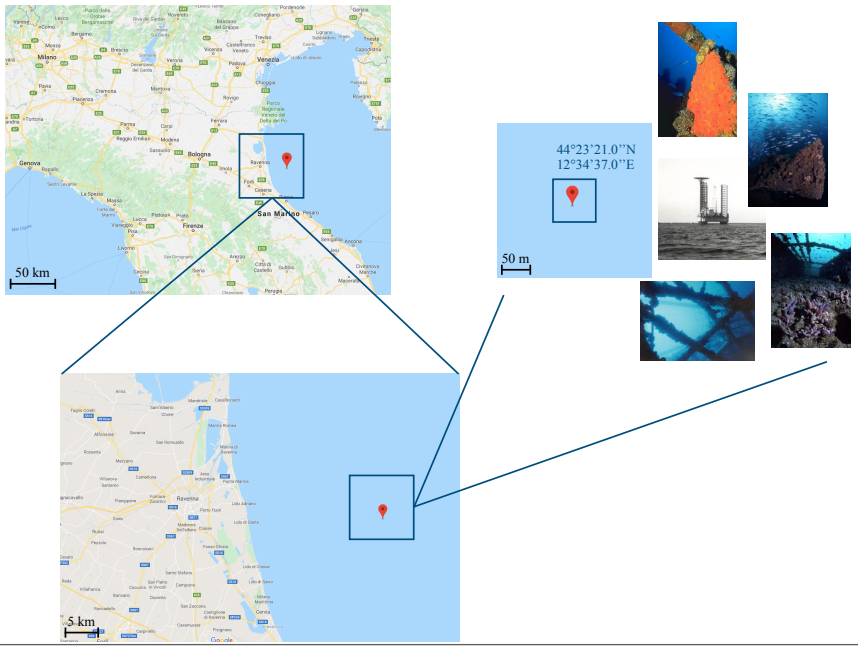

Figure S1 - **Maps and coordinates of "Il Paguro" site.** "Il Paguro" is located in the North Adriatic Sea, around 12 nautical miles offshore Ravenna. Its geographical coordinates are latitude 44°23'21.0''N and longitude 12°34'37.0''E. All the maps were collected from Google Maps and the pictures from the Associazione Paguro official website (http://www.associazionepaguro.org/coordinate.htm) with written authorization.

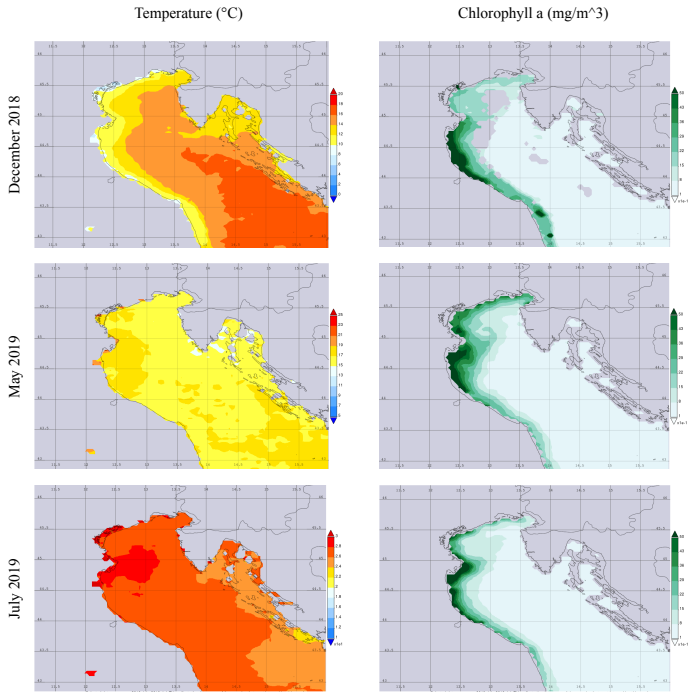

Figure S2 - **Monthly satellite maps of temperature and surface chlorophyll a.** All the maps were retrieved from NASA (https://giovanni.gsfc.nasa.gov/ giovanni/). Selected region is 11.1511E, 42.8522N, 15.9851E, 46.236N. Temperature and chlorophyll a were measured daily over the month of sampling and averaged.

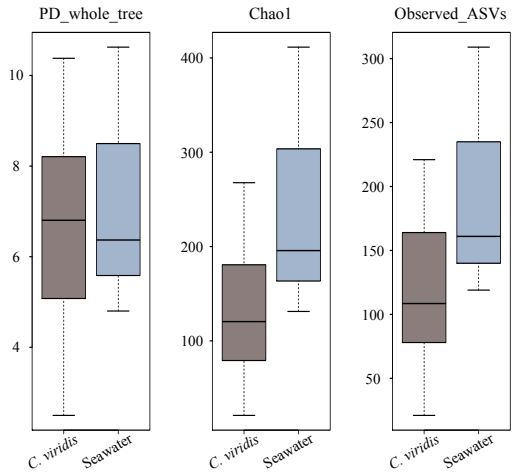

Figure S3 - **Alpha diversity of *C. viridis* and seawater bacterial communities.** Box-and-whiskers plots showing the distribution of the Faith's Phylogenetic Diversity (PD_whole_tree) α-diversity index, Chao1 index for microbial richness and observed ASVs, calculated for anemone and seawater samples. Data indicate a general tendency to higher richness in seawater than *C. viridis*-associated communities (Wilcoxon rank-sum test controlled for multiple testing using FDR, p-value > 0.05).

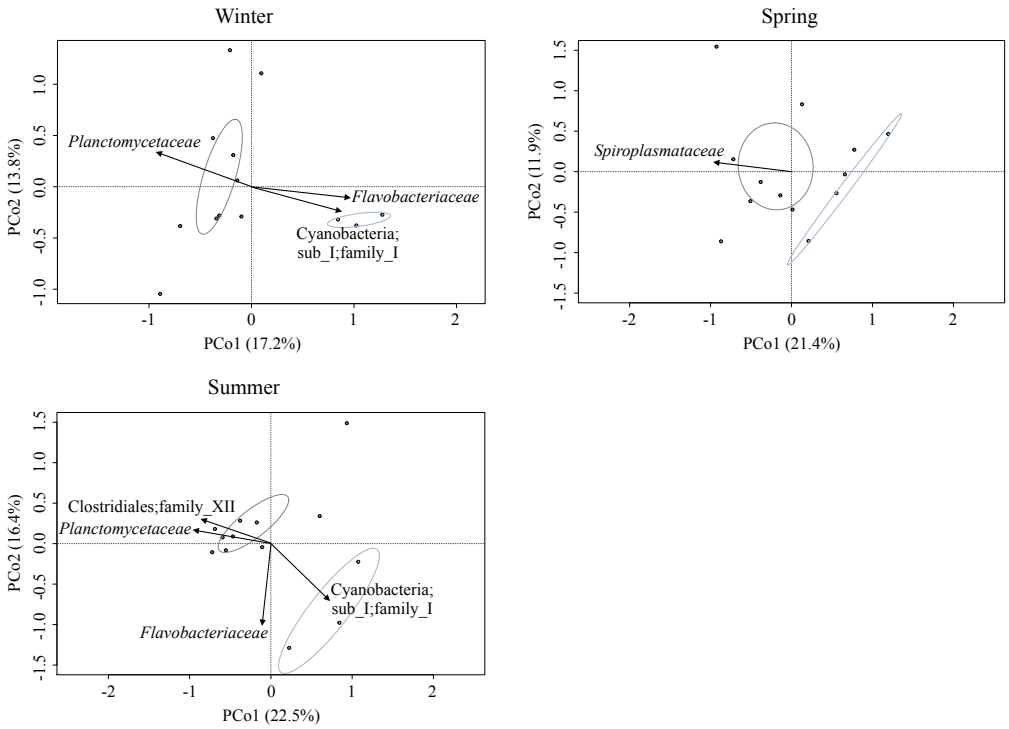

Figure S4 - **Beta diversity of *C. viridis* and seawater microbiomes per season.** Principal Coordinate Analyses (PCoA) of the overall compositional differences between *C. viridis* and seawater microbial communities for each season (winter, spring and summer). To identify the bacterial families most contributing to segregations, their relative abundance is superimposed on the PCoA plots (function envfit or the R package vegan). The separation between the *C. viridis* microbiome and that of seawater is significant and robust to seasonality (permutation test with pseudo F-ratio, p-value ≤ 0.01). Anemone samples are shown in brown and seawater samples in light blue. The first and second principal components (PCo1 and PCo2) are plotted and the percentage of variance in the dataset explained by each axis is reported. Ellipses include 95% confidence area based on the standard error of the weighted average of sample coordinates.

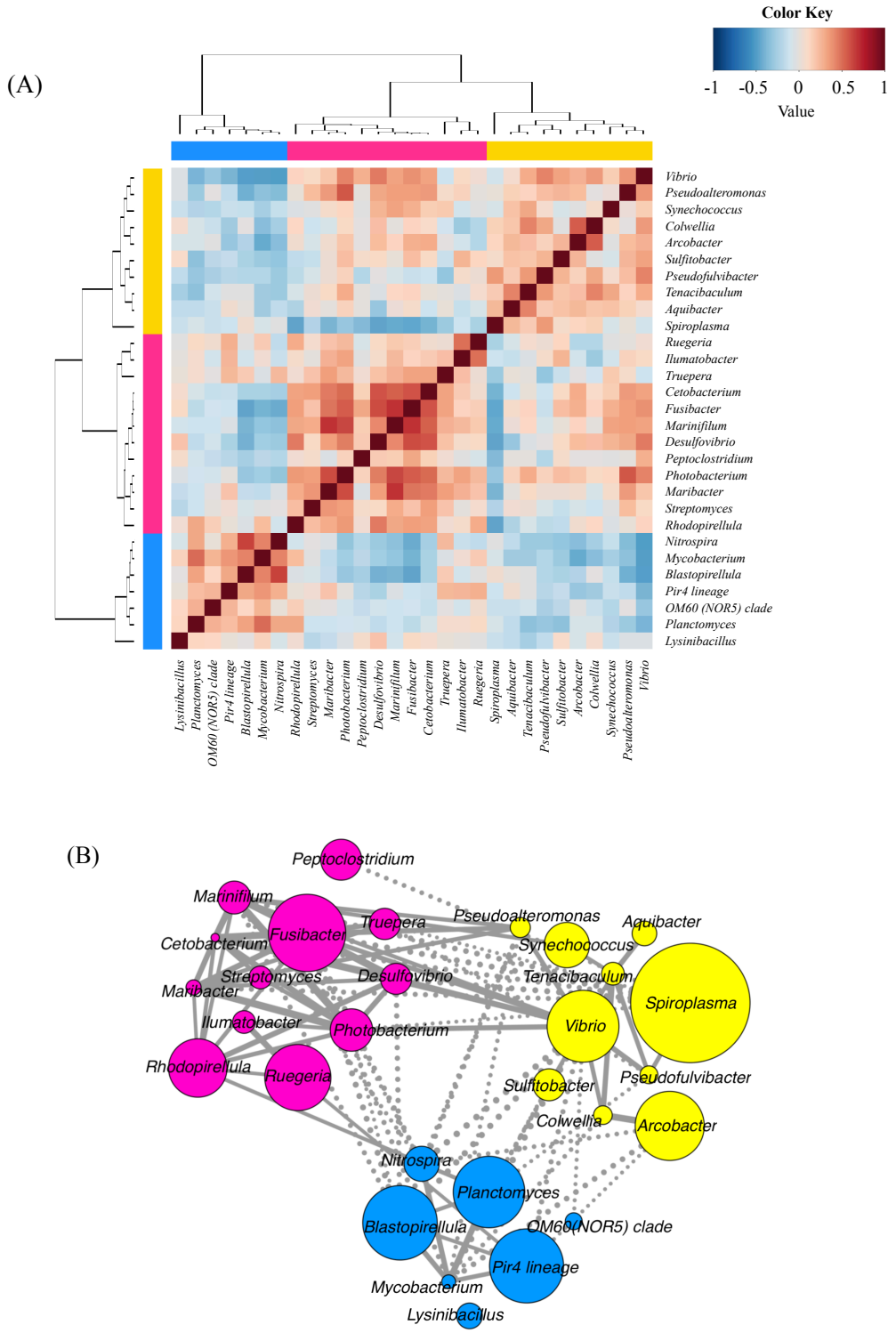

Figure S5 - **Co-abundance associations between *C. viridis* bacterial genera.** (A) The assignment of co-abundance groups (CAGs) relies on a heat plot showing Kendall correlations between genera clustered by the Spearman correlation coefficient and Ward linkage hierarchical clustering. Only genera with relative abundance higher than 0.5% in at least 10% of the samples are represented. Colors are indicative of the three identified CAGs. (B) Wiggum plot correlations between the three CAGs identified. Circle size is representative of the genus abundance and the connections between nodes represent positive (solid lines) and negative (dashed lines) significant Kendall correlations between genera (controlled for multiple testing using FDR, p-value ≤ 0.05).

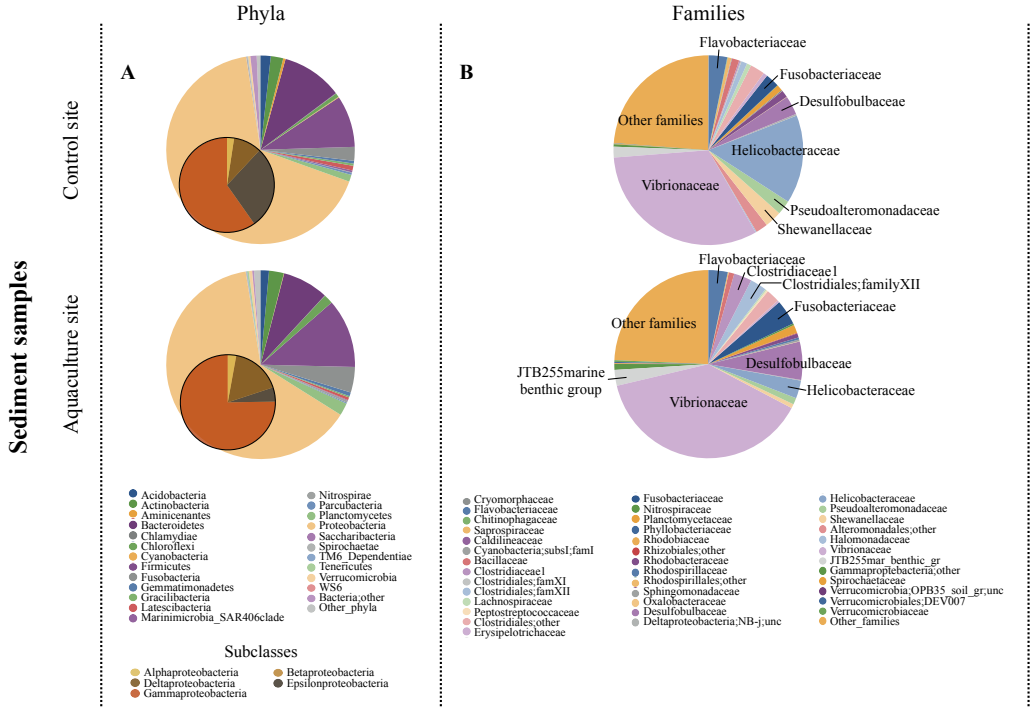

Figure S6 - Pie charts summarizing the phyla (A) and family (B) level microbiota composition of sediment samples in the two sampling sites. Phyla with relative abundance > 0.5% in at least one sample and families with relative abundance > 2% in at least 10% of samples are represented. Proteobacteria classes are expanded on the respective pie chart phylum slice. Subs = subset; fam = family; unc = uncultured; inc = incertae; mar =marine; gr = group.

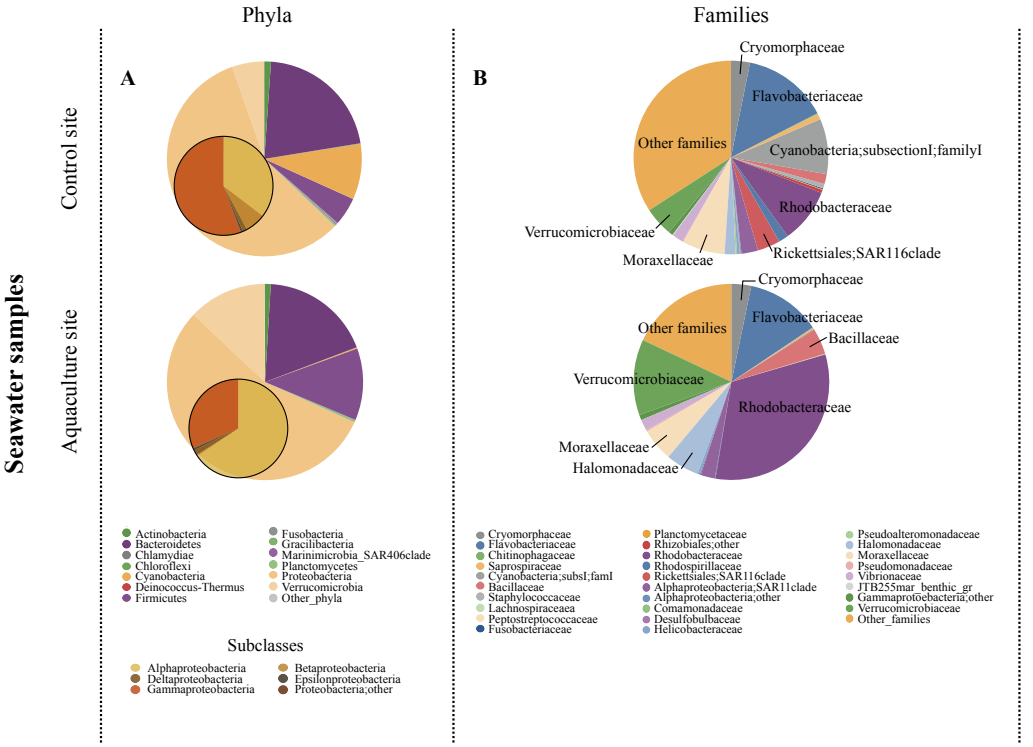

Figure S7 - Pie charts summarizing the phyla (A) and family (B) level microbiota composition of seawater samples in the two sampling sites. Phyla with relative abundance > 0.5% in at least one sample and families with relative abundance > 2% in at least 10% of samples are represented. Proteobacteria classes are expanded on the respective pie chart phylum slice. Subs = subset; fam = family; unc = uncultured; inc = incertae; mar =marine; gr = group.

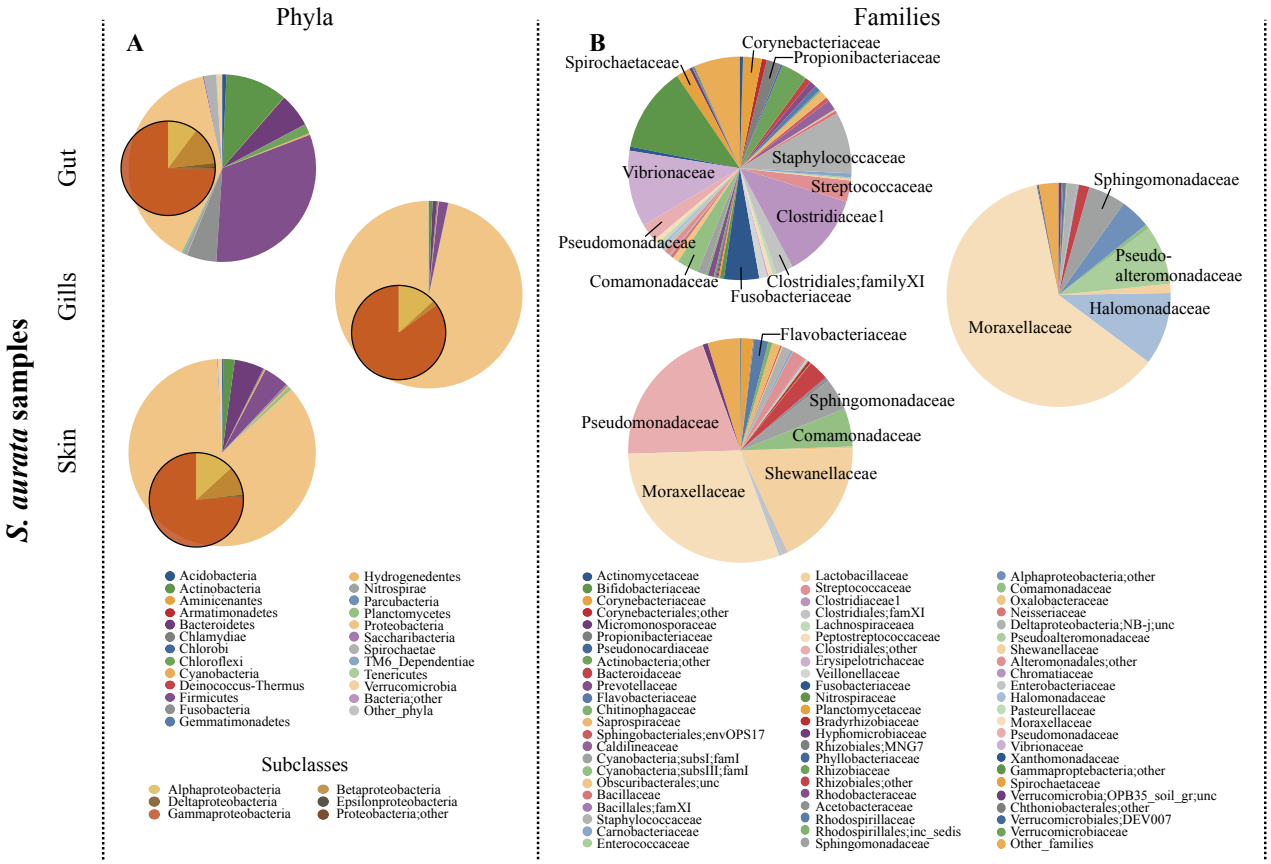

Figure S8 - Pie charts summarizing the phyla (A) and family (B) level microbiota composition of *S. aurata* samples in the three fish district (feces, gills and skin). Phyla with relative abundance > 0.5% in at least one sample and families with relative abundance > 2% in at least 10% of samples are represented. Proteobacteria classes are expanded on the respective pie chart phylum slice. Subs = subset; fam = family; unc = uncultured; inc = incertae; mar =marine; gr = group.

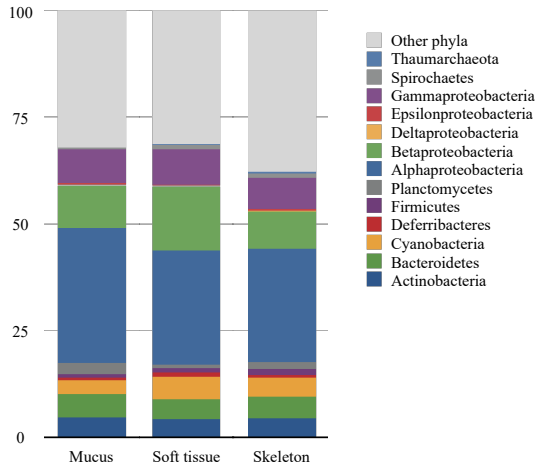

Figure S9 - ***B. europaea*** **microbiomes composition at phylum level.** Bar plots of the average microbiome composition at the phylum (and class for Proteobacteria) taxonomic level in the 3 different *B. europaea* anatomic compartments (mucus, soft tissue and skeleton). Composition is expressed as relative abundance (%) calculated on the phylogenetically assigned metagenomic reads. The dominant phylum in all tissues is represented by Proteobacteria, with the highest abundance of Alphaproteobacteria (mucus, 31.5%; soft tissue, 26.6%; skeleton, 26.5%), followed by Betaproteobacteria (10%, 15.1% and 8.6%) and Gammaproteobacteria (8.0%, 8.3% and 7.5%). Bacteroidetes is also present as dominant phylum (5.5%, 4.6% and 5.1%).

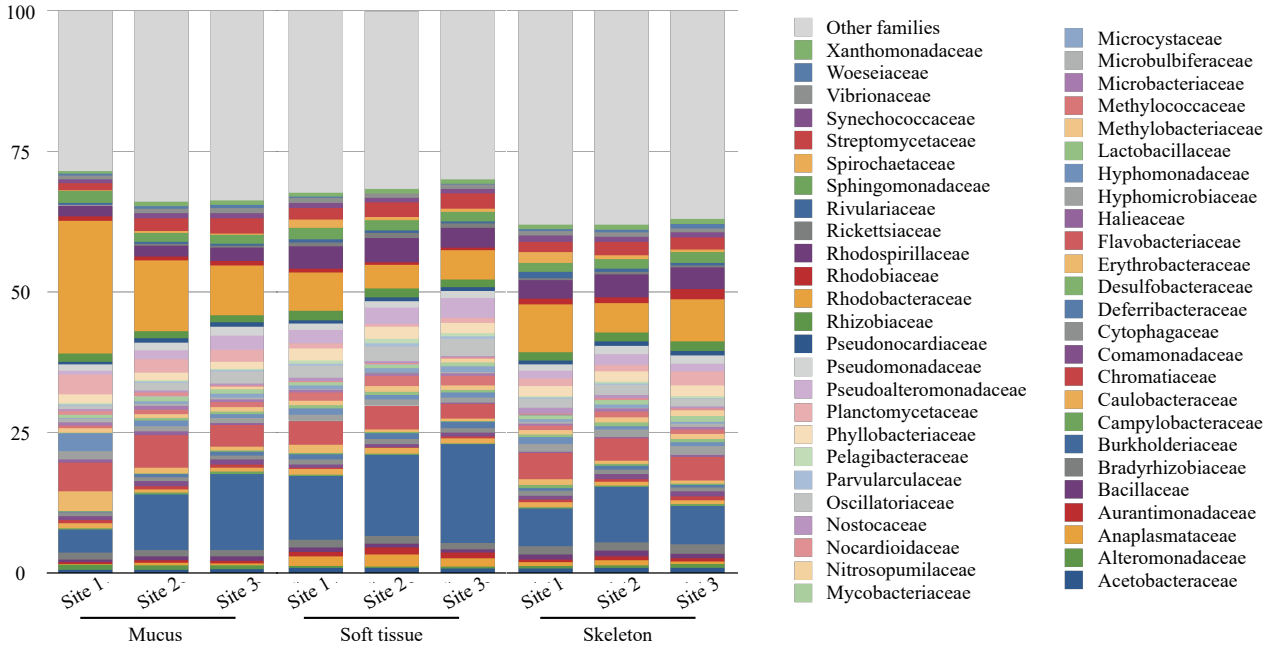

Figure S10 - ***B. europaea*** **microbial composition at family level.** Bar plots of the average microbiome composition at family taxonomic level in the 3 different *B. europaea* anatomic compartments (mucus, soft tissue and skeleton) and in the 3 different acidification conditions (Site 1, Site 2 and Site 3, corresponding to control conditions, mild acidification and high acidification, respectively). Compositions is expressed as relative abundance (%) calculated on the phylogenetically assigned metagenomic reads. In mucus samples, it can be observed a trend of increasing relative abundance of the family *Burkholderiaceae* from Site 1 to Site 2 and 3 (relative abundance 4.1%, 9.8% and 13.5% respectively) and of decreasing relative abundance of the family *Rhodobacteraceae* (relative abundance 23.6%, 12.6% and 8.1%).

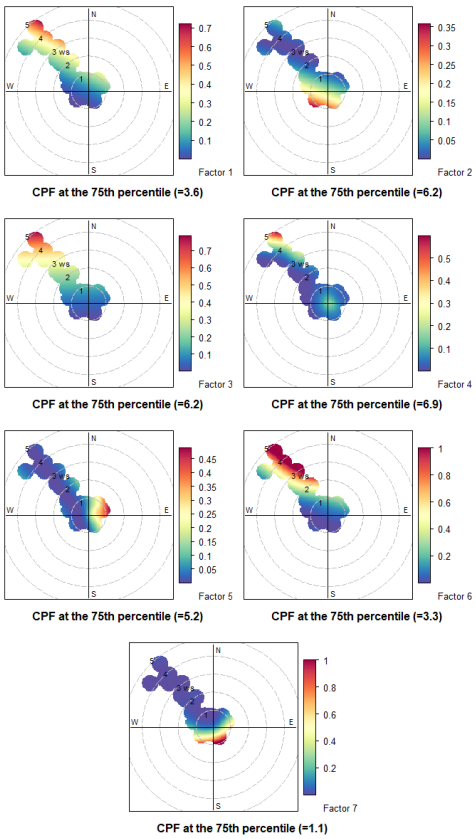

Figure S11 - **Association between the factors obtained by PMF analysis and the wind direction and intensity.** Polar plots of the seven factors obtained by the PMF model. ws, wind speed; CPF, conditional probability function.

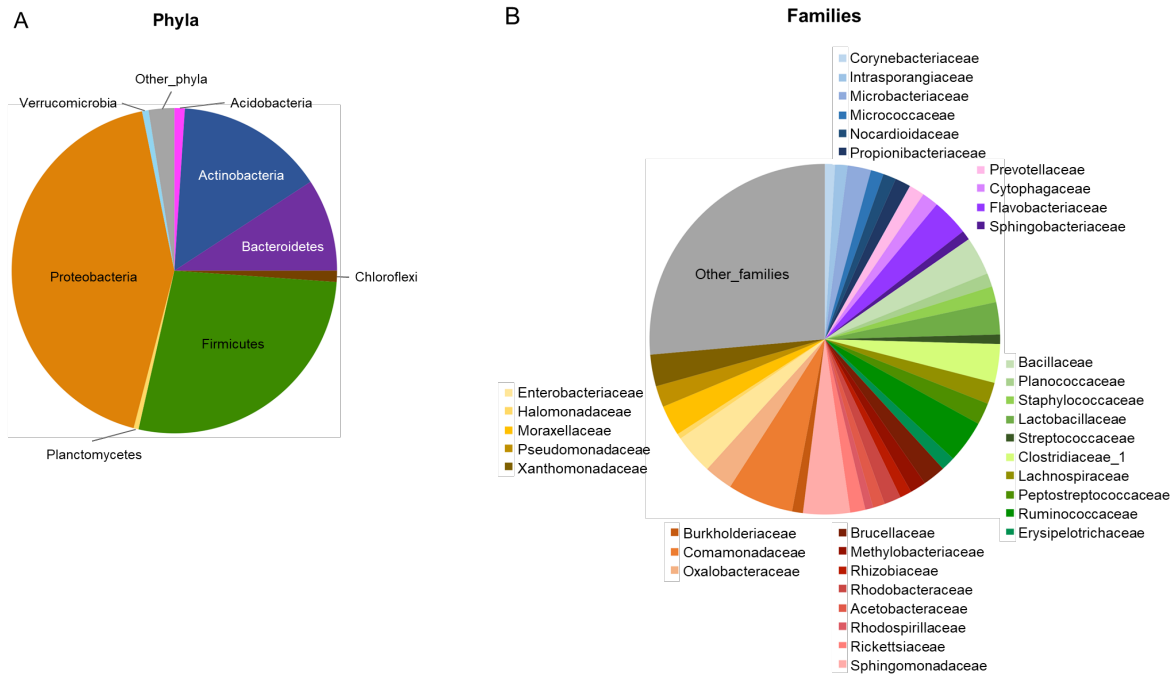

Figure S12 - **AM overall composition.** Pie charts summarizing the microbiota composition of air filter samples at phylum (A) and family (B) level. Only phyla with relative abundance >1.5% in at least 10 samples and families with relative abundance >3% in at least 10 samples are shown.

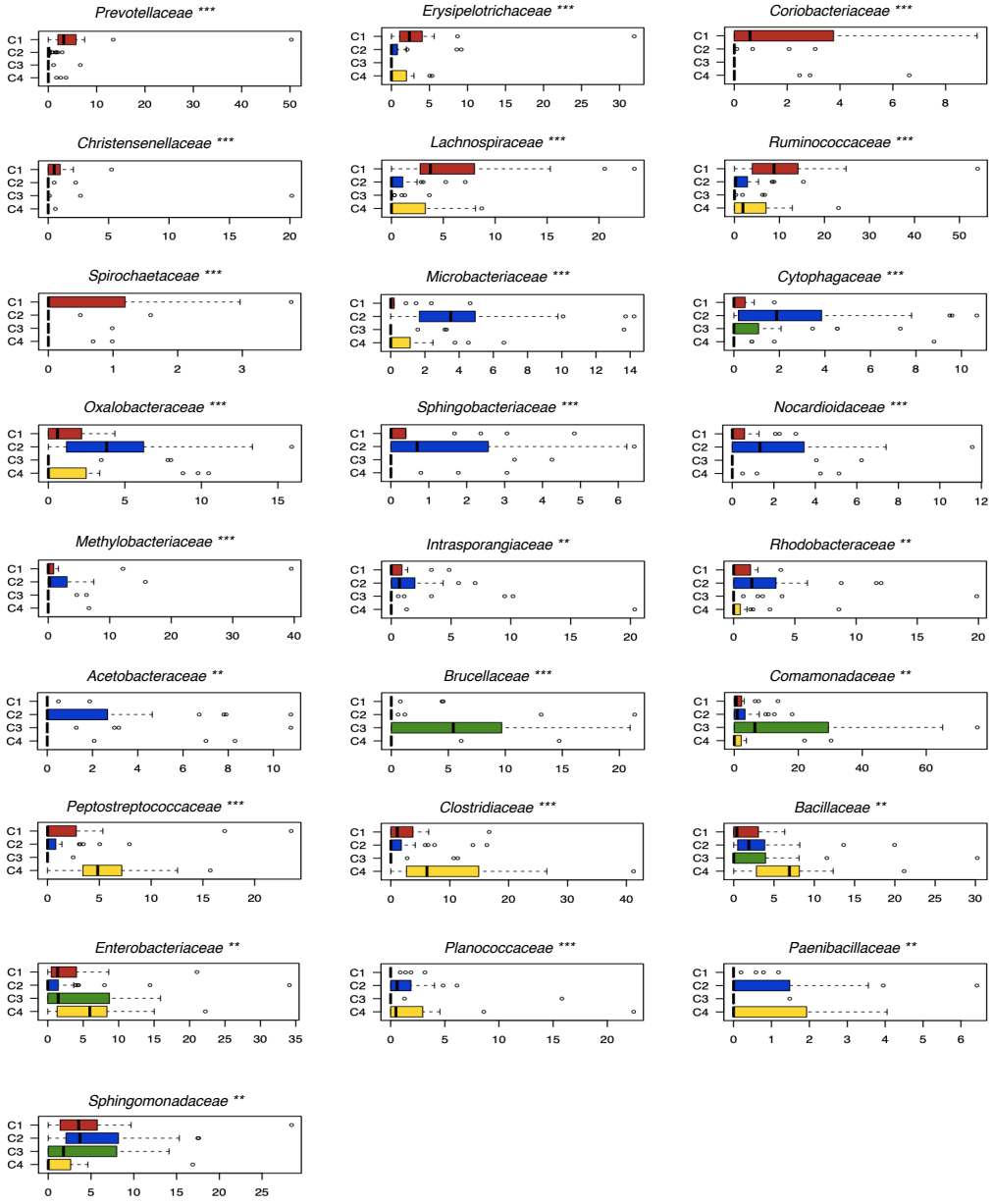

Figure S13 - **AM bacterial families differentially represented among the four microbial clusters.** Box plots showing the bacterial families whose relative abundance is significantly differently distributed among the microbial clusters C1-C4 (Kruskal-Wallis test, FDR- corrected p-value ≤ 0.05*, p-value ≤ 0.01** and p-value ≤ 0.001***). The central box represents the distance between the 25th and 75th percentiles. The median is marked with a black line. Whiskers identify the 10th and 90th percentiles.

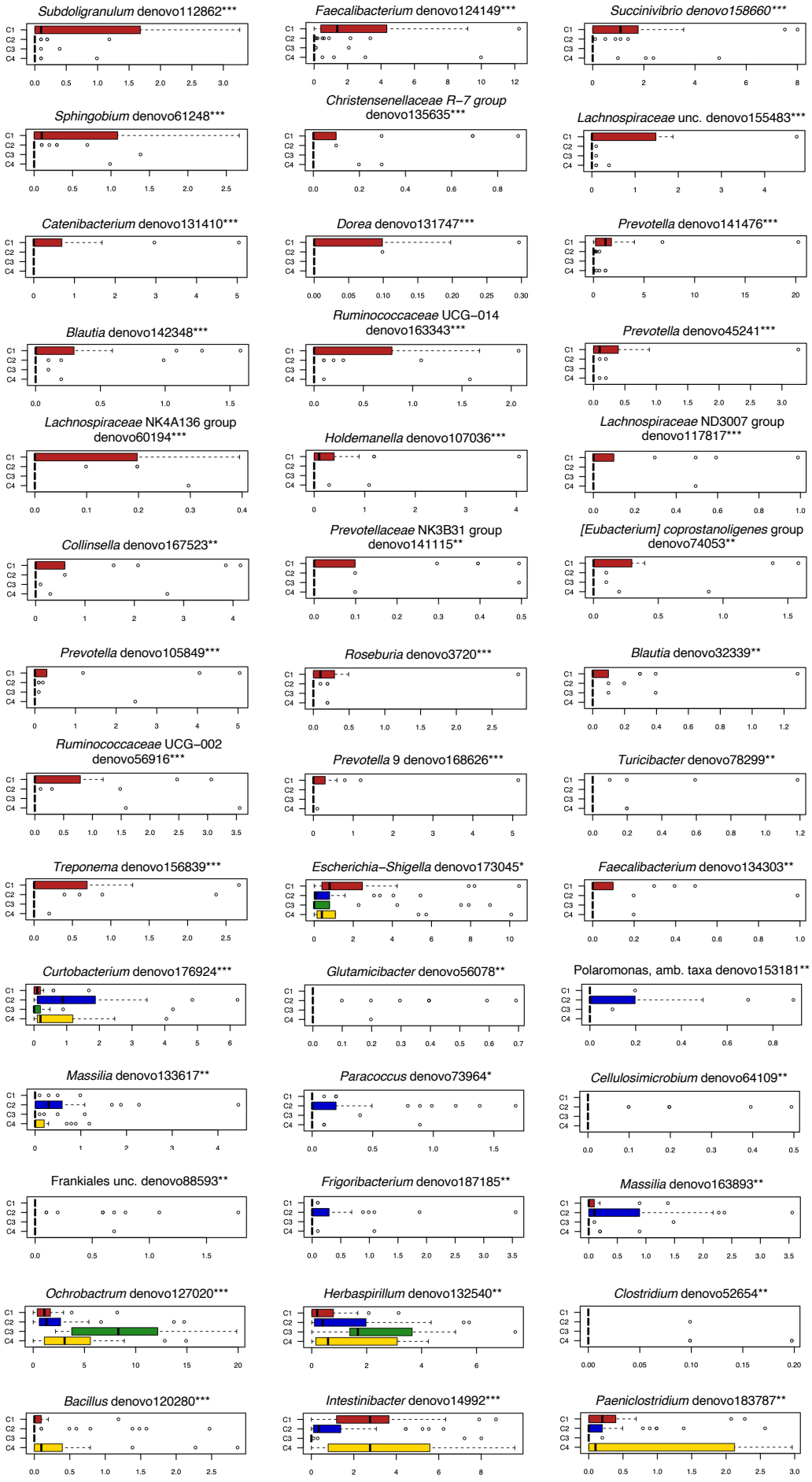
Subdoligranulum denovo112862***
Faecalibacterium denovo124149***
*Succinivibrio denovo158660****
Sphingobium denovo61248***
Christensenellaceae R–7 group denovo135635***
Lachnospiraceae unc. denovo155483***
Catenibacterium denovo131410***
Dorea denovo131747***
Prevotella denovo141476***
Blautia denovo142348***
Ruminococcaceae UCG–014 denovo163343***
Prevotella denovo45241***
Lachnospiraceae NK4A136 group denovo60194***
Holdemanella denovo107036***
Lachnospiraceae ND3007 group denovo117817***
Collinsella denovo167523**
Prevotellaceae NK3B31 group denovo141115**
[Eubacterium] coprostanoligenes group denovo74053**
Prevotella denovo105849***
Roseburia denovo3720***
Blautia denovo32339**
Ruminococcaceae UCG–002 denovo56916***
Prevotella 9 denovo168626***
Turicibacter denovo78299**
Treponema denovo156839***
Escherichia–Shigella denovo173045*
Faecalibacterium denovo134303**
Curtobacterium denovo176924***
Glutamicibacter denovo56078**
Polaromonas, amb. taxa denovo153181**
Massilia denovo133617**
Paracoccus denovo73964*
Cellulosimicrobium denovo64109**
Frankiales unc. denovo88593**
Frigoribacterium denovo187185**
Massilia denovo163893**
Ochrobactrum denovo127020***
Herbaspirillum denovo132540**
Clostridium denovo52654**
Bacillus denovo120280***
Intestinibacter denovo14992***
Paeniclostridium denovo183787**
C1
C2
C3
C4

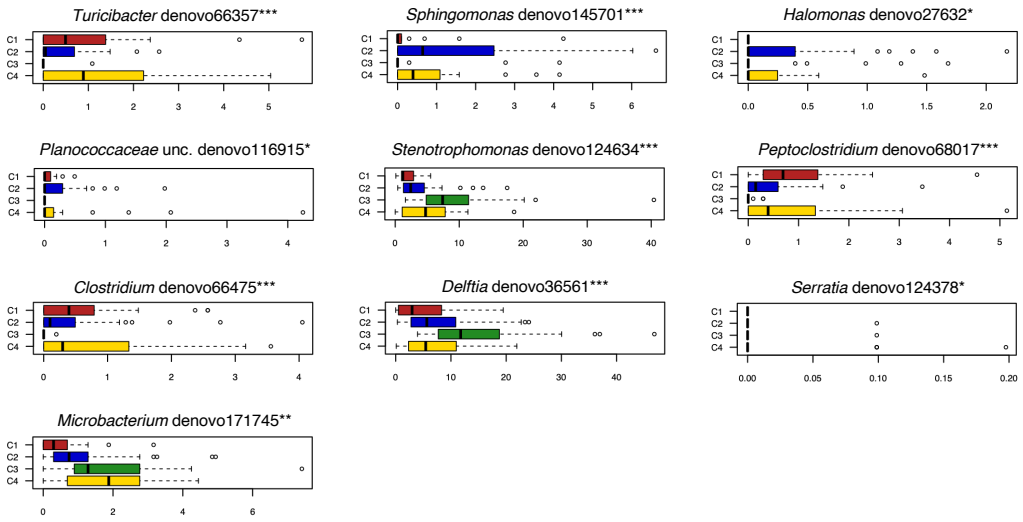

Figure S14 (two pages) - **AM-associated OTUs showing different distribution across microbial clusters.** Box plots showing the OTUs whose relative abundance is significantly differently distributed among the four microbial clusters C1-C4 (Kruskal-Wallis test, FDR-corrected p-value ≤ 0.05*, p-value ≤ 0.01** and p-value ≤ 0.001***). The central box represents the distance between the 25th and 75th percentiles. The median is marked with a black line. Whiskers identify the 10th and 90th percentiles. unc., unclassified; amb., ambiguous.

Supplementary tables

Table S1 (two pages) - Taxonomic assignment of the ASVs shared between all seasons or season pairs. The assignment is based on BLASTN algorithm, taking into account the BLAST best hit for each corresponding ASVs. Query cover and percentage identity are reported for each best hit, together with the respective strain, genus and family.

Winter-Spring-Summer shared ASVs					
ASV ID	ASV no.	BLASTN best hit			
		Description	Query coverage	Identity	Family
9e97d205c022389097ca4462aeda0f4e	ASV_1	*Spiroplasma apis* strain B31 16S ribosomal RNA, partial sequence	100%	80.22%	*Spiroplasmataceae*
cdd3b15b6fe13ff85537e4b729668b57	ASV_2	*Spiroplasma apis* strain B31 16S ribosomal RNA, partial sequence	100%	80.00%	*Spiroplasmataceae*
48c7d52e6c82b734826519880e779a31	ASV_3	*Spiroplasma apis* strain B31 16S ribosomal RNA, partial sequence	100%	80.00%	*Spiroplasmataceae*
e3c3d5f22646bf0781245a114e9ba63b	ASV_4	*Spiroplasma apis* strain B31 16S ribosomal RNA, partial sequence	100%	80.00%	*Spiroplasmataceae*
Winter-Spring shared ASVs					
ASV ID	ASV no.	BLASTN best hit			
		Description	Query coverage	Perc. Identity	Family
476800734964343f009a7dc110e60588	ASV_5	*Mariniblastus fucicola* strain FC18 16S ribosomal RNA, partial sequence	100%	93.98%	*Planctomycetaceae*
4dc541c84a9beec34f641e5e73f91109	ASV_6	*Geminicoccus roseus* strain D2-3 16S ribosomal RNA, partial sequence	100%	90.93%	*Geminicoccaceae*
846e2e400849bc88fd423716893b7c7f	ASV_7	*Albidovulum inexpectatum* strain FRR-10 16S ribosomal RNA, partial sequence	100%	94.77%	*Rhodobacteraceae*
8704273dc3b96e60f7103d1e5f9c35d7	ASV_8	*Pseudahrensia todarodis* strain KHS02 16S ribosomal RNA, partial sequence	100%	97.95%	*Phyllobacteriaceae*
a57690b07dd74e01c10eb0a9d65eb0f2	ASV_9	*Nitrospira lenta* strain BS10 16S ribosomal RNA, partial sequence	100%	89.91%	*Nitrospiraceae*
98997d2729a7002657452314ce086996	ASV_10	*Thiohalobacter thiocyanaticus* strain HRh1 16S ribosomal RNA, partial sequence	100%	93.64%	*Thiohalobacter*
2f2afd51237f3de4bbcac1f6cab5663d	ASV_11	*Sulfuriflexus mobilis* strain aks1 16S ribosomal RNA, partial sequence	100%	87.79%	*Granulosicoccaceae*
1bb079b333716591c77dace4f9be6954	ASV_12	*Thiohalobacter thiocyanaticus* strain HRh1 16S ribosomal RNA, partial sequence	100%	93.86%	*Thiohalobacter*
6430682cacad8ff963ad1421bfcdca7f	ASV_13	*Dialister invisus* strain JCM 17566 16S ribosomal RNA, partial sequence	100%	99.57%	*Veillonellaceae*
		Dialister invisus DSM 15470 strain E7.25 16S ribosomal RNA, partial sequence	100%	99.57%	*Veillonellaceae*

Spring-Summer shared ASVs					
ASV ID	ASV no.	BLASTN best hit			
		Description	Query coverage	Identity	Family
f1989a2ef35a2aab7afd4799d9e615c2	ASV_32	*Porphyromonas gingivalis* ATCC 33277 16S ribosomal RNA, partial sequence	23%	90.00%	*Porphyromonadaceae*
1c89ed5b14d2190798b526a3502ed4b5	ASV_33	*Vibrio lentus* strain CIP 107166 16S ribosomal RNA, partial sequence	100%	99.35%	*Vibrionaceae*
ede8abc42f0e494c7811adb4abbadf82	ASV_34	*Prochlorococcus marinus* subsp. pastoris strain PCC 9511 16S ribosomal RNA, partial sequence	100%	96.83%	*Prochloraceae*
495a1fe0b25d490f74bae884857aaf71	ASV_35	*Bythopirellula goksoyri* strain Pr1d 16S ribosomal RNA, partial sequence	96%	97.10%	*Planctomycetaceae*
845f3655e989ffab5832d471507e9077	ASV_36	*Lacinutrix venerupis* strain Cmf 20.8 16S ribosomal RNA, partial sequence	100%	98.91%	*Flavobacteriaceae*
8ce89250b73287faddb550e08c260ef5	ASV_37	*Sulfuriflexus mobilis* strain aks1 16S ribosomal RNA, partial sequence	100%	88.44%	*Granulosicoccaceae*
eb95260ff239c3c02b3421415b1a2d78	ASV_38	*Dichotomicrobium thermohalophilum* strain DSM 5002 16S ribosomal RNA, partial sequence	100%	92.95%	*Hyphomicrobiaceae*
		Nitratireductor basaltis J3 16S ribosomal RNA, partial sequence	100%	92.95%	*Phyllobacteriaceae*

Winter-Summer shared ASVs					
ASV ID	ASV no.	BLASTN best hit			
		Description	Query coverage	Identity	Family
70b9ac3d4d27ba08d578ba0578e2297e	ASV_14	*Foliisarcina bertiogensis* strain CENA333 16S ribosomal RNA, partial sequence	100%	93.23%	*Xenococcaceae*
73b6333986a432baa055722ce452a36f	ASV_15	*Roseimaritima ulvae* strain UC8 16S ribosomal RNA, partial sequence	99%	92.19%	*Planctomycetaceae*
1790e931b512a2119e06d48f4c0f4bb1	ASV_16	*Bythopirellula goksoyri* strain Pr1d 16S ribosomal RNA, partial sequence	96%	96.27%	*Planctomycetaceae*
75c88102e8fb110ae399001b13103e7e	ASV_17	*Ruegeria atlantica* strain NBRC 15792 16S ribosomal RNA, partial sequence	100%	99.55%	*Rhodobacteraceae*
7e995e366f362a5d90a0ca797cec9acf	ASV_18	*Mycoplasma hyorhinis* strain NBRC 14858 16S ribosomal RNA, partial sequence	100%	83.87%	*Mycoplasmataceae*
		Mycoplasma hyorhinis ATCC 17981 16S ribosomal RNA, partial sequence	100%	83.87%	*Mycoplasmataceae*
		Mycoplasma hyorhinis strain BTS7 16S ribosomal RNA, partial sequence	100%	83.87%	*Mycoplasmataceae*
984fdf14b57459f55a6d7c08366d5733	ASV_19	*Ichthyenterobacterium magnum* strain Th6 16S ribosomal RNA, partial sequence	100%	98.04%	*Flavobacteriaceae*
cf801faa8712369c3b52c02cb81b7388	ASV_20	*Prochlorococcus marinus* subsp. pastoris strain PCC 9511 16S ribosomal RNA, partial sequence	100%	97.29%	*Prochloraceae*
eb44b9da83eb7726fec80f23c4f3bc34	ASV_21	*Mariniblastus fucicola* strain FC18 16S ribosomal RNA, partial sequence	100%	94.78%	*Planctomycetaceae*
cc878c85296348a2d647295f6b7b92ca	ASV_22	*Ilumatobacter fluminis* YM22-133 16S ribosomal RNA, partial sequence	100%	90.02%	*Ilumatobacteraceae*
d64eb6b6a83ac66b81043bee1e2a5831	ASV_23	*Thioprofundum hispidum* strain gps61 16S ribosomal RNA, partial sequence	100%	91.83%	*Thioprofundaceae*
		Thioprofundum lithotrophicum strain 106 16S ribosomal RNA, partial sequence	100%	91.83%	*Thioprofundaceae*
3c750d7524e9de80b291817f2cc2a137	ASV_24	*Zobellia russellii* strain KMM 3677 16S ribosomal RNA, partial sequence	100%	95.87%	*Flavobacteriaceae*
95f2641e4f5a56a48458a73a506faa51	ASV_25	*Eudoraea chungangensis* strain CAU 1296 16S ribosomal RNA, partial sequence	100%	95.65%	*Flavobacteriaceae*
4c6a772bc39c2bac5c7b07fac62482ac	ASV_26	*Parasphingopyxis lamellibrachiae* strain JAMH 0132 16S ribosomal RNA, partial sequence	100%	98.86%	*Sphingomonadaceae*
e6c465ba19b4452d36ccb83030b4d258	ASV_27	*Nitrosomonas aestuarii* strain Nm36 16S ribosomal RNA, partial sequence	100%	95.70%	*Nitrosomonadaceae*
ca6ab15ffc67e8300d8d8e67c57ffd35	ASV_28	*Abyssivirga alkaniphila* strain L81 16S ribosomal RNA, partial sequence	100%	99.09%	*Lachnospiraceae*
		Vallitalea guaymasensis strain Ra1766G1 16S ribosomal RNA, partial sequence	100%	99.09%	*Defluviitaleaceae*
0b4d65c02c2b5a2299f649427252b03d	ASV_29	*Flagellimonas flava* strain A11 16S ribosomal RNA, partial sequence	100%	97.18%	*Flavobacteriaceae*
04de7f992d6f4084c801d75a08c24ebe	ASV_30	*Blastopirellula marina* strain DSM 3645 16S ribosomal RNA, partial sequence	100%	88.96%	*Planctomycetaceae*
dd1a8879b3249b4d4a3cfda66144fb2a	ASV_31	*Marispirochaeta aestuarii* strain JC444 16S ribosomal RNA, partial sequence	100%	84.09%	*Spirochaetaceae*

Table S2 - Ecological distribution and highest score alignment against NCBI 16S rRNA database of OTUs showing a significantly higher mean relative abundance in the limpets collected from control site with respect to those from the aquaculture cage and vice versa. P-values were calculated for the two *P. caerulea* groups (control vs. aquaculture, FDR-corrected Wilcoxon rank-sum test, p-value ≤ 0.05). Species, genera or families are retrieved on the BLAST column based on the last common taxonomic level shared between all BLAST best hits.

	OTU_ID	BLAST	Control site r.a. (%)			Aquaculture site r.a. (%)				p-value
			P. caerulea	Sediment	Seawater	*P. caerulea*	Sediment	Seawater	Fish	
Control site	4667	*Fodinicurvata halophila*	0.19	0.00	0.00	0.00	0.00	0.00	0.00	0.004
	11135	*Lactobacillus johnsonii*	0.10	0.00	0.00	0.04	0.00	0.00	0.00	0.05
	4454	*Fluviibacterium aquatile*	0.22	0.00	0.00	0.00	0.00	0.00	0.00	0.0004
	5034	*Robiginitalea biformata*	0.06	0.02	0.00	0.00	0.00	0.00	0.00	0.03
	12220	*Rhodobacteraceae*	0.13	0.00	0.00	0.00	0.00	0.00	0.00	0.0001
	1496	*Agaricicola taiwanensis*	0.48	0.00	0.00	0.02	0.00	0.00	0.00	0.01
	4069	*Amorphus coralli*	0.10	0.00	0.00	0.01	0.00	0.00	0.00	0.02
	4330	*Ochrobactrum oryzae*	0.11	0.00	0.00	0.00	0.00	0.00	0.00	0.02
	14127	*Rubinisphaera brasiliensis*	0.09	0.00	0.00	0.00	0.00	0.00	0.00	0.02
	5331	*Roseibacillus ponti*	0.06	0.00	0.00	0.00	0.00	0.00	0.00	0.0008
	2911	*Actibacter sediminis*	0.29	0.03	0.00	0.00	0.13	0.00	0.00	0.0004
	2289	*Psychrobacter celer*	0.03	0.00	0.17	0.00	0.00	0.07	0.06	0.008
	14154	*Phyllobacterium*	0.20	0.00	0.00	0.06	0.00	0.00	0.00	0.04
	3304	*Stappia taiwanensis*	0.31	0.00	0.00	0.00	0.00	0.00	0.00	0.00002
	11232	*Rubinisphaera italica*	0.07	0.00	0.00	0.00	0.00	0.00	0.00	0.03
	1355	*Prochlorococcus marinus*	0.02	0.02	1.18	0.00	0.01	1.88	0.01	0.007
	11155	*Lactobacillus rhamnosus*	0.24	0.00	0.00	0.00	0.00	0.00	0.00	0.006
	14091	*Bifidobacterium bifidum*	0.83	0.00	0.00	0.02	0.00	0.00	0.00	0.003
	11445	*Ahrensia kielensis*	0.13	0.00	0.00	0.00	0.00	0.00	0.00	0.0007
	3555	*Bifidobacterium longum*	0.50	0.00	0.00	0.01	0.00	0.00	0.00	0.0004
	2120	*Photobacterium swingsii*	0.23	0.02	0.00	0.01	0.00	0.00	0.00	0.003
	4234	*Hyphomicrobium*	0.07	0.00	0.00	0.00	0.00	0.00	0.00	0.03
Aquaculture site	4187	*Phyllobacteriaceae*	0.00	0.00	0.00	0.13	0.00	0.00	0.00	0.0003
	11247	*Rhodopirellula*	0.00	0.00	0.00	0.13	0.00	0.00	0.00	0.03
	11243	*Alienimonas californiensis*	0.00	0.00	0.00	0.35	0.00	0.00	0.00	0.001
	11205	*Wenxinia marina*	0.00	0.00	0.00	0.09	0.00	0.00	0.00	0.003
	6912	*Mycoplasma mobile*	0.45	0.00	0.00	2.92	0.00	0.00	0.00	0.0004
	5244	*Acinetobacter guillouiae*	0.03	0.00	0.00	0.16	0.00	0.00	0.00	0.04
	4203	*Mesorhizobium thiogangeticum*	0.00	0.00	0.00	0.36	0.00	0.00	0.00	0.003
	2259	*Mycoplasma mobile*	0.02	0.00	0.00	0.19	0.00	0.00	0.00	0.002
	4097	*Mesorhizobium camelthorni*	0.00	0.00	0.00	0.37	0.00	0.00	0.00	0.0002
	2073	*Halomonas*	0.05	0.00	0.00	0.18	0.00	0.00	0.00	0.05
	12731	*Sphingomonas*	0.37	0.00	0.00	1.96	0.00	0.00	0.00	0.001
	11913	*Sphingomonas*	0.06	0.00	0.00	0.40	0.00	0.00	0.00	0.0006
	4065	*Sulfitobacter pontiacus*	0.00	0.00	0.03	0.20	0.00	0.00	0.00	0.03
	4965	*Rhodopirellula baltica*	0.00	0.00	0.00	0.07	0.00	0.00	0.00	0.03
	2118	*Vibrio atypicus*	0.42	0.01	0.00	0.63	0.00	0.00	0.00	0.02
	1919	*Staphylococcus*	0.01	0.01	0.01	0.06	0.00	0.01	0.39	0.04
	2077	*Mycoplasma mobile*	0.05	0.00	0.00	0.33	0.00	0.00	0.00	0.005
	2154	*Mycoplasma mobile*	0.03	0.00	0.00	0.16	0.00	0.00	0.00	0.002
	11213	*Rubinisphaera italica*	0.01	0.00	0.00	0.27	0.00	0.00	0.00	0.005
	1397	*Foliisarcina bertiogensis*	0.00	0.00	0.00	0.10	0.00	0.00	0.00	0.002
	11152	*Bacteroides*	0.00	0.00	0.00	0.08	0.00	0.00	0.00	0.006
	2080	*Psychrobacter marincola*	0.00	0.00	0.19	0.13	0.00	0.03	0.00	0.02
	14234	*Sulfurovum lithotrophicum*	0.00	0.82	0.00	0.01	0.08	0.00	0.00	0.01
	4465	*Phyllobacteriaceae*	0.00	0.00	0.00	0.27	0.00	0.00	0.00	0.0001
	4305	*Marimonas arenosa*	0.00	0.00	0.00	0.14	0.00	0.00	0.00	0.04
	6020	*Pseudomonas*	0.00	0.00	0.00	0.07	0.00	0.00	0.08	0.01
	3237	*Bythopirellula goksoyri*	0.00	0.00	0.00	0.13	0.00	0.00	0.00	0.03
	6006	*Gimesia maris*	0.02	0.00	0.00	0.14	0.00	0.00	0.00	0.05

Table S3 - Seawater environmental data. Measurements (N = 6 per site) are shown for the control and aquaculture sites. Measured parameters, namely T, pH, TA and salinity (38‰ in control and 34‰ in the in the aquaculture site) were used to calculate the carbonate chemistry parameters through CO2SYS Software. T = Temperature; TA = Total Alkalinity; pCO2 = carbon dioxide partial pressure; HCO_3^{2-} = bicarbonate; CO_3^{2-} = carbonate; DIC = dissolved inorganic carbon; Ωarag = aragonite saturation; NS = not significant; **p<0.01, Mann-Whitney test. In brackets the 95% confidence interval.

	T (°C)	pH_{NBS}	TA ($\mu mol\ kg^{-1}$)	pCO_2 (μatm)	HCO_3^- ($\mu mol\ kg^{-1}$)	CO_3^{2-} ($\mu mol\ kg^{-1}$)	DIC ($\mu mol\ kg^{-1}$)	Ω_{arag}
Control	27.3	8.02	2319	667	1898	170	2086	2.67
	(26.9-27.6)	(8.00-8.04)	(2315-2324)	(620-714)	(1882-1914)	(164-177)	(2075-2097)	(2.57-2.76)
Aquaculture	24.8	7.96	2203	700	1877	132.1	2030	2.11
	(24.7-24.9)	(7.95-7.97)	(2191-2213)	(682-717)	(1872-1883)	(130-134)	(2026-2033)	(2.07-2.14)
Mann-Whitney	**	**	**	NS	**	**	**	**

Table S4 - **Variations in the abundance of cyanophycin synthetase (CphA) gene (K03802) in the metagenomes of all coral compartments in individuals collected at different acidification sites.** The values of relative abundance (r.a.) are calculated on the total number of reads assigned to KOs (i.e., number of reads assigned to K03802 divided by the sum of all reads in a given sample).

		Compartment	K03802 (r.a. %)
Site 1 – Control	Individual 1	Mucus	0.0058
		Soft tissue	0.0248
		Skeleton	0.0292
	Individual 2	Mucus	0.0013
		Soft tissue	0.0107
		Skeleton	0.0153
	Individual 3	Mucus	0.0447
		Soft tissue	0
		Skeleton	0.0126
Site 2 – Mild acidification	Individual 1	Mucus	0.0192
		Soft tissue	0.0017
		Skeleton	0
	Individual 2	Mucus	0.0112
		Soft tissue	0
		Skeleton	0.0261
	Individual 3	Mucus	0.0017
		Soft tissue	0.003
		Skeleton	0.0587
Site 3 – High acidification	Individual 1	Mucus	0.0092
		Soft tissue	0.0075
		Skeleton	0.0298
	Individual 2	Mucus	0.0091
		Soft tissue	0.0019
		Skeleton	0.0067
	Individual 3	Mucus	0.026
		Soft tissue	0.0046
		Skeleton	0.0124

Table S5 - **Variations in the abundance of genes associated with the Nif (nitrogen fixation) regulon in metagenomes of all coral compartments in individuals collected at different acidification sites.** The values of relative abundance (r.a.) are calculated on the total number of reads assigned to KOs (i.e., number of reads assigned to each Nif- associated KO divided by the sum of all reads in a given sample). The correspondence between KO numbers and genes is the following: K02584 - Nif-specific regulatory protein; K02585 - Nitrogen fixation protein NifB; K02586 - Nitrogenase molybdenum-iron protein alpha chain; K02587 - Nitrogenase molybdenum-cofactor synthesis protein NifE; K02588 - Nitrogenase iron protein NifH; K02591 - Nitrogenase molybdenum-iron protein beta chain; K02592 - Nitrogenase molybdenum-iron protein NifN; K02594 - Homocitrate synthase NifV; K04488 - Nitrogen fixation protein NifU and related proteins.

		Compartment	K02584	K02585	K02586	K02587	K02588	K02591	K02592	K02594	K04488
Site 1 – Control	Individual 1	Mucus	0.0019%	0.0011%	0.0036%	0.0038%	0.0011%	0.0036%	0.0019%	0.0016%	0.0011%
		Soft tissue	0.0215%	0.0148%	0.0101%	0.0228%	0.0020%	0%	0.0215%	0%	0.0040%
		Skeleton	0.0438%	0.0310%	0.0082%	0.0018%	0.0018%	0%	0.0100%	0%	0.0091%
	Individual 2	Mucus	0.0057%	0.6320%	0.0018%	0.0037%	0.0024%	0.0024%	0.0019%	0.0067%	0%
		Soft tissue	0.0107%	0.0164%	0.0100%	0.0064%	0.0014%	0.0136%	0.0157%	0.0050%	0.0050%
		Skeleton	0%	0%	0%	0%	0%	0%	0%	0%	0%
	Individual 3	Mucus	0.0147%	0.0018%	0.0159%	0.0196%	0.0184%	0.0257%	0.0037%	0.0159%	0.0098%
		Soft tissue	0%	0.0148%	0%	0.0485%	0%	0.0138%	0%	0%	0%
		Skeleton	0.0396%	0%	0.0108%	0.0126%	0.0459%	0.0027%	0%	0%	0%
Site 2 – Mild acidification	Individual 1	Mucus	0.0322%	0.0397%	0.0185%	0.0082%	0.0034%	0.0041%	0.0110%	0.0151%	0.0171%
		Soft tissue	0.0017%	0.0103%	0.0017%	0.0361%	0%	0.0456%	0.0103%	0.0112%	0.0103%
		Skeleton	0.0589%	0.0115%	0.0390%	0%	0.0115%	0.0269%	0.0115%	0%	0%
	Individual 2	Mucus	0.0284%	0.0022%	0.0203%	0.0081%	0%	0.0184%	0.0066%	0.0203%	0.0137%
		Soft tissue	0.0469%	0%	0%	0.0517%	0.0065%	0.0065%	0.0129%	0%	0.0016%
		Skeleton	0%	0.0095%	0.0165%	0%	0.0046%	0%	0%	0.0095%	0.0211%
	Individual 3	Mucus	0%	0%	0%	0%	0.0017%	0.0017%	0%	0.0017%	0.0083%
		Soft tissue	0.0161%	0.0030%	0%	0.0030%	0%	0.0030%	0.0030%	0%	0.0131%
		Skeleton	0%	0.0132%	0.0010%	0.0010%	0%	0.0122%	0.0243%	0.0435%	0.0851%
Site 3 – High acidification	Individual 1	Mucus	0.0031%	0.0010%	0.0212%	0.0212%	0.0010%	0.0031%	0.0041%	0.0092%	0.0256%
		Soft tissue	0.0115%	0.0020%	0%	0.0075%	0.0040%	0.0095%	0%	0.0075%	0.0055%
		Skeleton	0.0088%	0.0026%	0%	0%	0%	0.0175%	0.0079%	0.0070%	0.0079%
	Individual 2	Mucus	0.0155%	0.0155%	0.0255%	0.0091%	0.0027%	0.0255%	0.0027%	0.0428%	0%
		Soft tissue	0.0019%	0%	0.0055%	0%	0%	0.0055%	0.0019%	0%	0%
		Skeleton	0.0208%	0.0208%	0%	0%	0%	0.0208%	0%	0%	0%
	Individual 3	Mucus	0.0318%	0.0034%	0.0034%	0%	0.0134%	0.0042%	0.0151%	0.0017%	0.0184%
		Soft tissue	0.0158%	0.0164%	0.0053%	0.0184%	0.0066%	0.0099%	0.0197%	0.0092%	0.0132%
		Skeleton	0.0770%	0.0124%	0%	0%	0%	0.0028%	0.0289%	0.0422%	0.0298%

Table S6 (two pages) - Meteorological parameters during the PM sampling period. The first column reports the sample ID, while the second indicates the sampling date. The meteorological parameters taken into account are temperature (T, °C), relative humidity (RH, %), pressure (P, mbar), rainfall (Rain, mm), wind speed (ws, m/s, and wind direction (wd, °). All values were taken every 30 min and averaged on a daily basis.

Sample ID	Sampling date	T (°C)	RH (%)	P (mbar)	Rain (mm)	ws (m/s)	wd (°)
1	01-Feb-2012	0.2	62.5	1019.3	0	4.6	318
2	05-Feb-2012	-1.6	49.1	1029.3	0	2.3	316
3	06-Feb-2012	-1.1	41.1	1023.5	0	3.7	321
4	09-Feb-2012	5.6	30.5	1025.5	0	1.9	323
5	11-Feb-2012	-0.8	47.9	1024	0	3	323
6	14-Feb-2012	4.5	41.2	1020.3	0	0.9	315
7	15-Feb-2012	5.2	62.7	1016.6	0	0.5	242
8	17-Feb-2012	8.5	61.9	1027.2	0	0.5	219
9	18-Feb-2012	11.3	67.8	1026	0	0.8	237
10	19-Feb-2012	8.8	73.4	1023.7	0	0.1	270
11	23-Feb-2012	13.6	32.4	1028.4	0	1.9	318
12	25-Feb-2012	12.1	73.2	1026.6	0	0.2	197
13	26-Feb-2012	13	52.1	1019.3	0	0.6	35
14	27-Feb-2012	11.5	40.2	1026.3	0	0.7	318
15	28-Feb-2012	10.7	72.4	1028	0	0.4	232
16	06-Mar-2012	6.9	64.7	1023.5	1	3.7	314
17	09-Mar-2012	11.5	42.1	1035.4	0	4.2	306
18	10-Mar-2012	12.4	30.8	1034.6	0	3	324
19	11-Mar-2012	14.8	26.1	1026.9	0	2.5	317
20	12-Mar-2012	13.8	60	1025.3	0	0.5	334
21	14-Mar-2012	13.3	64.4	1031.5	0	0.8	326
22	19-Mar-2012	12.3	73	1028.7	1.4	0.7	150
23	21-Mar-2012	17	37.3	1037.4	0	3.4	313
24	23-Mar-2012	13.7	58.8	1031.8	0	0.4	92
25	24-Mar-2012	14.9	50.7	1028.5	0	0.5	358
26	25-Mar-2012	16	45	1029.2	0.8	0.7	350
27	27-Mar-2012	17.4	36.8	1031.3	0	0.7	260
28	28-Mar-2012	16.3	44.6	1029.7	0	0.3	79
29	29-Mar-2012	13.9	65.2	1024	0	0.4	76
30	02-Apr-2012	14.6	53.2	1017	0	1.9	330
31	03-Apr-2012	15	65.6	1015.2	0	0.5	67
32	04-Apr-2012	13.6	78.2	1014	23.4	0.3	307
33	05-Apr-2012	14.6	71.2	1013.7	4.6	0.8	279
34	08-Apr-2012	15.4	44.4	1006.9	0	0.9	42
35	09-Apr-2012	11.3	49.4	1017.1	0	0.3	303
36	10-Apr-2012	10.5	79.4	1015.9	5.2	0.1	61
37	11-Apr-2012	10	68.9	1006.6	18.6	1.6	313
38	12-Apr-2012	11.6	75.4	1009.5	0	0.3	115
39	13-Apr-2012	14.8	59.9	1005.5	8.8	1	304
40	14-Apr-2012	12.5	68.3	1001.5	0.6	1.5	306
41	15-Apr-2012	12.7	70.2	1003.3	0.8	0.4	38
42	16-Apr-2012	14	57.6	1009.7	1.2	1.2	305
43	17-Apr-2012	15.5	50.2	1011.7	0.2	0.6	272
44	18-Apr-2012	13.6	70.3	1004.1	0.6	0.5	95
45	23-Apr-2012	NA	NA	1012.7	0	0.1	270
46	25-Apr-2012	11.5	80.7	1016.4	0	0.3	252
47	26-Apr-2012	NA	NA	1024.2	0	NA	NA
48	02-May-2012	14.2	79.7	1022.8	0.2	0.3	68
49	10-May-2012	18.1	71.9	1029.4	0	0	68
50	14-May-2012	16.3	51.3	1020.1	0	1.2	287
51	16-May-2012	18.2	29.6	1017.4	0	0.7	56
52	17-May-2012	16.9	27.3	1022.9	0	0.5	268
53	18-May-2012	16.2	51.4	1021.4	0	0.1	354
54	19-May-2012	15.8	54.2	1020.8	0.4	0.1	277
55	20-May-2012	14.8	71.3	1017.5	11.4	0.3	291
56	22-May-2012	17.4	59.6	1012.3	0	0.2	256
57	23-May-2012	18.2	72.9	1019	0	0.1	68
58	26-May-2012	20.8	56.6	1021.4	0	0.2	276

Sample ID	Sampling date	T (°C)	RH (%)	P (mbar)	Rain (mm)	ws (m/s)	wd (°)
59	27-May-2012	20.5	64	1022.1	0	0.1	149
60	30-May-2012	20.4	75.5	1022.9	0	0.3	236
61	02-Jun-2012	19.7	85.8	1021.2	1.2	0.3	79
62	03-Jun-2012	20	86.8	1019.9	5.4	0.5	73
63	04-Jun-2012	20.4	77	1013.4	1	0.4	181
64	05-Jun-2012	19.5	71.1	1016.9	0	0.3	68
65	06-Jun-2012	18.6	78.6	1018.6	0	0.2	68
66	09-Jun-2012	21.3	75.3	1017.3	0	0.1	231
67	11-Jun-2012	20.8	74.7	1009.6	0	0.2	69
68	12-Jun-2012	19.6	72.8	1007.7	0	0.6	64
69	13-Jun-2012	19.7	71.1	1016.6	0	0.6	67
70	14-Jun-2012	20	69.9	1023.3	0	0.7	69
71	15-Jun-2012	20	62.7	1026.1	0	0.2	68
72	16-Jun-2012	25.3	51.7	1025.1	0	0.2	36
73	17-Jun-2012	24.2	55.3	1023.5	0	0.1	68
74	19-Jun-2012	25.8	61.8	1020.7	0	0.1	63
75	20-Jun-2012	24.6	58.3	1018.5	0	0.1	293
76	21-Jun-2012	23.3	66.9	1015.9	0	0.4	63
77	22-Jun-2012	24.1	71.4	1019.9	0	0.3	66
78	23-Jun-2012	24.9	69.3	1022.9	0	0.2	85
79	24-Jun-2012	24.8	70.2	1022.4	0	0.2	80
80	25-Jun-2012	23.6	74.9	1018	0	0.2	68
81	26-Jun-2012	25.2	66.2	1019.8	0	0.1	62
82	27-Jun-2012	28.6	49.1	1021.3	0	0.3	14
83	28-Jun-2012	26.6	58.5	1019.3	0	0.2	68
84	01-Jul-2012	25.8	71.2	1019.2	0	0.2	59
85	03-Jul-2012	23.4	68.8	1020.3	0	0.3	68
86	05-Jul-2012	24.5	61	1016.3	0	0.1	60
87	07-Jul-2012	23.9	76.4	1018.4	0.6	0.6	66
88	08-Jul-2012	24.4	73.5	1017.8	0	0.3	69
89	10-Jul-2012	25.4	71.9	1017.6	0	0.4	72
90	11-Jul-2012	24.9	74.3	1018.4	0.2	0.4	68
91	13-Jul-2012	23.6	69.7	1015	0	0.3	68
92	14-Jul-2012	23.7	76.5	1013.6	0	0.8	71
93	15-Jul-2012	23.5	68.4	1015.7	0	0.3	68
94	16-Jul-2012	25.7	39.8	1024	NA	0.8	281
95	17-Jul-2012	25.4	44	1025.9	NA	0.3	78
96	18-Jul-2012	24.8	55	1023.6	NA	0.3	69
97	19-Jul-2012	21.3	76.7	1021	NA	0	68
98	20-Jul-2012	0.2	62.5	1019.3	0	4.6	318

Table S7 (two pages) - Normalized contributions per sample of the seven factors resolved by PMF analysis. The first column reports the sample ID. All the other columns represent the contribution of each factor identified by PMF on the corresponding sample.

Sample ID	Factor 1	Factor 2	Factor 3	Factor 4	Factor 5	Factor 6	Factor 7
1	-0.01	-0.12	2.37	1.7	-0.2	2.96	-0.2
2	0.03	-0.2	3.73	1.17	0.18	3.04	-0.14
3	2.83	0.47	3.42	1.22	0.13	4.42	-0.2
4	4.17	1.34	2.84	1.24	0.31	5	0.18
5	0.89	-0.2	4.4	3.68	-0.2	3.34	0
6	0.94	0.96	0.98	1.96	-0.16	1.2	0.24
7	0.16	1.74	0.9	0.9	0.29	0.54	0.71
8	1.25	0.97	3.39	-0.2	1.21	0.55	0.59
9	-0.2	0.93	2.79	0.18	1.6	0.8	0.88
10	0.67	-0.2	0.28	-0.09	1.01	9.02	-0.07
11	2.29	0.09	-0.02	-0.2	0.79	5.42	-0.08
12	0.31	0.36	2.42	0.48	2.25	1.42	0.1
13	0.61	1.23	0.41	0.93	0.98	1.61	-0.01
14	1.9	2.14	0.3	0.11	0.4	2.38	-0.14
15	0.02	2.57	2.02	0.68	0.67	0	0.2
16	-0.05	0.36	1	0.65	-0.04	1.29	-0.09
17	1.74	0.28	3.35	0.39	0.14	0.9	-0.09
18	1.89	0.17	2.61	0.52	0.44	1.38	-0.13
19	0.75	0.38	3.12	0.34	0.57	1.39	-0.08
20	1.03	1.98	3.08	0.17	0.97	1.21	0.03
21	0.08	1.7	8.18	0.63	0.18	0.4	0.06
22	0.08	1.38	0.37	0.17	0.85	0.33	3.16
23	2.76	1.06	0.18	0.58	0.49	1.94	-0.2
24	1.58	3.06	1.85	1.71	0.54	2.5	-0.1
25	2.27	2.17	0.76	2.56	0.29	0.49	0.04
26	3.26	0.93	1.15	1.32	0.58	0.96	0.15
27	2.36	1.71	-0.2	1.7	-0.05	1.98	-0.17
28	1.71	3.84	-0.16	1.53	-0.2	3.08	-0.14
29	1.24	1.52	1.83	2.36	0.34	1.53	-0.03
30	4.01	0.15	1.05	-0.2	2.21	3.42	0.64
31	2.65	0.27	1.74	0.04	2.18	1.61	0.31
32	0.68	-0.1	4.53	1.13	0.46	1.42	0
33	0.12	0.99	0.41	0.51	0.26	0.11	0.13
34	1.32	0.35	0.08	0.39	0.12	0.3	0.43
35	0.54	0.72	0.53	0.34	0.41	0.29	0.65
36	-0.18	1.84	1.21	0.72	0.38	0.9	0.07
37	0.18	0.84	-0.16	0.09	-0.04	0.94	-0.05
38	0.17	0.79	0.7	-0.18	0.88	0.42	2.75
39	0.49	0.42	0.39	0.32	0.63	0.74	0.24
40	-0.13	0.57	0.01	0.4	-0.04	0.33	-0.01
41	-0.19	0.59	0.21	0.37	0.17	0.25	0.22
42	0.54	0.68	0.04	0.46	-0.05	0.3	-0.01
43	0.24	1.08	0.28	0.51	-0.1	0.75	0.33
44	0.18	1.94	0.83	0.01	0.81	1.26	3.35
45	0.14	0.66	0.09	0	-0.07	0.37	8.38
46	0.21	0.38	0.27	-0.12	0.79	0.13	6.81
47	0.26	0.6	0.61	-0.06	1.3	0.94	3.99
48	0.57	0.52	0.78	0.32	1.47	1.01	0.35
49	0.09	1.91	0.2	1.1	2.04	1.1	0.03
50	0.74	1.13	0.77	0.73	0.81	-0.2	0.82
51	3.12	1.29	-0.2	0.33	0.13	0.38	0
52	1.45	0.79	-0.1	0.4	0.26	0.73	0.08
53	1.62	2.78	0.21	0.34	0.31	0.59	-0.03
54	2.19	1.91	1.53	0.76	0.02	0.14	-0.02
55	0.74	0.5	4.04	0.58	0.11	-0.2	0.07
56	0.29	1.16	0.13	0.13	0.17	0.74	0.78
57	0.02	1.74	1.17	0.05	1.48	0.29	0.41
58	0.95	1.6	0.19	1.76	0.04	1.43	-0.09

Sample ID	Factor 1	Factor 2	Factor 3	Factor 4	Factor 5	Factor 6	Factor 7
59	0.25	1.47	0.18	1.9	-0.14	1.32	-0.08
60	-0.2	1.22	-0.06	2.94	0.44	0.7	-0.03
61	0.31	0.31	-0.2	1.71	0.62	1.08	-0.04
62	-0.16	-0.2	-0.2	3.74	2.36	0.79	0.13
63	0.13	0.85	0.23	0.94	1.11	0.07	2.08
64	0.11	0.83	1.31	0.08	1.99	0.05	1.68
65	0.34	0.53	0.57	-0.19	2.85	0.05	0.73
66	0.07	0.22	1.65	0.53	2.55	0.28	4.15
67	0.29	0.5	0.37	0.47	2.27	0.36	6.23
68	0.39	0.48	-0.2	0.2	0.62	0.27	8.04
69	0.17	0.31	0.53	-0.2	2.2	0.15	7.55
70	0.05	-0.2	1.14	0.18	1.92	0.18	5.54
71	0.31	1.37	0.66	0.44	2.36	0.48	0.11
72	1.23	1.38	0.3	1.66	1.22	0.65	-0.01
73	0.45	2.44	0.27	1.88	0.72	0.18	0.04
74	1.87	2.97	0.22	2.89	0.06	0.24	0
75	2.48	2.24	-0.11	2.57	0.1	1.39	-0.04
76	3.19	0.44	0.84	1.61	3.58	0.29	0.28
77	3.34	0.38	-0.1	3.68	2.98	0.62	-0.06
78	1.3	0.68	0.44	3.58	3.21	0.75	0.05
79	1.12	1.1	-0.02	3.3	2.47	0.92	0.01
80	0.13	0.74	0.88	2.93	2.8	-0.01	0.06
81	0.85	2.22	0.23	2.4	2.13	0.11	0.02
82	2.44	1.31	-0.16	0.23	1.18	1.02	-0.13
83	0.73	1.96	0.37	2.24	0.72	0.37	-0.02
84	3.45	0.53	-0.18	2.88	1.04	0.31	-0.11
85	1.6	0	1.45	0.92	1.27	0.53	3.41
86	2.4	1.89	0.08	1.78	0.36	0.22	-0.06
87	0.77	0.22	0.75	-0.16	3.71	0.55	0.34
88	0.48	0.76	0.01	1.72	1.81	0.2	0.01
89	0.19	-0.01	1.21	1.13	2.83	-0.2	0.38
90	0.33	0.06	1.22	1.24	3.15	0.26	0.45
91	0.28	0.53	1.51	-0.17	1.29	-0.09	9.64
92	0.24	-0.01	1.75	1.49	0.83	-0.02	5.21
93	0.43	0.45	0.74	-0.05	2.12	0.07	6.8
94	3.51	1.76	-0.03	0.42	0.44	0.63	0.36
95	2.07	2.15	0.02	0.62	0.51	0.6	0
96	1.37	2.47	0.11	1.42	0.36	0.48	-0.05
97	0.03	0.76	0.98	1.54	2.1	-0.2	0.19
98	0.2	0.12	0.45	1.93	2.33	0.76	0.07

Table S8 - Characteristics of the OTUs accounting for the compositional specificity of the four AM clusters. For each OTU, the following information is given: unique OTUs ID, taxonomy as assigned with SILVA database, the cluster/s to which each OTU is significantly correlated (i.e., the cluster/s in which the given OTU is significantly more represented), the BLAST best hit resulting from blasting OTU fasta sequences against the NCBI 16S rRNA sequence database, the percentage of identity (ID (%)) and coverage (coverage (%)) between the OTU sequences and the corresponding best hit, and the isolation source of each best hit as reported in the GenBank database.

unique OTU ID	Taxonomy	Cluster	BLAST best hit	ID (%)	Coverage (%)
denovo112862	D_0__Bacteria; D_1__Firmicutes; D_2__Clostridia; D_3__Clostridiales; D_4__Ruminococcaceae; D_5__Subdoligranulum; D_6__uncultured bacterium	C1	Bacteria; Firmicutes; Clostridia; Clostridiales; Ruminococcaceae;Gemmiger;Gemmiger formicilis strain X2-56 16S ribosomal RNA	99.55	100
denovo124149	D_0__Bacteria; D_1__Firmicutes; D_2__Clostridia; D_3__Clostridiales; D_4__Ruminococcaceae; D_5__Faecalibacterium; D_6__uncultured bacterium	C1	Bacteria; Firmicutes; Clostridia; Clostridiales; Ruminococcaceae; Faecalibacterium; Faecalibacterium prausnitzii strain ATCC 27768 16S ribosomal RNA	99.55	100
denovo158660	D_0__Bacteria; D_1__Proteobacteria; D_2__Gammaproteobacteria; D_3__Aeromonadales; D_4__Succinivibrionaceae; D_5__Succinivibrio; D_6__uncultured bacterium	C1	Bacteria; Proteobacteria; Gammaproteobacteria; Aeromonadales; Succinivibrionaceae; Succinivibrio; Succinivibrio dextrinosolvens strain 0554 16S ribosomal RNA	97.07	100
denovo61248	D_0__Bacteria; D_1__Proteobacteria; D_2__Alphaproteobacteria; D_3__Sphingomonadales; D_4__Sphingomonadaceae; D_5__Sphingobium	C1	Bacteria; Proteobacteria; Alphaproteobacteria; Sphingomonadales; Sphingomonadaceae; Sphingobium; Sphingobium ummariense RL-3 16S ribosomal RNA	99.32	100
denovo135635	D_0__Bacteria; D_1__Firmicutes; D_2__Clostridia; D_3__Clostridiales; D_4__Christensenellaceae; D_5__Christensenellaceae R-7 group; D_6__uncultured bacterium	C1	Bacteria; Firmicutes; Clostridia; Clostridiales; Christensenellaceae; Christensenella; Christensenella timonensis strain Marseille-P2437 16S ribosomal RNA	87.84	100
denovo155483	D_0__Bacteria; D_1__Firmicutes; D_2__Clostridia; D_3__Clostridiales; D_4__Lachnospiraceae	C1	Bacteria; Firmicutes; Clostridia; Clostridiales; Lachnospiraceae; Mediterraneibacter; Ruminococcus faecis JCM 15917 strain Eg2 16S ribosomal RNA	99.55	100
denovo131410	D_0__Bacteria; D_1__Firmicutes; D_2__Erysipelotrichia; D_3__Erysipelotrichales; D_4__Erysipelotrichaceae; D_5__Catenibacterium; D_6__uncultured bacterium	C1	Bacteria; Firmicutes; Erysipelotrichia; Erysipelotrichales; Erysipelotrichaceae; Catenibacterium; Catenibacterium mitsuokai strain DSM 15897 16S ribosomal RNA	96.76	99
denovo131747	D_0__Bacteria; D_1__Firmicutes; D_2__Clostridia; D_3__Clostridiales; D_4__Lachnospiraceae; D_5__Dorea; D_6__uncultured bacterium	C1	Bacteria; Firmicutes; Clostridia; Clostridiales; Lachnospiraceae; Dorea; Dorea longicatena strain 111-35 16S ribosomal RNA	99.55	100
denovo141476	D_0__Bacteria; D_1__Bacteroidetes; D_2__Bacteroidia; D_3__Bacteroidales; D_4__Prevotellaceae; D_5__Prevotella 9; D_6__uncultured bacterium	C1	Bacteria; Bacteroidetes; Bacteroidia; Bacteroidales; Prevotellaceae; Prevotella; Prevotella copri DSM 18205 strain JCM 13464 16S ribosomal RNA	99.35	100
denovo142348	D_0__Bacteria; D_1__Firmicutes; D_2__Clostridia; D_3__Clostridiales; D_4__Lachnospiraceae; D_5__Blautia; D_6__uncultured bacterium	C1	Bacteria; Firmicutes; Clostridia; Clostridiales; Lachnospiraceae; Blautia; Blautia luti strain BInIX 16S ribosomal RNA	99.32	100
denovo163343	D_0__Bacteria; D_1__Firmicutes; D_2__Clostridia; D_3__Clostridiales; D_4__Ruminococcaceae; D_5__Ruminococcaceae UCG-014; D_6__uncultured bacterium	C1	Bacteria; Firmicutes; Clostridia; Clostridiales; Vallitaleaceae; Petrocella; Petrocella atlantisensis strain 70B-A 16S ribosomal RNA	87.53	100
denovo45241	D_0__Bacteria; D_1__Bacteroidetes; D_2__Bacteroidia; D_3__Bacteroidales; D_4__Prevotellaceae; D_5__Prevotella 9; D_6__uncultured bacterium	C1	Bacteria; Bacteroidetes; Bacteroidia; Bacteroidales; Prevotellaceae; Prevotella; Prevotella copri DSM 18205 strain CB7 16S ribosomal RNA	97.17	100
denovo60194	D_0__Bacteria; D_1__Firmicutes; D_2__Clostridia; D_3__Clostridiales; D_4__Lachnospiraceae; D_5__Lachnospiraceae NK4A136 group; D_6__uncultured bacterium	C1	Bacteria; Firmicutes; Clostridia; Clostridiales; Lachnospiraceae; Kineothrix; Kineothrix alysoides strain KNHs209 16S ribosomal RNA	97.95	100
denovo107036	D_0__Bacteria; D_1__Firmicutes; D_2__Erysipelotrichia; D_3__Erysipelotrichales; D_4__Erysipelotrichaceae; D_5__Holdemanella; D_6__uncultured bacterium	C1	Bacteria; Firmicutes; Erysipelotrichia; Erysipelotrichales; Erysipelotrichaceae; Holdemanella; Holdemanella biformis strain DSM 3989 16S ribosomal RNA	99.35	100
denovo117817	D_0__Bacteria; D_1__Firmicutes; D_2__Clostridia; D_3__Clostridiales; D_4__Lachnospiraceae; D_5__Lachnospiraceae ND3007 group; D_6__uncultured bacterium	C1	Bacteria; Firmicutes; Clostridia; Clostridiales; Lachnospiraceae; Lachnospira; [Eubacterium] eligens ATCC 27750 16S	95	100
denovo167523	D_0__Bacteria; D_1__Actinobacteria; D_2__Coriobacteriia; D_3__Coriobacteriales; D_4__Coriobacteriaceae; D_5__Collinsella; D_6__uncultured bacterium	C1	Bacteria; Actinobacteria; Coriobacteriia; Coriobacteriales; Coriobacteriaceae; Collinsella; Collinsella aerofaciens strain JCM 10188 16S ribosomal RNA	99.55	100
denovo141115	D_0__Bacteria; D_1__Bacteroidetes; D_2__Bacteroidia; D_3__Bacteroidales; D_4__Prevotellaceae; D_5__Prevotellaceae NK3B31 group; D_6__uncultured bacterium	C1	Bacteria; Bacteroidetes; Bacteroidia; Bacteroidales; Prevotellaceae; Prevotella; Prevotella oris strain JCM 8540 16S ribosomal RNA	89.8	100
denovo74053	D_0__Bacteria; D_1__Firmicutes; D_2__Clostridia; D_3__Clostridiales; D_4__Ruminococcaceae; D_5__[Eubacterium] coprostanoligenes group; D_6__uncultured bacterium	C1	Bacteria; Firmicutes; Clostridia; Clostridiales; Eubacteriaceae; Eubacterium; Eubacterium coprostanoligenes strain HL 16S ribosomal RNA	91.84	100
denovo105849	D_0__Bacteria; D_1__Firmicutes; D_2__Clostridia; D_3__Clostridiales; D_4__Ruminococcaceae; D_5__Ruminococcus 2; D_6__uncultured bacterium	C1	Bacteria; Firmicutes; Clostridia; Clostridiales; Ruminococcaceae; Ruminococcus Ruminococcus bromii strain ATCC 27255 16S ribosomal RNA	98.64	100
denovo3720	D_0__Bacteria; D_1__Firmicutes; D_2__Clostridia; D_3__Clostridiales; D_4__Lachnospiraceae; D_5__Roseburia; D_6__uncultured bacterium	C1	Bacteria; Firmicutes; Clostridia; Clostridiales; Lachnospiraceae; Roseburia; Roseburia inulinivorans DSM 16841 strain A2-194 16S ribosomal RNA	100	100
denovo32339	D_0__Bacteria; D_1__Firmicutes; D_2__Clostridia; D_3__Clostridiales; D_4__Lachnospiraceae; D_5__Blautia; D_6__uncultured bacterium	C1	Bacteria; Firmicutes; Clostridia; Clostridiales; Lachnospiraceae; Blautia; Blautia faecis strain M25 16S ribosomal RNA	98.64	100
denovo56916	D_0__Bacteria; D_1__Firmicutes; D_2__Clostridia; D_3__Clostridiales; D_4__Ruminococcaceae; D_5__Ruminococcaceae UCG-002; D_6__uncultured bacterium	C1	Bacteria; Firmicutes; Clostridia; Clostridiales; Oscillospiraceae; Oscillibacter; Oscillibacter ruminantium GH1 16S ribosomal RNA	93.68	100
denovo168626	D_0__Bacteria; D_1__Bacteroidetes; D_2__Bacteroidia; D_3__Bacteroidales; D_4__Prevotellaceae; D_5__Prevotella 9; D_6__uncultured bacterium	C1	Bacteria; Bacteroidetes; Bacteroidia; Bacteroidales; Prevotellaceae; Prevotella; Prevotella copri DSM 18205 strain JCM 13464 16S ribosomal RNA	96.74	100
denovo78299	D_0__Bacteria; D_1__Firmicutes; D_2__Erysipelotrichia; D_3__Erysipelotrichales; D_4__Erysipelotrichaceae; D_5__Turicibacter; D_6__uncultured bacterium	C1	Bacteria; Firmicutes; Erysipelotrichia; Erysipelotrichales; Erysipelotrichaceae; Turicibacter; Turicibacter sanguinis strain MOL361 16S ribosomal RNA	97.42	100
denovo156839	D_0__Bacteria; D_1__Spirochaetae; D_2__Spirochaetes; D_3__Spirochaetales; D_4__Spirochaetaceae; D_5__Treponema 2; D_6__uncultured bacterium	C1	Bacteria; Spirochaetes; Spirochaetales; Spirochaetaceae; Treponema; Treponema porcinum strain 14V28 16S ribosomal RNA	90.99	100
denovo173045	D_0__Bacteria; D_1__Proteobacteria; D_2__Gammaproteobacteria; D_3__Enterobacteriales; D_4__Enterobacteriaceae; D_5__Escherichia-Shigella	C1	Bacteria; Proteobacteria; Gammaproteobacteria; Enterobacterales; Enterobacteriaceae; Shigella; Shigella sonnei strain CECT 4887 16S ribosomal RNA	99.57	100
denovo134303	D_0__Bacteria; D_1__Firmicutes; D_2__Clostridia; D_3__Clostridiales; D_4__Ruminococcaceae; D_5__Faecalibacterium; D_6__uncultured bacterium	C1	Bacteria; Firmicutes; Clostridia; Clostridiales; Ruminococcaceae; Faecalibacterium; Faecalibacterium prausnitzii strain ATCC 27768 16S ribosomal RNA	96.82	100
denovo176924	D_0__Bacteria; D_1__Actinobacteria; D_2__Actinobacteria; D_3__Micrococcales; D_4__Microbacteriaceae; D_5__Curtobacterium	C2	Bacteria; Actinobacteria; Micrococcales; Microbacteriaceae; Curtobacterium.; Curtobacterium flaccumfaciens strain BCCM/LMG 3645 16S ribosomal RNA	99.55	100
denovo56078	D_0__Bacteria; D_1__Actinobacteria; D_2__Actinobacteria; D_3__Micrococcales; D_4__Micrococcaceae; D_5__Glutamicibacter	C2	Bacteria; Actinobacteria; Micrococcales; Micrococcaceae; Glutamicibacter; Glutamicibacter halophytocola strain KLBMP 5180 16S ribosomal RNA	97.98	100
denovo153181	D_0__Bacteria; D_1__Proteobacteria; D_2__Betaproteobacteria; D_3__Burkholderiales; D_4__Comamonadaceae; D_5__Polaromonas; Ambiguous_taxa	C2	Bacteria; Proteobacteria; Betaproteobacteria; Burkholderiales; Comamonadaceae; Variovorax; Variovorax boronicumulans NBRC 103145 16S ribosomal RNA	98.28	100
denovo133617	D_0__Bacteria; D_1__Proteobacteria; D_2__Betaproteobacteria; D_3__Burkholderiales; D_4__Oxalobacteraceae; D_5__Massilia; D_6__uncultured bacterium	C2	Bacteria; Proteobacteria; Betaproteobacteria; Burkholderiales; Oxalobacteraceae; Massilia; Massilia aurea strain AP13 16S ribosomal RNA	99.35	100
denovo73964	D_0__Bacteria; D_1__Proteobacteria; D_2__Alphaproteobacteria; D_3__Rhodobacterales; D_4__Rhodobacteraceae; D_5__Paracoccus; D_6__uncultured bacterium	C2	Bacteria; Proteobacteria; Alphaproteobacteria; Rhodobacterales; Rhodobacteraceae; Paracoccus; Paracoccus cavernae strain 0511ARD5E5 16S ribosomal RNA	98.64	100
denovo64109	D_0__Bacteria; D_1__Actinobacteria; D_2__Actinobacteria; D_3__Micrococcales; D_4__Promicromonosporaceae; D_5__Cellulosimicrobium; D_6__Cellulosimicrobium cellulans	C2	Bacteria; Actinobacteria; Micrococcales; Promicromonosporaceae; Cellulosimicrobium; Cellulosimicrobium cellulans strain DSM 43879 16S ribosomal RNA	99.1	100
denovo88593	D_0__Bacteria; D_1__Actinobacteria; D_2__Actinobacteria; D_3__Frankiales; D_4__uncultured; D_5__uncultured bacterium; D_6__uncultured bacterium	C2	Bacteria; Actinobacteria; Geodermatophilales; Geodermatophilaceae; Geodermatophilus; Geodermatophilus pulveris strain BMG 825 16S ribosomal RNA	97.3	100
denovo187185	D_0__Bacteria; D_1__Actinobacteria; D_2__Actinobacteria; D_3__Micrococcales; D_4__Microbacteriaceae; D_5__Frigoribacterium	C2	Bacteria; Actinobacteria; Micrococcales; Microbacteriaceae; Frigoribacterium; Frigoribacterium endophyticum strain EGI 6500707 16S ribosomal RNA	99.33	100
denovo163893	D_0__Bacteria; D_1__Proteobacteria; D_2__Betaproteobacteria; D_3__Burkholderiales; D_4__Oxalobacteraceae; D_5__Massilia	C2	Bacteria; Proteobacteria; Betaproteobacteria; Burkholderiales; Oxalobacteraceae; Massilia; Massilia suwonensis strain 5414S-25 16S ribosomal RNA	98.92	100
denovo127020	D_0__Bacteria; D_1__Proteobacteria; D_2__Alphaproteobacteria; D_3__Rhizobiales; D_4__Brucellaceae; D_5__Ochrobactrum	C3	Bacteria; Proteobacteria; Alphaproteobacteria; Rhizobiales; Brucellaceae; Ochrobactrum; Ochrobactrum pseudogrignonense strain CCUG 30717 16S ribosomal RNA	99.77	100
denovo132540	D_0__Bacteria; D_1__Proteobacteria; D_2__Betaproteobacteria; D_3__Burkholderiales; D_4__Oxalobacteraceae; D_5__Herbaspirillum	C3	Bacteria; Proteobacteria; Betaproteobacteria; Burkholderiales; Oxalobacteraceae; Herbaspirillum; Herbaspirillum aquaticum strain IEH 4430 16S ribosomal RNA	99.78	100
denovo52654	D_0__Bacteria; D_1__Firmicutes; D_2__Clostridia; D_3__Clostridiales; D_4__Clostridiaceae 1; D_5__Clostridium sensu stricto 1; D_6__uncultured bacterium	C4	Bacteria; Firmicutes; Clostridia; Clostridiales; Clostridiaceae; Clostridium; Clostridium saudiense strain JCC 16S ribosomal RNA	95.68	100
denovo120280	D_0__Bacteria; D_1__Firmicutes; D_2__Bacilli; D_3__Bacillales; D_4__Bacillaceae; D_5__Bacillus; D_6__Bacillus megaterium	C4	Bacteria; Firmicutes; Bacilli; Bacillales; Bacillaceae; Bacillus; Bacillus aryabhattai B8W22 16S ribosomal RNA	99.78	100
denovo14992	D_0__Bacteria; D_1__Firmicutes; D_2__Clostridia; D_3__Clostridiales; D_4__Peptostreptococcaceae; D_5__Intestinibacter	C1, C4	Bacteria; Firmicutes; Clostridia; Clostridiales; Peptostreptococcaceae; Terrisporobacter; Terrisporobacter petrolearius strain LAM0A37 16S ribosomal RNA	99.09	100
denovo183787	D_0__Bacteria; D_1__Firmicutes; D_2__Clostridia; D_3__Clostridiales; D_4__Peptostreptococcaceae; D_5__Paeniclostridium; D_6__uncultured bacterium	C1, C4	Bacteria; Firmicutes; Clostridia; Clostridiales; Peptostreptococcaceae; Paeniclostridium; [Eubacterium] tenue strain ATCC 25553 16S ribosomal RNA	99.77	100
denovo66357	D_0__Bacteria; D_1__Firmicutes; D_2__Erysipelotrichia; D_3__Erysipelotrichales; D_4__Erysipelotrichaceae; D_5__Turicibacter; D_6__uncultured bacterium	C1, C4	Bacteria; Firmicutes; Erysipelotrichia; Erysipelotrichales; Erysipelotrichaceae; Turicibacter; Turicibacter sanguinis strain MOL361 16S ribosomal RNA	98.92	100
denovo145701	D_0__Bacteria; D_1__Proteobacteria; D_2__Alphaproteobacteria; D_3__Sphingomonadales; D_4__Sphingomonadaceae; D_5__Sphingomonas	C2, C4	Bacteria; Proteobacteria; Alphaproteobacteria; Sphingomonadales; Sphingomonadaceae; Sphingomonas; Sphingomonas aerolata strain NW12 16S ribosomal RNA	99.77	100
denovo27632	D_0__Bacteria; D_1__Proteobacteria; D_2__Gammaproteobacteria; D_3__Oceanospirillales; D_4__Halomonadaceae; D_5__Halomonas; D_6__uncultured bacterium	C2, C4	Bacteria; Proteobacteria; Gammaproteobacteria; Oceanospirillales; Halomonadaceae; Halomonas; Halomonas kenyensis strain AIR-2 16S ribosomal RNA	99.35	100
denovo116915	D_0__Bacteria; D_1__Firmicutes; D_2__Bacilli; D_3__Bacillales; D_4__Planococcaceae	C2, C4	Bacteria; Firmicutes; Bacilli; Bacillales; Planococcaceae; Planococcus; Planococcus donghaensis strain JH1 16S ribosomal RNA	98.92	100
denovo124634	D_0__Bacteria; D_1__Proteobacteria; D_2__Gammaproteobacteria; D_3__Xanthomonadales; D_4__Xanthomonadaceae; D_5__Stenotrophomonas; D_6__uncultured bacterium	C3, C4	Bacteria; Proteobacteria; Gammaproteobacteria; Xanthomonadales; Xanthomonadaceae; [Pseudomonas] geniculata ATCC 19374 = JCM 13324 16S ribosomal RNA	99.14	100
denovo68017	D_0__Bacteria; D_1__Firmicutes; D_2__Clostridia; D_3__Clostridiales; D_4__Peptostreptococcaceae; D_5__Peptoclostridium; D_6__uncultured bacterium	C1, C2, C4	Bacteria; Firmicutes; Clostridia; Clostridiales; Peptostreptococcaceae; Romboutsia; Romboutsia sedimentorum strain LAM201 16S ribosomal RNA	99.32	100
denovo66475	D_0__Bacteria; D_1__Firmicutes; D_2__Clostridia; D_3__Clostridiales; D_4__Clostridiaceae 1; D_5__Clostridium sensu stricto 1	C1, C2, C4	Bacteria; Firmicutes; Clostridia; Clostridiales; Clostridiaceae; Clostridium; Clostridium saudiense strain JCC 16S ribosomal RNA	98.41	100
denovo36561	D_0__Bacteria; D_1__Proteobacteria; D_2__Betaproteobacteria; D_3__Burkholderiales; D_4__Comamonadaceae; D_5__Delftia; D_6__uncultured organism	C2, C3, C4	Bacteria; Proteobacteria; Betaproteobacteria; Burkholderiales; Comamonadaceae; Delftia; Delftia acidovorans strain LMG 1226 16S ribosomal RNA	99.57	100
denovo124378	D_0__Bacteria; D_1__Proteobacteria; D_2__Gammaproteobacteria; D_3__Enterobacteriales; D_4__Enterobacteriaceae; D_5__Serratia; D_6__uncultured soil bacterium	C2, C3, C4	Bacteria; Proteobacteria; Gammaproteobacteria; Enterobacterales; Yersiniaceae; Serratia; Serratia quinivorans strain LMG 7887 16S ribosomal RNA	98.06	100
denovo171745	D_0__Bacteria; D_1__Actinobacteria; D_2__Actinobacteria; D_3__Micrococcales; D_4__Microbacteriaceae; D_5__Microbacterium	C2, C3, C4	Bacteria; Actinobacteria; Micrococcales; Microbacteriaceae; Microbacterium; Microbacterium tumbae strain T7528-3-6b 16S ribosomal RNA	99.33	100